

Contents

Zusammenfassung	V
Abstract	VII
1 Introduction & Objectives	1
2 Properties of chemically peculiar stars	5
2.1 Rotation	6
2.2 Magnetic field	15
2.3 The temperature scale of CP stars	20
3 Detection of chemically peculiar stars	29
3.1 Classification spectroscopy	36
4 Why studying open clusters?	41
4.1 Data compilation	43
5 The open cluster sample	45
5.1 Photoelectric Δa survey	45
5.1.1 Collinder 121	45
5.1.2 Collinder 132	45
5.1.3 Collinder 140	46
5.1.4 IC 2391	46
5.1.5 IC 2602	47
5.1.6 IC 4665	47
5.1.7 IC 4725	47
5.1.8 Melotte 20 (α Persei)	48
5.1.9 Melotte 22 (Pleiades)	48
5.1.10 Melotte 111 (Coma Berenices)	48
5.1.11 NGC 1039	49
5.1.12 NGC 1662	50
5.1.13 NGC 1901	50
5.1.14 NGC 2169	50
5.1.15 NGC 2232	50
5.1.16 NGC 2287	51
5.1.17 NGC 2343	51

5.1.18	NGC 2362	51
5.1.19	NGC 2422	51
5.1.20	NGC 2423	52
5.1.21	NGC 2447	52
5.1.22	NGC 2451 A/B	52
5.1.23	NGC 2516	53
5.1.24	NGC 2546	53
5.1.25	NGC 2632 (Praesepe)	53
5.1.26	NGC 3114	54
5.1.27	NGC 3228	54
5.1.28	NGC 3532	55
5.1.29	NGC 5460	55
5.1.30	NGC 5662	56
5.1.31	NGC 6087	56
5.1.32	NGC 6281	56
5.1.33	NGC 6405	57
5.1.34	NGC 6475	57
5.1.35	NGC 7092	57
5.1.36	NGC 7243	57
5.1.37	Trumpler 10	58
5.2	CCD Δa survey - Part I	58
5.2.1	Collinder 272	58
5.2.2	Lyngå 14	58
5.2.3	Melotte 105	58
5.2.4	NGC 2099	59
5.2.5	NGC 2169	59
5.2.6	NGC 2439	59
5.2.7	NGC 2489	60
5.2.8	NGC 2567	60
5.2.9	NGC 2658	60
5.2.10	NGC 3114	60
5.2.11	NGC 3960	61
5.2.12	NGC 5281	61
5.2.13	NGC 6134	61
5.2.14	NGC 6192	61
5.2.15	NGC 6204	62
5.2.16	NGC 6208	62
5.2.17	NGC 6250	62
5.2.18	NGC 6396	63
5.2.19	NGC 6451	63
5.2.20	NGC 6611	63
5.2.21	NGC 6705	63
5.2.22	NGC 6756	64
5.2.23	Pismis 20	64
5.3	CCD Δa survey - Part II	64

5.3.1	Berkeley 11	64
5.3.2	Berkeley 94	65
5.3.3	Haffner 15	65
5.3.4	King 21	65
5.3.5	Lyngå 1	66
5.3.6	NGC 1502	66
5.3.7	NGC 3105	66
5.3.8	NGC 3293	66
5.3.9	NGC 5999	67
5.3.10	NGC 6031	67
5.3.11	NGC 6268	67
5.3.12	NGC 6405	68
5.3.13	NGC 6802	68
5.3.14	NGC 6830	68
5.3.15	NGC 6834	68
5.3.16	NGC 7235	69
5.3.17	NGC 7296	69
5.3.18	NGC 7510	69
5.3.19	Ruprecht 44	69
5.3.20	Ruprecht 115	70
5.3.21	Ruprecht 120	70
5.3.22	Ruprecht 130	71
5.3.23	Stock 16	71
6	Open cluster parameters	73
6.1	Metallicity	73
6.1.1	A homogeneous approach to determine metallicity	76
6.2	The final open cluster parameters	102
7	Membership analysis	111
8	Results	123
8.1	The final dataset	123
8.2	Masses and fractional ages of CP stars.	127
8.3	Evolution with age	130
8.3.1	Former investigations	130
8.3.2	Results based on the Δa survey	132
8.4	Dependencies beside age	142
8.5	The early stage of chemically peculiar stars	146
9	Outlook	151
A	The data	153
	References	161

List of Abbreviations	171
List of Figures	173
List of Tables	181
Acknowledgements	183
Curriculum vitae	185

Zusammenfassung

Die Entstehung und Entwicklung von chemisch peculiaren (CP) Sternen ist nach wie vor nicht restlos geklärt, und das obwohl die ersten Vertreter dieser Sterngruppe bereits vor mehr als 110 Jahren entdeckt wurden. Aus astrophysikalischer Sicht sind diese Objekte von großem Interesse, da sie zahlreiche besondere Eigenschaften in sich vereinen.

Diese Dissertation widmet sich der Untersuchung einer Untergruppe der CP Sterne, die neben Überhäufigkeiten von Elementen der Eisengruppe (zB. Chrom) und seltenen Erden wie Europium, auch starke Magnetfelder und eine langsame Rotation aufweisen. Basierend auf einer Auswahl von gut untersuchten nahen Feldsternen wird der mögliche Zusammenhang zwischen diesen Eigenschaften betrachtet. Das Hauptaugenmerk galt jedoch der Untersuchung einer möglichen Abhängigkeit zwischen der Anzahl von CP Sternen und deren Alter. Für diesen Zweck wurden die Ergebnisse von mehreren Δa Studien in Sternhaufen herangezogen. Dieses fotometrische Filtersystem ermöglicht eine effiziente und zeitsparende Detektion der magnetischen CP Sterne auf Grund einer charakteristischen Flussdepression bei 520 nm. Im Vergleich zu Feldsternen bieten offene Sternhaufen den großen Vorteil, dass zum Beispiel das Alter und die Entfernung statistisch gesehen genauer bestimmt werden können. Der Grund dafür liegt in der mehr oder weniger gleichzeitigen Entstehung aller Mitglieder aus einer einzigen Molekülwolke.

Nach der Analyse der Mitgliedswahrscheinlichkeit aller mittels Δa untersuchten Objekte und der Bestimmung der jeweiligen Sternhaufenparameter konnte gezeigt werden, dass eine Abhängigkeit zwischen der Anzahl von CP Sternen und deren Alter besteht. Allerdings konnte dies durch die allgemeine Sternentwicklung erklärt werden. Das würde unter anderem bedeuten, dass CP Sterne spätestens beim Erreichen der Hauptreihe bereits ihre typischen Eigenschaften zeigen. Des Weiteren konnte zumindest ein Vertreter dieser Gruppe gefunden werden, der sich vermutlich noch auf der Vorhauptreihe befindet.

Abstract

The formation and evolution of chemically peculiar (CP) stars is still a matter of debate, although the first representatives were detected already more than 110 years ago. From the astrophysical point of view, these objects are of particular interest, since they combine a wide variety of specific properties.

This work deals with a subgroup of CP stars, showing beside overabundances of some iron-peak (e.g. Chromium) and rare earth elements like Europium, also strong ordered magnetic fields as well as a slow rotation. Based on a selection of well investigated close field stars, the possible connections of these properties were examined. However, the main research focus was the analysis of a relationship between the number of CP stars and their age. For this purpose, the results of the extensive Δa survey in open clusters were used. This photometric filter system allows an efficient and economic detection of magnetic CP stars due to a characteristic flux depression at 520 nm. Compared to field stars, open clusters offer the big advantage that for example the age and the distance can be determined more accurately on a statistical basis, since all member stars of an open cluster originate more or less at the same time from a single molecular cloud.

After the membership analysis of all in Δa investigated objects and the determination of the cluster parameters, it was shown that the occurrence of CP stars depend on age, but can be explained by the general evolution of stars. This entails amongst others that CP stars show their typical characteristics already as soon as they have arrived the main-sequence, or even before. Furthermore, we were able to detect at least one representative, probably still in its pre-main-sequence phase.

Chapter 1

Introduction & Objectives

For the first time, the term “peculiar” in combination with stellar spectra appeared in Maury & Pickering (1897). It was used to describe some special features found in the spectrum of α^2 CVn. They recognized a weak K line but also the striking SiII doublet at $\lambda 4128/30\text{\AA}$. Other stars designated in this respect were θ Aur or 81 UMa. We want to refer to Schnell (2008) and references therein for a more detailed historical review.

From then on, the phrase “peculiar” was often used to describe stars, which do not really fit into known groups. Spectral classifications are still contaminated by the frequent (often not justified) use of it, but also by a confusion of chemically peculiar objects and giants due to very low resolution spectra and similar equivalent widths of typical features.

Beside the spectral classification itself, also the used term for this star groups is far from being homogeneous. In the literature one can still find the designations Ap/Bp, CP, or mCP for the magnetic subgroups, or just “peculiar”, although Preston (1974) introduced a classification scheme for the chemically peculiar stars (see Table 1.1), which cover the spectral range from B to F type stars. Even though this classification has to be extended due to some “new” (sub)groups such as He-rich, PGa, or λ Bootis objects, it can and should serve to reduce the confusion in the literature. However, there are numerous objects, which cannot be assigned to a specific group. For example, “He wk Si” stars are often marked either as CP2 or CP4 objects, depending on the study and which feature was detected or used as to be more prominent. As can be seen in Table 1.1, also the temperature domains are often overlapping significantly. Furthermore, most known peculiar stars listed e.g. in the comprehensive catalogue of Ap, HgMn and Am stars by Renson & Manfroid (2009) are still based on a classification using objective prism plates (see e.g. Bidelman, 1983) or photometric peculiarity indices such as Δa or the *Geneva* $\Delta(V1 - G)$ (see Sect. 3).

Up to now more than 8000 probable chemically peculiar objects are known in the Milky Way (Renson & Manfroid, 2009), of which nearly one half belong to Ap and Am stars, respectively. The group of HgMn objects play a minor part with only 162 candidates listed in the aforementioned reference. However, this catalogue lists only 426 stars in total, which are well known and confirmed. This number clearly demonstrates the problems tersely mentioned above.

In this work we will concentrate on the magnetic representatives (Ap a.k.a. CP2/4,

Table 1.1: The classification scheme by Preston (1974).

CP Group	Classical name	Discovery criteria	Temperature domain
CP1	metallic line (Am)	wk Ca II and/or Sc II ; enhanced heavy metals	7000–10000 K
CP2	magnetic Ap	enhanced Si, Cr, Sr, Eu, et al	8000–15000 K
CP3	HgMn	enhanced Hg II λ 3894, Mn II	10000–15000 K
CP4	He-weak	$Q(\text{Sp}) > Q(\text{UBV})^a$	13000–20000 K

^aThe intrinsic colours of the spectral type and the measured photometry disagree

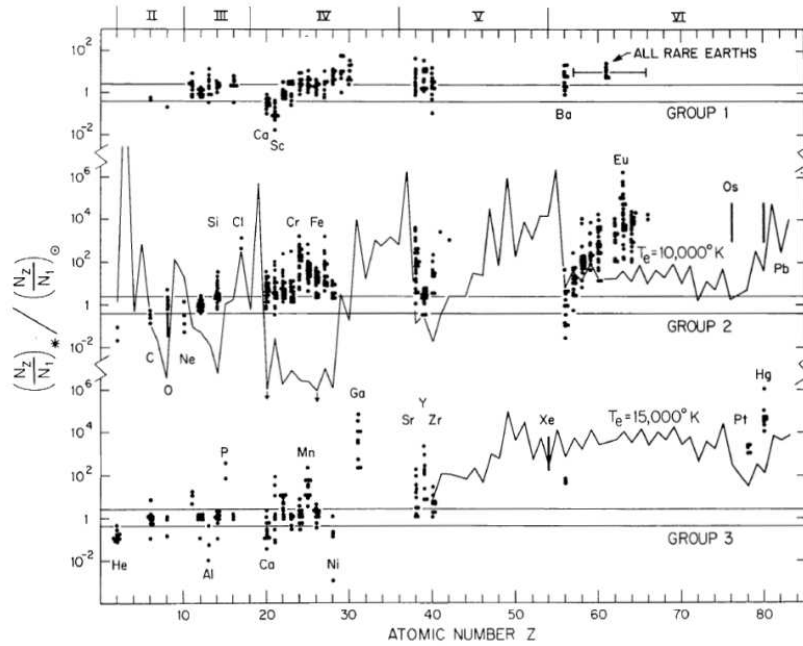


Figure 1.1: The observed abundances pattern in some groups of chemically peculiar stars, taken from Preston (1974).

see Table 1.1), which show a wide variety of element abundance patterns as can be seen in Fig. 1.1. This graph taken from Preston (1974) is still a representative and illustrative one and as can be seen, some elements like Europium show overabundances up to a factor of 10^6 times the solar value.

Although large overabundances are found, the stars exhibit in general a normal solar bulk composition and one can characterise them colloquially as a kind of “skin disease”. Although the mechanisms producing these chemical anomalies can still not completely be explained, it is understood that the main driver behind is atomic diffusion (Michaud, 1970) acting in the stellar photosphere. Whereas gravitational settling results in underabundances of e.g. He, radiative pressure leads to overabundances at the stellar atmosphere of some species such as Mn, Sr, and the rare earths. The Ap stars offer properties that diffusion processes are going to be important. They are slow rotators compared to normal stars of the same spectral type (see e.g. Abt & Morrell, 1995), which provides already a somewhat stable atmosphere. Furthermore,

strong globally organized magnetic fields up to several kG are found, which also act stabilising and prevent that convection dominates.

This work is dedicated to a statistical investigation of magnetic CP stars to explore their evolutionary status. Open clusters offer a perfectly suited laboratory for such a study, since cluster stars have all in general the same properties as a result from the respective gas and dust cloud, where they were formed. Hence, they are all more or less of the same age and chemical composition. Furthermore, since open clusters are rather compact ($\lesssim 15$ pc in absolute diameter; van den Bergh, 2006), all cluster stars can be assumed to be approximately at the same distance from the Sun. Therefore, compared to single field objects, the individual parameters of open clusters can be determined more accurately on a statistical basis using e.g. evolutionary models. Nevertheless, a significant number of almost homogeneously investigated open clusters with respect to their CP star content is necessary in order to study e.g. their time dependent incidence. Fortunately, photometry - the Δa system - offers a powerful and economic way to detect these objects thanks to a characteristic flux depression in the optical region (see Sect. 3). In total, 79 open clusters were used for the presented study to evaluate the evolution of the CP phenomenon, which is also somehow connected to stellar magnetism in general. Concerning this topic, the present study helps also to supply further clues about the origin of the magnetic field of CP objects, which is either a fossil one, frozen-in during star formation from the interstellar cloud or due to a dynamo acting in the star, like in the Sun. However, more and more the fossil field hypothesis is being accepted as responsible, since the fields are found to be rather stable and were already detected in pre-main-sequence objects. Since the final stellar stages of the mass range of CP stars incorporates both, white dwarfs and neutron stars, the CP objects may provide also a hint for the magnetism found in these degenerate stars (Wade et al., 2007).

Several intermediate steps were necessary to reach the goals of this study. Since the magnitudes of the detected CP stars reach down to $V_{\text{mag}} \sim 17$, effective temperatures derived from high resolution spectra are hardly available, so that one has to rely on photometrically calibrated data. Due to the chemical anomalies of the CP stars, available temperature calibrations for normal stars can not be used safely, therefore new and revised calibrations tuned for CP objects were presented by Netopil et al. (2008). Furthermore, although open clusters offer a big advantage to derive their properties (age, distance, metallicity) the actual state of data is often rather poor, what can be noticed also in the investigations by Paunzen & Netopil (2006) and Paunzen et al. (2010). Therefore, a homogeneous approach based on the method by Pöhl & Paunzen (2010) was carried out to determine the cluster parameters, including metallicity. Since photometry has to be transformed into the $T_{\text{eff}}/\log(L/L_{\odot})$ plane, also revised photometric temperature calibrations for normal type stars were introduced. A further crucial topic is membership of the individual stars (CP as well as normal cluster objects). Since this work was performed in the pre Gaia mission era, whose dataset will revolutionize cluster research, accurate parallax and proper motions were provided by the Hipparcos/Tycho mission only within a rather limited area around the Sun. Although current available proper motion catalogues (e.g. PPMXL, UCAC-4) are a valuable source, they have still limitations which have to be considered. Finally,

also individual photometric studies (especially CCD ones) used for the determination of effective temperature and the derivation of the cluster parameters were often found to be erroneous due to a probably wrong standardisation. The use of all available data in different photometric systems and the incorporation of surveys such as APASS or 2MASS helped to overcome these problems and to produce datasets as consistent as possible.

This brief introduction should just serve as an easy entry to the wide topics covered by this thesis, in the following chapters further introductory words are given connected to the respective subjects.

Chapter 2

Properties of chemically peculiar stars

Although cluster stars would offer a more appropriate way to study the properties of chemically peculiar objects (e.g. thanks to a restriction in age), several parameters such as rotational period, or magnetic field are naturally better known for brighter and closer field stars. However, an investigation of field objects would also allow a comparison to cluster stars e.g. in respect to the mass distribution. At the beginning of writing this thesis, the latter was also the main motivation to compile such a sample. We therefore used as a starting point the CP catalogue by Renson & Manfroid (2009), which was restricted to field stars using their notes concerning cluster affiliation. An additional cross-check was made using the open cluster catalogue by Dias et al. (2002) to remove further objects which are in the vicinity of open clusters. Furthermore, Renson & Manfroid (2009) list a “quality flag” for the peculiarity. This way, we removed all probably doubtful CP stars. The given spectral type was used to sort out non-magnetic Am or HgMn objects. Since it is important to determine temperature and luminosity as accurate as possible, further restrictions were made concerning errors of the Hipparcos parallax (van Leeuwen, 2007) and available photometric data. We therefore included only such objects with errors in the parallax $< 15\%$ (a compromise between accuracy and a sufficient large sample), as well as stars with data in at least two photometric systems (out of *UBV*, *Geneva*, or Strömgren data), extracted from the *General Catalogue of Photometric Data*¹ (GCPD, Mermilliod et al., 1997). This way, we compiled a sample of 282 CP stars within ~ 500 pc around the Sun. The temperature and luminosity was calculated as presented in Sect. 2.3. However, as soon as “fundamental” temperatures for the stars were listed by Netopil et al. (2008), these were adopted instead (this holds for 75 objects in total).

In the following sections we concentrate on rotation and magnetic field. The third important property, which can be noticed already in the designation “chemically peculiar”, are of course their element abundances. This topic is strongly connected with a flux depression visible mostly in magnetic CP stars, which can be also measured using photometric systems (e.g. Δa , *Geneva*). Therefore, an investigation of the observed abundances was merged with the explanation of these systems in Section 3.

¹<http://obswww.unige.ch/gcpd/gcpd.html>

2.1 Rotation

It is well known that CP stars are slow rotators compared to normal objects (see e.g. Abt & Morrell, 1995). The reference suggested also that the slow rotation is a sufficient property that the CP phenomenon occurs. One assumption is that the magnetic field is responsible for the slow rotation.

Due to the slow rotation the stellar atmospheres are stable, and in the absence of a surface convection zone and significant mass loss, the work by Michaud (1970) is still accepted that atomic diffusion is responsible to explain the observed abundance patterns. This means that some elements like He settle down due to gravitation, others such as Si (guided also by the magnetic field) assemble at the outer layers.

The magnetic field is not a necessity to produce chemical inhomogeneities on the stellar surface, since also in CP3 (HgMn) stars such a behaviour was observed, which do not show measurable magnetic fields so far (Kochukhov, 2011).

Due to the resulting (e.g. Si) spots on the stellar surface, the rotational period of magnetic CP stars can be determined accurately using e.g. photometric timeseries. Recently, several stars were investigated in this respect e.g. by Wraight et al. (2011) using the STEREO satellites or by Paunzen et al. (2011b) based on Strömgren data. Unfortunately, up to now the most recent compilation of rotational periods is still the one by Renson & Catalano (2001), which includes period values for 362 CP objects. As can be seen e.g. in Fig. 8 by Wraight et al. (2011), the individual results can sometimes differ significantly, presenting often harmonics of the real rotational period. For numerous stars, the only photometric source is the one by the Hipparcos mission, whose lower time resolution makes it also often difficult to extract the proper period.

We used the compilation by Renson & Catalano (2001) as starting point and performed a cross-match with the sample defined above. If meanwhile new or revised periods were published, these were adopted instead. Beside the work by Wraight et al. (2011), also Koen & Eyer (2002), Bychkov et al. (2005), or the series by Adelman (2008) were consulted. In total, we compiled periods for 169 objects of the sample defined above, of which six are longer than 100 days, with some extremely slow rotators of up to several years. We noticed a broad gap in period between those and the remaining stars and therefore restricted the sample to stars with periods below 34 days.

Additionally, we queried the catalogue by Glebocki & Gnacinski (2005), which presents homogenized projected rotational velocities ($v \sin i$). Again, it was updated with more recent determinations and some values overseen by these authors by following their weighting system. For most stars of our sample (228 out of 282), a $v \sin i$ value is available. Finally, for 144 objects, both information (period and $v \sin i$) exist, allowing to calculate e.g. the inclination of their rotation axis.

We also tried to exclude known binaries, since such objects would introduce an error in luminosity, if the magnitudes of the individual components are not exactly known, but also e.g. co-rotation of these systems may cause a bias if investigating the actual evolution of rotation. We therefore used the works (and references therein) by North et al. (1998), Leone & Catanzaro (1999), Wade et al. (2000), Carrier et al. (2002), and Balega et al. (2012) to reject binaries/multiples. In total 29 such candidates were

found, resulting in an incidence of about 10%. However, this value is very probably an underestimation, since the majority of the objects were not investigated in this respect. The study by Balega et al. (2012) using speckle interferometry of 117 CP stars with a measured magnetic field, resulted e.g. in an incidence of 25% binaries among the magnetic chemically peculiar stars, but this value is probably affected also by chance projections.

As can be seen in the Hertzsprung-Russell diagram (HRD; see Fig. 2.1) some stars are located below the ZAMS (using the $Z=0.02$ models by Schaller et al., 1992). One possible reason can be that a too hot temperature was adopted. Since only objects with proper photometry in several systems were selected and among these deviating stars also some with spectroscopic results are available, a more likely explanation is an underestimation of the Hipparcos distances. These stars, as well as the few above the TAMS, which can be either evolved stars or unrecognised binaries, were therefore rejected for the further analysis. In total 125 stars with available periods remain.

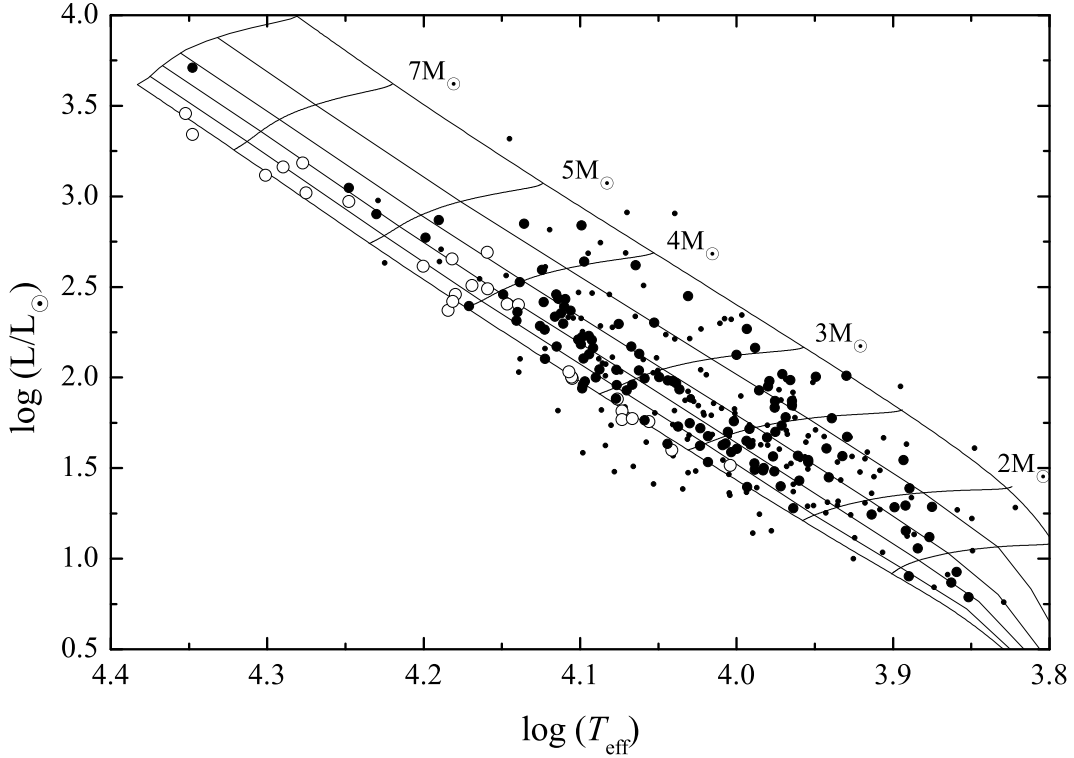


Figure 2.1: The HRD of the stars used for the analysis. Large filled circles represent single stars within the main-sequence band and with available periods, whereas the smaller symbols represent the remaining sample. Open circles are CP members of OB associations.

First, we present in Fig. 2.2 a comparison of the projected rotational velocities ($v \sin i$) of CP stars to normal main sequence (of mid B to mid F type) stars, the latter compiled from Abt & Morrell (1995) and Abt et al. (2002) (753 stars in total), whose $v \sin i$ values were updated with the homogenized mean entries listed by Glebocki & Gnacinski (2005). We also performed a cross-match of the compiled normal stars

with the Ap catalogue by Renson & Manfroid (2009) and found that about 15% of this sample were at least mentioned as peculiar (mostly as Am star) somewhere in the literature. After exclusion of these objects, 650 stars remained. All of them show no significant photometric peculiarity indices $\Delta(V1 - G)$ and Z of the *Geneva* system (see also Sect. 3).

Additionally, Fig. 2.2 (small insert) shows the percentage of Ap stars to all objects (normal + CP) for the various velocity bins, indicating that at least almost all of the very slowest rotating stars ($< 20 \text{ km s}^{-1}$) are CP stars, with a decrease of the incidence to higher velocities. Since both samples (normal and CP stars) are definitely incomplete, we restricted them also to stars within 100 pc, assuming that this would represent a somewhat more complete coverage. Here, one can notice a similar distribution, but with a significant lower CP percentage of 60% at $v \sin i < 20 \text{ km s}^{-1}$. If including also the other groups of chemically peculiar stars such as Am or HgMn objects (CP1 and CP3, respectively), the discrepancy will be surely reduced, but still several slow rotating stars can be considered as normal ones.

According to Abt & Morrell (1995) using subsamples of the spectral type, the velocity ratio between normal and CP stars is about four, what can be also followed from Fig. 2.2. Considering the velocity distributions, the CP objects are not the slow-rotation tail of main-sequence stars (Abt & Morrell, 1995). The origin of the slow rotation is not yet known, but is probably the result from an enhanced loss of angular momentum already during the pre-main-sequence phase (Stępień, 2000).

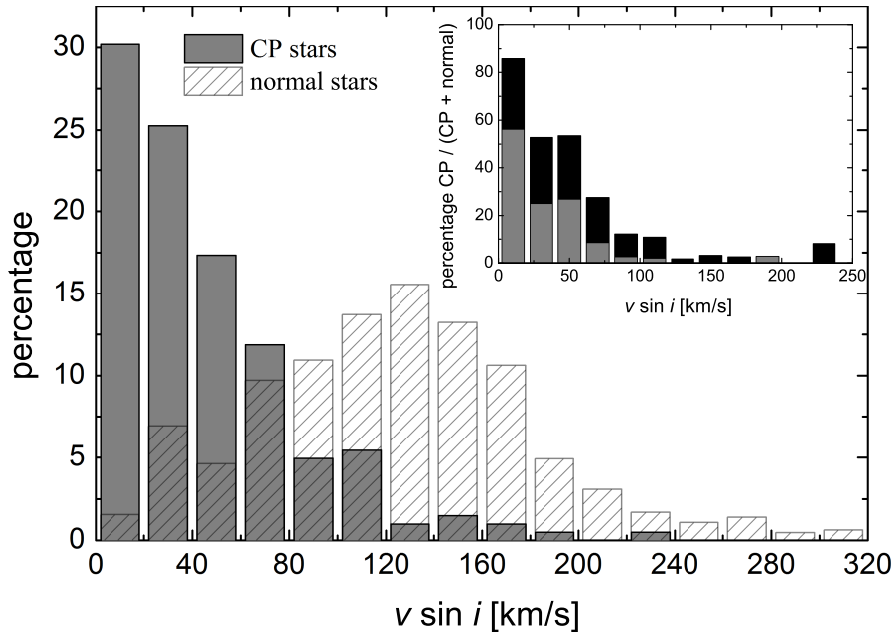


Figure 2.2: The distribution of observed $v \sin i$ for CP stars compared to normal main-sequence stars. Additionally, the smaller insert shows the percentage of CP stars to normal ones. Whereas the black columns represent the complete sample, the grey columns gives the sample restricted to stars within 100 pc.

Of course, based on Fig. 2.2, the slow rotation of CP stars can be also due to projection, in the sense that their inclination axes are not randomly orientated and show a preference of pole-on in the line of sight. However, this argument is very unlikely and was already disproved e.g. by Abt (2001). Using the sample with available $v \sin i$ and equatorial velocities, calculated by means of rotation period P_{rot} [d], stellar radius R [R_{\odot}], and the well known formula

$$V_{eq}[\text{km s}^{-1}] = 50.57877 R P_{rot}^{-1}$$

if assuming rigid rotation, the inclination can be easily derived. In Fig. 2.3 one can find the distribution of this property. We want to note that throughout this work we used the solar fundamental data suggested by Harmanec & Prša (2011). A number of objects exhibit a lower V_{eq} value than the measured $v \sin i$, indicating at least one erroneous parameter (R and/or P_{rot}). Therefore, Fig. 2.3 shows also a sharp drop at large inclinations. We included also such objects with differences smaller than 10 km s^{-1} in the last (highest inclination) bin, indicated by an open bar. This value represents somehow the error in equatorial velocities, if the accuracy of the radius determination is $\sim 20\%$. Based on this figure one can conclude an equal distribution of the rotation axes. We derived a χ^2 of 8.6, which is less than the needed 11.1 to obtain at least a 95% probability for non-uniformity.

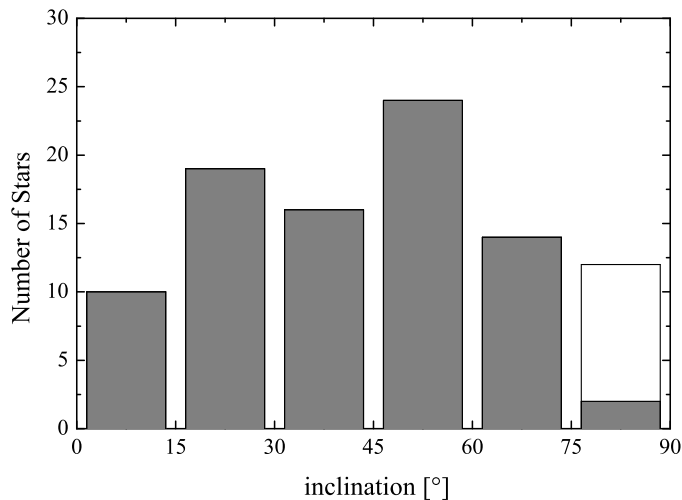


Figure 2.3: The distribution of the inclination for CP stars. The open bar represents objects including also stars with $(v \sin i - V_{eq}) \leq 10 \text{ km s}^{-1}$ (see text).

So, what about normal stars, exhibiting also low $v \sin i$ values? In principle, slow rotation can be just a necessary condition to produce a chemical peculiarity. Abt (2009) concluded at least for early/mid A type stars that most of the normal slow rotators did not have enough time yet to develop their peculiarities, which takes at least about 186 Myr according to the reference (slightly less than half of their main-sequence lifetimes). The evolutionary models by Vick et al. (2011), however, yield

~ 3 Myr for a $2.5 M_{\odot}$ star to develop peculiarities due to diffusion processes, which would be still during the pre-main sequence phase (see also Sect. 8.5).

In Fig. 2.4 one can find the HRD of the cleaned CP star sample as defined above together with 65 normal objects slower than 50 km s^{-1} (taken from the compilation explained above). For the latter selection also both peculiarity indices ($\Delta(V1 - G)$ and Z) of the *Geneva* photometry are completely inconspicuous (see Sect. 3). As can be seen in Fig. 2.4, the slowly rotating normal objects occupy the same region as the CP stars. There are several CP stars close to the ZAMS, but also several more evolved normal stars. Hence, either another property seems to be necessary (such as magnetic field) or the slow rotation is due to projection and their rotational axes are close to pole on in the line of sight, which was ruled out already for the CP stars above. Concerning the latter argument, it is worth to mention e.g. Vega, showing a rather low $v \sin i$ of 20 km s^{-1} . Although a pole-on view was suggested since long-time, the first absolute proof using interferometric observations was presented by Peterson et al. (2006), resulting in a velocity of about 93% of the breakup speed.

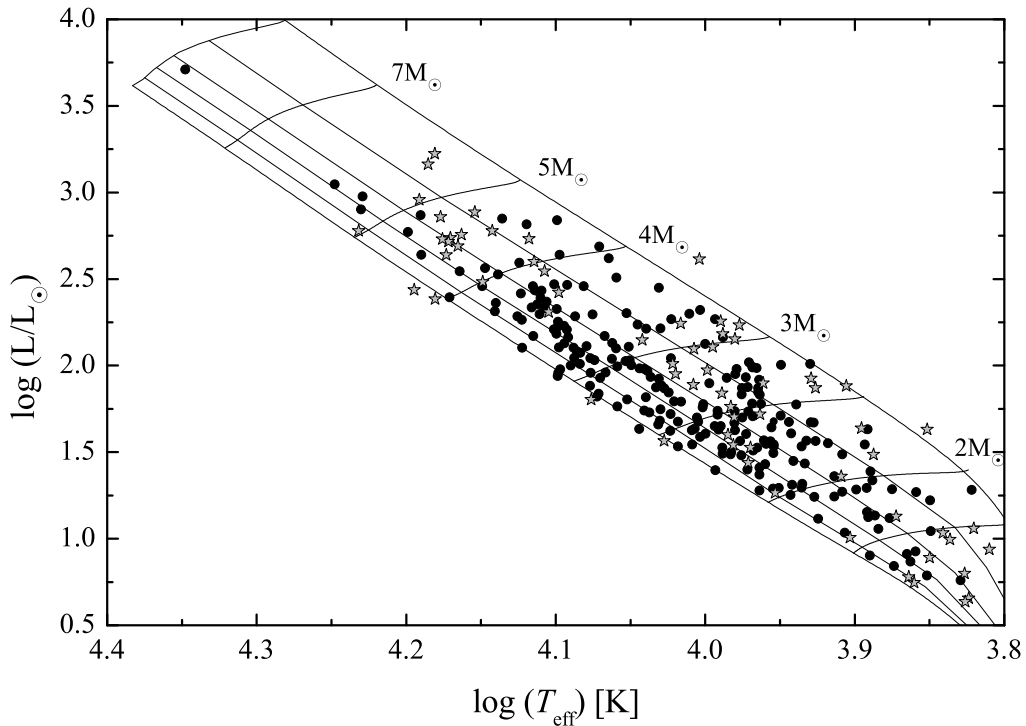


Figure 2.4: The HRD of the cleaned field star CP sample and the slow rotating normal objects with $v \sin i < 50 \text{ km s}^{-1}$, the latter represented by star symbols.

Since Ekström et al. (2008) presented evolutionary grids with rotation, it is worth to compare these models with the observed periods for the chemically peculiar stars. The latter reference calculated models for several initial rotation rates ($\Omega/\Omega_{\text{crit}}$) up to

the critical limit of the angular velocity Ω . In the following we adopted their $3 M_{\odot}$ model for metallicity $Z = 0.020$, since this is the most appropriate one if considering the mass distribution of chemically peculiar stars. Furthermore, these models include an interplay between meridional circulation and mass loss by stellar winds to trace the evolution of equatorial velocities, but conservation of angular momentum is always given (see the reference for details). The mass loss is zero for the $3 M_{\odot}$ model, but at this mass range shear mixing is more important. In Fig. 2.5 the models for initial $\Omega/\Omega_{crit} = 0.1, 0.3, \text{ and } 0.5$ are plotted, which corresponds to $v/v_{crit} = 0.07, 0.20, \text{ and } 0.35$. These velocities can be transformed to equatorial ones with

$$\frac{v}{v_{crit}} = \left(\frac{\Omega}{\Omega_{crit}} 2(f - 1) \right)^{1/3} v_{crit} = \sqrt{\frac{2}{3} \frac{GM}{R_{p,crit}}}$$

as given by Ekström et al. (2008), with f being the ratio of equatorial to polar radius and $R_{p,crit}$ the polar radius at critical velocity, which can be replaced by the polar radius since $R_{p,crit}/R_p \simeq 1$ (see also Fig. 3 of the latter reference). The critical equatorial velocity is defined in the context of the Roche model and is reached if gravitational acceleration is exactly balanced by the centrifugal force. Since chemically peculiar stars are slow rotators, one can furthermore set $R_p \simeq R_{eq}$, the latter being the radius at the equator.

In Fig. 2.5 the evolution of the rotational periods is shown using $\log g$ as evolutionary parameter. Such a diagram was already presented e.g. by North (1998). Beside the $3 M_{\odot}$ models by Ekström et al. (2008), we included also rather simplified ones with the same initial periods assuming concentric shells without exchange of angular momentum, hence only the external shell has to be considered. Therefore, the rotation period follows $P_{rot} \propto R^2$. In addition to the complete sample, the mass range of 2.4 to $3.5 M_{\odot}$ is highlighted, representing a sufficient large sample of 68 stars. The lower mass range was chosen, since in the range of 2.4 to $2.5 M_{\odot}$ several stars are available, which cover a broad range of the main sequence band (see Fig. 2.1). Using this sample we calculated mean periods for various $\log g$ bins, rejecting always the most deviating stars in each bin. From Fig. 2.5 one can already deduce that the population of the individual bins vary significantly, with only five to seven objects in the earliest and most evolved groups, respectively, and up to 15 in the more covered middle regions.

Nevertheless, as can be seen in Fig. 2.5, these mean values are rather well represented by an interpolated rotational model of $\Omega/\Omega_{crit} = 0.22$ ($v/v_{crit} \sim 0.15$), except at the beginning of the main-sequence, where the models predict a somewhat faster rotation. In contrast, the simple model shows a somewhat too steep trend. Surprisingly, Huang et al. (2010) found a good agreement of such a model to their B-type stars sample with the same mass range (see upper panel of their Fig. 10), but that can be also due to the considerable scatter of their data, which is also noticeable in our sample.

We used the calculated mean periods and $\log g$ values presented in Fig. 2.5 to derive the factor, which has to be applied to correct the period due to stellar evolution and to normalize the periods to the ZAMS ($\log g = 4.3$).

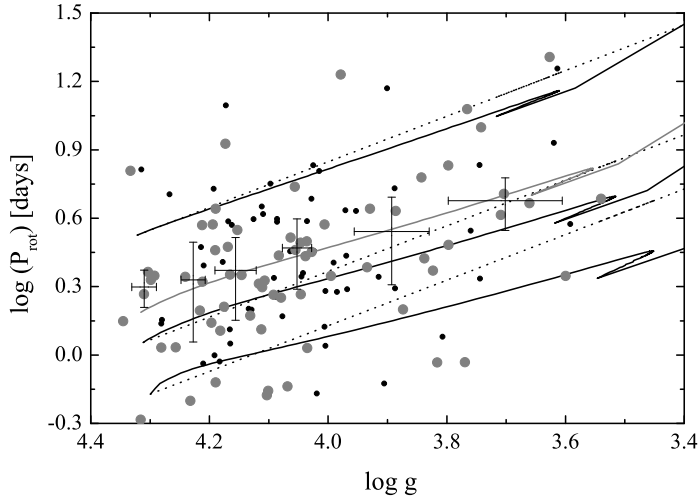


Figure 2.5: The gravity/period relation for chemically peculiar stars. The thick lines represent the $3 M_{\odot}$ models by Ekström et al. (2008) for initial (ZAMS) values of $\Omega/\Omega_{crit} = 0.1, 0.3,$ and 0.5 (from top to bottom). The dotted lines show the evolution assuming a simple model with conservation of angular momentum ($P_{rot} \propto R^2$). The subsample of 2.4 to $3.5 M_{\odot}$ stars are given by larger grey symbols and their mean values (plus standard deviation) by the crosses. Furthermore, the models were interpolated to $\Omega/\Omega_{crit} = 0.22$ ($v/v_{crit} \sim 0.15$) shown as grey line.

$$P_{factor} = 40.337 - 17.090 \log g + 1.847 (\log g)^2$$

Although the sample of more evolved stars in Fig. 2.5 is still rather low, all gravity bins (except the earliest ones as mentioned above) follow nicely the models by Ekström et al. (2008). We present a somewhat larger CP sample than given by North (1998), but the conclusion is the same. The data suggest conservation of angular momentum and no noticeable magnetic braking along the main sequence.

One of the few stars for which a rotational braking was detected by Mikulášek et al. (2008) is HD 37776, located in the Ori OB1b association. They found a considerable rate of period increase, which amounts to 0.524 s/yr . However, they ruled out that magnetic braking is effective enough to explain that large spin-down and favoured angular momentum loss via its magnetically confined stellar wind.

Although one can not approve that the increase of period shown in Fig. 2.5 is also valid for other masses, simply since at lower/higher masses no significant number of stars are available covering the full main-sequence band to test this behaviour, we normalized the periods to the ZAMS for the complete sample. Using the adopted stellar masses, we calculated the radii on the ZAMS using the evolutionary models by Schaller et al. (1992). Hence, with $P_{rot,Z}$ and $R_{*,Z}/R_{\odot}$ (Z representing ZAMS values) one can estimate the equatorial velocity on the ZAMS. However, the differences to the actual velocities are rather small, only $\sim 10 \text{ km s}^{-1}$ for the majority of the stars.

As can be seen in the works by Ekström et al. (2008) or Huang et al. (2010), the ratio v/v_{crit} also hardly depends on the time elapsed on the main sequence, especially for slow rotating stars like CP objects. Similar to the approach before, we averaged the periods

$P_{rot,Z}$ and velocities ($V_{eq,Z}$; v/v_{crit}), but now for various mass bins, again rejecting strong outliers in each subsample. The equatorial velocities deduced via the averaged v/v_{crit} values are in excellent agreement (within a few km s^{-1}) to those obtained by the corrected periods. In addition to this sample, we compiled CP stars with known periods, which are members of young clusters/associations, as it is HD 37666 mentioned above. The work e.g. by Landstreet et al. (2007) presented such objects, for which we re-determined the fundamental parameters such as temperature, luminosity, and mass, following the same procedure as before. These stars are members of the Orion Associations, Upper Sco, Lower Cen Cru, and Upper Cen Lup, which are all young enough ($\lesssim 15$ Myr) to represent stars reasonable close to the ZAMS (see also Fig. 2.1). If the corrections above were also applied to these stars, the velocities are only slightly higher by about 10 km s^{-1} for the higher mass objects. We therefore adopted the uncorrected values in order not to include additional errors. The results can be found in Fig. 2.6, where the mass dependency of the equatorial velocity is shown.

In general a rather good agreement of the corrected field stars and the young association sample can be found, suggesting that the correction is properly defined. Several fast rotating stars in the mass range of 2 to $4 M_{\odot}$ are present in Fig. 2.6, reaching up to about 60 % of the critical velocity. We assume that we have probably adopted the false rotational period, since for numerous stars divergent results in the literature can be found: e.g. for HD 22470 Bychkov et al. (2005) report 0.68 d (corresponds to $V_{eq,Z} = 260 \text{ km s}^{-1}$), whereas Renson & Catalano (2001) list 1.93 d ($V_{eq,Z} = 90 \text{ km s}^{-1}$); or for HD 55579 values of 0.70 ($V_{eq,Z} = 170 \text{ km s}^{-1}$) and 2.32 d ($V_{eq,Z} = 50 \text{ km s}^{-1}$) are available, taken from Koen & Eyer (2002) and Renson & Catalano (2001), respectively. There are several other such examples available. We examined also another “fast rotator” (HD 72634), for which Koen & Eyer (2002) quote a period of 0.93 d. Using photometric timeseries taken from the All Sky Automated Survey (ASAS)² and the analysis package Peranso³, we noticed that the strongest signal seems to be present around one day, but the examination of the phase curve would support a much longer period of 13.94 d. This clearly shows the difficulties in finding or adopting the correct rotational period. Extensive efforts are still necessary in this respect. Several surveys such as ASAS, TASS⁴, or Superwasp⁵ are already available, offering huge timeseries datasets. These have to be evaluated in a homogeneous manner like by Wraight et al. (2011) for the Stereo satellites data. However, also some of their results are among the “fast rotators”.

On the contrary there are also several very slow rotators with more than 100 days or even in the range of years, as mentioned at the beginning, but which are not included in the present analysis. Mathys et al. (1997) list 29 such stars with established or probable periods longer than 25 days. Stępień & Landstreet (2002) give the necessary conditions for such slow rotation, which are:

- low mass stars so that the PMS phase is long enough,

²<http://www.astrouw.edu.pl/asas>

³<http://www.peranso.com>

⁴<http://www.tass-survey.org>

⁵<http://www.wasp.le.ac.uk/public/>

- strong magnetic fields of several kG,
- that the accretion disk disappears during the PMS phase and the magnetized wind remains for a sufficient long time afterwards.

Landstreet & Mathys (2000) concluded that almost all of these very slow rotators have their magnetic and rotation axes nearly aligned, whereas the shorter period representatives show an inclination of the axes of 60° and more. Stępień (2000) has also suggested that the presence of a disk around a magnetic CP star during the PMS phase is able to produce rotation rates around a few days, which seems to be the majority as can be also seen in the sample presented here.

Using the mean velocity values for the various mass bins, we determined the following linear fit for the mass dependency of the equatorial velocity.

$$V_{eq}[\text{km s}^{-1}] = -13.57(4.19) + 23.53(1.37) \frac{M}{M_\odot}$$

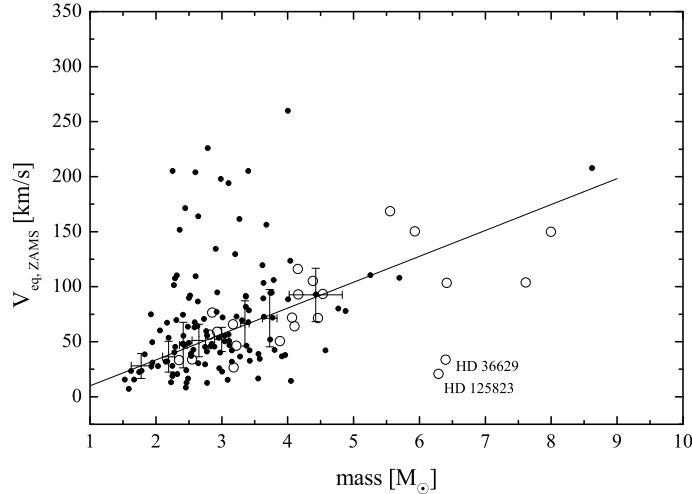


Figure 2.6: The mass/equatorial velocity relation on the ZAMS. Small dots represent the sample defined in Sect. 2.1, open circles are CP stars in OB associations listed by Landstreet et al. (2007), and the crosses equatorial velocities deduced using the mean v/v_{crit} velocities of the field star sample. Additionally, the linear fit of these averages is given as straight line.

Its continuation also retraces quite well the velocity distribution of the higher mass association stars. However, this mass/velocity dependency has to be verified by a much larger sample, especially in the higher mass regime. As can be seen in Fig. 2.6, two stars (HD 36629 and HD 125823) exhibit significantly lower velocity values. These are members of the OriOB1c and Upper Cen Lup association, respectively. Recently, HD 125823 was investigated by Bohlender et al. (2010), classifying it as the first well established magnetic star of the small helium-3 group (see e.g. Hartoog & Cowley, 1979). According to Bohlender et al. (2010), the helium abundance varies by a factor of 125 from one hemisphere to the other. The long period of about 8.8 days is confirmed

by several studies, also the $v \sin i$ value of 17.7 km s^{-1} listed by Glebocki & Gnacinski (2005) suggest a slow rotation. Since also the magnetic field strengths for both objects (HD 36629 and HD 125823) are inconspicuous compared to the other CP stars in the respective associations, other not yet known mechanisms are probably responsible for the slow rotation.

2.2 Magnetic field

The chemically peculiar subgroups CP2 and CP4 are known to exhibit strong organized magnetic fields. The first detected field was announced by Babcock (1947) for 78 Vir (HD 118022). This work was followed by the first catalogue of magnetic stars (Babcock, 1958) and the detection of an extra ordinary large field of 34 kG in HD 215441 (Babcock, 1960), still known as Babcock's star. Although some other stars with magnetic fields in this range were detected in the meanwhile (e.g. HD 75049 with 30 kG by Elkin et al., 2010), it is still the strongest magnetic CP star known so far.

The detection of variations of the magnetic field strength led to the Oblique Rotator model (Stibbs, 1950), which explains the periodicity of the variations just as a geometrical effect as the star rotates, using a simple dipolar geometry. Hence, also magnetic field measurements can be used to determine the rotational period. Meanwhile several quadrupole or even higher order configurations are known. As mentioned in Sect. 2.1, the rotational and magnetic axes mostly do not coincide, or there is even a decentred (dipole) geometry (Landstreet, 1970).

The origin of the magnetic field is still an open question, although the overall opinion tend to a fossil origin (e.g. Braithwaite & Spruit, 2004), after which it is a relic of the frozen-in interstellar magnetic field. The other theory is that there is a dynamo operating in the convective core. Both theories were critically examined e.g. by Moss (1989).

Since there are excellent reviews available, about measuring the magnetic field using the Zeeman effect, we do not want to go into details and refer to Mathys (2009) or Landstreet (2011), but it is worth to mention two main magnetic field moments, which are being measured: the (mean) longitudinal magnetic field (B_l), which is the average over the observed stellar hemisphere of the magnetic vector component along the line of sight. This is by far the most often measured moment, but to obtain a hint about the surface field strength, it is necessary to cover the whole rotational period. If only a single or few measurements are available, which are furthermore unfortunately badly timed with phase, one can even fail to detect a magnetic field. The other moment, worth to mention, is the mean magnetic field modulus (B_s), which is the average of the modulus of the magnetic field vector over the observed stellar hemisphere. Since it shows only slight variations during a rotation cycle, it is a quite good measure of the actual surface field strength. It can be determined only if the star exhibits a strong field and narrow lines (slow rotation). Its detection limit lies currently at about 2 kG (Romanyuk, 2010), whereas the one for the longitudinal field is significantly lower; the work e.g. by Aurière et al. (2007) increased the precision to a median σ of 40 G. The latter reference concluded thanks to their Zeeman detection rate of 100 % in their

sample that probably all Ap/Bp stars host a detectable magnetic field, and that there seems to be a threshold of ~ 300 G, below which fields are uncommon or even absent.

As mentioned above, using timeseries of B_l measurements one can determine also the rotational period, but its investigation allows also to estimate the actual surface fieldstrength. With B_0 as the observed average field strength and B_1 half of the amplitude, the maximal longitudinal field can be easily derived with $B_l^{max} = |B_0| + B_1$. Of course also several double wave variations were found (see e.g. Bychkov et al., 2005). According to Preston (1967) for a centred dipole configuration one can derive the surface polar field strength B_d :

$$B_d = B_l^{max} \left(\frac{15 + u}{20(3 - u)} (\cos\beta\cos i + \sin\beta\sin i) \right)^{-1}$$

with u as limb darkening coefficient ($u \sim 0.5$), i the inclination of the rotational axes, and β the obliquity angle. However, the latter parameters are rather inaccurate (see e.g. Table 2 by Aurière et al., 2007). Therefore, if skipping these one obtains the approximation

$$B_d \geq 3.23 B_l^{max} \sim B_s.$$

To examine the magnetic properties of chemically peculiar stars and their probable dependency with other parameters, we compiled stars which have either the mean magnetic field modulus B_s measured or the longitudinal field B_l with a sufficient large number. Bychkov et al. (2005) presented a catalogue of magnetic rotational phase curves for 136 stars in total, of which we adopted only their single-wave results for CP stars. Additionally, Aurière et al. (2007) investigated some further weak magnetic stars and list their B_l^{max} values. Furthermore, results of the mean magnetic field modulus were compiled from the literature, for which the most substantial investigation was performed by Mathys et al. (1997), but also Elkin et al. (2012) studied several stars recently. In order not to overlook further data in this respect, we also checked the catalogue by Romanyuk (2008). If for an object both determinations are available, we adopted always the mean magnetic field modulus as indicator of the field strength.

In total, data for 156 objects were compiled which have either a parallax available or are members of open clusters. Several stars coincide with the sample presented in Sect. 2.1, for the remaining ones we determined their fundamental parameters (temperature and luminosity) accordingly or adopted spectroscopic temperatures from the respective reference.

As in the previous section, we excluded known binaries, and objects strongly deviating from the ZAMS/TAMS, but concerning errors in the parallax we used a more conservative error of 20 % in order to have a sufficient large sample available. This way, still a considerable number of 52 stars has to be excluded from the sample, resulting in a final list of 104 objects.

In Fig. 2.8 the evolution of magnetic field strength as a function of gravity ($\log g$) is presented. A decrease along the main sequence is unambiguous. Additionally, we included an evolutionary model for a $3 M_\odot$ star, with initial (ZAMS) field strengths of 1.5, 7.5, and 30 kG, respectively, and a decrease with increasing stellar radius $(R/R_Z)^2$.

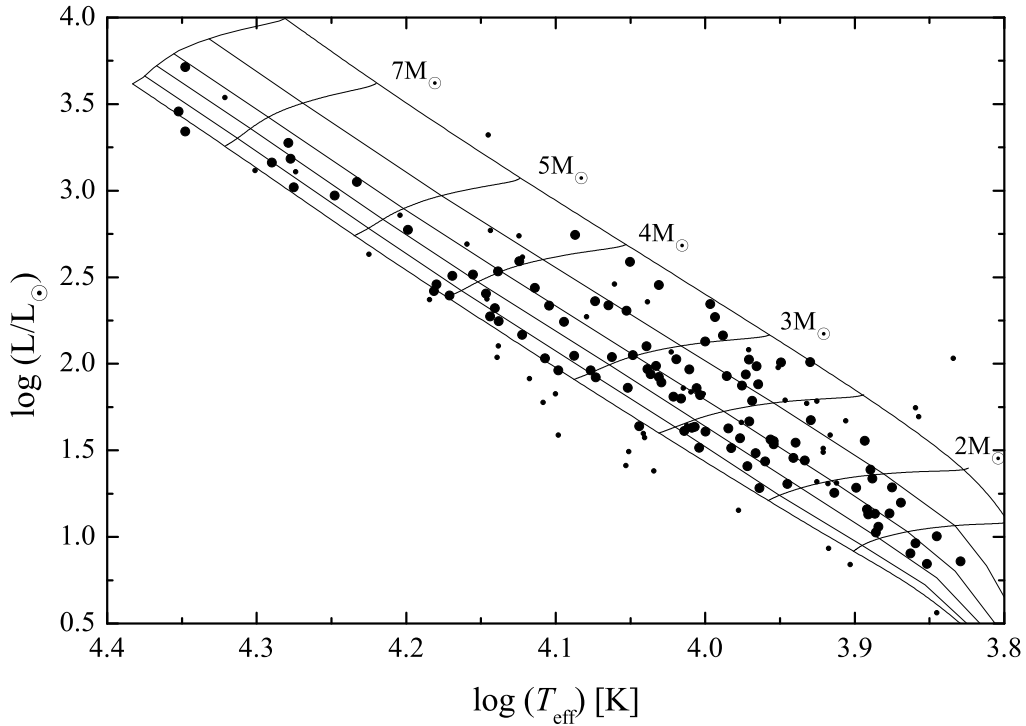


Figure 2.7: The HRD of the stars used for the investigation of the magnetic field. Large filled circles represent the adjusted sample (see text), whereas the smaller symbols represent the remaining stars.

Again, we used radii relative to the ZAMS value. The good agreement implies that the magnetic flux of the stellar magnetic field remains constant.

All presented mass ranges show a rather good agreement, indicating that there seems to be no further mass dependency. If applying $(R/R_Z)^2$ to the observed field strengths, these will be all normalized to their respective ZAMS values. The resulting distribution of the initial field strengths is given in Fig. 2.9, showing a peak at about 5 kG.

For 96 objects of the sample also rotational periods are available, allowing to calculate equatorial velocities like in the previous section. As explained above, we determined also the respective velocity on the ZAMS, which are compared to the magnetic field strengths in Fig. 2.10 for various mass ranges. Based on this Figure, one has the visual impression that the magnetic field strength declines with increasing equatorial velocity, or vice versa that the stronger the magnetic field, the slower the stellar rotation. This would support the theory of magnetic braking, which occurs probably already during the PMS phase. This behaviour is best seen especially in the lower mass regime, but a larger sample is definitely necessary for a profound conclusion. The magnetic field strength seems to be also a contributor to the scatter of the mass/velocity relation presented in Fig. 2.6. Although few objects show a higher magnetic field,

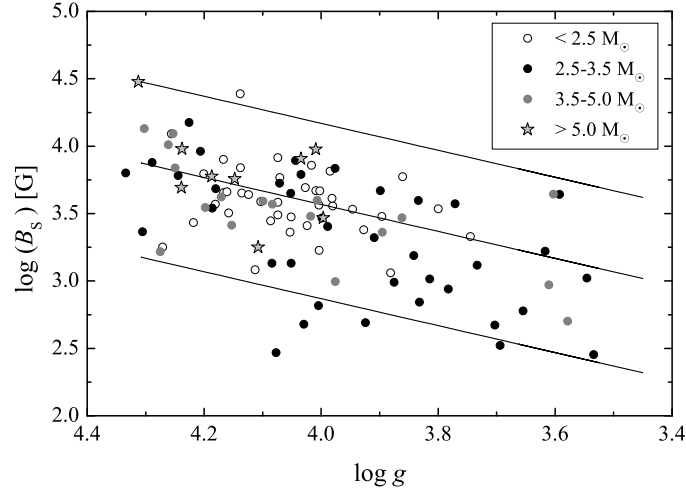


Figure 2.8: The magnetic field as a function of gravity for various mass ranges. The full lines assume initial magnetic field strengths of 1.5, 7.5, and 30 kG, respectively, decreasing with $(R/R_Z)^2$. The $3M_\odot$ evolutionary model by Schaller et al. (1992) was used for that purpose.

there appears to be a kind of upper limit for the field strength of about 15 kG in each mass subsample.

Some stars in the 2.5 to $3.5 M_\odot$ range show extremely low magnetic fields compared to the others (see also Fig. 2.8). These are HD 10221, HD 32650, and HD 89822. The latter was adopted from the work by Bychkov et al. (2005), where it is listed as A0p. See also Section 1 about the confusion in the literature in the classification schemes and designations. The additional literature (e.g. Netopil et al., 2008) assign it to the HgMn (CP3) group, which is known to exhibit rather small (if any) magnetic fields. In contrast, HD 10221 can be considered as unambiguous CP2 star (Glagolevskii et al., 2005), whose weak magnetic field is verified by the latter reference and later on by Aurière et al. (2007). These findings led to the conclusion by Glagolevskii et al. (2005) that the slow rotation rather than the magnetic field is the major origin for the formation of chemical anomalies. This is consistent with the group of HgMn stars, for which also some spots on their surface were already found spectroscopically (see also the short discussion in Sect. 2.1), but hardly a magnetic field. For the third weak magnetic object (HD 32650) unfortunately no detailed abundance analysis is available, but Marakov & Kaplan (2005) list it as astrometric binary, by comparing the proper motion data of Hipparcos and Tycho. Hence, the rotational braking was possibly due to the companion rather than because of a strong magnetic field. However, a detailed investigation of this object is necessary, since a binarity can influence parallax and measured brightness.

Also among the highest mass stars, two objects show up with rather low velocities. These are HD 36629 and HD 125823, already discussed at the end of Section 2.1. If their slow rotation can be assured, there has to be an additional braking, probably explained by the conditions listed by Stępień & Landstreet (2002) (see also Sect. 2.1).

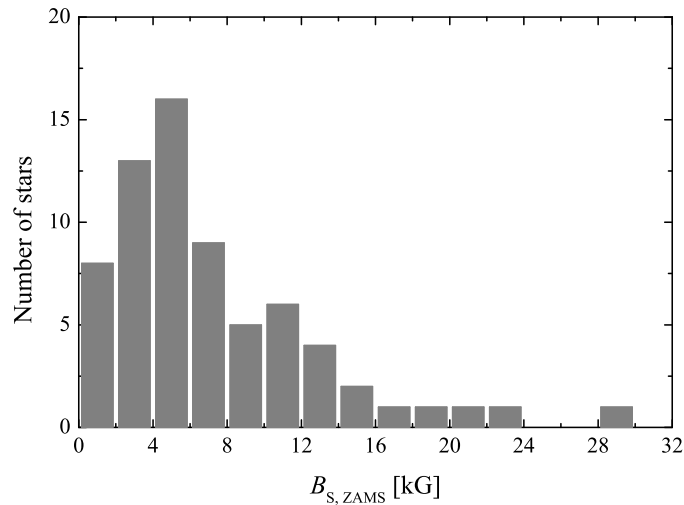


Figure 2.9: The distribution of the magnetic field strengths at the ZAMS.

For both objects also rather low $v \sin i$ values of 12.6 and 16.8 km s⁻¹ for HD 36629 and HD 125823, respectively, were compiled, a further hint of slow rotation. These stars are therefore worth of more detailed investigations, especially with respect to photometric/spectroscopic time series.

In Section 3 we investigated the temperature dependency of observed abundances based on a larger sample than Ryabchikova (2005). The findings are mostly in agreement with diffusion theory (see discussion by the latter reference). Therefore it is worth to study also possible dependencies of abundances with rotation and magnetic field, but the sample for which all data are available is rather small. Due to the temperature dependency of e.g. iron (see Fig. 3.4) the sample has to be further limited to the temperature range of $\sim 9000 - 12000$ K, where a plateau of the Fe abundances can be noticed. One can use instead e.g. the *Geneva* peculiarity indices (see Section 3 for details) for that purpose, which are available for the majority of stars, in contrast to Δa measurements. In Fig. 2.11 one can find the indices $\Delta(V1 - G)$ and Z compared to equatorial velocity, magnetic field, and iron abundance using the samples defined above and in Section 3. We have to note that here the actual observed values of equatorial velocity and magnetic field are given, and not to the ZAMS corrected values as e.g. in Fig. 2.10, since the peculiarity indices are the actual observed ones as well. To take into account the aforementioned temperature dependency of iron abundances, but still to present the behaviour of the indices for the whole temperature range, the symbol size was scaled with effective temperature. As can be seen in the left lower panel, $\Delta(V1 - G)$ shows the strongest relationship with iron abundance for the whole temperature range. There seems to be a kind of saturation at $\Delta(V1 - G) \sim 0.03$, where the indices still increase but the abundances remain at the same level. This index compared to magnetic field strength shows that it is not usable for the coolest and hottest stars, respectively, but for the temperature range defined above a strong correlation with the magnetic field can be found. The same can be noticed in the upper

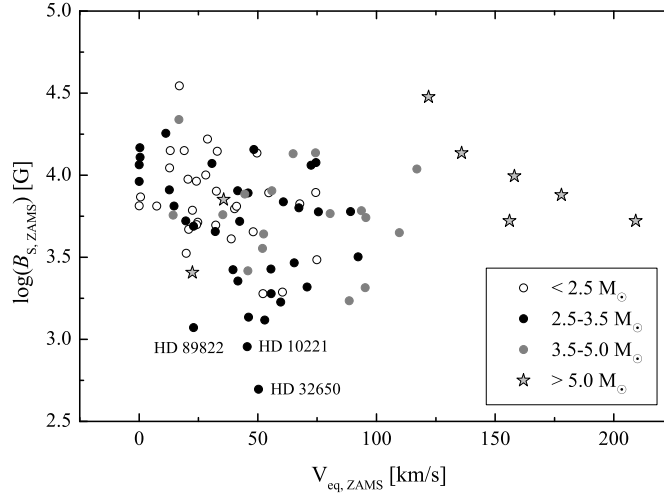


Figure 2.10: The magnetic field strength at the ZAMS vs. equatorial velocities.

left panel for equatorial velocities, but the latter is also affected by the mass/velocity dependency shown in Fig. 2.6. Using the Z index, only the hottest stars do not follow a relation with magnetic field strength, whereas for abundances (lower right panel of Fig. 2.11) the coolest objects deviate.

Hence, according to Fig. 2.11, there seems to be a correlation between all investigated parameters (equatorial velocity, magnetic field strength, and iron abundances), but these properties are also influenced by variations with phase of the rotation period (see also Sect. 3). Together with the findings of the magnetic field / velocity relation presented in Fig. 2.10 one can conclude that in general the stronger the magnetic field, the slower the rotation due to magnetic braking. Furthermore, the slower the rotation the higher the iron abundance, which implies that diffusion acts more efficiently since the stellar atmospheres are stabilised because of slow rotation and magnetic field. However, the latter assumption is valid for the temperature range of $\sim 9000 - 12000$ K only. A thorough study based on a sufficient large sample for which all observed parameters are available is necessary for a more profound conclusion.

2.3 The temperature scale of CP stars

Effective temperature is a very important astrophysical parameter, necessary to study several processes. However, for chemically peculiar stars the situation is more complicated compared to “normal” ones due to several reasons. There is only a small fraction available with direct (e.g. spectroscopic) temperature determinations, a rather small sample to be able to investigate evolutionary effects in detail. Therefore, the most convenient solution is a temperature estimate by using available photometric data. Unfortunately, existing standard calibrations for normal stars cannot be used safely, due the properties of chemically peculiar objects. They appear bluer than they actually are. Such a behaviour was already noticed by Adelman (1980). Additionally,

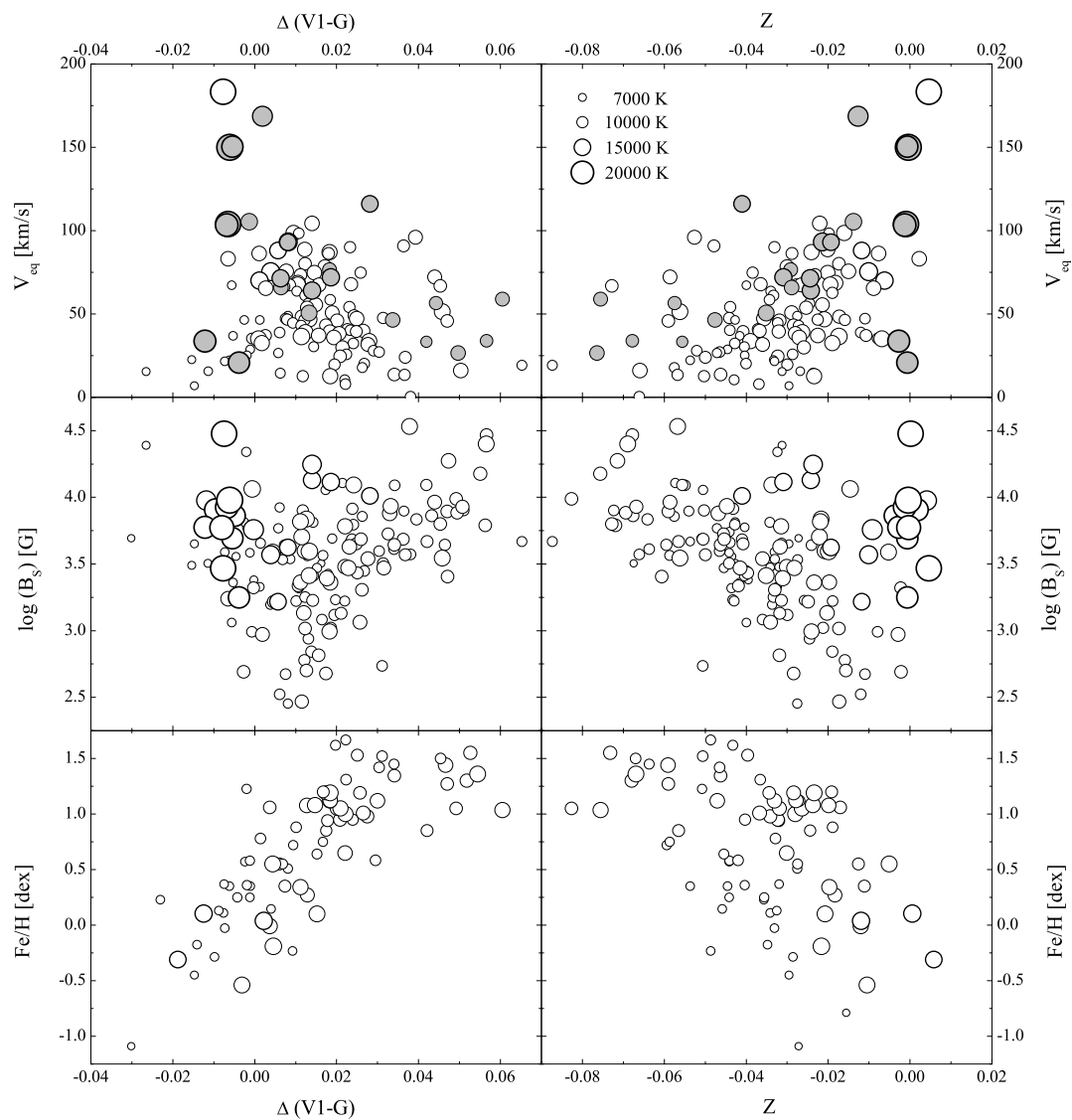


Figure 2.11: The Geneva peculiarity indices $\Delta(V1 - G)$ and Z compared to equatorial velocities, surface magnetic field strength ($\log B_s$), and iron abundances. In the upper panel also the young magnetic association members are given with grey symbols. The symbol size corresponds with the effective temperature.

blanketing effects, individual abundances or strong magnetic fields prevent a temperature determinations by means of standard calibrations for normal stars.

To overcome this problem, many attempts were presented to correct existing methods so that the temperature scale of chemically peculiar stars can be matched. Such corrections for the main systems Johnson UBV , Strömgren $wby\beta$, or *Geneva* photometry were determined e.g. by Mégessier (1988); Napiwotzki et al. (1993); Hauck & North (1993); Stępień (1994); Hauck & Künzli (1996) or Lipski & Stępień (2008).

All of these are based mostly on a very limited comparable sample of some “fundamental” CP objects, whereas the latter reference used their new own sample. Since in the meanwhile several new temperature determinations have been published, Netopil et al. (2008) have re-examined the necessary corrections based on a much larger sample. They have compiled direct temperature determinations for 176 chemically peculiar stars of the different groups (CP1–4) together with available photometric data. To reduce the influence of individually wrong determined temperatures, only such objects were used, for which at least two independent determinations are available. In case of CP2 stars, 51 out of 79 objects remained using this restriction (see Fig. 2.12).

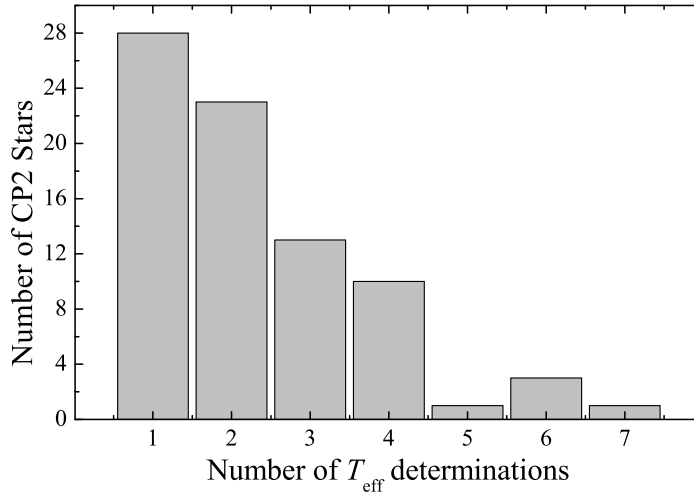


Figure 2.12: Histogram of the number of individual temperature determinations for CP2 stars.

However, due to the variable nature (e.g. spots on the surface), which can be found for several objects, photometry is surely affected. This fact can be only reasonably reduced by using averaged values of individual measurements. Anyway, the compiled sample comprises several prominent representatives, which are extensively studied. The temperatures obtained by using the averaged photometric data and well known calibrations for normal stars (e.g. the TEFLOG routine by Napiwotzki et al. (1993) for Strömgren data) were then corrected by appropriate relations, which can be found in Table 2.1. The deviations of these results compared to the compiled direct temperatures can be found in Figs. 2.13 and 2.14 for the CP2 and CP4 objects respectively. Except some strong outliers, which are discussed by Netopil et al. (2008), one can adopt errors of ~ 500 K for CP2 stars. For the hotter He (weak/rich) representatives a slightly

larger error of ~ 700 K has to be taken into account.

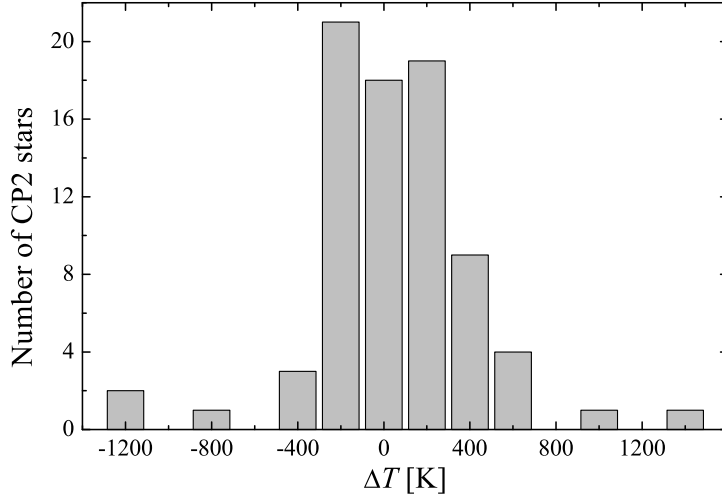


Figure 2.13: The temperature deviations for CP2 objects determined by Netopil et al. (2008).

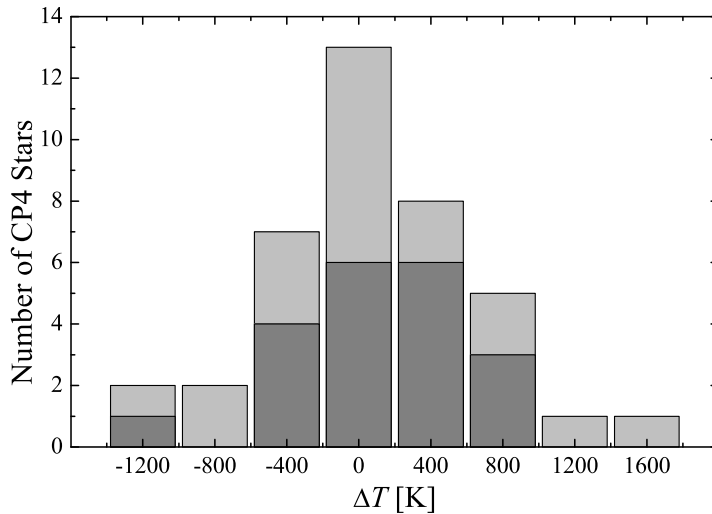


Figure 2.14: The temperature deviations for CP4 objects determined by Netopil et al. (2008). The dark grey portion serves to discriminate He-weak objects from He-rich stars.

In most cases a fair agreement with former studies was found, but for the group of CP4 the temperature was slightly overestimated until now, influencing all former evolutionary studies (see Fig. 2.15). Previous investigations suggested the e.g. the direct use of the *Geneva X/Y* temperatures.

It is obvious that the accuracy strongly depends on the availability of data in the various photometric systems. Especially for cooler stars without Strömgren data, the determination of individual reddening values is rather difficult. Certainly, one can use

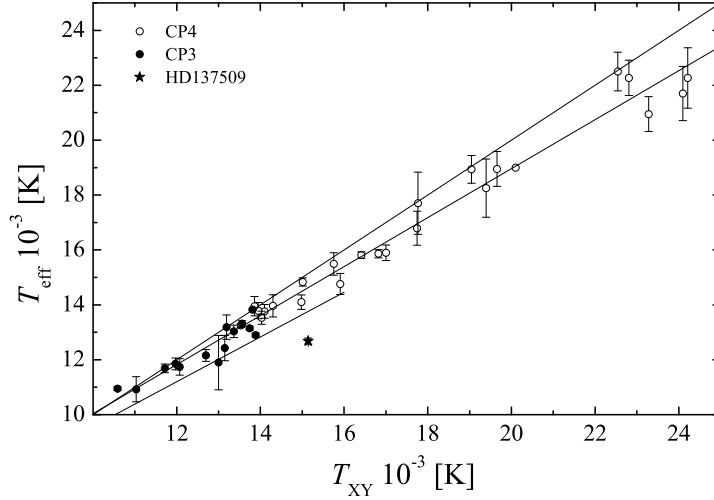


Figure 2.15: The corrections for CP3 and CP4 objects based on Geneva photometry by Netopil et al. (2008). The upper line shows the one-to-one relation, the middle line the determined fit, and the lower one the CP2 relation as comparison. Furthermore, the position of the strong magnetic star HD 137509 is given.

e.g. the mean open cluster reddening, but if these exhibit a differential reddening, the resulting temperatures are erroneous. Additionally, for most (distant) clusters in general only $(B - V)$ measurements are available for the temperature determination of the CP stars. We therefore made use of additional data in other passbands such as Bessell I and R , as well as near infrared 2MASS JHK_s measurements (Cutri et al., 2003), in order to fit the spectral energy distribution (SED). For this purpose we applied the tool provided by Robitaille et al. (2007), which allows to set reddening as free parameter. However, using the mean cluster reddening, a constraint of that parameter is already given. This approach for the determination of temperatures for CP stars was already presented by Wraight et al. (2011), where we defined a correction of the SED results, which takes into account the abnormal colours of CP stars.

$$T_{\text{eff}} = 1032(167) \text{ [K]} + 0.873(16) T_{\text{SED}} \text{ [K]}$$

In total, 62 CP2 objects out of 72 calibrated ones taken from the list by Netopil et al. (2008) was used to determine the necessary correction. As can be seen in Fig. 2.16, some stars exhibit strong deviations. Most of these objects can be also found in Table 3 of the work by Netopil et al. (2008), which lists the strongest deviating stars if comparing spectroscopic temperatures and the corrected photometric ones. The stars HD 26571, HD 37470, HD 133880, HD 157751, as well as HD 215441 coincide with the above mentioned list and are showing also deviations in the SED analysis of more than 1000 K. Except the first star, all of them were already investigated concerning magnetic field strength. However, it is difficult to conclude about the influence of the magnetic field strength on the temperature deviations noticed above. Whereas for HD 215441 (Babcock's star) one of the strongest magnetic field was measured so far, the object HD 37470 exhibit hardly a magnetic field (a non-detection was presented by Bagnulo et

al. (2006)). Another possibility for the discrepancy can be the degree of “peculiarity”, in the sense that these objects show stronger overabundances compared to the majority of the CP stars such as HD 101065 (see discussion in the following). Unfortunately, there is no detailed abundance analysis available for these stars so far. Finally, except for HD 133880, in each case there is only a single temperature determination available as listed in Netopil et al. (2008). Hence, faulty results can be an additional possibility for the large deviations.

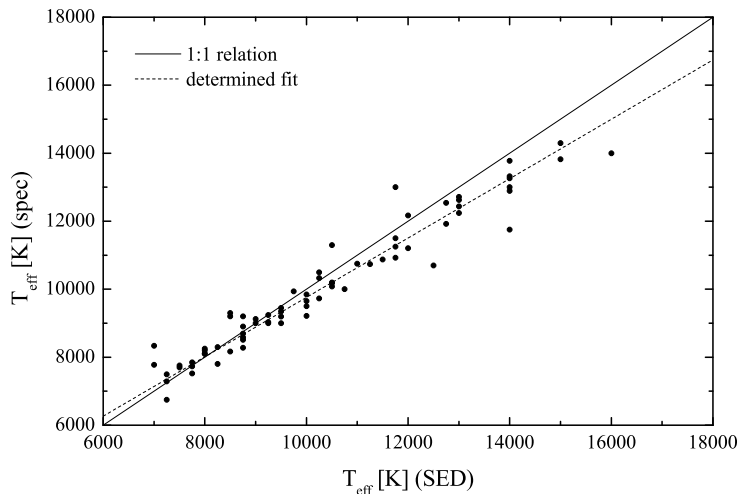


Figure 2.16: The temperatures for CP2 stars deduced using SED fitting compared to spectroscopic temperatures.

To investigate the extent of the above mentioned “blueing effect” in more detail, we have made use of the temperature compilation for CP2 and CP4 stars by Netopil et al. (2008), in addition to temperatures of some further cool roAp stars taken from the literature. In contrast to the latter reference, a back calculation to the colour index ($B - V$) was performed by using the CP temperatures and established calibrations (Flower, 1996) for normal stars. We made use of the work by Harmanec & Božić (2001), which provides transformations between the UBV , *Geneva*, and Strömgren photometric systems, to calculate a mean ($B - V$) colour index for the CP objects based on the three photometric systems to exclude a possible erroneous standardization within a single system, resulting in standard deviations below 0.02 mag for the majority of the stars. The result as a function of temperature can be found in Fig. 2.17. Hotter CP2 stars (>9500 K) compared to normal stars of same temperature exhibit bluer colour indices of about 0.05 mag, whereas the effect diminishes for cooler and hotter ones, respectively. The cool CP stars seem to appear even redder. That can be either the result of a wrong reddening estimate, since for cooler objects (later than spectral type A0) only Strömgren photometry offers a reasonable possibility for such a determination. Furthermore, there is also the possibility of a systematic error in the temperatures what can be responsible for the redder appearance. Bruntt et al. (2008) have determined for the first time the temperature of the cool CP object α Circini by

means of angular diameter measurements and bolometric correction. They obtained a value ~ 500 K lower than previously available spectroscopic results. However, more studies in this respect are necessary for a meaningful conclusion. It can be noticed in Fig. 2.17 that the coolest object - HD 101065, also called Przybylski's star - deviates significantly. It is probably the most peculiar object known so far, investigated recently by Shulyak et al. (2010). They have shown that especially the observed Strömgren $c1$ colour index can not be reproduced well using theoretical models, which influences also e.g. the reddening calibration.

In contrast to the CP2 stars, the He-weak objects (CP4) are not suspicious in Fig. 2.17, showing even a marginal redder colour index compared to normal stars. As mentioned already above, the work by Netopil et al. (2008) proposed an overestimate of the photometric temperature (using a calibration for normal stars) of some hundreds K also for this star group (see also Fig. 2.15). That can be also noticed, if comparing the Q -index temperature relation for normal stars (presented in Sect. 6.1 and Fig. 6.6) with the one for CP stars given in Table 2.1. The differences are similar to those for *Geneva* photometry (Fig. 2.15). However, considering a star with temperature of about 12000 K, the corrections transformed to a $\Delta(B - V)$ results in only about -0.01 mag. Furthermore, on the one hand a shift of the “blueing” more to the Ultraviolet (UV) region or an underestimate of reddening via the photometric calibrations can be responsible, on the other hand a slight offset of the photometric scale/zero point by Flower (1996) can not be excluded. If compared to the relations (equations 11) given by Napiwotzki et al. (1993), the offset to Flower (1996) for the hotter CP4 stars are of the order of ~ 0.01 mag, placing them around zero or slightly below.

However, looking at Fig. 2.17 one can conclude that CP4 stars follow the sequence of CP2 representatives not only in the temperature domain, but also with respect to the blueing. Although the effect is in principle rather small, it has to be also taken into account, if the colour-magnitude-diagram is the only possibility for a membership analysis of CP stars in open clusters, but the marginal deviation from the main sequence will probably not be recognizable in the typical scatter of individual colour-magnitude-diagrams.

To be able to determine also the luminosity properly, we have furthermore presented in Netopil et al. (2008) a new calibration for the bolometric correction of CP stars. For this undertaking we have made use of the available literature to compile integrated fluxes F_t for stars in our sample. Using a total sample of 42 magnetic peculiar objects we have calculated the following relation depending on temperature

$$BC = -5.737 + 18.685\theta_{\text{eff}} - 15.135\theta_{\text{eff}}^2$$

which is valid for the temperature range 7500–19000 K. Using this estimation, errors of ~ 0.1 and 0.15 mag have to be adopted for stars cooler or hotter than 14000 K. The results are illustrated in Fig. 2.18. A comparison to other recent studies in this respect (Lipski & Stępień, 2008; Landstreet et al., 2007) shows a rather good agreement with the latter reference at least for objects cooler than 14000 K. The deviation for hotter ones can be explained by their use of photometrically determined temperatures and the non-use of corrections for hotter (CP4) stars. The study by Lipski & Stępień (2008) deviates to ours over a rather large temperature range. They have used their

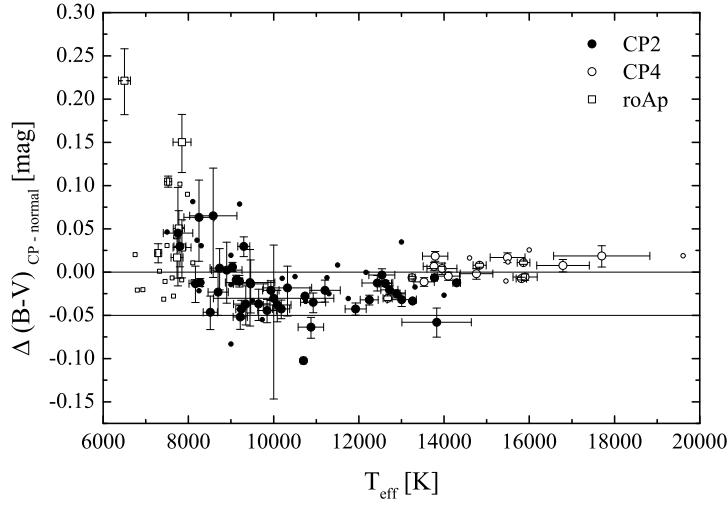


Figure 2.17: The “blueing effect” of CP2 (filled circles) and CP4 (open circles) objects as a function of temperature. Additionally, the group of roAp stars is given separately as open squares. Smaller symbols indicates that only one fundamental temperature is available. The lower vertical line represents the typical maximal blueing of 0.05 mag. The error bars correspond to the standard deviation of the averaged temperatures and the resulting errors for the colour indices.

own data for the presented relation, but the obtained temperatures are somewhat too low compared to others. Furthermore, they assumed a non-reddening for several stars. The differences to relations for normal stars like Balona (1994) or Flower (1996) do not exceed 0.1 mag. This result is considerable lower than the one obtained by Lanz (1984), who has presented a relation based on the *Geneva* colour index ($B2 - G$). His study revealed a difference to normal stars of up to 0.3 mag. Finally, Netopil et al. (2008) have shown that standard calibrations for the investigated photometric systems can be used to deduce interstellar reddening at a reasonable accuracy (~ 0.02 mag). All these results above allow to determine the position of CP objects in the HRD at highest possible precision and hence the estimation of masses using evolutionary models.

Table 2.1: The temperature calibrations for the individual CP groups and photometric systems determined by Netopil et al. (2008).

CP Type	System	Relation	Errors ^a	Restriction
CP1	<i>UBV</i>	$\theta_{\text{eff}} = 0.527 + 0.515(B - V)_0$	0.003/0.013	$-0.160 \leq (B2 - V1)_0 \leq +0.730$ $(B2 - V1)_0 < -0.160$
	<i>Geneva</i>	$\theta_{\text{eff}} = 0.632 + 0.640(B2 - V1)_0$ ^b direct use of T_{XY}		
CP2	<i>UBV</i>	direct use of $T_{uvby\beta}$		
		$\theta_{\text{eff}} = 0.541 + 0.389Q$	0.004/0.014	$T_{\text{eff}} \gtrsim 9000$
		$\theta_{\text{eff}} = 0.572 + 1.177(B - V)_0$	0.011/0.089	$-0.20 \leq (B - V)_0 \leq -0.05$
	<i>Geneva</i>	$\theta_{\text{eff}} = 0.542 + 0.388(B - V)_0$	0.005/0.030	$-0.05 \leq (B - V)_0 \leq 0.40$
		$\theta_{\text{eff}} = 0.835 + 0.458(B2 - G)_0$ ^c		$T_{\text{eff}} \lesssim 9000$
		$T_{\text{eff}} = 1420 + 0.815T_{XY}$	280/0.023	$T_{\text{eff}} \gtrsim 9000$
<i>uvbyβ</i>	direct use of $T_{uvby\beta}$		$T_{uvby\beta} < 9000$	
	$T_{\text{eff}} = 2090 + 0.756T_{uvby\beta}$	300/0.025	$T_{uvby\beta} \geq 9000$	
	$\theta_{\text{eff}} = 0.234 + 0.213[u - b]$	0.009/0.008	$T_{\text{eff}} \gtrsim 9000$	
CP3/4	<i>Geneva</i>	$T_{\text{eff}} = 1120 + 0.892T_{XY}$	350/0.021	
CP3/4	<i>uvbyβ</i>	$T_{\text{eff}} = 2230 + 0.809T_{uvby\beta}$	300/0.018	
CP3a	<i>UBV</i>	$\theta_{\text{eff}} = 0.501 + 0.323Q$	0.007/0.026	
	<i>uvbyβ</i>	$\theta_{\text{eff}} = 0.233 + 0.196[u - b]$	0.014/0.014	
CP3b/4	<i>UBV</i>	$\theta_{\text{eff}} = 0.540 + 0.418Q$	0.009/0.017	
	<i>uvbyβ</i>	$\theta_{\text{eff}} = 0.173 + 0.286[u - b]$	0.005/0.008	

^aErrors of the linear fits

^btaken from Hauck (1985)

^ctaken from Hauck & North (1982)

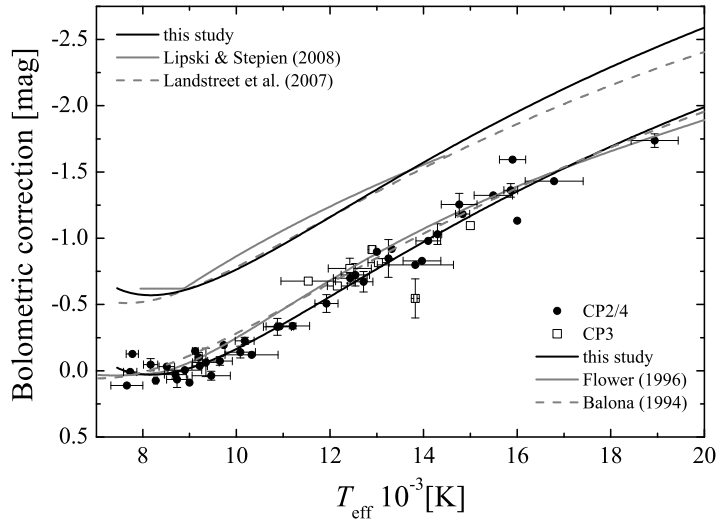


Figure 2.18: The bolometric corrections for CP2/4 objects by Netopil et al. (2008). There is only data for a few CP3 stars available, insufficient to conclude about their behaviour.

Chapter 3

Detection of chemically peculiar stars

The most conclusive way to detect chemically peculiar stars is by means of spectroscopic studies. In principle, low (classification) resolution with $R \sim 2000$ is sufficient for a proper classification into the various CP groups as performed recently by Paunzen et al. (2011c). However, also photometric investigations allow their detection. Beside using *Geneva* photometry or Strömgen data (see e.g. Masana et al., 1998), also the Δa photometric system is able to detect especially the magnetic CP2 and CP4 stars.

The Δa photometric system was introduced by Maitzen (1976) to detect chemically peculiar stars in an economic and efficient way. One can imagine that a survey by means of spectroscopy would be a very time consuming task. Furthermore, the limiting magnitude would prevent an investigation of more distant objects. A photometric detection method offers therefore an easy possibility to extend a rather volume limited sample. The characteristics of the filters were adjusted with time to be more efficient, the most recent filter sets are defined as listed in Table 3.1; the filter curves can be found in Fig. 3.1. At the beginning, the third filter (y) was taken over directly from the Strömgen system, and its designation remained afterwards due to “historical” reasons. An overview of the different used filter sets is presented by Paunzen et al. (2005b), where they have not found any systematic differences between the various measurements.

The system takes advantage of the characteristic flux depression at $\lambda 5200\text{\AA}$, which was first noticed by Kodaira (1969) in the spectra of the peculiar star HD 221568 beside other depressions at $\lambda 4200$ and 6300\AA . Similar effects were also found in the ultraviolet regions by Jamar (1977, 1978). All these features can be mostly noticed in (magnetic) CP stars, the most conspicuous and usable turned out to be the one at

Table 3.1: The characteristics of the recent Δa filter set.

Filter	Central wavelength [\AA]	FWHM [\AA]
g_1	5010	130
g_2	5200	130
y	5470	130

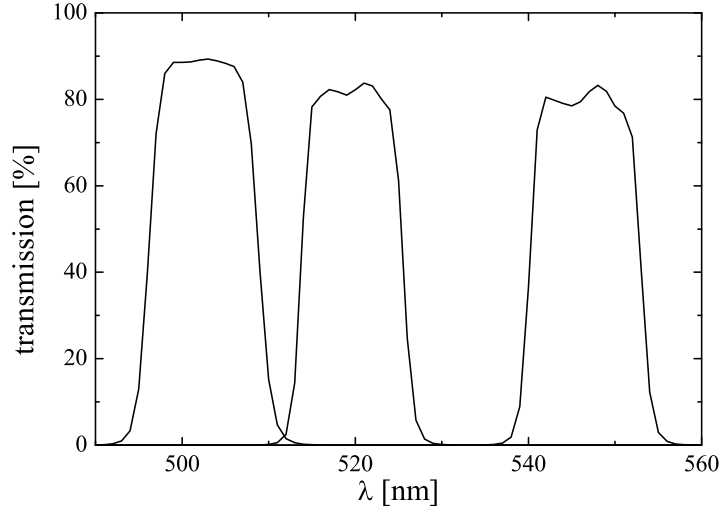


Figure 3.1: The filter curves of the most recent Δa system, produced by Custom Scientific in 2005.

5200Å. By measuring its flux depth compared to the adjacent regions, the resulting Δa index can be easily calculated as

$$a = g_2 - \frac{g_1 + y}{2}$$

$$\Delta a = a - a_0,$$

where a_0 is called the “normality line”, presenting the a -values of non-peculiar objects. Therefore, Δa gives the difference between the individual a -values and those of non-peculiar objects of the same colour.

Since for this quantity there is a slight dependency with temperature (increase towards lower temperature / larger colour) the peculiarity index has to be defined as

$$\Delta a = a - a_0[(b - y), (B - V), (g_1 - y)].$$

In Fig. 3.2 one can see an example of a Δa diagnostic diagram for the open cluster Ruprecht 115 taken from Netopil et al. (2007). Magnetic chemically peculiar objects (CP2 and CP4) show a positive Δa index, whereas for example emission line (Be/Ae objects) or λ Bootis stars exhibit a negative one (see also Fig. 3.3). In case of Be/Ae stars, the observed negative values are very probably due to emission of iron and magnesium lines in the domain of the g_2 filter (see e.g. Paunzen et al., 2005b), whereas those of λ Bootis stars are a result of strong underabundances of the iron peak elements (Kupka et al., 2004).

The close correlation of the colour index $(g_1 - y)$ with other colour indices such as Strömgen $(b - y)$ or Johnson $(B - V)$ allows also the transformation into these systems and hence an estimate of temperature. The works by Paunzen et al. (2005a) and Paunzen et al. (2006c) presented e.g. effective temperature calibrations for B to F type stars by using the $(g_1 - y)$ index. However, for this purpose photometric zero

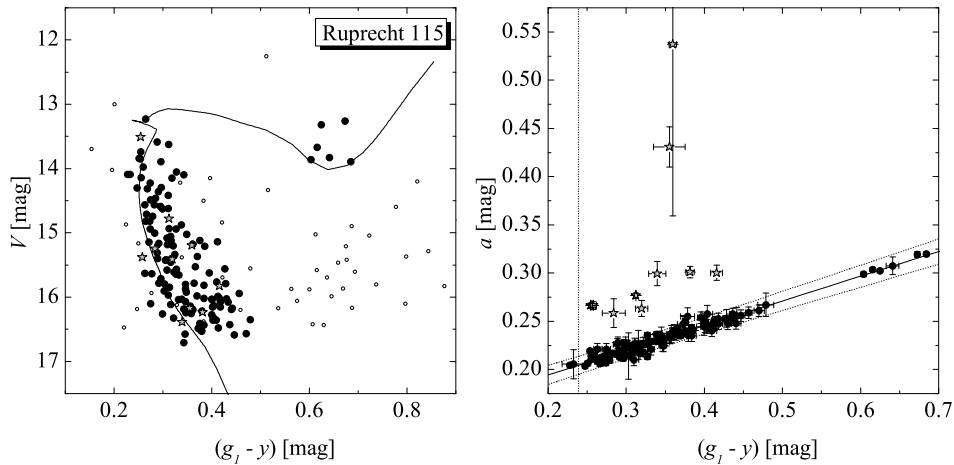


Figure 3.2: The CMD (left panel) and diagnostic Δa diagram (right panel) for the open cluster Ruprecht 115 taken from Netopil et al. (2007). The isochrone for an age of $\log t = 8.6$ is over plotted. In the right panel, the vertical line represents the transformed position of spectral type A0. The detected chemically peculiar objects are shown with star symbols, non-members with small open circles.

points have to be determined, which implies that at least some comparative values in other photometric systems are available.

At the very beginning, Δa was applied in the photoelectric technique, but the very first approach to switch to CCDs was performed by Maitzen et al. (1997) by means of 22 CP2 stars in the galactic field. Later on, the first CCD results on the open clusters NGC 2169, Melotte 105 and NGC 6250 were presented by Bayer et al. (2000), showing an excellent agreement with the photoelectric measurements by Maitzen (1993) for NGC 2169. Further comparisons were made afterwards for the open clusters NGC 6405 and NGC 3114 which confirm the capability of the CCD Δa technique.

Beside the economic way to detect CP candidates via photometry, another big advantage is that comparison (normal) stars - essential to calculate the normality line - are always on the same frame. Therefore, standard field observations are not necessary, which allows also observations at non-photometric (in traditional sense) conditions. Furthermore, observations in all three filters have not to be accomplished within one night. Beside different zero points of a_0 , even different instruments have no effect on the results. Until now, the Δa system was in use at 17 different telescopes to go from several instruments at ESO La Silla Observatory to CASLEO (Argentina), Rozhen (Bulgaria), Sierra Nevada (Spain), or Hvar Observatory (Croatia).

The next improvement was made by the work of Claret et al. (2003), who introduced also isochrones for Δa . Thence it was possible to determine independently the important open cluster parameters age, distance, and reddening on the Δa system alone. The isochrones were applied already to 23 open clusters, published in four works (the most recent one by Netopil et al., 2007). The comparison of the results with literature values shows very good agreement.

Since Kupka et al. (2003) have shown by means of models of synthetic Δa photom-

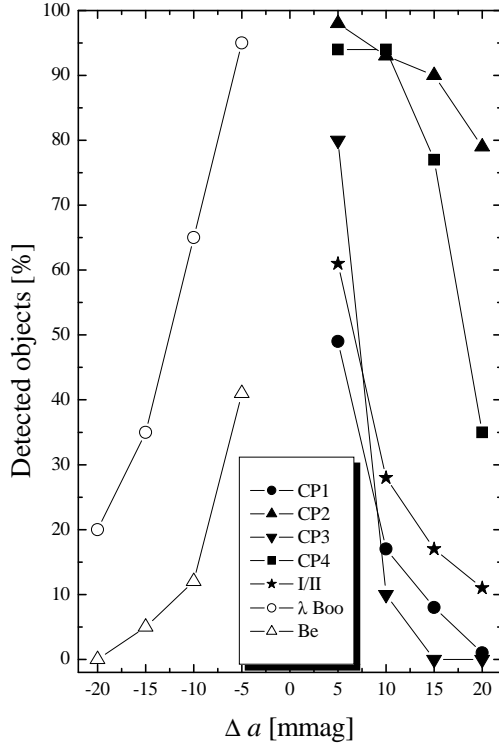


Figure 3.3: The detection probability of the Δa system for various peculiar groups as a function of the detection limit investigated by Paunzen et al. (2005b). Additionally, the group of supergiants (luminosity class I/II) is also given (see the latter reference for details), which can be easily distinguished from classical CP stars by their photometric properties.

etry, that different environments (metallicities) have hardly any influence on Δa , this system can be also safely used in other environments like globular clusters or even in the Magellanic Clouds. We have already presented studies in this respect, Paunzen et al. (2006a) is the currently last investigation summarizing the CP content in the Large Magellanic Cloud (LMC) by means of several studied clusters and a comparison field. They derived an occurrence of classical chemically peculiar stars of 2.2(6)%, a value considerably lower than assumed for the Milky Way.

Paunzen et al. (2005b) explored the detection capability of the Δa system. They compiled all measurements for 1474 galactic field stars and found an efficiency of up to 95% (depending on the detection limit) to detect all relevant magnetic CP objects. It is also possible to detect a smaller percentage of non-magnetic chemically peculiar objects or Be/shell stars, as well as the group of metal weak λ Bootis objects, as can be seen in Fig. 3.3. Based on this investigation, it would be possible to derive the former unknown bias of undetected CP candidates. However, they have not presented an efficiency taking into account various temperatures/masses or ages of CP stars, necessary for a correct application of the bias of undetected stars.

Several works studied the flux depression and the Δa photometric system on a theoretical basis (e.g. Kupka et al., 2003, 2004). They were able to reproduce observed Δa values with computed model atmospheres, taking into account individual abundances for a sample of stars. At least for cool CP2 objects they correspond within a few mmag, but for somewhat hotter representatives (~ 9000 K) with rather large Δa , the models underestimate the peculiarity index significantly by ~ 30 mmag. They concluded that it is probably caused by the limitation of the available stellar atmospheres.

Later on, Kochukhov et al. (2005) presented new stellar model atmospheres with

magnetic line blanketing, where they investigated also the behaviour of Δa considering the magnetic field strength for various metallicities. They noticed especially for the cool model (8000 K) a significant influence of the field strength on the Δa values, which amounts up to 65 mmag if comparing a 40 kG model with a non magnetic one. They also recognized an increase of Δa with increasing metallicity for all three temperature models (8000, 11000, and 15000 K), as well as a further rise of Δa , if taking into account a high Cr overabundance of +2.0 dex.

In a follow up paper, Khan & Shulyak (2006) confirmed the sensitivity of Δa to the magnetic field, but at a much lower level (less than 30 to 50 % compared to Kochukhov et al., 2005), but they did not reconfirm the influence of metallicity for the 8000 K model. They found that no peculiarity parameters (Δa and the *Geneva* ones, for the latter see below) are showing a linear trend in respect to magnetic field strength (except Δa for the 8000 K model).

Finally, Khan & Shulyak (2007) investigated the contribution of individual elements on the 5200 Å flux depression and hence on Δa . In agreement with the previous studies they conclude that Fe is mainly responsible for it, but also Cr and Si are major contributors at least for lower effective temperatures, which explains positive Δa values for magnetic CP stars, and negative ones for e.g. the λ Bootis stars, which exhibit underabundances of Fe-peak elements. Hence, the Δa values are affected by the effective temperature, individual abundances, as well as by the magnetic field strength. An application of the new model atmospheres was done e.g. by Shulyak, Kochukhov, & Khan (2008) for the strong magnetic star HD 137509 (29 kG). Under consideration of all properties, they were able to reproduce the observed large Δa of +66 mmag within a few mmag (+62 mmag). If neglecting the magnetic field, the value would be significantly lower (+37 mmag).

Since Ryabchikova (2005) presented also an observational evidence of the strong temperature dependency for the elements Fe and Cr, and these are mainly responsible for the degree of Δa , it is worth to do such a presentation also for the photometric peculiarity index. We therefore used the list of the latter reference as a starting point, and updated it with the recent literature. If more investigations are available for one object, an average of the abundances were derived. In total, we compiled abundances of the major elements for 87 magnetic chemically peculiar objects, nearly doubled compared to the compilation by Ryabchikova (2005). If averaged effective temperatures are available in the lists by Netopil et al. (2008), these were adopted, otherwise we used the values given in the respective references. Unfortunately, for only 50 stars observed Δa values are available. We therefore included also *Geneva* photometry, which offers the index $\Delta(V1 - G)$ (Hauck, 1974) or Z (Cramer & Maeder, 1979) as peculiar parameter, whereas the latter is due to a temperature dependency only safely applicable for stars hotter than about 10000 K. For completeness, their definition is given below:

$$\Delta(V1 - G) = (V1 - G) - 0.289(B2 - G) + 0.302$$

$$Z = -0.4572 + 0.0255 U - 0.174 B1 + 0.4696 B2 - 1.1205 V1 + 0.7994 G$$

Due to the temperature dependency of the Z index, in the following we consider

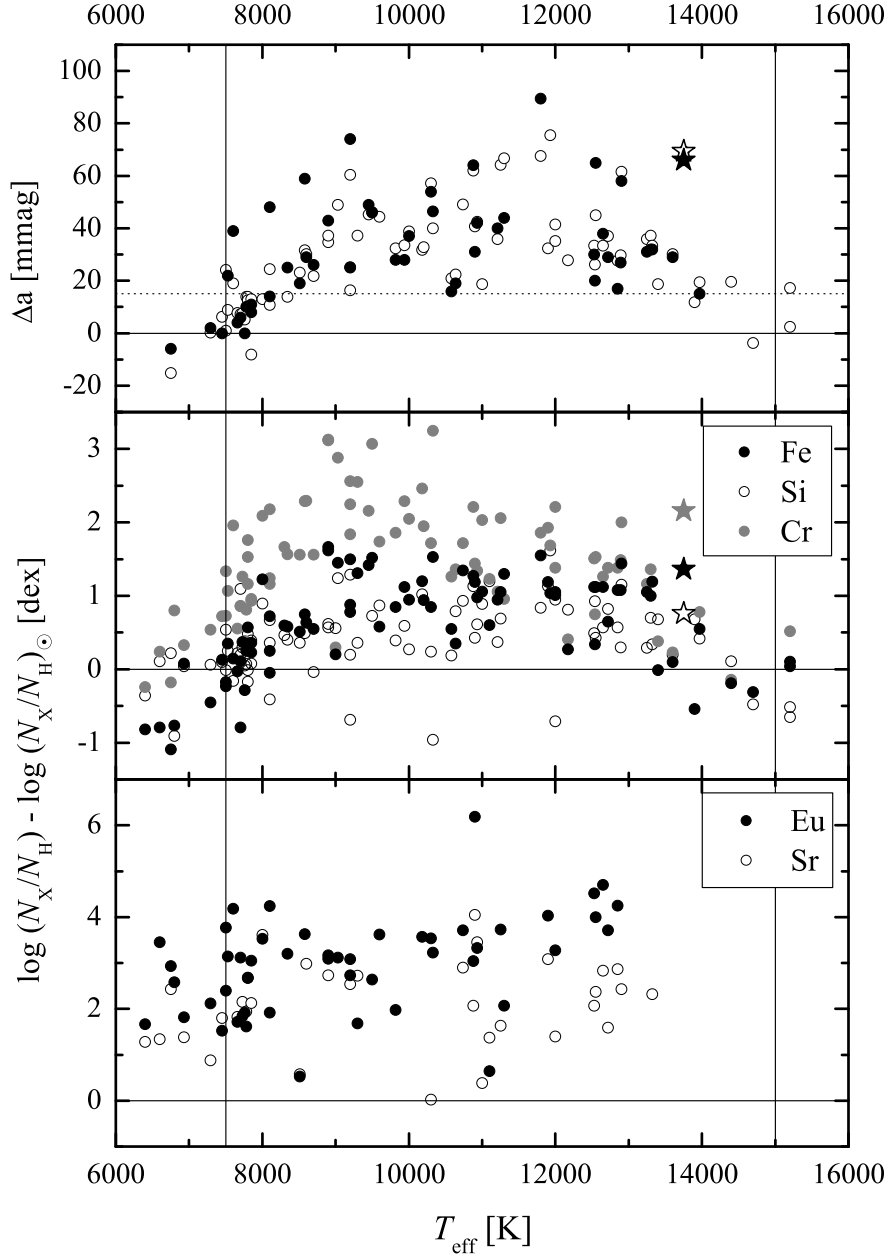


Figure 3.4: Temperature dependency of $\Delta a / \Delta(V1-G)$ and abundances of some selected elements. In the upper panel the black circles represent direct Δa measurements, whereas open circles are *Geneva* $\Delta(V1-G)$ values shifted by +15 mmag in order to bring them on the scale of Δa . The solid lines indicate the zero point of Δa at ~ 7400 K and the dotted line a Δa limit of +15 mmag. The position of the strong magnetic star HD 137509 is given with star symbols (see discussion in the text).

only $\Delta(V1 - G)$. In contrast to Δa this index does not measure the 5200 Å depression directly, since the filters $V1$ and G are shifted somewhat to the red. Furthermore, since these are much broader filters, they are not that sensitive on specific spectral features such as Cr (Khan & Shulyak, 2006). This index was also investigated by Paunzen et al. (2005b), showing a similar efficiency like Δa to detect magnetic chemically peculiar stars. If comparing these two peculiarity indices, one can notice a linear relationship with an offset of ~ 15 mmag, in the sense that $\Delta(V1 - G)$ is somewhat lower. Whereas normal stars or metallic line Am stars in the latter index mostly do not exceed 0 mmag, in Δa especially Am stars can also show slight positive values.

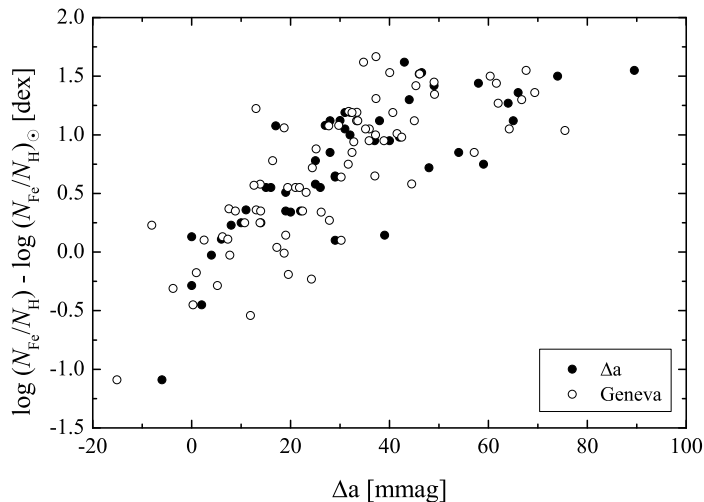


Figure 3.5: The photometric peculiarity indices Δa and $\Delta(V1 - G)$ compared to iron abundances. Again, *Geneva* $\Delta(V1 - G)$ values were shifted by +15 mmag in order to bring them approximately on the scale of Δa .

Although due to the different sensitivity of these two peculiarity indices on specific spectral features, a direct comparison should not be made, we applied the offset mentioned above to the $\Delta(V1 - G)$ values to obtain a comparable peculiar index for all objects, which is presented in Fig. 3.4. The upper panel shows the temperature dependency of the photometric indices, whereas the others the dependency of selected elements. The good agreement between Fe and the peculiar indices can be easily recognized also in Fig. 3.5, supporting the conclusion by Khan & Shulyak (2007) that Fe is the main contributor to the flux depression at 5200 Å and hence for positive Δa values. Its “zero point” is located at $T_{\text{eff}} \sim 7500$ K, coinciding also with solar Fe abundances, whereas the respective solar reference values were taken from Asplund et al. (2009). The hotter end is unfortunately not that good covered, but is roughly estimated at ~ 15000 K. However, Δa values can be designated as significant only at a level of $\gtrsim +15$ mmag, depending on the scatter of the normal stars (see e.g. Fig. 3.2), but also to avoid a mix up with members of the Am group. Some of these can even reach $\sim +20$ mmag, like three objects in the Praesepe cluster (HD 73618, HD 73709, and HD 73711), but these are rather exceptional ones in this respect. A confirmation of their Am characteristic was presented e.g. by Fossati et al. (2007).

Hence, taking into account a Δa level of +15 mmag, the temperature range decreases to ~ 8000 to 14000 K. Cooler or hotter stars will be detected probably only if excessive overabundances of e.g. Si or Cr are present and/or a rather strong magnetic field contributes to a larger Δa . The overall lower Δa values at higher temperatures can be also noticed in the models by Khan & Shulyak (2006). Nevertheless, in this temperature range all stars presented in Fig. 3.4 would have been unambiguously detected by its Δa measurement.

Since the elements are distributed inhomogeneously on the stellar surface, Fig. 3.4 is also affected in this respect. One can notice three stars (HD 8441, HD 22316, and HD 108662) in the middle temperature range, which exhibit even underabundant Si (about a factor 100 lower than the majority of stars). At least for one object of these (HD 108662; $T_{\text{eff}} = 10\,300$ K) a time resolved spectroscopic study was performed. Rice & Wehlau (1994) found that the abundances of iron and chromium vary by a factor of 100 going down to even a solar abundance value, but unfortunately they have not analysed also silicon in this respect. Hence, the available abundance analysis (see Ryabchikova, 2005) for this element was probably badly timed.

Due to these variations also Δa measurements are very probably influenced. Unfortunately, so far no dedicated photometric time series are available, but for some stars at least a few observing runs are available. However, as mentioned above, the filter sets varied slightly in time, making a conclusion about a possible dependency difficult. For the object HD 108662 (see above) also two Δa measurements are available. Maitzen (1976) list +50 mmag, whereas Maitzen & Pavlovski (1987b) presented a only slighter value of +43 mmag. One of the largest differences of Δa can be found for the star HD 188041: +59 and +90 mmag (by Maitzen, 1976; Maitzen & Seggewiss, 1980, respectively). For the presentation in Fig. 3.4 we adopted only the lower value, and even this is rather outstanding (at $T_{\text{eff}} = 8\,580$ K) thanks to the chromium overabundance (like most of the deviating stars). For this object it would be therefore desirable to obtain timeseries with Δa and high-resolution spectroscopy.

The efficiency of Δa was proven already by several works (theoretical as well as by observations). However, a spectroscopic re-investigation of the photometric peculiar candidates is always desirable, as was presented e.g. by Paunzen et al. (2011a) with the first spectroscopic confirmation of a classical Si CP star in the LMC (Fig. 3.6), which was previously detected with Δa photometry. Beside this star, also an emission object was confirmed, detected by its negative Δa index. This study proves that Δa can be used confidently also in other environments than the Milky Way.

3.1 Classification spectroscopy

Additional spectroscopic classifications for some with Δa selected CP candidates were presented by Paunzen et al. (2011c). They investigated 23 open cluster stars down to about 14^{th} magnitude, of which only one star turned out to be of normal type (A1V for NGC 6475 #23, although showing a Δa of +20 mmag). In the following we present some further objects (nine in total) with classification resolution spectra ($\sim 2\text{\AA}/\text{px}$) obtained at the CASLEO (May 11-14th 2012 by O. I. Pintado) and ROZHEN (August

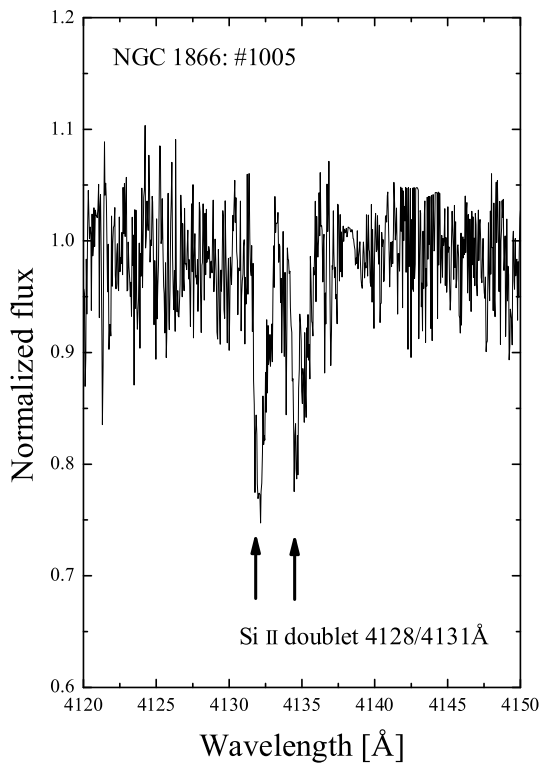


Figure 3.6: Spectroscopic confirmation of an extragalactic CP star by Paunzen et al. (2011a). The measured equivalent widths of the Si doublet ($\sim 0.3 \text{ \AA}$) are about two times larger compared to normal late B type stars.

17/18th 2012 by I. Kh. Iliev) observatories in Argentina and Bulgaria, respectively. After the basic IRAF¹ reductions, including normalization, they were classified analogous as given in the reference above, based on a refined Morgan-Keenan system (Gray & Garrison, 1987, 1989a,b). The results can be found in Figs. 3.7 and 3.8 as well as in Table 3.2.

For two objects classified as peculiar, the combination of photometry and kinematic data suggest a non-membership (Collinder 140 #60 and NGC 3114 #184). Both are probable background stars of the rather close ($< 1000 \text{ pc}$) and hardly reddened open clusters.

Two programme objects turned out to be foreground stars of normal type (NGC 6830 #38 and NGC 2546 #258), whereas for the latter erroneous photometry resulted in a positive Δa index (see Sect. 5.1.24), the other star is located in front of a rather reddened cluster ($E(B - V) = 0.51$). Due to the lower reddening of the assumed CP candidate it mimics a positive Δa . Such a behaviour was also concluded for candidates in e.g. NGC 5999 (see Sect. 5.3.9). The spectroscopic data confirm the (probable) non-membership based on photometry and kinematic data. Using the spectral types as additional criteria, a definite non-membership was therefore adopted for both stars.

In the open cluster Melotte 105 two objects with a rather marginal Δa were investigated (see Table 3.2). Whereas one was classified at least as weak Si star, the spectrum of the other star is completely inconspicuous. Unfortunately, the other two CP candidates in this cluster are too faint ($\sim 14.8 \text{ mag}$) to be observed with the used 2m class telescopes.

¹<http://iraf.noao.edu/>

Table 3.2: Spectral classifications for some additional CP candidates based on data obtained at CASLEO (upper panel) and ROZHEN observatory (lower panel).

Cluster	WEBDA #	V [mag]	Δa [mmag]	member ^a	Spec
Collinder 140	60	10.72	39	nm	A0 CrSrEu
NGC 2546	258	10.54	30	pnm	A7 V
NGC 3114	184	11.39	59	pnm	B9 Si
Melotte 105	107	13.15	15	pm	B9 Si
Melotte 105	133	13.48	17	pm	B9 V
NGC 1502	27	12.46	88	pm	B7 Si
NGC 7296	14	13.68	23	m	A0 Si
NGC 6830	38	13.04	38	nm	F8 V
NGC 6830	166	13.25	35	m	B8 Si

^amembership according photometric and kinematic data

Although the Δa system is efficient for the selection of CP stars, these results clearly show that an additional spectroscopic information is extremely useful, especially for more distant and high reddened clusters, where e.g. cooler foreground stars can influence a proper detection. Still, for numerous fainter CP candidates no spectra are available. The Chinese LAMOST project² has already started to obtain spectroscopic data (R=1800) within the galactic plane. The yet available pilot survey covers already several open clusters, but unfortunately without an overlap to our programme stars. Nevertheless, these data will allow a direct investigation of the peculiar incidence in open clusters without the intermediate step of Δa photometry. However, the first results have to be evaluated in respect of coverage and S/N at the fainter magnitude end.

²<http://www.lamost.org>

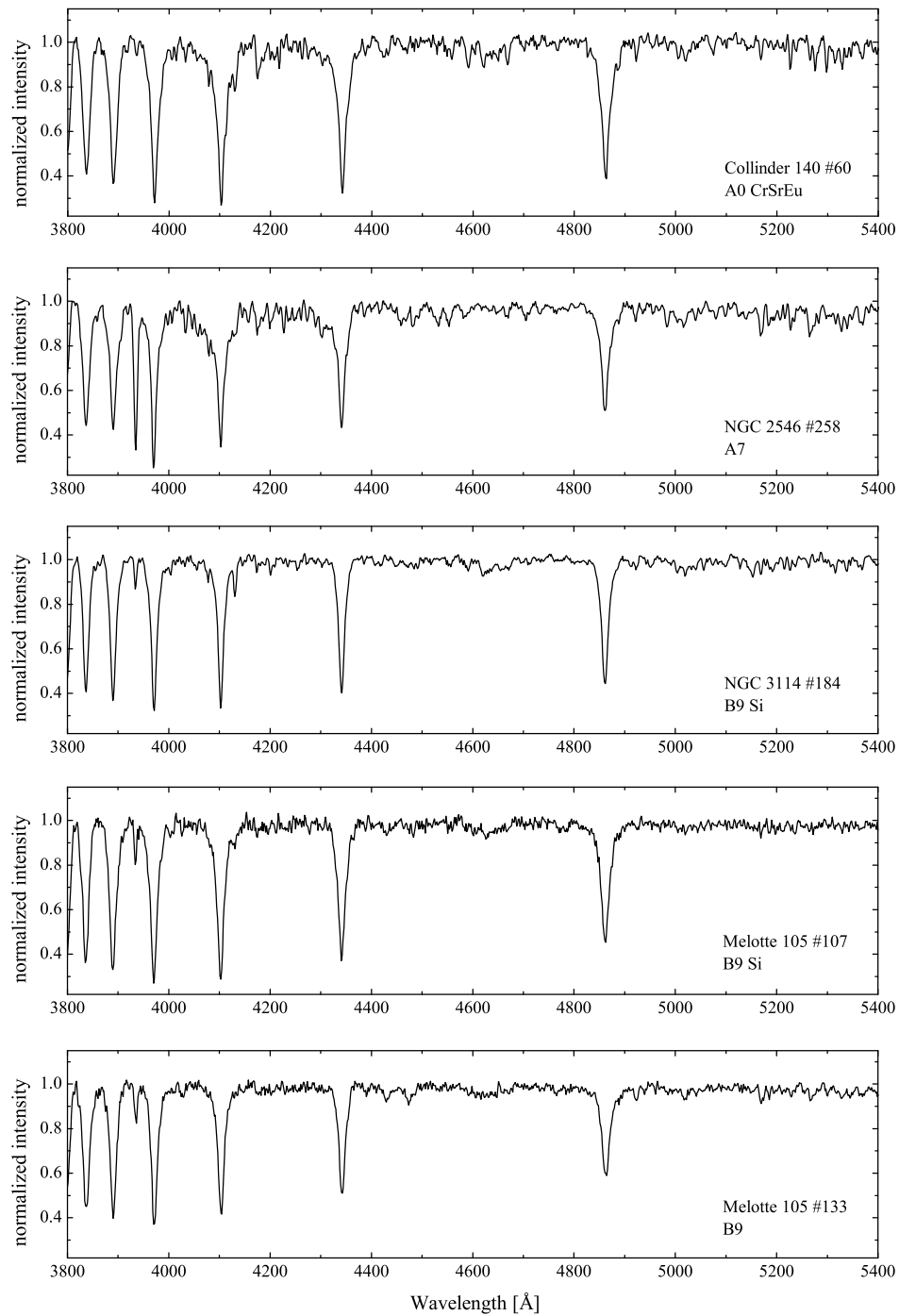


Figure 3.7: Classification resolution spectroscopy of some further open cluster CP candidates taken at CASLEO observatory.

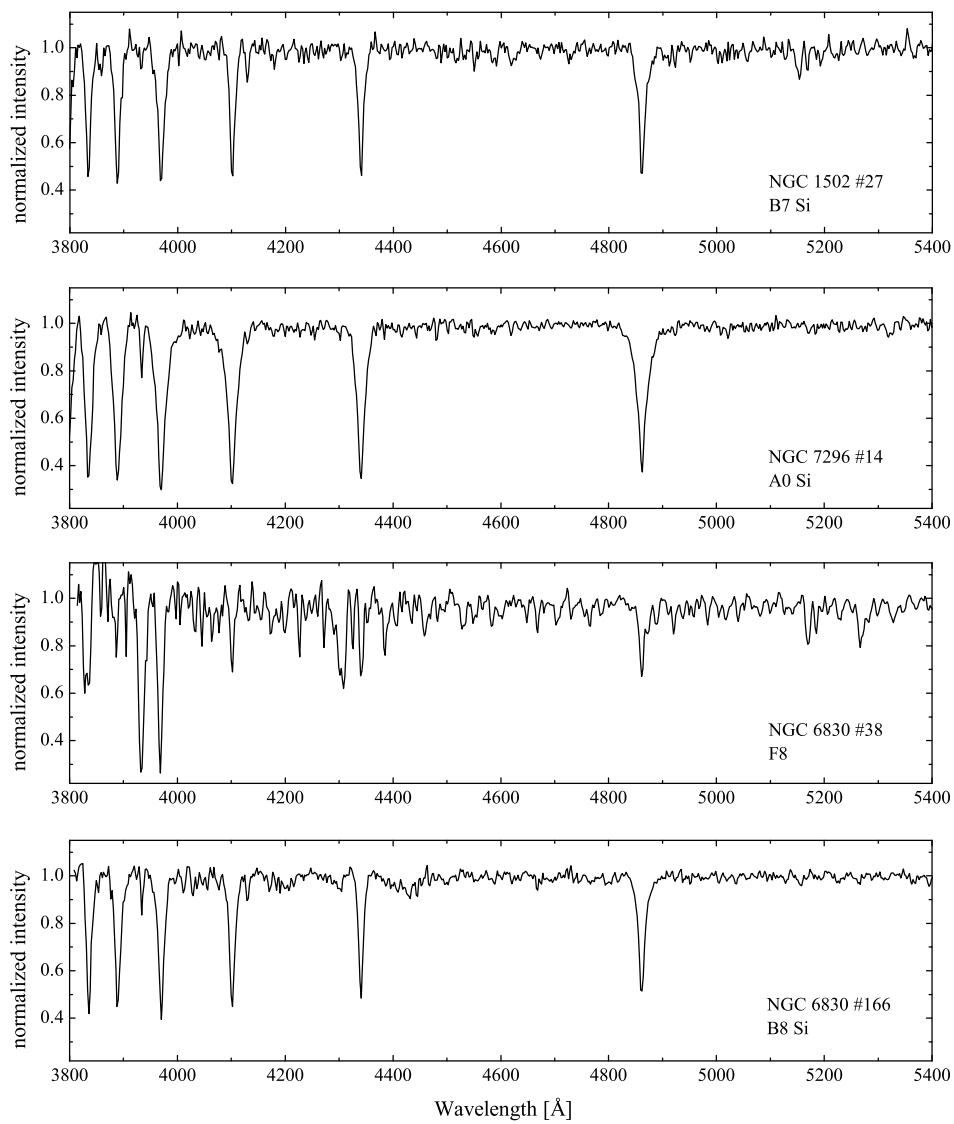


Figure 3.8: Classification resolution spectroscopy of some further open cluster CP candidates taken at ROZHEN observatory.

Chapter 4

Why studying open clusters?

Open clusters are an ideal astrophysical laboratory to study the content of several star groups, like chemically peculiar stars. They are physically related groups of stars held together by mutual gravitational attraction, populating a limited region in space which is normally much smaller than their distance. Hence, for all cluster stars the same distance can be assumed, which can be determined on a statistical basis over all members using for example the method of isochrone fitting. The same holds for the cluster/star age. Since the formation process takes only about a few million years - a short time compared to the cluster lifespan - all cluster stars are about the same age (excluding sequential star formation). They originate from large gas and dust clouds, which are predominantly homogeneous in their initial chemical composition. Therefore, the cluster metallicity represents also more or less the one of the individual member stars. Furthermore, open clusters exhibit member stars with different masses, ranging from about $120 M_{\odot}$ in very young aggregates to less than $\sim 0.08 M_{\odot}$.

Thus, all parameters within an open cluster are quite homogeneous. However, if investigating a large sample of different clusters, one can notice that the individual clusters span a wide variety of these parameters (distance, age, reddening, and metallicity), what can be seen in Fig. 4.1. These figures are based on the updated catalogue (version 3.2, 26th January 2012) of optically visible open clusters and candidates by Dias et al. (2002). Their list includes currently 2135 clusters or candidates together with the different known parameters. As can be deduced from the figures, ages and distances are known in some respects for a majority of the sample. Whereas distances are given for 1530 (72%) and ages for 1490 (70%) clusters, the knowledge of metallicity is available only for 189 (9%) aggregates. However, this compilation is certainly far from being complete and homogeneous, since the data were collected from several sources, but can serve for studies in a statistical way. As one can see in the Fig. 4.1, open clusters span an age range of 1 Myr to 10 Gyr, are found at distances between the immediate surrounding of the sun until ~ 15 kpc and offer the possibility to explore their star contents at environments (metallicities) in the range of $-0.9 \leq [\text{Fe}/\text{H}] \leq 0.5$.

In Fig. 4.2 the galactic distribution of the cluster sample is shown together with the spiral arm models by Hou et al. (2009). Different age groups are used to demonstrate the capability of young open clusters to trace the spiral arms of the Milky Way. Several approaches were made already in this respect (e.g. Janes & Adler, 1982; Dias & Lépine,

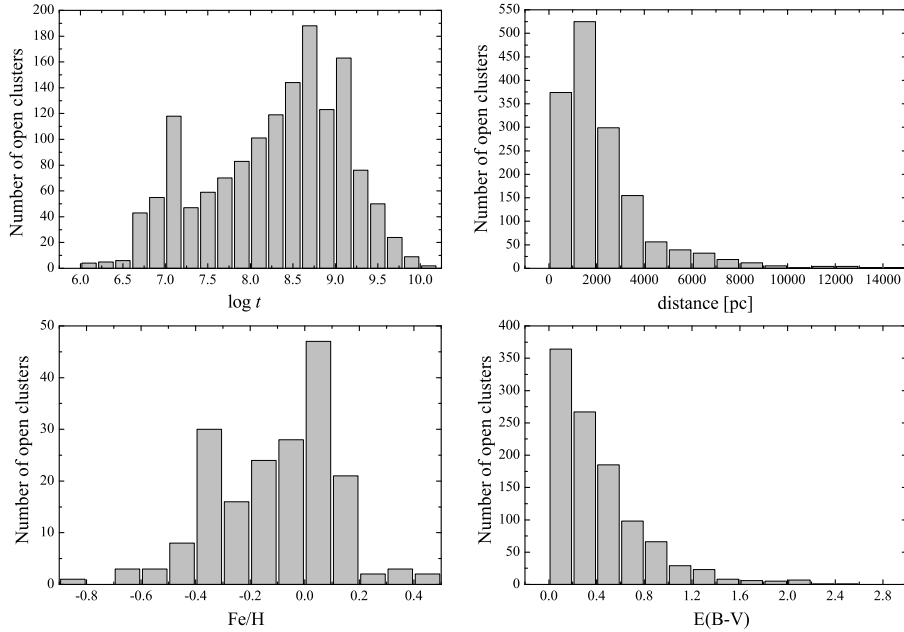


Figure 4.1: Distribution of age, distance, reddening, and metallicity of the clusters in the updated catalogue by Dias et al. (2002).

2005; Vázquez et al., 2008). Even the use of a compilation such as Dias et al. (2002) can help for such studies, but only in a statistical sense. If e.g. distance has to be used for individual cluster objects to calculate luminosity, a more homogeneous determination of distance (which also holds for all other parameters) is necessary. Due to interstellar extinction, the sample above is certainly limited. Within the galactic plane more distant clusters are hardly detected in the visual, they are hidden in the galactic field; other approaches are necessary to detect further ones. Froebrich et al. (2007) started to explore density maps obtained from the Two-Micron All-Sky Survey (2MASS) and found 1788 star cluster candidates, of which 767 turned out to be already known open or globular clusters. They conclude that only about 50% of the remaining ones are true cluster candidates. However, a verification in the optical passbands will be a difficult task - large telescopes and extremely long exposures are needed. It is expected that approximately 10000 open clusters are domiciled in the Milky Way.

All these facts clearly demonstrate that open clusters offer a unique possibility to study the evolution with age and/or galactic location of individual star groups, since most groups are present in clusters - also chemically peculiar objects. One can get for example age, distance, reddening, and metallicity more or less for “free”, necessary for a detailed study. With distance one is able to determine luminosity, together with effective temperature (for which the knowledge of reddening is important if this parameter is photometrically defined) the position in evolutionary diagrams can be calculated and hence the mass and age can be estimated, whereas for the latter a comparison with cluster age allows a further check of consistency. So, cluster stars allow an accurate investigation within different environments. Currently, by using parallaxes - for example those by the Hipparcos mission (Perryman et al., 1997) - one is limited

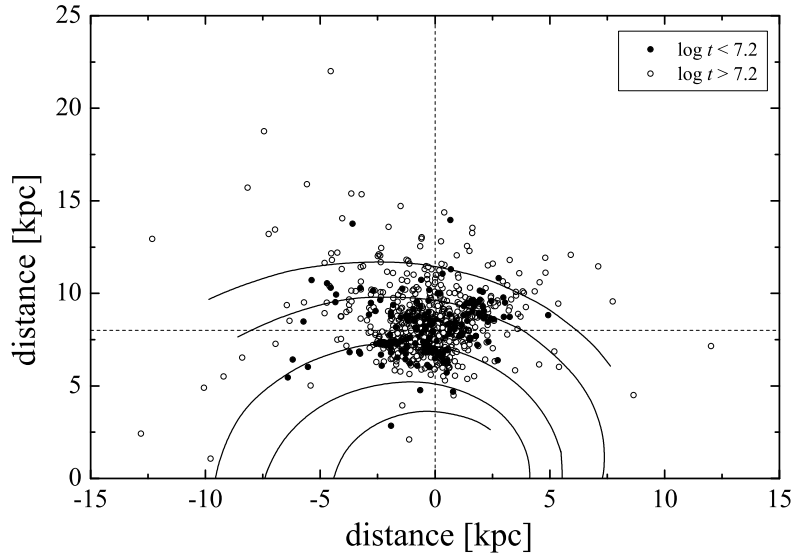


Figure 4.2: The positions of open clusters within the Milky Way by using the updated catalogue by Dias et al. (2002). Furthermore, the spiralarm models by Hou et al. (2009) are given. The galactic center is at 0/0, the position of the Sun at 0/8.0kpc. The youngest open clusters are highlighted to demonstrate their capability as spiral arm tracers.

to the immediate solar neighbourhood, but even there a further comparison with age is not possible if examining field stars. The forthcoming Gaia satellite mission will improve the knowledge of the outer area significantly. For cluster research the impact will be enormously, since a more detailed membership analysis is possible. Therefore, also e.g. the cluster ages can be determined very accurately.

4.1 Data compilation

With appearance of the CCD technique, the amount of photometric data for open clusters increased significantly. Unfortunately, most studies are using their own numbering system and do not provide equatorial coordinates, which makes a comparison of different works difficult. Furthermore, there is also the difficulty caused by the use of different filters, even within a single photometric system such as UBV . Not to mention errors resulting due to an erroneous standard transformation or correction of atmospheric extinction. In Fig. 4.3 one can see probably one of the worst example by means of a comparison of two studies presenting $(B - V)$ data for the open cluster NGC 1513. Fortunately, this cluster is not among our programme clusters, but also for these from time to time significantly different photometric solutions were found.

The open cluster database WEBDA¹ is able to reveal such problematic data sets very easily. This database was initially developed at the former Institute for Astronomy at the University of Lausanne (now EPFL) by Jean-Claude Mermilliod (Mermilliod,

¹<http://www.univie.ac.at/webda>

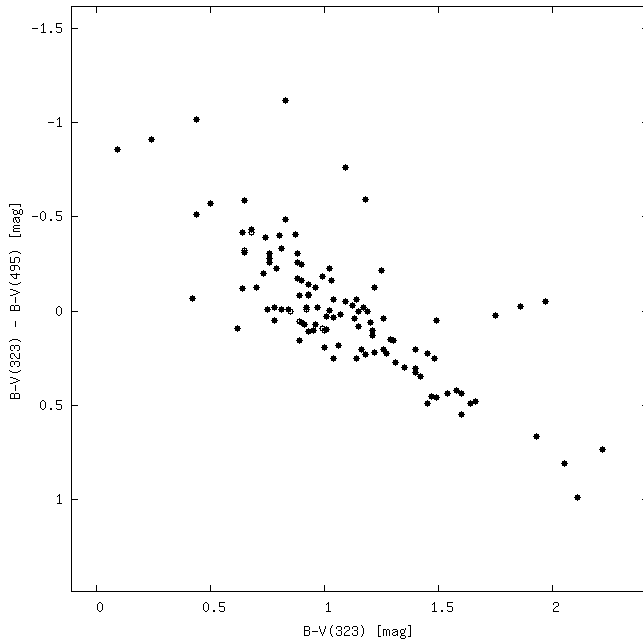


Figure 4.3: Comparison of two different studies presenting $(B - V)$ data for NGC 1513 taken from the WEBDA database. In an ideal case, there has to be a small scatter around zero at the ordinate.

1995) to combine available data for open clusters by using a homogeneous numbering system, which allows to compare different measurements. In October 2005 this database was handed on Univ. Doz. Dr. Ernst Paunzen (University of Vienna) to expand this project. Currently, about four million individual measurements in more than 1000 open clusters can be found in this database, and it is growing continuously. It provides several data types such as photometry in different systems, spectral classification, membership probabilities and much more. Star lists of e.g. red giants, CP or Be/Ae stars as well as bibliographic references can be also found. WEBDA is therefore the first place to go concerning open clusters, what is reflected by more than 500 refereed publications which acknowledge the use of it. The “usual” astronomical tools like SIMBAD² are not able to provide such an extensive knowledge and data match for open clusters, since in several studies only X/Y coordinates of the respective areas are presented. The database management tools within WEBDA allow even such an inclusion. Furthermore, the strategy behind the database results in an appearance of data sets which are not available elsewhere. Authors, who obtained measurements but do not provide them electronically, are contacted personally. So, in WEBDA one can find a nearly complete overview of individual open clusters.

Beside the *General Catalogue of Photometric Data*³ (Mermilliod et al., 1997), surveys (such as APASS or 2MASS), and the additional literature, WEBDA was therefore the main source to compile data (photometry, spectroscopy, membership probabilities ...) for the chemically peculiar stars as well as all via Δa studied “normal” objects. However, a careful comparison of all measurements is necessary to correct or exclude erroneous data like those presented in Fig. 4.3.

²<http://simbad.u-strasbg.fr/simbad/>

³<http://obswww.unige.ch/gcpd/gcpd.html>

Chapter 5

The open cluster sample

Within the following sections a brief description of the individual clusters and the detected CP candidates within the published photoelectric and CCD Δa surveys are presented, the latter subdivided into parts without (Part I) and with contribution (Part II) by the author of this thesis.

5.1 Photoelectric Δa survey

5.1.1 Collinder 121

A discussion about the nature of this open cluster, similar to Collinder 132, took place over the last three decades. Eggen (1981) suggested a distance of more than 1 kpc for it and pointed out that most early type stars are located much closer and form the OB Association CMa OB2. The cluster itself is a probable extension of the association CMa OB1, which is located at about the same distance. Using Hipparcos parallaxes, Robichon et al. (1999) found a mean distance of 556 pc based on some selected Collinder 121 members, much closer than the previous investigation. In Kaltcheva (2000) and Kaltcheva & Makarov (2007) a discussion about the different results can be found. Furthermore, they have identified 11 photometric cluster candidates at a distance of ~ 1085 pc in agreement with Eggen's cluster definition. In Maitzen & Wood (1983) ten stars in this area were investigated by means of Δa photometry. They have detected one CP candidate (HD 51088) among this small group of studied objects. Using the works by Kaltcheva and the position of the objects in the HRD we conclude that eight objects are probable members of Collinder 121, but the CP candidate belongs to the closer OB association. It is also listed as CMa OB2 member in the work by Landstreet et al. (2007). We keep this very young cluster as CP free in our sample.

5.1.2 Collinder 132

The nature of this cluster has been debated in literature. Clariá (1977) concluded based on UBV and $H\beta$ measurements that two clusters (Collinder 132 A and B) are present in this area. Eggen (1983a) found evidence for the existence of two unbound groups, one of them associated to the nearby cluster Collinder 140, and the other belonging to

the CMa OB2 association. The allocation of members to the different groups differs between these two studies. A further investigation about the nature of this aggregate was performed by Baumgardt (1998). He has used parallaxes and proper motions to clarify the situation and found that at least Clariá's Collinder 132B is doubtful since most stars do not follow a common motion. This study tried to divide objects in the area into probable cluster, association (CMa OB2), and field stars. More recently, Orellana et al. (2010) presented a thorough astrometric study of this area, and found a poorly populated cluster at a distance of 360 pc, as well as a bound association between 417 and 660 pc from the Sun.

Maitzen (1993) measured 27 objects in this area with Δa photometry, about half of them probably belonging to the more distant association. One star (HD 56343, WEBDA #27) with $\Delta a = +35$ mmag seems to be a CP2 candidate, supported by the rather large magnetic field measured by Bagnulo et al. (2006). According to Baumgardt (1998), the object belongs to the CMa OB2 association, but Landstreet et al. (2007) listed it as member of Collinder 132, which is according to them 470 pc away. The same distance was adopted by the reference also for the CMa OB2 association. They argued that proper motion as well as parallax of the peculiar star are in agreement with the cluster mean values. The new Hipparcos reduction by van Leeuwen (2007) shows a somewhat larger distance for this object than the previously catalogued value, but if taking the errors of both parallax results into account, the object can be assigned to the outer border of the extended association. Concerning proper motion it is difficult to decide, if it belongs to the closer cluster or the association, since both exhibit according to Orellana et al. (2010) a rather similar value. Nevertheless, in combination with photometric criteria we conclude a probable membership to the Collinder 132 association for the CP object.

5.1.3 Collinder 140

No photometric peculiar member was detected by Jenkner & Maitzen (1987) in this moderately young (~ 40 Myr) cluster. However, one object exhibits a Δa index of $+39$ mmag, but it can not be classified as member of the cluster according to proper motion as well as using photometric criteria. The position in the colour-magnitude diagram was also discussed by the above reference. The deviation to the cluster main sequence in all available CMDs is too large to be explained by the blueing effect (see Sect. 2.3).

5.1.4 IC 2391

Maitzen & Catalano (1986) have investigated 32 stars in the area of the open cluster IC 2391. They have found three objects showing a positive Δa index, of which one (HD 74168) was already denoted as non-member. Proper motion as well as parallax confirm this assumption. The other two stars (HD 74535 and 74169) are bona fide members of the cluster according to proper motions and additional literature (e.g. Platais et al., 2007). These two objects also remain as CP cluster members in the study by Landstreet et al. (2007).

5.1.5 IC 2602

Two suspected CP2 candidates (HD 92385 and HD 92664) in IC 2602 were confirmed by Maitzen et al. (1988) with Δa photometry. They were already targets of the Δa introduction paper by Maitzen (1976) and by Maitzen & Vogt (1983), but with a somewhat lower Δa for the first mentioned object. Both seem to be definite members according to proper motion data as well as by the position in the HRD. Furthermore, Landstreet et al. (2007) list them also as definite CP cluster members. No further candidates seem to be present in the cluster. The latter reference excluded the suspected candidate HD 93030, which was not measured by Maitzen et al. (1988), from their sample since neither membership nor CP nature can be confirmed.

5.1.6 IC 4665

This aggregate is located closer than 400 pc from the Sun and is about 40 Myr old. No CP2 candidate was detected by Maitzen & Schneider (1984) among the 33 investigated stars (24 members), in agreement with some spectroscopic surveys as well as *Geneva* photometry. The most recent spectroscopic study in this cluster was performed by Gray & Corbally (2002). They have found some CP2 stars, but all of them are non-members. Two stars are in common with Maitzen & Schneider (1984), but no significant Δa was found, to be explained by the non-membership and a reddening different from the cluster one.

5.1.7 IC 4725

Three photometric peculiar candidates were found by Maitzen (1985) among 29 investigated objects in the cluster area. We have extracted 22 stars which belong to the cluster, including the three above mentioned peculiar candidates. One object (BD-19 5044L) is a probable non-member according to Dias et al. (2006), who list a membership probability of only 20% for it. However, recent UCAC-4 proper motions as well as those of the PPMXL catalogue do not contradict membership. Furthermore, the peculiar nature was rather uncertain, since Maitzen (1985) mentioned a peculiar Δa index varying from non significant to +25 mmag during the various observing runs. Furthermore, no magnetic field was detected by Bagnulo et al. (2006), but the study by Paunzen et al. (2011c) showed that it is a B9 Si star with a probable SB nature. For the other candidates, proper motion as well as photometry confirm membership. Dias et al. (2001) have used Tycho-2 data to determine membership probabilities of more than 85% for both stars. Concerning peculiarity, Landstreet et al. (2008) indicates strong Si lines in HD 170860 in agreement with the positive Δa index, and for HD 170836 Bagnulo et al. (2006) have detected also a magnetic field. Paunzen et al. (2011c) list a He-weak nature for it in agreement with Luck et al. (2000), who found an underabundant He content of -0.45 dex. The position in the HRD is in good agreement with the determined cluster age of 75 Myr. However, a slightly higher metallicity has to be taken into account since e.g. Gratton (2000) list $[\text{Fe}/\text{H}]=0.17$. In Landstreet et al. (2007) all three stars remained as probable CP cluster members and they list a somewhat older age (105 Myr) for the cluster. Since we have not found any reference which lists

such an age, they have probably determined it by fitting solar composition isochrones to the three stars (see the reference for details). The above mentioned He-weak star was calibrated by them as CP2, resulting in a lower temperature, which suggests an earlier turn-off point and hence an older age. Furthermore, their given true distance modulus of 10.44 mag for IC 4725 is erroneous. Since we have obtained a similar value for the apparent modulus, based on several individual determinations, it is most likely a mix-up by them.

5.1.8 Melotte 20 (α Persei)

In the 12th paper of the photoelectric Δa survey, Maitzen & Pavlovski (1987a) have investigated the prominent open cluster Alpha Persei (Melotte 20). They have obtained data for 48 cluster stars, of which most remained to be true cluster members after applying a membership analysis. Although some CP candidates were already suspected in this cluster, the above cited authors were only able to confirm the peculiar nature of HD 21699 (WEBDA #985), a He-weak star. In Landstreet et al. (2007) the assumed peculiar stars in Alpha Persei were investigated, and also the above mentioned object remained as true CP cluster member after their analysis. Proper motion as well as parallax (e.g. by van Leeuwen, 2007) are in perfect agreement with the cluster mean values. To determine its position on the HRD, we have used the calibration for CP4 stars as given in Table 2.1 and found a very good coincidence with the cluster age of ~ 50 Myr.

5.1.9 Melotte 22 (Pleiades)

Apart from the detection of a strong variable Δa index for the shell star Pleione, Maitzen & Pavlovski (1987b) have not detected any CP2 candidate in the well known open cluster Pleiades. Beside Coma Berenices it is the closest studied aggregate in our sample. However, some spectroscopically identified CP2 stars can be found in the literature (Abt & Levato, 1978), but for all a normal Δa value was measured. Additionally, Landstreet et al. (2007) have excluded all those candidates, since for none of them a CP nature can be concluded.

5.1.10 Melotte 111 (Coma Berenices)

This prominent close and rather old cluster was already target of the Δa introduction paper by Maitzen (1976), but a more detailed study was presented by Maitzen & Pavlovski (1987b), showing a very good agreement of the stars in common. For two former spectroscopically detected CP2 stars (HD 108662 and 108945) the Δa measurements confirm their peculiar nature. Furthermore, magnetic fields were found for both objects. However, membership analysis shows that only one (HD 108945) is a CP cluster member. The proper motion and the position in the HRD of the other object deviate significantly from the cluster mean values. Therefore, HD 108662 can not be identified as member of Melotte 111. This result is in agreement with the study by Landstreet et al. (2007).

5.1.11 NGC 1039

The study by Maitzen et al. (1986) listed two positive CP detections among 31 via Δa investigated stars. Whereas one (HD 16605) exhibits a large Δa index of +56 mmag, confirmed by spectral classification and a large magnetic field of about 2 kG, the other star (HD 16728) deviates from the normality line only by +15 mmag. This object appears also as mild peculiar by means of the *Geneva* $\Delta(V1 - G)$ and Z indices. In Landstreet et al. (2007) the first mentioned strong peculiar star is listed in their final table of probable CP cluster stars, but can not be found in the foregoing table which provides membership and peculiarity analysis. However, both objects are investigated in the follow-up work by Landstreet et al. (2008). For all stars probable cluster membership was assigned, and HD 16728 being rejected by them as normal type object. We can not retrace the conclusion for the latter object due to in the reference mentioned observational problems with unexpected low S/N and large uncertainties in the magnetic field measurements. Furthermore, based on a small section of their ESPaDOnS I spectrum they found atmospheric abundances which are close to solar values. However, since Δa and *Geneva* indices are rather low, but definitely positive, one can not expect a strong peculiarity. This object is known to be a binary with a separation of about 1.5", and Landstreet et al. (2008) also notes a probable SB2 nature. The first spectroscopic investigation on this object was carried out by Ianna (1970), who determined a spectral type of B8 SiCr. Later, Abt & Levato (1977) argued that if a higher luminosity class is taken into account, the Si II lines appear as normal. Therefore, they list a spectral type A0 III-IV for it. The most recent study was performed by Grenier et al. (1999), who classified it as B9 Si. Since the binary nature has hardly an effect on Δa (Stütz & Paunzen, 2006), we conclude that at least one component is indeed peculiar. The Tycho-2 catalogue (Høg et al., 2000) list resolved magnitudes for the components ($V_T = 8.461/8.957$ mag), whose total intensity is in perfect agreement with the V magnitude of ~ 7.95 mag, measured photoelectrically in all available systems (UBV , *Geneva*, Strömgren) for both components together. Furthermore, since the Tycho colour indices (and hence temperature) are nearly identical, there is hardly an influence on the temperature deduced from photometry measuring the binary system as a whole. By placing both objects on the HRD (with and without CP temperature correction), we assume that the fainter component is the CP star, since the resulting HRD position agrees much better with the age of about 140 Myr. Both stars are probable members according photometry, also proper motions are in agreement with the cluster mean. However, Tycho-2 lists the same motion for both stars and the latter membership criteria can be of course also affected by the binary nature. Finally, even if using the total intensity of the system, one can not infer that it is an evolved object as Abt & Levato (1977) proposed, hence a further argument in favour of the peculiar nature. Since both stars have rather similar masses due to the different bolometric correction for normal and CP stars, we adopt a suitable mean of $3 M_{\odot}$ for HD 16728B.

5.1.12 NGC 1662

This open cluster was target of two Δa studies (Maitzen & Hensberge, 1981; Maitzen & Wood, 1983). However, in total only eight objects in this poorly populated aggregate were measured. The first reference mentioned three mild peculiar objects, whereas in the latter reference only HD 30598 remained as peculiar candidate, since they have taken into account also the reddening effect on the a values. For this object Young & Martin (1973) identified slightly enhanced Sr II, but Bagnulo et al. (2006) and Kudryavtsev et al. (2006) failed to detect a magnetic field. Anyhow, we consider the object as CP star (as Landstreet et al., 2007). It was recognized as cluster member in several kinematic studies (e.g. Kharchenko et al., 2004; Dias et al., 2001, 2006). Furthermore its position in the HRD agrees perfectly with the cluster age of 400 Myr.

5.1.13 NGC 1901

In this rather old and poorly populated aggregate no CP2 candidate was detected in the study by Maitzen (1993). All observed 11 stars in the field turned out to be true cluster members. A recent deep study by Carraro et al. (2007) combined photometric and spectroscopic data for the analysis. Based on radial velocity measurements, they concluded that several binaries are present in the cluster. Taking this result into account as well as the confirmed membership of a giant, they obtained the youngest age found in the literature for this open cluster. The individual results range from ~ 400 –850 Myr, whereas distance is in very good agreement among most studies. Our analysis supports an age at the upper border. Furthermore, Carraro et al. (2007) obtained a slight sub-solar metallicity of $[\text{Fe}/\text{H}] = -0.08$, but only based on a single cool star.

5.1.14 NGC 2169

The photoelectric Δa investigation by Maitzen (1993) detected one CP candidate (WEBDA #12) among 15 observed stars in this rather sparse cluster, of which all remained as cluster members after our analysis, including the peculiar candidate for which photometry and all available proper motions agree perfectly. Since also radial velocity data follow the mean motion, it can be considered as definite cluster member. This object was also observed in Δa by using the CCD technique (Bayer et al., 2000) with a very good agreement for the detected CP star. Controversial spectral types were obtained for this star, as discussed in Maitzen (1993), but its variability (also in Δa) and the detection of a rather strong magnetic field of about 3 kG (Bagnulo et al., 2006) strengthens its peculiar nature.

5.1.15 NGC 2232

Beside the confirmation of the already known Si star HD 45583, Jenkner & Maitzen (1987) have not detected any further candidate in the cluster NGC 2232. For this object also a definite magnetic field was measured by Bagnulo et al. (2006). Furthermore, the work by Semenko et al. (2008) found an unusual curve of longitudinal magnetic field

variations. According to measured parallax and proper motions it is a member of the cluster; e.g. Dias et al. (2001) list a probability of 95%.

5.1.16 NGC 2287

One strongly deviating object was found in the Δa survey by Maitzen & Wood (1983). The star HD 49299 exhibits a large Δa index of +74 mmag, and a strong magnetic field was detected by Bagnulo et al. (2006). All other investigated stars appear to be normal in Δa . Furthermore, a He-weak object (HD 49333) in the cluster area was measured by Maitzen (1981), who found a significant Δa value for it, but it is definitely no member of the cluster in contrast to HD 49299 which seems to be a member based on kinematic data as well as by using photometric criteria. In Landstreet et al. (2007) a further object is listed as a probable CP star (CpD-20 1640), but which is neither noticeable in Δa and *Geneva* indices nor a magnetic field was detected. Their assumption is only based on the spectral type A5 (Si Sr) obtained by Harris et al. (1993). Since no photometric indications of peculiarity are given and this object shows only kinematic membership probabilities of 39% (Dias et al., 2001) and 18% (Ianna, Adler, & Faudree, 1987), we do not take into account this star in our analysis.

5.1.17 NGC 2343

NGC 2343 is another cluster investigated by Maitzen (1993) with a non-detection of CP stars. This cluster was also subject of the study by Jenkner & Maitzen (1987). Both references have most stars in common, but a re-investigation was performed since a rather large scatter compared to other clusters was noticed. It seems that this poorly populated cluster with an age of ~ 120 Myr shows no evidence of any peculiar object. The survey by McSwain & Gies (2005) has also found no Be/Ae type star in it, confirming the Δa results, since such stars should exhibit significant negative Δa indices.

5.1.18 NGC 2362

No photometric CP candidate was detected by Maitzen (1982) in this very young (< 10 Myr) open cluster. It is the most distant (~ 1500 pc) cluster in the photoelectric Δa survey. In total 28 objects were investigated by this reference, of which 23 remained after a membership analysis of all individual stars, with five stars more massive than $7 M_{\odot}$.

5.1.19 NGC 2422

In Maitzen & Wood (1983) one object (HD 61045) deviates +34 mmag from the normality line in the Δa diagnostic diagram. It was recognized as Si star in several spectroscopic studies. Parallax and proper motion of the newly reduced Hipparcos data by van Leeuwen (2007) support cluster membership, as well as its position in the HRD. Furthermore, a magnetic field was detected by Bagnulo et al. (2006). In Landstreet et

al. (2007) several other suspected CP candidates in NGC 2422 were investigated, but except for the above mentioned star they seem not to be of peculiar type according to their criteria. The majority of the individually determined cluster parameters are in very good agreement, which establish an age and distance of 120 Myr and 480 pc, respectively.

5.1.20 NGC 2423

In the cluster NGC 2423 two CP candidates were found by Maitzen (1993), whereby one of them, the pair ADS 6223, was measured as single object (such as CP-60 944AB in NGC 2516). Furthermore, the brighter component is composed of two very close objects. However, the photometry of both components contradict membership as well as the proper motion for the brighter star (Dias et al., 2001, list a 2% membership probability for it). The other CP candidate (HD 61044) is too bright and located too much above the cluster turn-off to be a member. Furthermore its proper motion listed in the Tycho-2 catalogue differs from the cluster mean (e.g. determined by Loktin & Beshenov, 2003) and it is located too far from the cluster center. In Maitzen (1993) the erroneous photometry by Hassan (1976) is discussed, probably the reason for differing results of the cluster parameters. The recent study by Clariá et al. (2008) confirmed membership of some red giants in this cluster. With an age of 1 Gyr it is one of the oldest aggregates in our sample.

5.1.21 NGC 2447

This is another cluster studied by Maitzen (1993) showing beside an object with negative Δa index of -21 mmag no other peculiar candidates among 36 investigated member stars. With an age of about 500 Myr it is in respectable society with other clusters of comparable ages, showing no or only one CP candidate. The only exception is the somewhat older aggregate Ruprecht 115 with three listed candidates.

5.1.22 NGC 2451 A/B

Maitzen & Catalano (1986) proposed the existence of two clusters at different distances in the direction to NGC 2451, which have been meanwhile confirmed based on several studies. We have extracted from their Δa measurements four objects with significant deviations from the normality line (HD 61622(B), 62251(B), 62992(-), 63401(A)); the affiliation to the respective clusters is given in parenthesis. All stars have been also identified at least once based on spectroscopic results. We have used the above reference as well as additional literature (e.g. Carrier et al., 1999) to determine membership of all the investigated stars in the individual clusters. Carrier et al. (1999) have used proper motion, parallax, and photometry to separate their sample, showing also a significant difference in motion for the two open clusters. This allows an easier division of the objects. From the above mentioned four CP stars only one (HD 62992) seems to be a field star; proper motion and position in the HRD contradict membership in any of both clusters. Landstreet et al. (2007) have included five candidates in their study,

but unfortunately only one in common with our sample (HD 63401). This is also the only one which remains as CP cluster star in their investigation, in agreement with our analysis. Surprisingly, they have also included HD 62376, for which a weighted Δa index of +23 mmag is listed in Maitzen & Catalano (1986). However, this star was nowhere mentioned as peculiar in the text of the above reference. Based on the other given values in the table by Maitzen & Catalano (1986) we conclude that the positive index is most likely a typo. In total, they have investigated 58 stars in the cluster areas. We were able to identify 20 and 29 stars belonging to NGC 2451A and NGC 2451B, respectively. Both clusters seem to be of comparable age (~ 50 Myr), but are located at ~ 200 (A) and 400 (B) pc.

5.1.23 NGC 2516

See Chapter 7 for a cluster description.

5.1.24 NGC 2546

Three photometric CP candidates are mentioned in the work by Maitzen (1982) in the open cluster NGC 2546 (WEBDA # 197, 258, 567). Since he noticed a differential reddening in this cluster, a reddened as well as unreddened Δa diagnostic diagram were used for the analysis. For one object (#258) we presented additional classification spectroscopy in Sect. 3.1, showing a normal star of spectral type A7. Since Maitzen (1982) has used at least for this object photographic data by Lindoff (1968) for the Δa diagrams, and the $(B - V)$ colour is too blue (e.g. 2MASS shows also a much redder colour), this object is shifted in the diagrams to the left and hence producing a false positive Δa peculiarity. Except from #567, the CP candidates were investigated also by Landstreet et al. (2007), who concluded a probable CP nature for them, and they list a questionable cluster membership for #258, in agreement with our conclusion. For the remaining two objects, photometric as well as kinematic data support membership. Landstreet et al. (2007) have investigated three further suspected CP objects in this cluster, of which two turned out to be probable non-members. The remaining star (#201) has only a moderate Δa index of +12 mmag and lies due to the scatter, caused by the differential reddening, on the border of the detection limit, but a magnetic field of about 500 G was detected by Bagnulo et al. (2006). It is difficult to decide how to handle such objects, which are not really suspicious in Δa , but are recognized as peculiar (or magnetic in this case) in another study. However, inspecting the available photometric data we assume that this object is probably a significantly less reddened foreground object, although proper motions agree with the cluster mean. Finally, two CP members (#197 and 567) remain among 40 probable cluster stars.

5.1.25 NGC 2632 (Praesepe)

Praesepe is another prominent, rather close (~ 180 pc) and old (~ 720 Myr) cluster studied by Maitzen & Pavlovski (1987a). Beside some confirmed Am stars (e.g. Fossati et al., 2007), which exhibit unusual positive Δa indices of around +20 mmag, no CP2

candidates were found in this open cluster. One formerly suspected marginal Si star (HD 73666) turned out to be a Blue Straggler as can be clearly seen in the colour-magnitude diagram and its location in the Δa diagnostic diagram is also inconspicuous. Furthermore, another star showing $\Delta a = +14$ mmag is a δ Scuti type pulsator, whose variability might be the reason for the marginal positive Δa index. The non-presence of CP2 objects is well in line with other studied aggregates in this age range.

5.1.26 NGC 3114

A rather large number of cluster stars (127) were observed in NGC 3114 with Δa photometry by Maitzen et al. (1988). In total, they have found six objects with a positive deviation from the normality line, suggesting a CP2 nature. Some of them were already confirmed by spectroscopic results or *Geneva* photometry (see discussion by Maitzen et al., 1988). However, we were able to determine a positive membership for only four of them (HD 304841, HD 304842, HD 87240, HD 87405). For all others the position in the HRD suggest a location in the background. The latter conclusion holds especially for CP-59 1669 (WEBDA #22), which lies noticeable below the ZAMS, strengthening the assumption by Schneider & Weiss (1988) that it is a background object. Unfortunately, not all objects are included in the study by Landstreet et al. (2007), but for the stars in common a good agreement of membership and CP nature can be found. Additionally, this cluster was studied with Δa by Paunzen et al. (2003b) in the CCD survey, allowing to merge both datasets.

5.1.27 NGC 3228

In this poorly populated cluster (15 members according to Lyngå's catalogue) 12 objects were measured by Maitzen (1982). He detected one possible CP candidate (HD 89856). We have noticed that the membership probabilities by Dias et al. (2001) based on the Tycho2 data seem to be erroneous. They listed a proper motion of $-12.3/2.3$ (pmRA/pmDE [mas/yr]) for the cluster and 12% probability for the above mentioned star with a proper motion of $-11.9/4.3$. On the other hand, for strongly deviating stars a probability of 100% is listed. In Fig. 5.1 one can find their results.

Based on this figure we conclude that the listed probabilities are inverted, since the probability increases with higher deviation from the cluster mean motion. However, their result of the mean cluster motion and that of the field stars is nearly identical. Another study dealing with membership analysis was carried out by Javakhishvili et al. (2006). They introduced a new method based on a cumulative effect of the proper motions and listed a membership probability of 72% for HD 89856. They also discussed the discrepancies between both studies, and conclude that one of the reasons is a low cluster-to-field star ratio. Furthermore, Baumgardt et al. (2000) analysed membership using Hipparcos data resulting in 0% for the CP candidate. However, the study is based only on a very limited number of cluster stars. Seven objects measured by Hipparcos are in this field; the cluster motion was then calculated on the basis of three stars. After a careful membership analysis by us, nine stars remained from the Δa sample, but again HD 89856 was rejected as non-member, since its position deviates strongly in

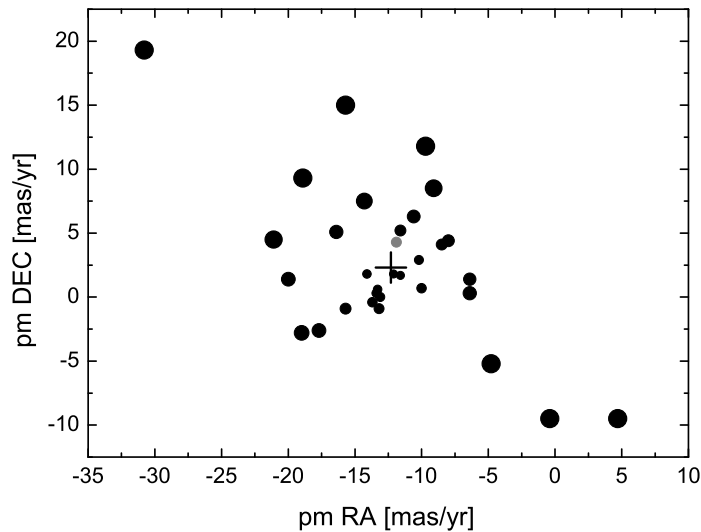


Figure 5.1: The Tycho2 proper motions of the stars in the area of NGC 3228. The membership probabilities by Dias et al. (2001) are given with increasing size of the symbols (larger symbols represent higher probability). The cross indicates the listed mean cluster motion, the grey symbol the proper motion of the CP candidate HD 89856.

the HRD and contradicts membership. The temperatures obtained by means of *UBV* and *Geneva* photometry are in perfect agreement, so an error due to photometry can be excluded. Another object with a Δa of +15 mmag is also present (HD 298053), but which was spectroscopically identified as Am star. Most cluster age determinations found in the literature are around 100 Myr, in contrast to Kharchenko et al. (2005) who list 250 Myr. Mermilliod et al. (2008) have determined membership of a red giant by means of radial velocity data, which would justify such an higher age. However, our analysis results in a much lower age of 85 Myr (Sect. 6.2).

5.1.28 NGC 3532

See Chapter 7 for a cluster description.

5.1.29 NGC 5460

Two photometrically detected CP candidates are listed by Maitzen (1985) in this intermediate age cluster (~ 150 Myr). Both are probable kinematic members according to Dias et al. (2001), Kharchenko et al. (2004), or Dias et al. (2006) and still remained as members after re-investigation of all available kinematic data. Furthermore, their position in the HRD strengthen their cluster membership. In Landstreet et al. (2007) these objects are listed also as probable or definite members of the cluster including their peculiar nature. In total, 25 objects were measured by means of Δa photometry and the majority of them seem to be indeed cluster members.

5.1.30 NGC 5662

In the work by Maitzen & Schneider (1987) two CP candidates were found, of which one is a probable non-member as mentioned in the reference, and also e.g. Tycho-2 data deviate especially in declination from the cluster mean by about 10 mas. Therefore, Dias et al. (2001) list only 19% probability for CpD-56 6330 to be a cluster member. However, the data of the recent UCAC-4 catalogue are in much better agreement with the cluster mean. Photometrically, this star would be classified as definite member (see also discussion by Paunzen et al., 2011b). Also the determined reddening using Strömgren and UBV data are in excellent agreement with that of the cluster. We therefore keep this object as probable member in our sample. Paunzen et al. (2011c) list a spectral type of A0 Si for it, but Bagnulo et al. (2006) has not detected a magnetic field. Nevertheless, it was classified as probable peculiar in Landstreet et al. (2007). A discrepancy can be found if comparing the spectral type and the adopted temperature of 12000 K. However, it can be also a late B-type star, if taking a possible He-wk nature into account. High resolution spectroscopy is necessary for a more profound investigation. For the other peculiar object (HD 127924) most studies list a high probability to be a kinematic member, except Dias et al. (2006) whose mean cluster motion differs significantly compared to all other investigations, probably due to the inclusion of numerous faint photometric non-members. Furthermore, Landstreet et al. (2007) list it also as probable CP cluster star. An analysis of photometry as well as all kinematic data confirm membership. This time, the spectral type of B8 Si (Paunzen et al., 2011c) is in agreement with temperature, but again no magnetic field was detected by Bagnulo et al. (2006). However, its peculiar nature was also defined as probable by Landstreet et al. (2007).

5.1.31 NGC 6087

In this ~ 80 Myr old aggregate Maitzen (1985) has detected two CP candidates, both of them already verified spectroscopically as Si stars. Only a hint of a magnetic field was found by Bagnulo et al. (2006) for HD 146555, whereas for the other (CpD-57 7817) a definite field was measured. The position of the CP stars in the HRD supports membership as well as kinematic data do. Also King (1982) lists a membership probability of more than 90% for both stars. Furthermore, Tycho photometry suggests duplicity for the object CpD-57 7817.

5.1.32 NGC 6281

In this rather close (~ 500 pc) intermediate age cluster (280 Myr) one peculiar candidate out of 30 investigated stars was detected by Maitzen & Schneider (1984). Most of the studied objects are definite members, it was necessary to reject only a few stars. The CP2 candidate is also a member according to proper motion and its position in the HRD. This object is included in the investigation by Landstreet et al. (2007), and they also confirmed membership as well as CP nature for it, based on available spectral classification, the Δa result, photometric variability, and a weak but detected magnetic field (see Bagnulo et al., 2006).

5.1.33 NGC 6405

The investigation by Maitzen & Schneider (1984) obtained Δa photometry for 67 objects in this cluster. They detected three CP2 candidates, of which two were also confirmed by *Geneva* photometry. All candidates seem to be definite cluster members, Landstreet et al. (2007) have also assigned membership and peculiar nature for these objects. In addition, this open cluster was studied by Paunzen et al. (2006b) to obtain a comparison between the CCD and photoelectric Δa survey, showing very good agreement for the three CP objects.

5.1.34 NGC 6475

This open cluster was intensively studied by Maitzen & Floquet (1981). They have obtained Δa data for 50 objects in the cluster area, 41 remained as members after our membership analysis. With five positive Δa detections (HD 162576, 162725, 162305, 162588, and 320764), this cluster is one of the most CP rich aggregates beside NGC 2516. For four of them Folsom et al. (2007) provide chemical abundance analyses, confirming their peculiar nature. However, HD 320764 seems to be a normal star. Also the recent classification spectroscopy presented by Paunzen et al. (2011c) found no hint of peculiarity. Therefore, this object was rejected from our sample. For the remaining peculiar candidate (HD 162588) Landstreet et al. (2008) found that Cr is overabundant, in contrast to Abt (1975) who listed slightly strong Si. Since this cluster is rather close and bright, several studies confirm membership for these peculiar objects. Concerning cluster age, one can find rather different results in the literature, ranging from 130 to more than 400 Myr. Our analysis supports an age of about 250 Myr.

5.1.35 NGC 7092

By means of Δa photometry and spectroscopic data Maitzen et al. (1986) confirmed the mild peculiar nature of the star HD 205331. Furthermore, they report indications of spectrum variability for the Si II and K-line. The study by Gray & Corbally (2002) strengthens this result, they list a SiCr peculiarity for this object. All these investigations were not taken into account by Landstreet et al. (2008), who classified it as normal star using spectral synthesis of two short spectral regions in their ESPaDOnS *I* measurement. This result is comparable to HD 16728 in NGC 1039. Examining only a short spectral region will probably not reveal such mild CP stars. Kinematic data, parallax, radial velocity, and photometric criteria all suggest a definite membership for this object.

5.1.36 NGC 7243

Maitzen & Pavlovski (1987a) presented Δa photometry for 20 objects in this cluster, and we were able to determine a positive membership status for 19 of them. In this reference in total four objects were listed as at least marginal Δa peculiar candidates. Two of them (WEBDA # 377 and 493) have Δa indices of +11 and +10 mmag respectively, rather low values to be significant, and were rejected from the sample. The

remaining two (#370 and 490) seem to be definite CP stars. Although Landstreet et al. (2008) were not able to measure a magnetic field due to low precision, but by synthesis of two small spectral windows they were able to confirm the positive CP nature of these objects. Their affiliation to the cluster is confirmed by several kinematic membership studies (e.g. Jilinski et al., 2003; Kharchenko et al., 2004), but also after re-investigating all available kinematic data and radial velocity. All the aforementioned references list probabilities of 70–98% for the CP stars. Furthermore, the position in the HRD additionally supports membership.

5.1.37 Trumpler 10

One previously suspected CP star (HD 75239) was included in the Δa study by Jenkner & Maitzen (1987). Levato & Malaroda (1975) list a spectral type of B9p Si 4200 for this object, but Jenkner & Maitzen (1987) determined an unsuspecting Δa value of -1 mmag, which disproves a peculiar nature. Furthermore, Bagnulo et al. (2006) found no evidence of a magnetic field. Since proper motions do not contradict membership, we conclude that it is a normal cluster member. No further CP candidates were detected in this ~ 40 Myr old aggregate.

5.2 CCD Δa survey - Part I

5.2.1 Collinder 272

The peculiar content of the very young aggregate Collinder 272 (~ 14 Myr) was studied by Paunzen et al. (2002). They found no CP candidate among the investigated objects. All individual results for the cluster parameters found in the literature are quite homogeneous, allowing to determine them very accurately. Due to the youthfulness of this aggregate, there are most probably many objects still in the pre-main-sequence phase. Taking this into account as well as membership studies, we have extracted from their list about 60 main-sequence cluster stars in the appropriate mass domain.

5.2.2 Lyngå 14

Another very young open cluster with an age of about 6 Myr is Lyngå 14. It was studied by Paunzen et al. (2002) and they found like in some other very young clusters no peculiar object. Since also a differential reddening is present, they had to de-redden all measured objects to achieve an accurate Δa diagram. The obtained detection limit is rather low, but all investigated stars follow the normality line without any deviation. Finally, we have determined 22 main-sequence cluster members for further analysis.

5.2.3 Melotte 105

This was one of the first studied clusters using Δa with the CCD technique. Bayer et al. (2000) detected four objects deviating from the normality line. However, as mentioned in the reference, they are not substantial photometric peculiar candidates, since

their Δa indices hardly reach +20 mmag. For the two brightest objects we obtained classification resolution spectra (see Sect. 3.1), whereas the one with the lower Δa value (+15 mmag) turned out to be a weak Si star, and the other (+17 mmag) appears to be a normal type object. The remaining two stars with a Δa of +15 and +19 mmag are somewhat too faint (~ 14.7 mag) to obtain spectra with a sufficient S/N at the used observatories, but one can not a priori exclude a peculiarity for them. We therefore adopt three CP stars for this open cluster. Due to its distance of ~ 2000 pc and the compact appearance, not many cluster stars are included in the available proper motion catalogues, the resolution of the photographic plates was probably too low. This is most likely the reason why the study by Dias et al. (2006) list only 12 members compared to 50 field stars in the cluster area.

5.2.4 NGC 2099

In Paunzen et al. (2003b) the open cluster NGC 2099 was studied with Δa photometry. It shows a rather well defined main-sequence and red giant clump. They found no CP star in this ~ 370 Myr old aggregate. However, they have observed only the brightest members down to V 13 mag, still resulting in an sample of 27 main sequence stars with masses down to $\sim 2 M_{\odot}$.

5.2.5 NGC 2169

This cluster was included in the Δa CCD study by Bayer et al. (2000) to obtain a comparison with the results of the photoelectric survey by Maitzen (1993) (see Sect. 5.1.14), showing very good agreement for the stars in common and the detected CP star (WEBDA # 12). No measurements of additional objects in this cluster were presented by Bayer et al. (2000).

5.2.6 NGC 2439

No peculiar object was found by Paunzen & Maitzen (2002) in this cluster, although peculiar values of Δa could be expected since McSwain & Gies (2005) detected several Be candidates in agreement with former studies. Unfortunately, there is only one object in common for these two references, but for which the Δa measurements show no hint of such a nature. Although this young cluster shows a rather well defined main sequence and no conspicuous colour-colour diagrams, Kaltcheva et al. (2001) conclude that it is probably not a real cluster. According to them, it is located in an area of lower absorption, giving the impression of a cluster (see also Eggen, 1983b), which is supported by their kinematic investigation. In contrast, Ramsay & Pollaco (1992) stated that it is physical and not an optical effect. Since Kaltcheva et al. (2001) used Tycho data for their analysis, which is rather limited in case of this cluster, we have examined the UCAC catalogue and found strong hints of a proper motion clustering at $\sim -3/3$ [mas/yr] in RA/DE. We therefore rely on the study by Ramsay & Pollaco (1992) and keep this cluster in our sample.

5.2.7 NGC 2489

Rather different open cluster parameters can be found in the literature for this open cluster, ranging from ~ 1000 – 4000 pc in distance and 20 to 500 Myr in age. Furthermore, the reddening values vary between 0.3 and 0.45 mag. Piatti et al. (2007) used CORAVEL data to confirm membership of red giants in the cluster by means of radial velocity, supporting an older age. Our analysis results in ~ 530 Myr and a distance of 1800 pc. Three peculiar candidates were detected by Paunzen & Maitzen (2001), which are all at least probable members. Landstreet et al. (2007) has included two stars in their sample (WEBDA #40 and 58) and classified both as probable non-members. Furthermore, they deny peculiarity for the investigated objects, since Bagnulo et al. (2006) were not able to detect a magnetic field and the only hint of peculiarity is the Δa index. However, since they show rather large values of more than +30 mmag, we keep these objects as probable cluster CP stars in our sample.

5.2.8 NGC 2567

No classical chemically peculiar candidates were detected by Paunzen & Maitzen (2001) among 22 studied main sequence cluster members, but three stars are lying significantly below the normality line, suggesting a Be/Ae object nature. However, all of them are probable background stars. The individual results for the cluster parameters are quite homogeneous resulting in an average age of ~ 300 Myr and a distance of 1700 pc. Inspecting the final results for clusters in this age range one can notice that most of them exhibit a rather low or zero CP frequency.

5.2.9 NGC 2658

There is a cluster parameter set deviating significantly from the other ones: Lyngå's catalogue and the follow-up compilation by Dias et al. (2002) list an age of 1.4 Gyr. Since several late B and mid A type stars (deduced from photometry) are in this cluster, such an old age is improbable. The adopted parameters show that NGC 2658 is located about 4000 pc away from the Sun and a representative of the middle aged clusters (~ 250 Myr). It is therefore one of the most distant clusters in our sample. The study by Paunzen & Maitzen (2001) revealed the presence of two possible classical chemically peculiar objects. Due to distance and the compactness of the cluster, as well as the brightness of the objects (V 15–16 mag), a membership analysis based on proper motions has to be given lower weight. However, the position in the HR diagram together with the determined age of the cluster shows a perfect agreement.

5.2.10 NGC 3114

NGC 3114 was already observed photoelectrically in Δa by Maitzen et al. (1988). A further investigation by Paunzen et al. (2003b) was carried out to obtain an additional comparison of CCD to the photoelectric technique. However, due to brightness and the field-of-view, only a limited number of objects are in common with the former study

and it was not possible to measure the detected CP candidates also with CCD, but still very good coincidence between the two systems was found.

5.2.11 NGC 3960

One CP star with a very large Δa index of +85 mmag was detected in the cluster NGC 3960 by Paunzen & Maitzen (2002). Recently, spectral classifications by Paunzen et al. (2011c) showed a very peculiar SrCrEu type nature for that object. Its membership is confirmed by the position in the HRD as well as by proper motions. Since it is close enough (~ 1900 pc), these data can still be used safely. The work by Dias et al. (2006) lists a probability of 81% for this object. In total, 36 cluster members with masses higher than $1.5M_{\odot}$ were extracted from the investigated sample in this rather old aggregate (~ 1 Gyr). The well recognizable turn-off point and red giant clump in the colour-magnitude diagram allows a rather accurate determination of the cluster parameters.

5.2.12 NGC 5281

In the study by Paunzen & Maitzen (2001) one single CP candidate was detected, for which the proper motion study by Sanner et al. (2001) does not contradict membership. Unfortunately, this object is too faint to be observed by the Tycho mission, and too close to the bright star HD 119699, which probably influences all proper motion studies. However, according to the CMD presented in Paunzen & Maitzen (2001) it is a probable member. A cluster age of 60 Myr was determined, as well as a distance of 1300 pc.

5.2.13 NGC 6134

Although a very low detection limit of 9 mmag is presented by Paunzen & Maitzen (2002) for this cluster, they were not able to find any peculiar object among the 102 investigated stars. Since this cluster is very old (~ 1 Gyr) - the second oldest cluster in our sample - many red giants or stars with masses lower than $1.5M_{\odot}$ are present. Finally, we have extracted 36 main sequence cluster members in the mass range occupied by CP stars.

5.2.14 NGC 6192

This open cluster was studied by Paunzen & Maitzen (2002) and they found one CP candidate (#68 according to WEBDA) within the investigated sample. A follow-up work (Paunzen et al., 2003a) presented additional Strömgren *uvby* data for this open cluster, which is located ~ 1600 pc away from the Sun. Based on the new Strömgren photometry, they concluded that it is a probable B8 Si star. However, they mentioned the possibility of a problematic photometric standardization due to the use of only three (spectrophotometric) standard stars. Indeed, during preparation of the photometric data for the parameter study presented in Sect. 6.1.1, we have noticed slight gradients in the colours if compared with available *UBV* photometry. For this purpose,

the Strömgren data were transformed to the Johnson system using the equations given by Harmanec & Božić (2001). Nevertheless, the zero point seems to be near the colours of the peculiar candidate, resulting in an agreement of the temperature deduced using UBV and the original Strömgren photometry. We determined a temperature of 11500 K, supporting the estimated spectral type by Paunzen et al. (2003a). The position of the star in the HRD agrees perfectly with the determined age of ~ 140 Myr. Inspecting the proper motion of this object, one can notice that the data of PPMXL support a definite kinematic membership, whereas based on UCAC-4 data by no means a positive membership can be concluded. However, since the determined reddening for the object coincides with the cluster mean, we adopt a probable membership for it.

5.2.15 NGC 6204

The observations of the 100 Myr old cluster NGC 6204 by Paunzen et al. (2003b) cover the whole cluster area with a magnitude range of ~ 9 mag. In total, 319 stars were measured in the Δa system. However, since many objects have masses well below $1.5 M_{\odot}$, we rejected them for further analysis, since CP stars are not expected anymore at lower masses; 59 main-sequence members remained. Although the latter reference obtained a very low detection limit of 7 mmag, no CP candidate was detected.

5.2.16 NGC 6208

NGC 6208 is another cluster that seems to have no CP stars. Furthermore, Paunzen & Maitzen (2001) found no evidence of other peculiar objects such as Be/Ae or metal-weak stars among 41 studied objects. Most of them turned out to be non-members (16 stars remained), which is in agreement with Lindoff (1972) who concluded that only half of the objects in the innermost cluster region are true members. With an age of ~ 1.2 Gyr it is the oldest aggregate in our sample. The non-presence of CP stars is in agreement with other old programme clusters.

5.2.17 NGC 6250

Two definite CP2 candidates were found by Bayer et al. (2000) in this rather young (~ 20 Myr) obscured cluster, located at a distance of ~ 900 pc. Sufficient photometry is available for these objects to determine effective temperature and masses. Their position in the HRD perfectly agrees with the estimated age, further indicating membership. Inspecting available proper motions and membership probabilities, we have noticed a similar result like for NGC 3228 (see Fig. 5.1). Dias et al. (2006) seem to have calculated the probabilities in an inverse way. The most deviating objects have highest value probability, in contrast to stars following the mean cluster motion. However, the individual proper motions for these two stars do not contradict membership.

5.2.18 NGC 6396

With an age of about 30 Myr, the open cluster NGC 6396 is the oldest cluster in the investigation by Paunzen et al. (2002), but no chemically peculiar candidate was detected, as in the other surveyed clusters. It also exhibit differential reddening, therefore a de-reddening of all individual objects was necessary. Several of the studied objects have masses below $1.5 M_{\odot}$, the lower limit where CP stars are expected. After a careful member selection, 51 observed cluster members in the mass range of $1.5\text{--}7 M_{\odot}$ remained.

5.2.19 NGC 6451

Rather different cluster parameters can be found in the literature for this open cluster, as it was already discussed by Paunzen & Maitzen (2002). These data are ranging from ~ 600 to 2100 pc in distance, and 60 Myr to 4 Gyr in age. Our analysis results in an age of 130 Myr and a distance of 2070 pc. The above mentioned reference found one CP candidate in this cluster with a high Δa index of +78 mmag. Additional Strömgen photometry was published by Paunzen et al. (2003a), but as for NGC 6192 (see Sect. 5.2.14) the photometry is affected by a slightly wrong standardization. The same holds for the V magnitudes measured by Piatti et al. (1998), which is about 1 mag too bright (see also Sect. 6.2). Based on the new Strömgen data, Paunzen et al. (2003a) concluded that the peculiar candidate (WEBDA #714) is a unreddened G-type star. Taking the somewhat erroneous photometry into account in combination with additional data we confirm their assumption, but it is probably even a cooler object of spectral type K. This result is similar to the findings for NGC 5999 (see Sect. 5.3.9), where also cool foreground objects have pretended a CP nature due to their large Δa indices. We therefore also rejected NGC 6451 #714 from our sample.

5.2.20 NGC 6611

NGC 6611 is located in the Eagle nebula and hence another very young aggregate in our sample with an age of ~ 3 Myr. Like all clusters in the study by Paunzen et al. (2002) it also shows no evidence of chemically peculiar objects. However, two stars deviate from the normality line (WEBDA #198 and 229), but both are most likely non-members according to Paunzen et al. (2002). The star #198 is listed as Herbig Ae/Be type object in the *Catalogue of Stellar Spectral Classifications* (Skiff, 2012). Furthermore, in Hillenbrand et al. (1993) for one object (#468) in the vicinity of the cluster a spectral type of B1 Vp is listed. Although its proper motion does not contradict membership, it is somewhat too distant from the cluster center to belong to it. We therefore conclude that NGC 6611 is another open cluster free of classical CP2 stars.

5.2.21 NGC 6705

Two CP candidates were found by Paunzen et al. (2003b) in this intermediate age (~ 200 Myr) very rich open cluster. For one object (# 863 according to WEBDA)

we have found several membership studies (e.g. Dias et al., 2006; McNamara et al., 1977), both listed a high percentage for this star. Since the other object (#987) is located in a crowded group of stars, the latter reference has not investigated it on their photographic plates. In contrast to Dias et al. (2006) using UCAC-2 data, who list only 39% probability. However, due to the crowded field, we conclude that this result is unreliable. Both objects are well within the cluster boundaries and do not deviate in the colour-magnitude diagrams compared to other members. This cluster exhibits a somewhat overabundant metallicity compared to the Sun. Gonzalez & Wallerstein (2000) have determined a metallicity of $[Fe/H]=0.1$ or Thogersen et al. (1993) even a value of 0.21 dex. The work by Paunzen et al. (2003b) also discussed the divergent photometric results for the cluster. We therefore used as far as possible the data by Stetson (2000), who has established photometric standard stars in this field.

5.2.22 NGC 6756

In total, three photometric peculiar objects were found by Paunzen et al. (2003b), whereas one of them belongs probably to the group of λ Bootis stars. From the remaining two CP2 candidates, one (WEBDA #33) is according to the Strömgren indices, measured by Delgado et al. (1997), an unreddened late-type star (see Paunzen et al., 2003b). Furthermore, the proper motions deviate significantly from the cluster mean, Dias et al. (2006) list a probability to be a cluster member of only 15%. Unfortunately, the other one (#24) is in a rather crowded area in the very center of the cluster, therefore no proper motion data are available for it. However, as mentioned in Paunzen et al. (2003b), the photometric indices are typical for a B8 Si-type object. Furthermore, its position in the HRD agrees nicely with the cluster age of 130 Myr.

5.2.23 Pismis 20

Pismis 20 is a highly reddened young open cluster located at a distance of ~ 2800 pc. With an age of ~ 5 Myr it is among the youngest representatives of our programme clusters. However, the accurate determination of age in such aggregates is rather difficult, since no turn-off point is visible; results ranging from 2–10 Myr can be found in the literature. Photometry in the Δa system was performed by Paunzen et al. (2002) and they found no CP objects in this cluster although in total 80 exposures were obtained. Since strong differential reddening is present in this area, they had to de-redden all individual objects to obtain a useful Δa diagnostic diagram. Out of the 238 stars measured in the cluster area, we have estimated the number of main-sequence cluster stars to about 80.

5.3 CCD Δa survey - Part II

5.3.1 Berkeley 11

Although 80 Myr years old, this cluster exhibits a strong differential reddening. Furthermore, the extinction law towards Berkeley 11 seems to be not standard. We there-

fore adopted $R = 2.6$ obtained by Yadav & Sagar (2002). Three CP candidates were detected by Paunzen et al. (2006b), which are members according literature (e.g. Yadav & Sagar, 2002), but also proper motions do not contradict their membership. Two further stars show rather large positive Δa indices of more than +100 mmag. On the one hand they are probably not classical CP objects, on the other hand membership is doubtful due to their position in the colour-magnitude diagram.

5.3.2 Berkeley 94

Paunzen et al. (2006b) examined the peculiar content of the very young distant cluster Berkeley 94. Unfortunately, it is another poor investigated cluster. For none of the two detected CP candidates suitable photometric data is available, since these are rather faint ($V \sim 15-16$ mag). Furthermore, due to the small total number of investigated stars in other photometric systems, a calibration of e.g. $(B - V)$ based on $(g_1 - y)$ is hardly possible. We found 33 main sequence members and also positive membership of the CP candidates.

5.3.3 Haffner 15

Haffner 15 is another young cluster with an age of 25 Myr. Paunzen et al. (2006b) detected two CP candidates among 83 studied cluster members. Unfortunately, additional photometry by Vogt & Moffat (1972) is only available for some stars, insufficient for a proper transformation to $(B - V)$, and therefore no estimation of temperature and mass for the studied cluster members is possible. For one of the identified CP objects (WEBDA # 109) UBV measurements by Vogt & Moffat (1972) are available. The determined high temperature indicates that this star, if it is of peculiar nature, probably belongs to the CP4 group. The position in the HRD is close to the TAMS, but if fitting isochrones to the CMD of the cluster, this object is well below the turn-off point to the red giant branch. Furthermore, the fitted isochrone in Paunzen et al. (2006b) is far from being satisfactory, indicating additional difficulties in this cluster. Due to all mentioned problems, we decided to exclude this cluster from our sample.

5.3.4 King 21

Five CP candidates were detected in this open cluster. It is one of the few northern clusters in our sample studied by Netopil et al. (2007) using Δa photometry, obtained at the 1.5 m telescope of the Sierra Nevada Observatory (OSN) in the province of Granada. Unfortunately, not many additional photometric measurements were available at that time, making a decision about membership difficult. Although the peculiar objects deviate somewhat from the cluster main sequence, the authors assumed that they are members. This conclusion was based on their position in the cluster and the results by Mohan & Pandey (1984); the only available UBV study for King 21 at that time, which determined a non-uniform reddening in this cluster with a scatter of 0.21 mag. However, for the faint CP candidates in the range of V 15-17 mag our Δa photometry was the only available source. Examining e.g. the near-Infrared 2MASS diagrams one

can notice that the locations of the CP stars is dominated by the field population. Even the strong differential reddening can not explain the position of the stars in the CMD. Hence, all CP stars turn out to be no cluster members. For two of them considerable Δa indices of about +80 mmag were measured. They are probably, similar to the findings in NGC 5999 (see Sect. 5.3.9), less reddened cool-type foreground objects. However, additional photometry such as in the Strömgen system and/or spectroscopic follow-up observations are desirable.

5.3.5 Lyngå 1

The study by Paunzen et al. (2006b) has detected numerous stars that are deviating from the normality line. Even after a restriction to stars earlier than spectral type F5, one third of the investigated objects show different kinds of peculiar nature. Including one star with a doubtful positive Δa index due to variability, in total six CP candidates were found as well as seven Be/Ae or metal-weak objects. After a further membership analysis, five CP members out of about 60 cluster stars remained in our sample, of which most have masses below $1.5 M_{\odot}$. Also the CP candidates have all masses at the lower border, or even slightly below. Additionally, this cluster exhibit a non standard reddening law. We used the result of $R = 3.5$ by Vázquez et al. (2003) for the further analysis.

5.3.6 NGC 1502

In the study by Paunzen et al. (2005c) the northern young cluster NGC 1502 (< 10 Myr) was included. They have detected one strong positive Δa object (# 27 according to WEBDA). With an Δa index of +88 mmag, it exhibits one of the highest value ever observed. Several studies based on proper motion and photometry confirm the cluster membership. Furthermore, the peculiar nature is also approved by *Geneva* photometry. North & Cramer (1981) list a rather high value of +58 mmag for $\Delta(V1 - G)$. Since the reddening law towards NGC 1502 is not standard, we used $R = 2.57$ instead (Pandey et al., 2003).

5.3.7 NGC 3105

Rather different results for the distance, ranging from $\sim 5 - 9$ kpc, can be found in the literature for NGC 3105. Our analysis resulted in a distance of 7.3 kpc as well as in an age of about 20 Myr. This open cluster is therefore the most distant object in our sample. Paunzen et al. (2005c) found one single CP candidate within the cluster boundaries, which is a probable member. Due to the large distance, the cluster exhibits an angular diameter of only $\sim 1.5'$ and an interstellar reddening of $E(B - V) \sim 1$ mag.

5.3.8 NGC 3293

The CP content of NGC 3293, a very young (~ 10 Myr old) cluster located at a distance of ~ 2400 pc was studied by Netopil et al. (2007). They have found no single CP

candidate among 241 investigated cluster stars, although the detection limit was rather low. After a careful membership analysis and estimation of masses for all objects, about 100 cluster main-sequence members remained for the further analysis.

5.3.9 NGC 5999

In the 400 Myr old open cluster NGC 5999 three CP candidates were detected by Ne-topil et al. (2007). All objects deviate somehow in the Δa CMD as presented by the latter reference, which can be interpreted as higher reddening. However, only one star (WEBDA #119) can be considered as probable member if the $(B - V)$ data by Piatti et al. (1999) are used as criteria. In addition, 2MASS data and the corresponding CMD show only a reasonable agreement for the latter object, whereas the other two stars deviate significantly. This cluster is located in a rather crowded area, making an additional membership analysis with proper motion difficult. While UCAC-4 data suggest membership for that object, the PPMXL catalogue entry would imply a definite non-membership. However, since all candidates exhibit unusual large Δa values (+92 mmag for # 119), especially if considering the estimated temperature of < 8500 K and the temperature dependency of Δa (see Fig. 3.4 in this respect), we conclude that all three objects are not real CP stars. The combination of optical and near-infrared (NIR) 2MASS data suggest that they are close-by nearly unreddened G/K type dwarf stars. The large Δa values can be explained by their lower reddening as well as the much steeper slope of the normality line at such cool temperatures.

5.3.10 NGC 6031

Two CP2 candidates (#73 and 85 according to WEBDA) were detected by Paunzen et al. (2006b) in the open cluster NGC 6031, whereas only for the first one additional BV CCD measurements are available. For the second one only photographic data in the UBV and RGU system can be found, which do not offer a reliable use. We therefore had to use transformed Δa colours. Unfortunately, the available proper motion data are inconclusive, rather large deviations between UCAC-4 and PPMXL can be found for these objects. Therefore, these two CP candidates, of which one shows a slight Si nature (Paunzen et al., 2011c), remained in our sample as cluster members.

5.3.11 NGC 6268

The study by Clariá et al. (2006) confirmed the presence of some red giants in the cluster NGC 6268, not taken into account in several previous studies such as Paunzen et al. (2005c). Therefore, the age was sometimes somewhat underestimated. Using only such investigations and our analysis, which include their presence, we estimated an age of 160 Myr. Five possible CP candidates were found in the Δa study by Paunzen et al. (2005c), of which four remained after a further careful membership analysis using e.g. also the results by Dias et al. (2006). Additionally, for three stars Paunzen et al. (2011c) confirmed the peculiar nature by means of classification spectroscopy.

5.3.12 NGC 6405

This close (~ 500 pc) cluster with an age of ~ 80 Myr is well studied in several photometric systems, allowing an accurate determination of mass for the individual objects. Additionally, it was a further aggregate studied in the photoelectric (Maitzen & Schneider, 1984) and CCD Δa survey (Paunzen et al., 2006b), yielding excellent agreement for the three detected CP candidates. Their probable CP nature and cluster membership was determined by Landstreet et al. (2007), an additional spectroscopic confirmation was presented by Paunzen et al. (2011c).

5.3.13 NGC 6802

Five positive Δa detections were made in this rather old cluster (1 Gyr) by Netopil et al. (2007), but except one all of them are either too cool to be classical CP stars or are placed along the giant branch. No additional measurements in other photometric systems were available at that time for the remaining star, but its position in the Δa colour-magnitude diagram already suggested membership. Recently, Janes & Hoq (2011) presented a thorough photometric analysis of this cluster, strengthening its membership. They also flagged that star with positive membership.

5.3.14 NGC 6830

In total, four objects show a positive Δa index in the investigation by Netopil et al. (2007), whereas at least two of them are probably classical CP stars according to their colours. However, if inspecting the corresponding colour-magnitude diagrams, one of them (WEBDA # 38) is shifted to redder colours. Since no differential reddening is evident in this cluster, we conclude after inspecting 2MASS data that it is a probable non-member. Also the available proper motions deny cluster membership for the three objects. For the remaining star (# 166 in WEBDA), Dias et al. (2006) list 35% probability of membership, but their determined mean cluster motion differs somewhat compared to several other studies like Loktin & Beshenov (2003) or Kharchenko et al. (2005). Using their results, this object will obtain a much higher probability. Also the recent UCAC-4 and PPMXL catalogues support membership. Therefore, this star remains in our sample.

5.3.15 NGC 6834

Beside several Be/Ae objects, two CP2 candidates were found by Paunzen et al. (2006b) in this 60 Myr old aggregate, but just for one peculiar object (WEBDA # 412) photographic UBV measurements are available. Due to the low accuracy of photographic data, into $(B - V)$ transformed Δa colours were used for the further analysis. No entries in the proper motion catalogues PPMXL and UCAC-4 can be found. On the other hand, the position of the stars in the CMD's does not contradict membership.

5.3.16 NGC 7235

According to Paunzen et al. (2005c), three CP candidates were found in this young and distant cluster (< 10 Myr, ~ 3000 pc). With positive Δa indices between ~ 30 – 60 mmag, they are well separated from the normality line. Due to their faintness (V 16–17 mag), no additional measurements in other photometric systems are available. Also the few available proper motion data are not meaningful due to the low number of individual measurements and the resulting errors. Therefore, a membership analysis is only possible by means of their position in the cluster and in the colour-magnitude diagram. Both criteria do not contradict membership. Using temperature and luminosity, determined via the Δa data, masses around $2 M_{\odot}$ were estimated.

5.3.17 NGC 7296

This cluster is the only one in our sample, for which no other data were available before the study by Netopil et al. (2005). They combined BVR photometry and Δa measurements, obtained at two different sites. One positive CP star detection was presented by this reference. Furthermore, several Be and metal-weak candidates were found in this aggregate. Concurrently, a study for this cluster by means of near infrared 2MASS data was published by Tadross (2006). He obtained a much older age of 315 Myr compared with Netopil et al. (2005), who determined 100 Myr. Using data taken from the recent APASS survey release, we found some disagreement of the optical measurements mentioned above. After a correction and the application of the method presented in Sect. 6.1.1, we confirm the age presented by Tadross (2006). However, a somewhat higher reddening was determined. Both, photometric and kinematic data support a definite membership of that CP candidate.

5.3.18 NGC 7510

Beside the confirmation of two previously known Be stars, no classical CP objects were detected in NGC 7510 by Paunzen et al. (2005c), although nearly the complete mass range occupied by CP stars is covered. Inspecting its galactic location and distance, one can notice that the cluster lies in the Perseus arm of the Milky Way close to NGC 7235, an aggregate of comparable age (~ 10 Myr), located at about the same distance (2900 pc). Furthermore, more or less the same number of cluster members were observed. Although both are probably born in a similar environment, the number of detected CP objects differs. The only difference at first sight is their visual appearance. Whereas NGC 7235 looks like a loose conglomerate of stars, NGC 7510 is more compact, corresponding to the Trumpler classification (III 2 p and II 2 m for NGC 7235 and NGC 7510, respectively).

5.3.19 Ruprecht 44

This cluster was included in the survey by Netopil et al. (2007), who have listed several CP candidates. Some difficulties are combined in this cluster, making a membership investigation difficult. It is a rather distant (~ 4400 pc) and very young (~ 10 Myr)

open cluster, exhibiting also differential reddening. Therefore, a membership analysis by means of proper motions is not expected to be successful. Furthermore, due to the differential reddening, it is out of scope to determine accurate effective temperatures for individual stars. No additional photometry is available for the CP candidates and all other stars measured in this field, which allow to determine individual reddening values. The differential reddening also complicates a membership analysis by means of photometry. We therefore had to exclude this cluster from our sample.

5.3.20 Ruprecht 115

The peculiar content of Ruprecht 115 was investigated by Netopil et al. (2007). They found 10 objects that show a positive Δa index. Some of them were already excluded by this reference due to extreme Δa values of ~ 200 mmag and more, variability, or colour index (temperature). From the remaining six stars, we had to reject three further ones, since they are deviating too much from the main sequence. Although for one star (WEBDA #38), the UCAC-4 proper motions deviate from the cluster mean, we keep the star as member, because data of two epochs were used only to calculate its motion. In general, we noticed strong differences between UCAC-4 and PPMXL data, especially of the motion in declination. We therefore have not used proper motions as additional membership criteria. The brightest CP candidate (WEBDA #7) was also a target by Paunzen et al. (2011c), who determined a spectral type B8 SiEuSr. According to the CMD and HRD, this object (if it is a member) would be located close to the TAMS, and the position in the HRD agrees excellently with the cluster age of ~ 500 Myr. However, the spectral type is completely inconsistent with the cluster age and the determined temperature of about 8500 K, using the mean cluster reddening and the available $(B - V)$ data. Hence, it can not be a cluster member and is probably a slightly higher reddened background object. Hence, only two probable CP objects out of about 90 investigated member stars remain for further analysis. This cluster nicely demonstrates that the availability of various data is needed for a detailed study. Nevertheless, additional spectroscopic data for the other CP candidates as well as at least UBV or even better Strömgen photometry for the whole cluster is desirable.

5.3.21 Ruprecht 120

Netopil et al. (2007) list eight CP candidates, but most of them are either too cool to be classical ones, or are located close to the border of the confidence interval. The remaining four seem to be bona fide CP stars thanks to their Δa indices and their temperature, which was estimated based on photometric indices. Since most of the stars appear to be rather hot, and the cluster shows a slight differential reddening, the determination of effective temperatures, based only on $(B - V)$ measurements by Piatti et al. (1999) and the mean cluster reddening, can be probably affected. However, their position in the HRD agrees within the errors with the adopted cluster age of 220 Myr. Unfortunately, they are too faint to be observed by TYCHO, and the data taken from available proper motion catalogues are mostly in disagreement. Hence, we have not made an additional membership analysis beside the photometric criteria.

5.3.22 Ruprecht 130

Five CP candidates were detected by Paunzen et al. (2006b) in this 560 Myr old and ~ 2000 pc distant aggregate (see discussion about the parameters and the problems with available photometry in Sect. 6.2). One object (WEBDA #108) is about two magnitudes above the cluster turn off, hence very probably a non-member. A second candidate (# 570) is slightly too red and was also classified as probable non-member. Unfortunately, the available proper motions of UCAC and PPMXL deviate strongly, allowing no further membership analysis. The remaining three peculiar objects are not conspicuous in the colour-magnitude diagram as well as concerning kinematic data, and were classified as (probable) members.

5.3.23 Stock 16

This is a poorly populated very young cluster with an age of ~ 5 Myr, located at a distance of ~ 1800 pc. A detailed study was performed by Vázquez et al. (2005), who identified several pre-main-sequence stars in it. In the area of Stock 16 they found also two other populations belonging to more distant OB associations. The peculiar content was examined by Paunzen et al. (2005c), and they reported the detection of a single CP candidate (WEBDA # 12) in this young aggregate. The follow-up study by Paunzen et al. (2011c) show that it is indeed a peculiar star of Si type. A positive cluster membership status was determined by Fenkart et al. (1977) and Turner (1985), in contrast to Vázquez et al. (2005), who list it as probable non-member. Furthermore, Dias et al. (2006) presented membership probabilities based on UCAC-2 data by Zacharias et al. (2004). They determined a mean cluster motion of $-8.55 / -2.11$ (pmRA / pmDE [mas/yr]). Other studies in this respect (Kharchenko et al., 2005; Loktin & Beshenov, 2003) list values much closer to zero. We estimated the cluster motion using the UCAC-2 data to $-2.8 / -1.3$ [mas/yr], which is in very good agreement with the latter two references. The difference to Dias et al. (2006) are explained by their wrong cluster coordinates, which are $\sim 10'$ SE of the actual cluster position. This discrepancy was already mentioned by Kharchenko et al. (2005). Due to the wrong coordinates, the detected CP star was therefore not included in the study by Dias et al. (2006). Nevertheless, PPMXL as well as UCAC-4 data confirm a probable kinematic membership. This object is of special interest, since it is probably still on the pre-main-sequence (see Sect. 8.5).

Chapter 6

Open cluster parameters

In Paunzen & Netopil (2006), the current status of the open cluster parameters age, distance, and reddening was investigated. Based on a collection of parameters for several hundreds of open clusters, taken from the various literature sources, they compiled a list of open clusters with the most accurate (in a statistical sense) parameters, which can be used for testing or developing theoretical models. However, only 72 open clusters remained, which meet the therein defined criteria. For completeness, in Fig. 6.1 one can find the error distribution of the complete compiled sample. For this thesis, the above mentioned work was used as starting point to determine the parameters for the programme clusters in an iterative way. At the beginning, the collection was updated with parameter estimates overseen before, or newer ones, to calculate average values for each cluster. The various colour-magnitude diagrams (CMD's) were then examined using appropriate isochrones and the collected parameters. If a set of parameters did not yield an appropriate fit at all, it was rejected and a recalculation of the remaining parameters was carried out. This procedure was necessary only for some cluster parameters, mostly for results which were based on too few stars, a low magnitude limit, or too inaccurate data (e.g. photographic ones).

6.1 Metallicity

The majority of the above compiled cluster parameters are based on the assumption of solar metallicity, which is probably correct for most (closer) open clusters, but by far not for more distant ones, since a radial metallicity gradient within the Milky Way is well known (e.g. Chen et al., 2003), but also perpendicular through the disc. To provide an insight in the differences of stellar evolution at various metallicities, in Fig. 6.2 a comparison of 100 Myr isochrones with different initial metallicities is given, which were taken from the database of Geneva stellar evolution tracks and isochrones by Lejeune & Schaerer (2001).

Some photometric systems are capable to provide such information, most commonly the Johnson UBV , Strömngren $uvby\beta$, as well as the Washington and DDO systems, but also the Vilnius and *Geneva* systems are efficient in this respect. In order to investigate the knowledge of metallicity, Paunzen et al. (2010) have compiled such photometric metallicity estimates. In total, for 188 open clusters at least one metallicity estimate

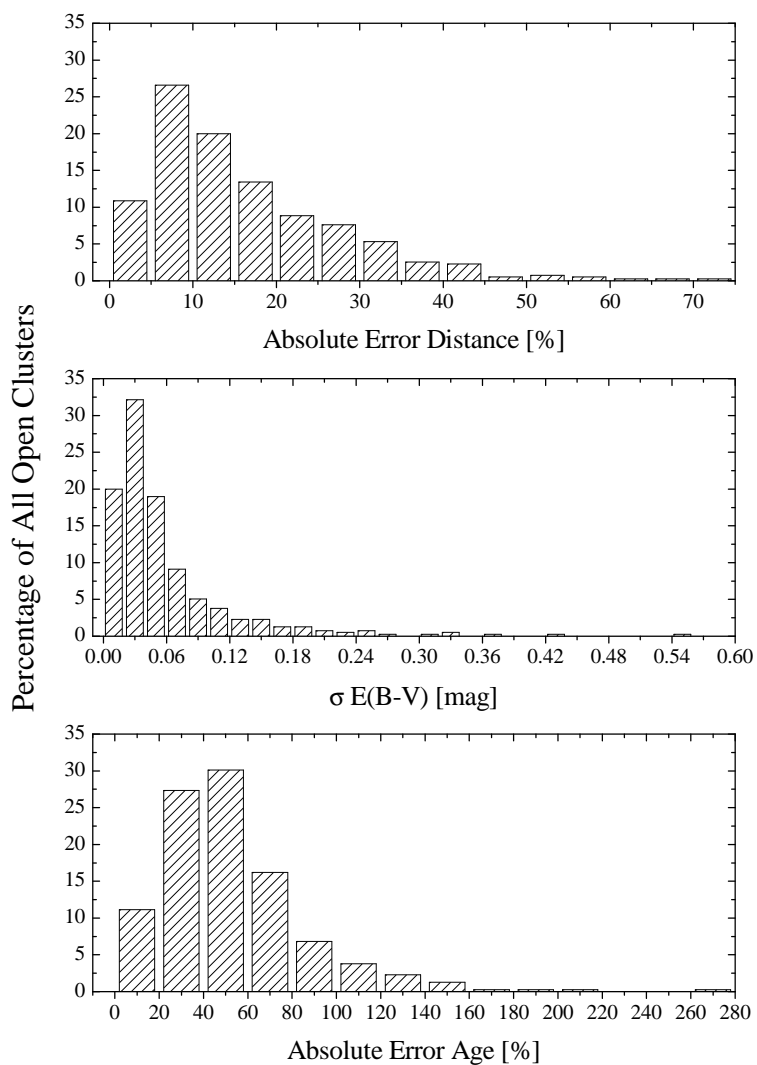


Figure 6.1: The distribution of the mean absolute errors of the distance and age as well as the standard deviation of the reddening for the complete sample of 395 open clusters with more than three independent measurements from the literature; taken from Paunzen & Netopil (2006).

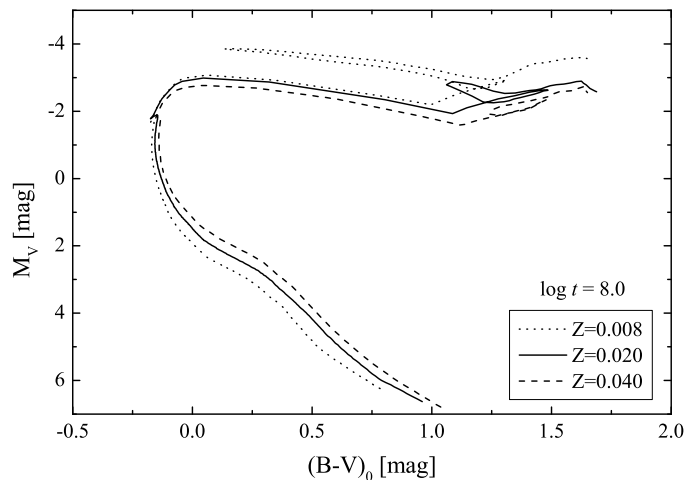


Figure 6.2: Geneva isochrones for $\log t=8.0$ in the $(B - V)_0/M_V$ plane for some metallicities.

is available, and for only 88 clusters more than one determination. Based on this sample, this reference tried to investigate the metallicity gradient within the Milky Way (see their Fig. 5). Although a gradient is recognizable, its value can by far not be determined due to the large scatter.

The second paper of this series (Heiter et al., 2013) will deal with spectroscopic metallicity determinations of open cluster stars, which should provide a more accurate information for this cluster parameter. However, if restricting them to more accurate high-resolution ($R \geq 25000$) and high signal-to-noise ($S/N \geq 50$) data, only 370 objects in 59 open clusters remained, whereas for about 40% of these clusters only data for three or less stars are available. In this respect one has to mention that also a temperature and gravity restriction was defined to sort out objects, for which the results are probably affected by non-LTE effects, but only six clusters were rejected by the latter criteria. However, the use of different reduction/analysis methods and line-lists makes it often difficult to merge available datasets, as seen in Fig. 6.3, showing the comparison of the results by Friel et al. (2003), Carretta et al. (2005), De Silva et al. (2007), and Sestito et al. (2008) for the old (1 Gyr) open cluster Collinder 261 (see Heiter et al., 2013, for details). As one can see, the mean cluster metallicity varies between $[Fe/H] \sim -0.2$ to about 0.15 dex, whereas two studies result in roughly solar metallicity. An inhomogeneous metallicity distribution within the cluster can be fairly excluded as explanation, since there are some stars in common between the studies, showing also significant offsets. Unfortunately, there are not many clusters extensively studied like Collinder 261, for the majority one has to rely on a single investigation. This clearly shows that an extensive homogeneous approach concerning metallicity determination is necessary. In this respect it is worth to mention the Gaia-ESO Public Spectroscopic Survey (Gilmore et al., 2012), which will provide high-resolution spectroscopy for about 100 000 Milky Way stars (including objects in about 100 open clusters) as preparation for the upcoming Gaia mission.

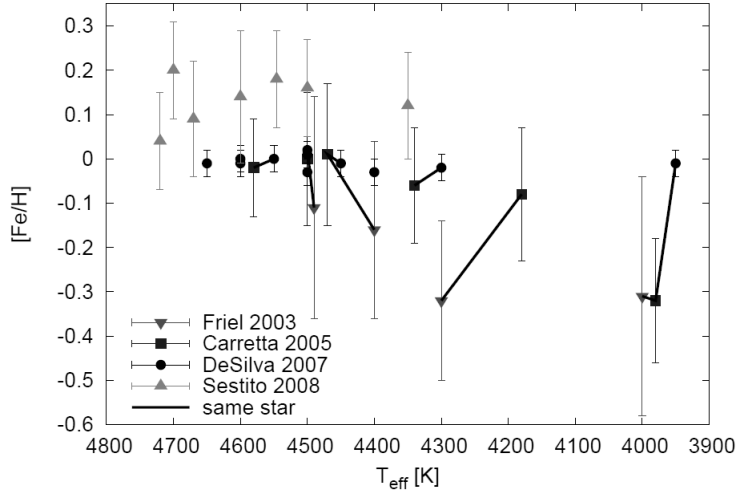


Figure 6.3: Comparison of available high resolution and high S/N metallicity determinations for the open cluster Collinder 261, taken from Heiter et al. (2013).

Nevertheless, 20 of our programme clusters were studied with respect to metallicity yet using high-resolution and high S/N spectra as listed in Heiter et al. (2013). Including also some further ones with mid-resolution and rejected ones due to the criteria of the latter reference, as well as recent additional studies, 28 clusters are covered in total.

6.1.1 A homogeneous approach to determine metallicity

In order to investigate the open cluster parameters, especially metallicity, as homogeneous as possible, we applied the method by Pöhl & Paunzen (2010). This approach takes advantage of differential evolutionary tracks (compared with the ZAMS), produced for various metallicity/age combinations (see Fig. 6.4), which have to be compared with the observed HRD of the open clusters.

Therefore, available photometric data have to be transformed into the $T_{\text{eff}}/\log(L/L_{\odot})$ plane. We made use of almost all available photometric data in the $UBV(RI)$, $wbyH\beta$, and *Geneva* systems, which are included in the WEBDA open cluster database (Sect. 4.1). However, as soon as photoelectric data cover the respective open cluster sufficiently down to lower mass stars, these were preferred over CCD studies. The transformation equations between the three above mentioned photometric systems by Harmanec & Božić (2001) were used to check the individual zero points. Whenever we noticed a significant offset, the photometric data were adjusted to the most “reliable” one. If sufficient data in the *Geneva* system are available, these were generally used for that purpose, since it provides probably the most homogeneous all-sky photometry. However, among the photoelectric studies we hardly recognized an offset or gradient, in contrast to some CCD studies (in this respect see also e.g. Fig. 4.3).

Furthermore, if several studies are available in a specific photometric system, a straight average for the stars in common was calculated. For some poorly studied

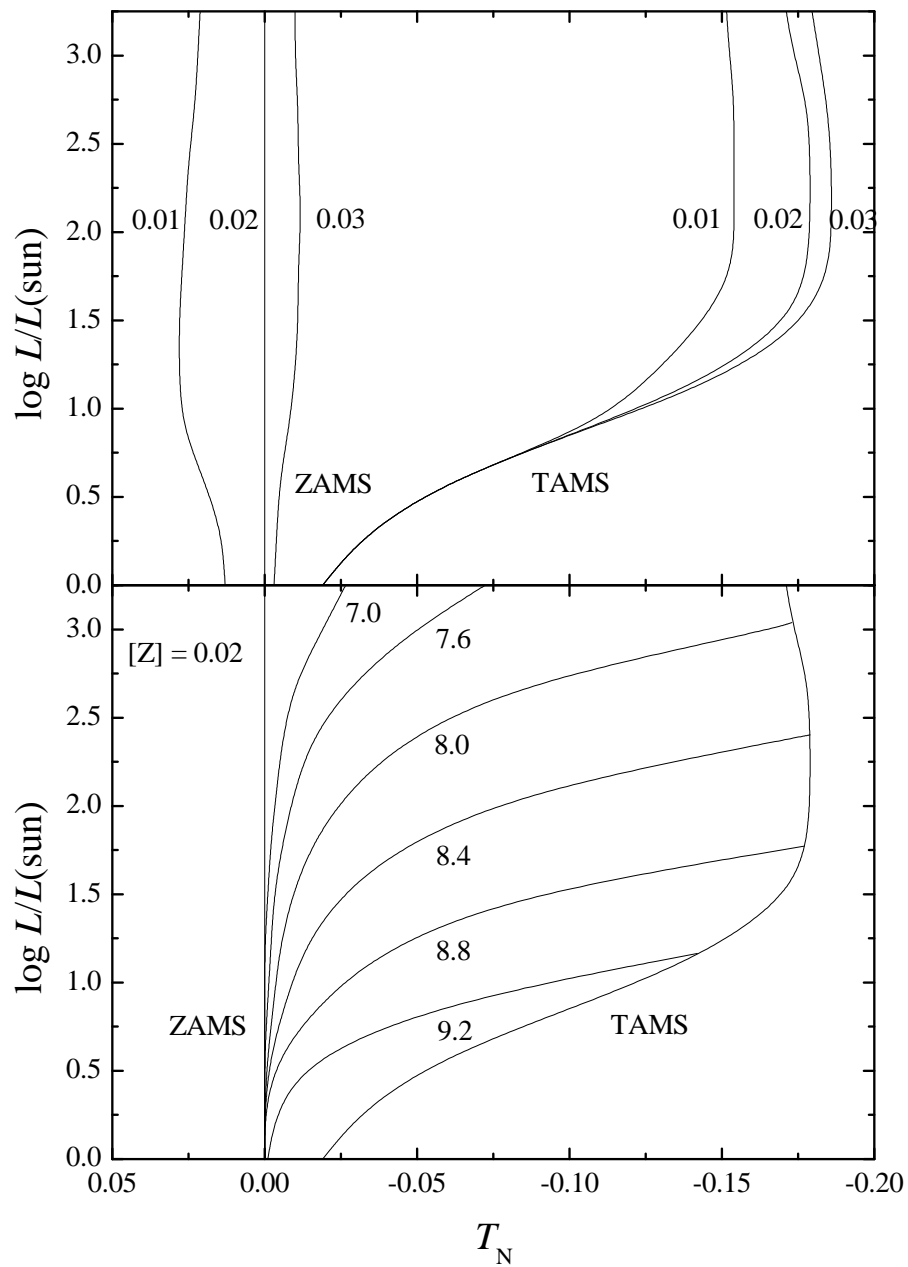


Figure 6.4: The differential evolutionary tracks by Pöhl & Paunzen (2010), which were used to deduce metallicity, as well as the other open cluster parameters. T_N stands for to the ZAMS normalised effective temperatures.

clusters, we included also B, V data taken from the APASS¹ survey (data release 6), as well as 2MASS NIR JHK_s measurements (Cutri et al., 2003), in order to use e.g. $(V - K_s)$ as temperature indicator, which provides a broad wavelength range and hence the resulting temperature is less affected by photometric errors.

However, it is crucial to define a proper temperature scale to transform the photometric data accurately. In Pöhl & Paunzen (2010), for example the metallicity dependent relations by Alonso et al. (1996) were used for the colour index $(B - V)$. We proceeded likewise and adopted also their relations for $(V - R)$. Since it is defined for the original Johnson system, and most CCD studies are on that of Cousins, the colour index was transformed using

$$(V - R)_C = 0.715(V - R)_J - 0.02$$

by Bessell (1983). Further adopted colour indices are $(V - I)$ and $(V - K)$, which are assumed to be rather metallicity independent (see Alonso et al., 1996). Since this reference provides temperature calibrations for stars of spectral type F0 and cooler only, we used directly the relations by Bessell, Castelli, & Plez (1998) for $(V - I)$ and those of Di Benedetto (1998) for $(V - K)$, which are valid for stars up to about 10 000 K. Again, the latter colour index is on the Johnson system, but since we are incorporating 2MASS NIR K_s data, which are slightly different, these have to be transformed properly. The work e.g. by Carpenter (2001) lists such transformations for a wide variety of NIR systems. In order to extend the temperature calibration also to stars earlier than spectral type F0 as given by Alonso et al. (1996) for $(B - V)$, the results by Flower (1996) were used. This author provides a compilation of “fundamental” temperatures like those of Code et al. (1976) for numerous stars of different luminosity classes, in order to derive temperature based on $(B - V)$, but also to define a calibration of the bolometric correction as a function of colour/temperature. We adopted his list, but using only luminosity class IV/V objects, and searched for available photometric data in other passbands using the General Catalogue of Photometric Data (GCPD)².

This way, we defined an extension of the relation by Alonso et al. (1996) for $(V - R)$, valid for the range of 5 000 to 10 000 K, based on a sample of 82 objects (see Fig. 6.5 and the equation below):

$$\theta_{\text{eff}} = 0.487(3) + 0.947(13)(V - R)_C$$

with a mean standard deviation of $\sigma = 140$ K.

Please note that here already the colour index in the Cousins system was used, and θ_{eff} is defined as $5040/T_{\text{eff}}$, in order to avoid a higher order polynomial fit. The use of a polynomial fit does not provide any significant improvement, the good linear regression is justified by the correlation coefficient $R = 0.993$. A comparison to Alonso et al. (1996) in the overlapping range gives an excellent agreement with differences of the order of about 50 K only, using $[\text{Fe}/\text{H}]=0$ in Alonso’s relation.

Due to the narrower spacing of the colour indices at temperatures higher than about 10 000 K, the results will be too erroneous in consideration of photometric and

¹<http://www.aavso.org/apass>

²<http://obswww.unige.ch/gcpd/gcpd.html>

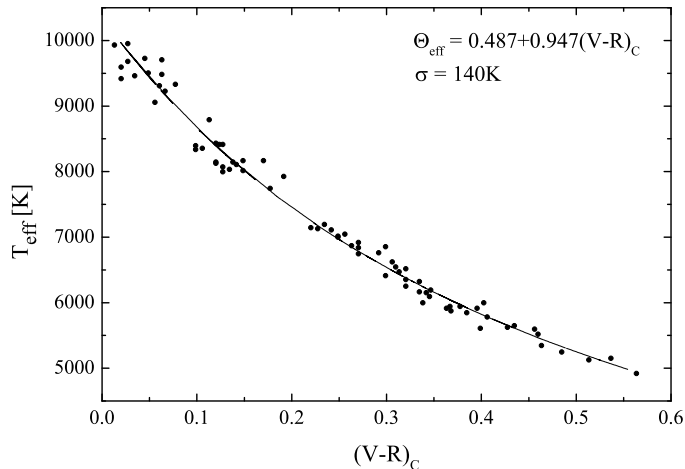


Figure 6.5: Empirical temperature calibration for the colour index $(V - R)$ on the Cousins systems.

interstellar reddening errors. For such objects, it is more efficient to use directly reddening free indices such as Johnson Q or Strömgren $[u - b]$. The first index was defined by Johnson (1958), but in the following we make use of the refined definition $Q = (U - B) - 0.71(B - V)$ given by Bessell, Castelli, & Plez (1998), in order to be consistent since also their reddening ratios to $E(B - V)$ (including the listed colour terms) for the various colours are in use. However, the difference to the “original” definition is marginal and within the errors. For completeness, the $[u - b]$ index is defined as $[u - b] = [c_1] + 2[m_1]$ with $[c_1] = c_1 - 0.2(b - y)$ and $[m_1] = m_1 + 0.32(b - y)$ (Crawford & Mandwewala, 1976). As for the previous temperature relation presented above, we made use of the hotter stars given by Flower (1996). These were extended with results for O/B type stars presented in the works by Morel et al. (2008), Przybilla et al. (2008), Simón-Díaz (2010), Nieva & Simón-Díaz (2011), and Lefever et al. (2010), whereby from the latter reference only the “well-studied” objects were adopted (see the reference for details). If more than a single temperature estimate was available, an average was calculated. No significant offsets or trends (within the respective errors) were found between common stars of the different studies. The compiled list of stars was checked for luminosity class and variability, if known. Several Beta-Cephei type stars or slowly pulsating B-type objects (SPB) were rejected, in order to prepare a list of non-variable main-sequence stars. Furthermore, using photometric data in the Johnson, Geneva, and Strömgren systems, we estimated the reddening of the objects to exclude also stars, which exhibit $E(B - V) > 0.1$ mag, in order not to influence the results with objects probably exhibiting an interstellar reddening law different from the “normal” total-to-selective extinction value $R_V = 3.1$ (e.g. stars in associations). However, using the latter criterion only a few stars were rejected. In total, 44 objects define our final list of fundamental temperatures, whose relations to the Johnson Q and Strömgren $[u - b]$ index are presented in Figs. 6.6 and 6.7, respectively, with mean standard deviations of about 350 K for both empirical calibrations:

$$\theta_{\text{eff}} = 0.522(2) + 0.417(4)Q$$

$$\theta_{\text{eff}} = 0.169(3) + 0.236(20)[u - b] + 0.074(33)[u - b]^2 - 0.044(15)[u - b]^3$$

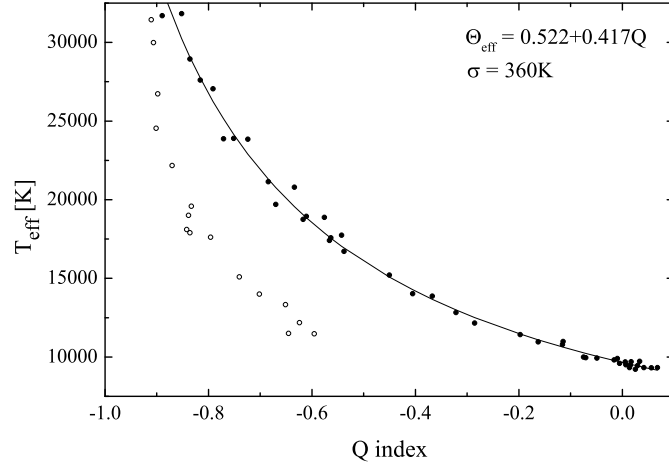


Figure 6.6: Empirical temperature calibration for normal B-type stars (the restricted sample) using the *UBV* *Q*-Index. Open circles represent supergiants (luminosity class I a/b).

Furthermore, we defined the equations also for the whole sample, consisting of 90 objects, including the above mentioned higher reddened stars, as well as luminosity class III objects, Beta Cephei, and SPB ones, which are in good agreement with the equations given above, but with mean standard deviations twice of the previous results (~ 700 K). These equations, which can be found for completeness below, are also resulting in slightly higher temperatures (1% only) at the upper temperature end:

$$\theta_{\text{eff}} = 0.523(3) + 0.420(5)Q$$

$$\theta_{\text{eff}} = 0.167(3) + 0.232(22)[u - b] + 0.088(40)[u - b]^2 - 0.052(19)[u - b]^3$$

As can be seen in Figs. 6.6 and 6.7, supergiants deviate significantly from the relation of main-sequence objects, but the use of the investigated reddening-free indices as temperature indicator would result in rather large errors due to the steep slope, especially at the hotter part. Nevertheless, up to 15 000 K it is possible to use them for temperature determination. However, for the present study such an investigation is not required, since only main-sequence stars are considered for the following metallicity determination.

It is essential to compare the above defined temperature scale with various results from the literature, which is presented in Fig. 6.8. Using *Geneva* photometry, the grids by Künzli et al. (1997), as well as the reddening free parameters X and Y, as defined by Cramer & Maeder (1979) (see their definition also below), we determined the effective temperature for the above defined reference star sample.

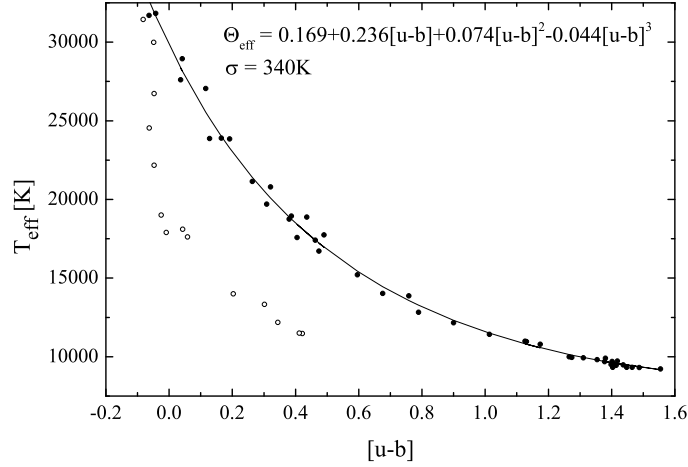


Figure 6.7: Empirical temperature calibration for normal B-type stars (the restricted sample) using the reddening free $[u - b]$ Strömrgren index. Open circles represent supergiants (luminosity class I a/b).

$$X = 0.3788 + 1.3764U - 1.2162B1 - 0.8498B2 - 0.1554V1 + 0.8450G$$

$$Y = -0.8288 + 0.3235U - 2.3228B1 + 2.3363B2 + 0.7495V1 - 1.0865G$$

However, for cooler stars ($< 10\,500$ K) these parameters are not generally applicable, therefore the pT/pG parameters have to be used (see Künzli et al., 1997). Although a scatter of about 5% can be noticed, the *Geneva* results are in excellent agreement compared to the reference sample, with a negligible median offset of 5 K, or a straight mean deviation of -160 K (literature – this work). The noticeable scatter is due to the decrease of the sensitivity of photometry towards higher temperatures (Künzli et al., 1997).

A further widely used temperature calibration was provided by Napiwotzki et al. (1993) for Strömrgren $wby\beta$ photometry. They presented updated routines of those by Moon & Dworetzky (1985), using extended grids of the latter reference with an additional empirical temperature determination based on the reddening free $[u - b]$ index. However, the latter calibration rests upon only 14 “fundamental” stars in total. Compared to our new relation for this colour index, the former calibration results in somewhat lower values of the order of 500 K at about 22 000 K. On the other hand, the “TEFLOG” routines by Napiwotzki et al. (1993) applied to Strömrgren photometry gives offsets from the reference stars below -70 K for both average functions (mean and median). We have to note that for the latter two calibrations (*Geneva* and TEFLOG) we always used solar metallicity, which can be justified by the rather bright and therefore close-by objects.

The work by Lyubimkov et al. (2002) presented a temperature relation for the Johnson Q index using the model atmospheres by Kurucz (1993). As can be seen

in Fig. 6.8, this temperature scale compared to our one results in significantly lower values, reaching already a 2 000 K difference at a temperature of 30 000 K.

Another calibration for Strömgren photometry, making use of models by Kurucz (1979) and synthetic colours, is given by Balona (1984). The difference to our temperature scale is included in Fig. 6.8, showing also a significant underestimation of temperature for the hotter stars. Balona (1994) presented a revision of this temperature calibration using more recent model atmospheres together with an additional correction to match “fundamental” stars with synthetic colours, showing a rather good linear agreement with our scale, but with an offset of about -200 K.

In Daflon et al. (1999) an empirical temperature relation for the Q -index was defined based on a sample of stars with temperature determinations using an iterative procedure with Strömgren and spectroscopic data. Their Q relation results in somewhat higher temperatures (~ 500 K, see Fig. 6.8). In a follow-up work (Daflon et al., 2004), they supposed that their former temperature scale is 1 300 K too high. However, they used the scale by Balona (1984) and the $[u - b]$ relation of Napiwotzki et al. (1993) for this conclusion with an additional comparison to Lyubimkov et al. (2002). They noted that the first two scales are in agreement within 100 K, but we are not able to retrace this. Although at lower temperatures ($\sim 10\,000$ K) they are in very good agreement, at higher temperatures they differ significantly (1 500 K at a temperature of 30 000 K).

Furthermore, we made use of the models by Bessell, Castelli, & Plez (1998) to construct an additional theoretical relation for the Q -index. These models are based beside others also on those by Kurucz (1993). We restricted their grid to entries with $\log g = 4.0$, resulting in a similar (lower temperature) behaviour like Lyubimkov et al. (2002) (see Fig. 6.8). See the discussion in the Appendix E by Bessell, Castelli, & Plez (1998) about the problems of reproducing synthetic colours and their mismatch with observational data, especially for the $(U - B)$ index, but also for the $(B - V)/(U - B)$ plane.

We therefore conclude that theoretical relations have to be used with caution, if not properly corrected (e.g. like by Balona, 1994). For cool stars (G-K5 dwarfs), Sekiguchi & Fukugita (2000) even found a disagreement of the synthetic Kurucz colours with significant 0.07 mag in $(B - V)$. Finally, we derived a mean photometric temperature for the restricted sample using our new defined calibrations together with the *Geneva* results and the TEFLOG determinations by Napiwotzki et al. (1993). Compared to the “fundamental” effective temperatures, about 70% of the sample exhibit a deviation lower than 2%, and only three objects more than 5%, but one can not exclude systematic errors also in these “fundamental” values. Since stars with temperatures above 25 000 K are under represented (see Figs. 6.6 and 6.7), but also the standard deviation of the mean photometric temperatures shows a linear increase with temperature, in the following analysis we adopt this temperature as limit to avoid erroneous results.

Using the compiled and defined photometric calibrations, which are summarized in Table 6.1, the observational data of the programme open cluster stars were transformed into effective temperatures. As for the comparisons shown above, *Geneva* and Strömgren photometry were calibrated also for the programme clusters using the routines by Künzli et al. (1997) and Napiwotzki et al. (1993), respectively, whereas our

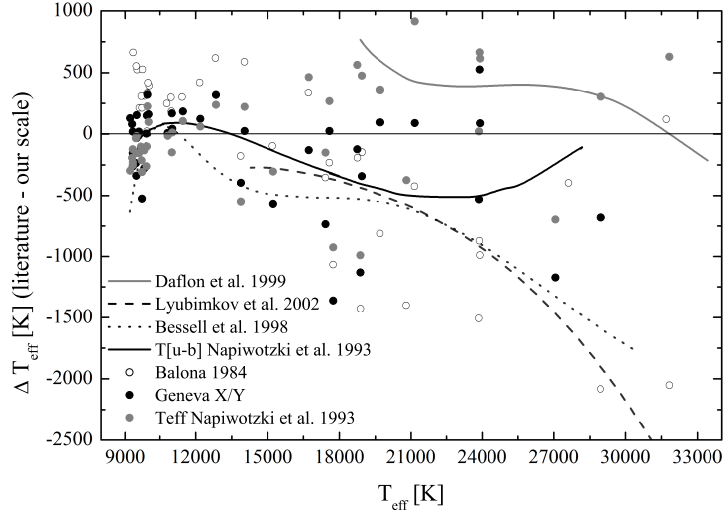


Figure 6.8: Comparison of the temperature scale in the present work to various literature results using the restricted sample defined above.

Table 6.1: Adopted temperature calibrations.

Colour / System	calibration
$UBVQ$ index	this study
$(B - V)$	Alonso et al. (1996) / Flower (1996) (for cooler / hotter stars)
$(V - R)$	Alonso et al. (1996) / this study (for cooler / hotter stars)
$(V - I)$	Bessell, Castelli, & Plez (1998)
$(V - K)$	Di Benedetto (1998)
<i>Geneva</i>	Künzli et al. (1997)
$wby\beta$	“TEFLOG” routine by Napiwotzki et al. (1993)
$[u - b]$	this study

new $[u - b]$ relation was used instead of the original one. The remaining calibrations for $(B - V)$, $(V - R)$, $(V - I)$ or $(V - K)$ were already mentioned above. Whenever possible, individual reddening values for the cluster stars were determined and averaged, if several calibrations were applied. Although in most cases these are B-type stars, which were generally calibrated using the reddening-free indices, one has a further possibility to check the temperature using e.g. $(B - V)_0$. Furthermore, the mean reddening of such objects were used also to de-redden cooler stars. As already mentioned above, we used the reddening-ratios listed by Bessell, Castelli, & Plez (1998) to be able to transform $E(B - V)$ to other colours. For completeness, Strömgren and *Geneva* reddening values were transformed as given below (see also Netopil et al., 2008):

$$E(B - V) = 1.43E(b - y) = 0.84E[B - V] = 1.14E(B2 - V1) = 0.83E(B2 - G).$$

If the available data do not allow the determination of individual reddening values, the mean cluster reddening of the compiled literature was used as a starting value, which also holds for the remaining parameters age and distance, respectively (see Section 6). Whenever we noticed a significant temperature offset e.g. between temperatures deduced via $(B - V)$ and $(V - I)$, these were scaled to the results obtained via $(B - V)$ by applying a different reddening to the other colours. This can be due to either pho-

tometric offsets or an abnormal reddening-law, but mostly it is difficult to distinguish between these possibilities. However, in Table 6.2, these few cases are marked with “reddening law?” in the last column.

Finally, all obtained temperatures were averaged, and the bolometric correction as well as luminosity were calculated. Using an iterative procedure, the parameters were changed until a best fit with the grids by Pöhl & Paunzen (2010) converged. The Figs. 6.12 to 6.21, as well as Table 6.2 represent the results for the programme clusters. In order to avoid an erroneous result, the parameters were checked also by common isochrone fitting using Geneva and Padova isochrones. It was possible to apply this method to 58 clusters in total. For the remainder there are too few usable data available, or the majority of the other clusters are simply too young for this method.

Unfortunately, it is difficult to list a meaningful error of these fits. Although the standard deviation of $[Z]$ (as listed in Table 6.2) can be used as a hint, also the number of objects, the coverage down to solar luminosity, and last but not least the quality and number of available photometric datasets has to be considered. A good example is the poorly populated open cluster NGC 1901, with only 11 main-sequence member stars usable for the metallicity determination, since several objects are already somewhat evolved. We obtained a quite accurate result of $[Z]=0.019(2)$, but the error is very probably underestimated. Also, the mean standard deviation of all investigated clusters is twice as large.

Nevertheless, a comparison of these metallicity determinations to high-resolution spectroscopic results taken from Heiter et al. (2013) and the additional literature shows an excellent agreement for $[Fe/H]$ within < 0.05 dex (see Fig. 6.10 and Table 6.2) using in total 31 open clusters. In this comparison we also included results presented by Pöhl & Paunzen (2010). Since most spectroscopic works do not provide a $[Z]$ value, which incorporates all metallic elements, it is necessary to compare the iron abundances only, which were deduced from $[Z]$ as given in the latter reference.

The isochrones defined by Pöhl & Paunzen (2010) are standardised on evolutionary grids with the former known solar metal abundance of $Z=0.020$ (Anders & Grevesse, 1989), which was in the meanwhile scaled down to $Z=0.0134$ by Asplund et al. (2009). Using a reduced solar metal content, Mowlavi et al. (2012) presented new stellar models ranging from $[Z]=0.006$ to 0.040. However, these were unfortunately provided after the begin of our investigation, and the models are yet only available up to $M = 3.5 M_{\odot}$. Nevertheless, it is worth to investigate the influence of the different metallicity scale. Therefore, we searched for a suitable open cluster with sufficient photometry and well defined parameters. Due to the aforementioned mass restriction of the new models, one is further limited to clusters with an age of $\log t \sim 8.3$, to cover the complete main-sequence and the widest possible range in luminosity. Among our programme clusters we have chosen NGC 6475 to be a good candidate for such a comparison.

Following the instructions by Pöhl & Paunzen (2010), we constructed new differential grids based on those by Mowlavi et al. (2012), using their $Z=0.014$ model as reference. This was performed for ages around $\log t=8.4$, our final result, which is in rather good agreement with the starting value ($\log t=8.34$) compiled from the literature. The best fit was obtained with the same age as in the previous analysis and $Z=0.017(4)$ (see Fig. 6.9). With the relation given in the appendix by Mowlavi

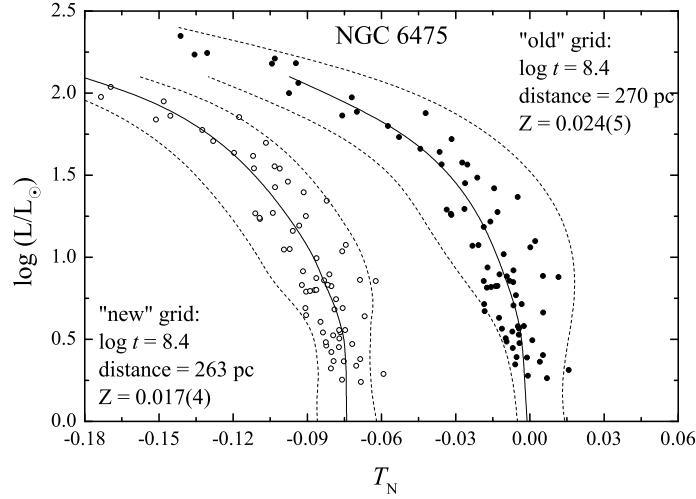


Figure 6.9: Comparison of the old and new differential grids applied to NGC 6475. For better visibility, the results based on the new grids were shifted by $T_N = 0.07$ to the left. Additionally, some isochrones for the same age but for different metallicities are shown as comparison with dashed lines: $Z=0.010/0.040$ (old grid) and $Z=0.010/0.030$ (new grid)

et al. (2012), this results in a $[\text{Fe}/\text{H}]$ ratio of 0.14 dex, whereas the original grids provide with $Z=0.024(5)$ an only slightly lower value of $[\text{Fe}/\text{H}]=0.11$. Also the applied distances correspond within a few percent, 263 pc (new grid) vs. 270 pc (old grid), whereas the latter is equal to the Hipparcos distance derived by van Leeuwen (2009). Since the overall differences are quite small, it seems that the differential grid method is rather independent of the used stellar models, the respective $[Z]$ -results just have to be transformed properly to $[\text{Fe}/\text{H}]$. However, the results have to be used with caution, since iron is not the only contributor to the overall metallicity $[Z]$. Nevertheless, both determinations are in good agreement with the mean spectroscopic iron abundance of 0.08(2) dex, derived from two sources (Sestito et al., 2003; Villanova et al., 2009), providing $[\text{Fe}/\text{H}]=0.14(6)$ and 0.03(2), respectively. Such differing results are found for some open clusters (e.g. Melotte 20 or Praesepe).

As can be seen in Fig. 6.10, the coverage of a broader range of metallicity is necessary for a more profound comparison, but already yet the agreement with spectroscopic data indicates that the method by Pöhl & Paunzen (2010) offers a rather good possibility to investigate larger cluster samples and hence to study e.g. metallicity gradients within the Milky Way.

Since ten of our programme clusters were investigated in the work by Pöhl & Paunzen (2010), we have an additional possibility to compare the results. These clusters were re-investigated according to the procedure explained above to be as consistent as possible, hence based on averaged temperatures instead of the use of a single colour index. For the majority of the objects, the resulting metallicity is in good agreement (within ~ 0.05 dex), but for three clusters (Melotte 20 a.k.a. Alpha Per, NGC 2516, and NGC 7092) the results differ significantly by more than 0.1 dex. Especially for the prominent cluster Alpha Per, the determined age shows also absolutely no agreement.

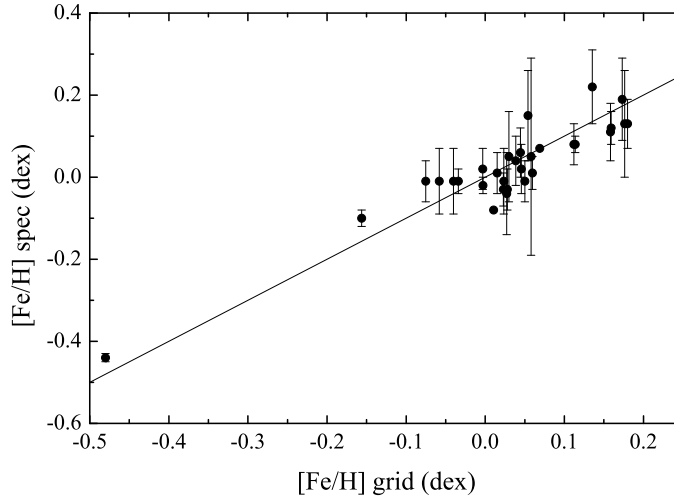


Figure 6.10: Comparison of the metallicity estimates using the method by Pöhl & Paunzen (2010) to spectroscopic values. The one-to-one relation is given as straight line.

We examined the used data by Pöhl & Paunzen (2010) for that cluster and noticed a problem with the deduced effective temperatures. For some reason these were underestimated by the reference as a function of temperature, reaching substantial 3 000 K for the hottest (brightest) stars. Hence, they obtained a much older age. This fact together with the used distances explains the differences. Whereas they adopted directly 185 pc as given in WEBDA, the present work used the mean parallax by van Leeuwen (2009) (172 pc) as starting point, reaching a comparable value of 168 pc after several iterations. The used distances are very probably also responsible for the metallicity differences of the other clusters, mentioned above. Generally, our obtained errors are smaller than those given by Pöhl & Paunzen (2010), indicating a more appropriate fit thanks to more accurate temperatures. Anyway, the cluster Alpha Per is a rather puzzling object, for which e.g. Gonzalez & Lambert (1996) found a mean $[\text{Fe}/\text{H}] = 0.17 \pm 0.06$ using three dwarf stars, whereas Boesgaard & Friel (1990) determined $[\text{Fe}/\text{H}] = -0.054 \pm 0.046$ based on four dwarf objects. Only one star is in common in both studies with a difference of 0.15 dex. Our result represents a suitable average of these spectroscopic studies. The mean metallicity presented by Heiter et al. (2013), using the defined restrictions in temperature and gravity, resulted in $[\text{Fe}/\text{H}] = 0.15 \pm 0.11$, but only two determinations remained in total. Unfortunately, no further recent study is available on this nearby open cluster.

As already mentioned at the beginning of Sect. 6.1, *UBV* and Strömgren photometry allow a photometric metallicity estimate. Another system, the *Geneva* one, was not extensively used so far to estimate this property, although it also provides a good capability. Whereas the first system makes use of the ultraviolet excess $\delta(U - B)$ at $(B - V)_0 = 0.6$, Strömgren data offers δm_1 and the *Geneva* system the index Δm_2 for that purpose. In all cases, the intrinsic colours are compared with respect to the Hyades and are calibrated to $[\text{Fe}/\text{H}]$ using a sample of well investigated field stars. For

UBV photometry we used the grid and calibration by Karataş & Schuster (2006), and *wbyβ* and *Geneva* data were treated using the work by Berthet (1990). For all systems we used only available photoelectric data listed in WEBDA. Since an accuracy better than ~ 0.01 mag for the photometric data is needed, the use of CCD measurements can often result in extreme and doubtful underabundant metallicity values (see e.g. Tadross, 2001, 2003). It is rather difficult to reproduce the standard Johnson ($U - B$) at this accuracy with the CCD technique (see e.g. Bessell, 2005). Using cluster members, selected on the basis of CMD's, colour-colour diagrams, as well as kinematic data if available, we then applied the above mentioned calibrations and calculated the respective mean values.

In Table 6.3 one can find the mean metallicity results using the three above mentioned systems, together with the determinations via the differential grid method as well as the spectroscopic measurements as comparison. Generally, a good agreement between the various methods can be found, although some deviations are also present like for Trumpler 10. However, the *wbyβ* result for this cluster is based on three stars only, making it rather uncertain. Nevertheless, for Alpha Per all systems suggest a near solar metallicity value, in agreement with the previous new result based on the differential grids and the spectroscopic study by Boesgaard & Friel (1990).

If compared to the spectroscopic results, we found the offsets

$$[Fe/H]_{spec} = [Fe/H]_{wby\beta} - 0.02 = [Fe/H]_{UBV} + 0.03 = [Fe/H]_{Geneva} + 0.03,$$

which were applied in order to calculate a mean metallicity using all available results, tightened to spectroscopic data. For those obtained via differential grids we found an excellent agreement with a negligible deviation below 0.01 dex, excluding the result for Alpha Per (see discussion above) and NGC 1901, which spectroscopic value is based on a single star only. Hence, no correction was applied to this dataset. Since the mean photometric metallicities by Paunzen et al. (2010) are more or less an uncritical combination of various results, we do not incorporate these values as additional source. It is of great importance to have a large set of clusters investigated in a homogeneous way, which have to be compared and scaled to spectroscopic results. We therefore decided to use the work by Twarog et al. (1997), which offers in total 76 open clusters (17 of our sample) based on a combination of metallicities deduced from DDO photometry and the low-resolution study by Friel & Janes (1993), brought to a common scale.

In Fig. 6.11 we show a comparison of their results to spectroscopic mean values by Heiter et al. (2013) and further spectroscopic studies listed in Carrera & Pancino (2011) with an overlap of 45 open clusters. As one can recognize, these photometric determinations underestimates metallicity somewhat. Rejecting the two deviating clusters Tombaugh 2 and NGC 6791, and restricting Twarog's list to clusters with $[Fe/H] > -0.4$, since no cluster in common with our programme sample is that underabundant, we determined a correlation of $[Fe/H]_{spec} = 0.768[Fe/H]_{Twarog} + 0.032$.

Finally, we obtained metallicity estimates via several approaches, ranging from spectroscopic data to various photometric results (*UBV*, *wbyβ*, *Geneva*, *DDO*), but also those applying the new differential grid method by Pöhl & Paunzen (2010). Although spectroscopic determinations give probably the best results, they are also

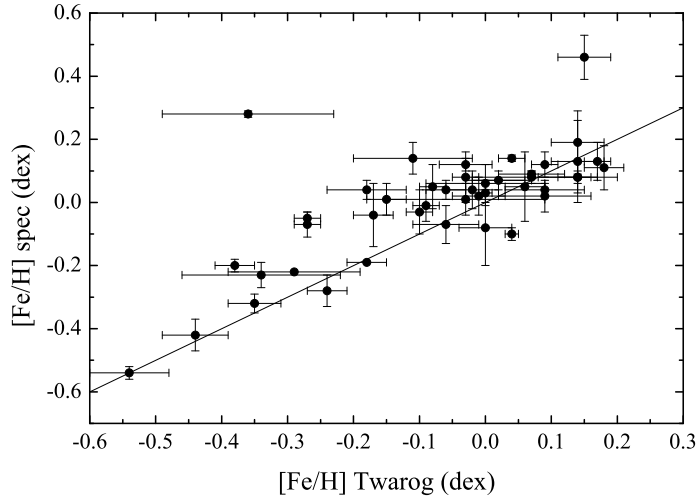


Figure 6.11: Comparison of photometric and low-resolution metallicity mean values listed by Twarog et al. (1997) compared to high resolution spectroscopic results by Heiter et al. (2013) and additional sources listed by Carrera & Pancino (2011). The one-to-one relation is given as straight line.

not error free, as can be seen e.g. in Fig. 6.3 for Collinder 261. We therefore decided to calculate weighted mean values using the following weights: spectroscopy (6), grid-method (3), for the other photometric results (2). Due to the excellent agreement with spectroscopic data without the need of an additional correction, we apply a slightly higher weight for the grid-method compared to the other photometric estimates (see e.g. Fig. 6.10). However, if individual results are based only on a limited number of stars (≤ 2 for spectroscopy or ≤ 5 for photometric mean values), the weights were reduced to 4 and 0.5, respectively. The weight of the differential grid results were set to 1, if they do not provide a clear solution, which is indicated in Table 6.2.

This way we obtained a mean metallicity for 60 open clusters in total, of which 38 are based on at least two different methods. The remaining 19 programme objects are mostly too young (13 with $\lesssim 10$ Myr) and offer no usable cool giants or dwarf stars, being too faint and probably still on the pre-main-sequence. Just for a handful of older objects, the poor available data do not allow an estimate at least via the grid-method.

Additionally, we calculated also straight mean values, which do not differ significantly from the weighted ones, indicating a rather good agreement of the various metallicity determinations. Both mean values of metallicity are presented in Table 6.5, together with the number of available estimates.

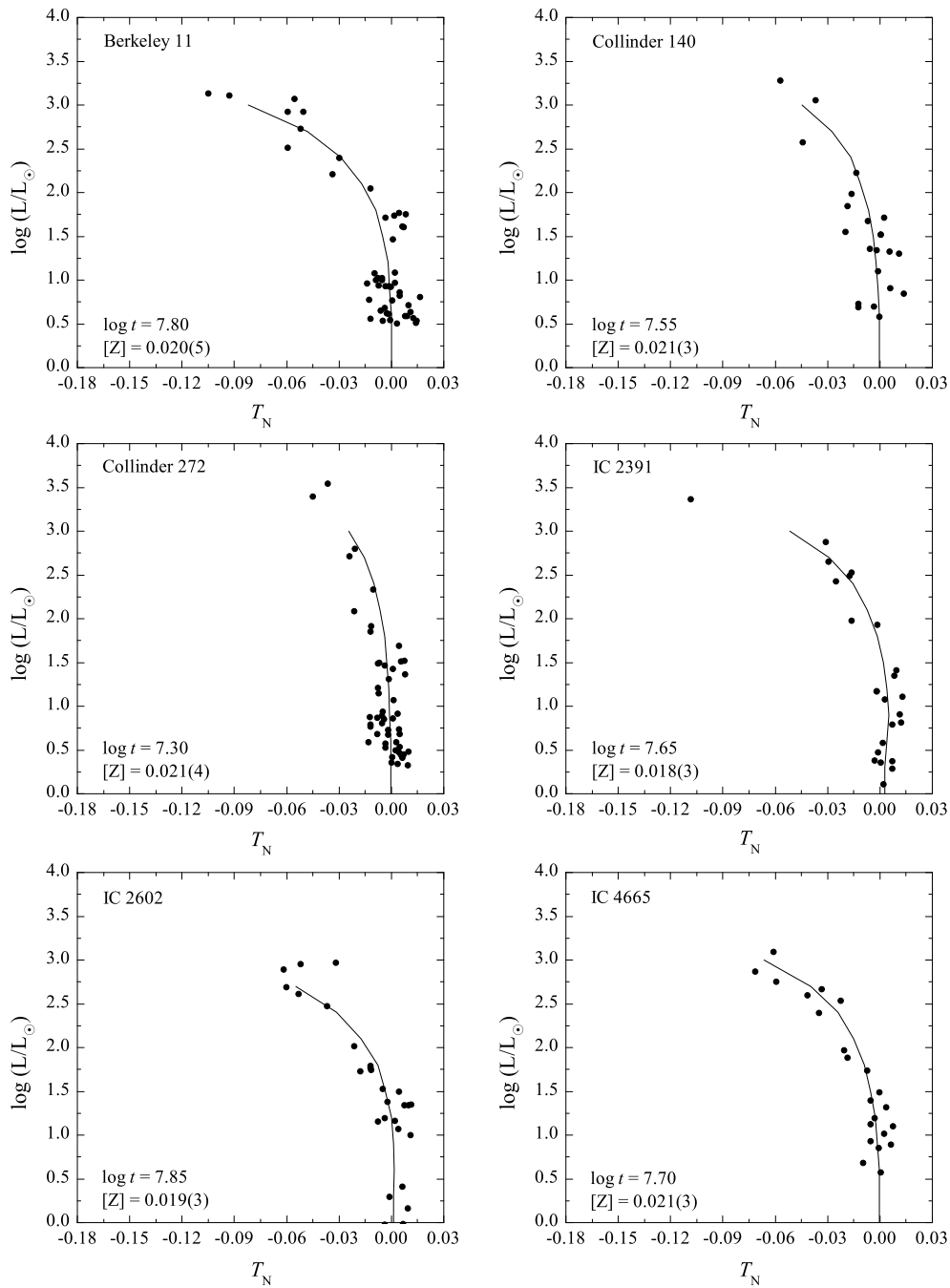


Figure 6.12: The best fits of the differential grids by Pöhl & Paunzen (2010) to the program open clusters, in order to determine the fundamental parameters including metallicity. For clarity, T_N is the to the ZAMS normalised effective temperature. An equal scale is used for a better recognition of different ages and metallicities. Due to interpolation in the available grids, the hotter stars are sometimes not covered by the isochrone.

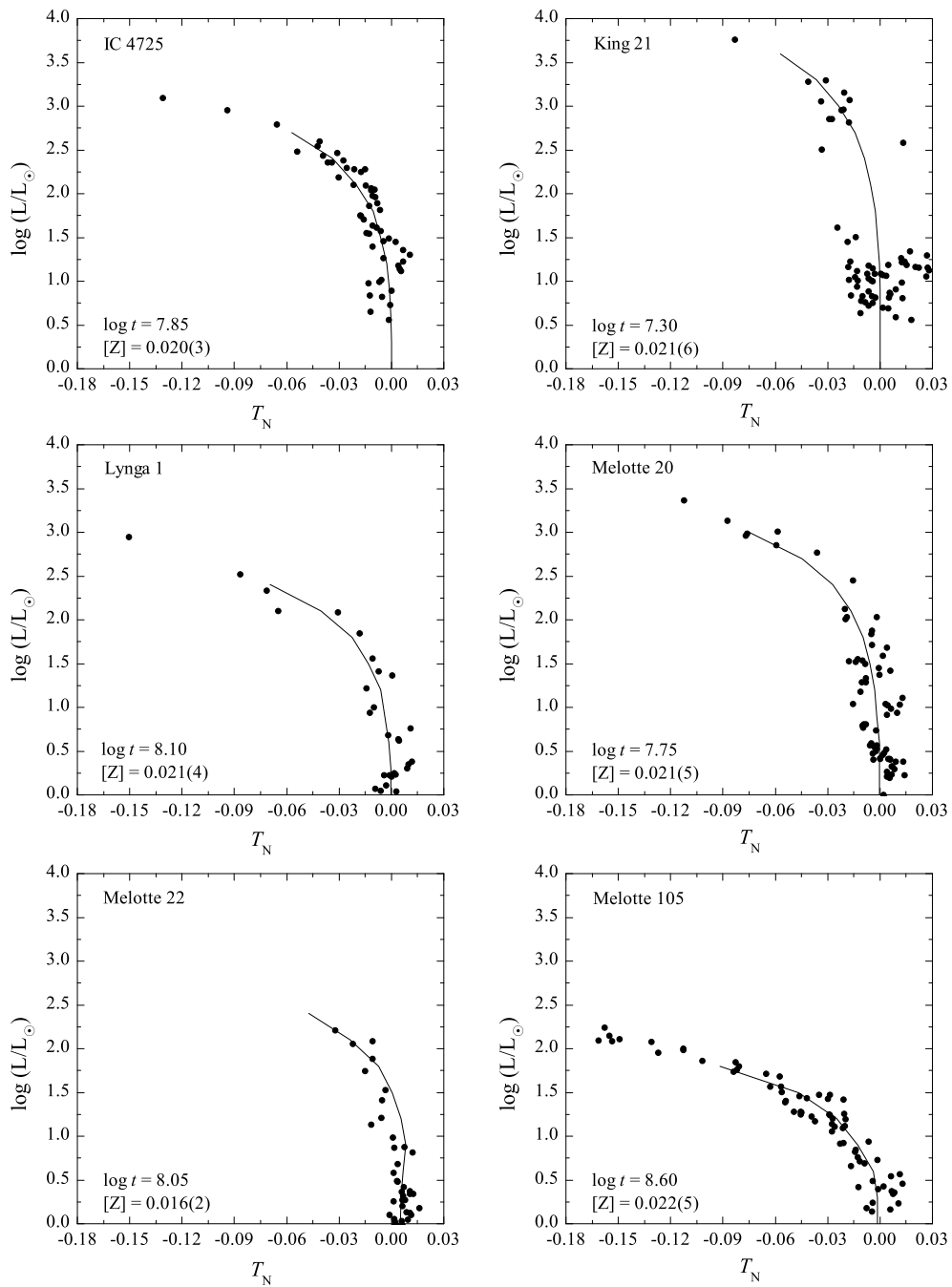


Figure 6.13: Continuation of Figure 6.12.

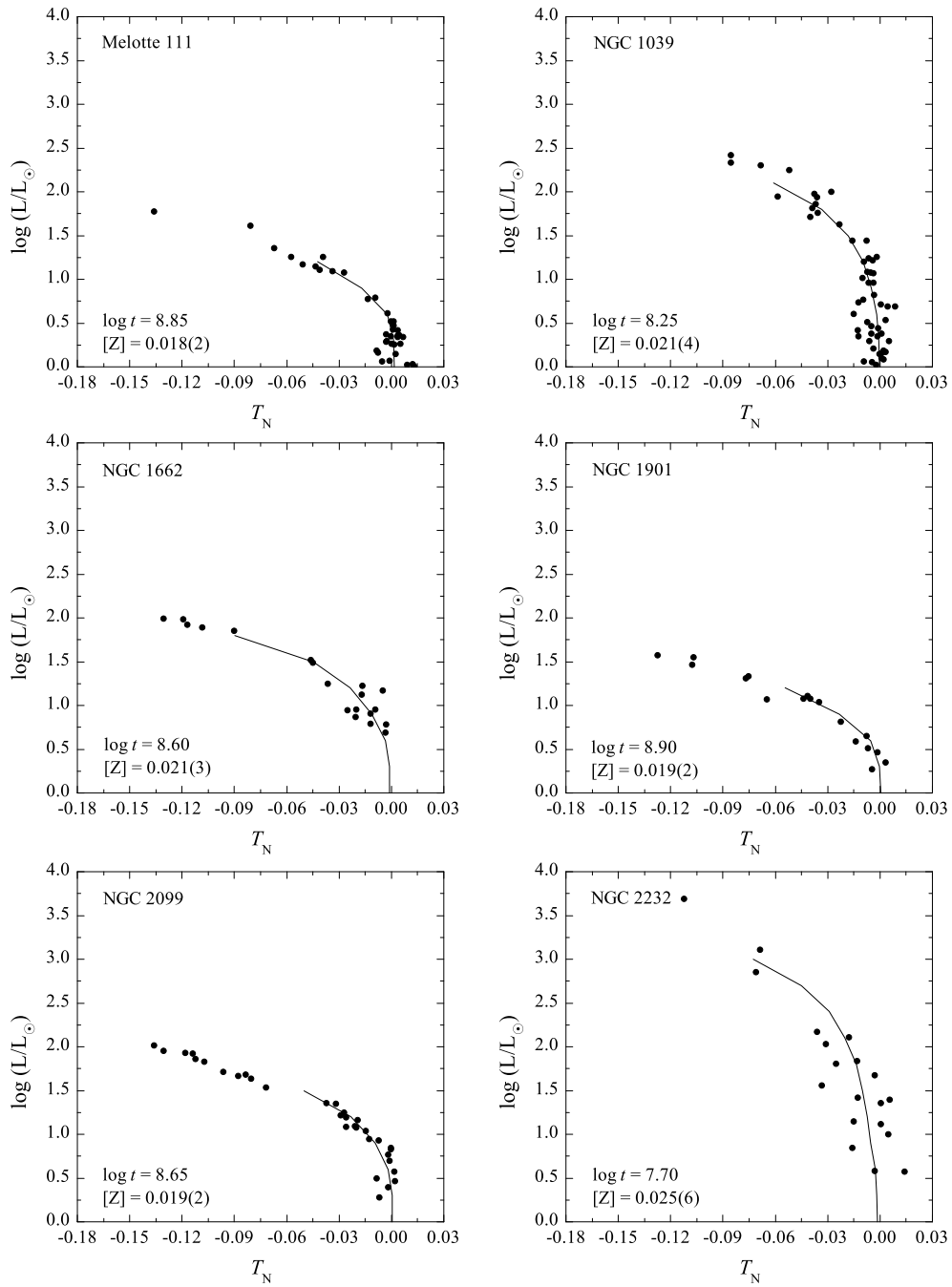


Figure 6.14: Continuation of Figure 6.12.

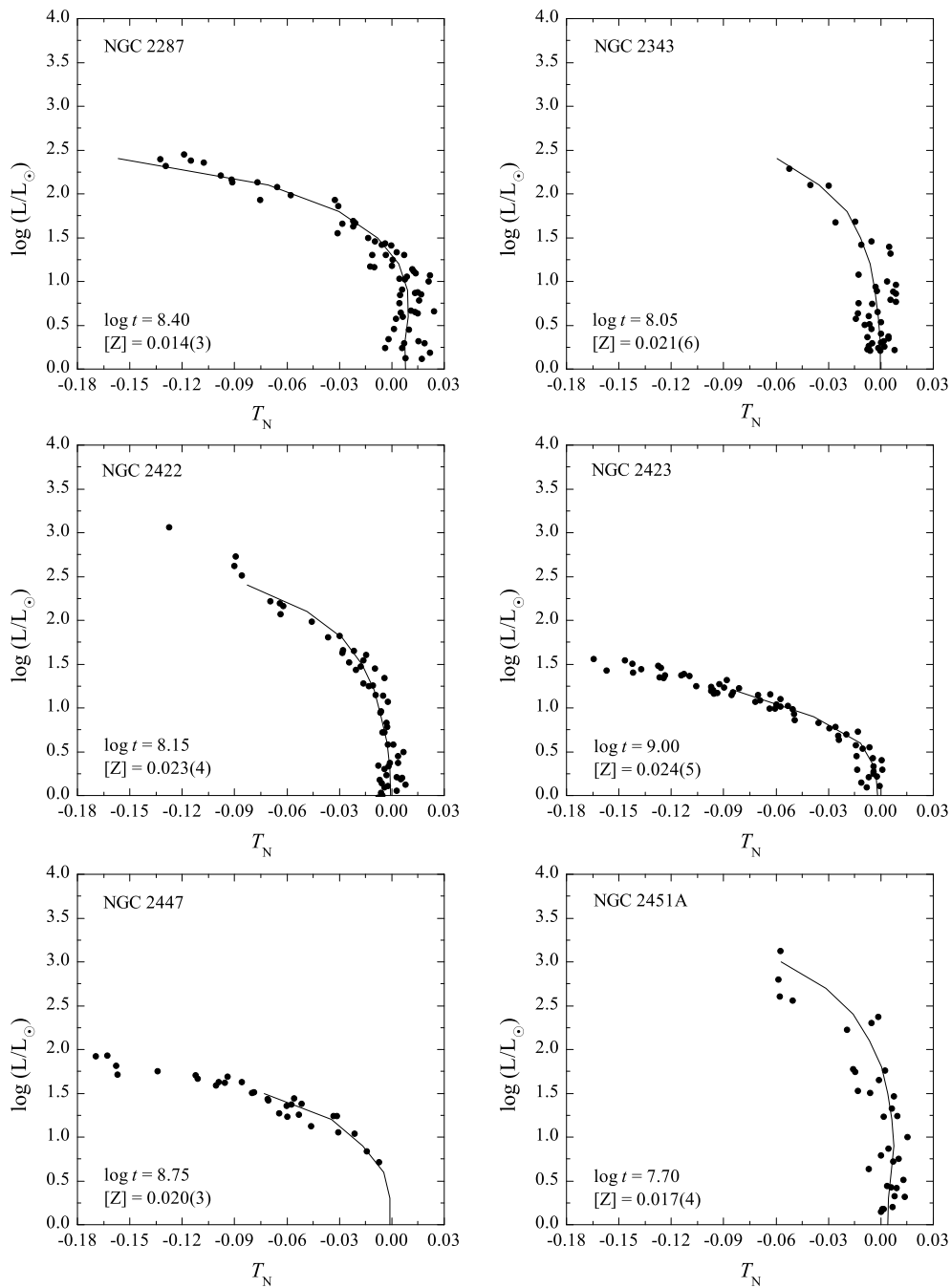


Figure 6.15: Continuation of Figure 6.12.

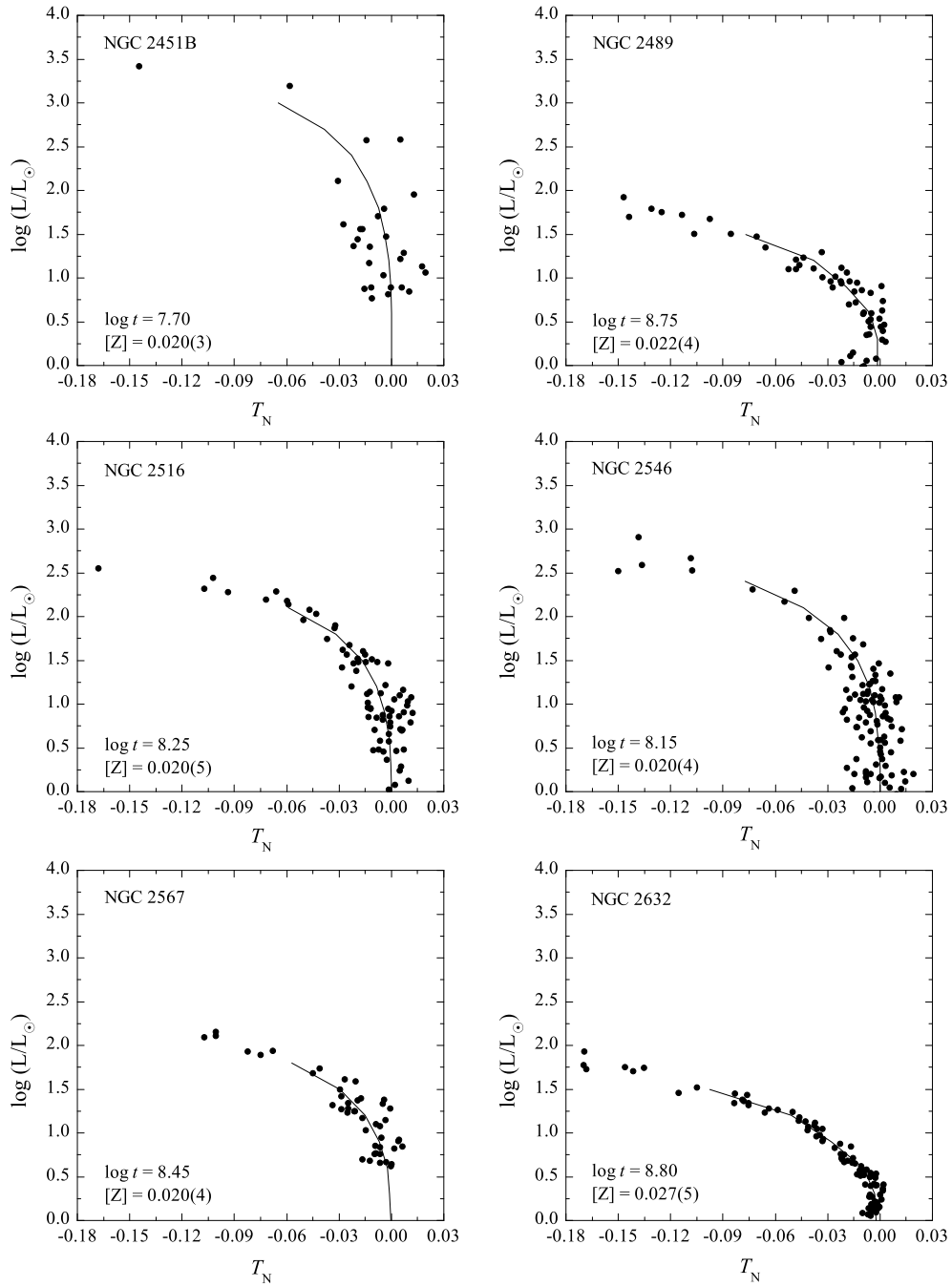


Figure 6.16: Continuation of Figure 6.12.

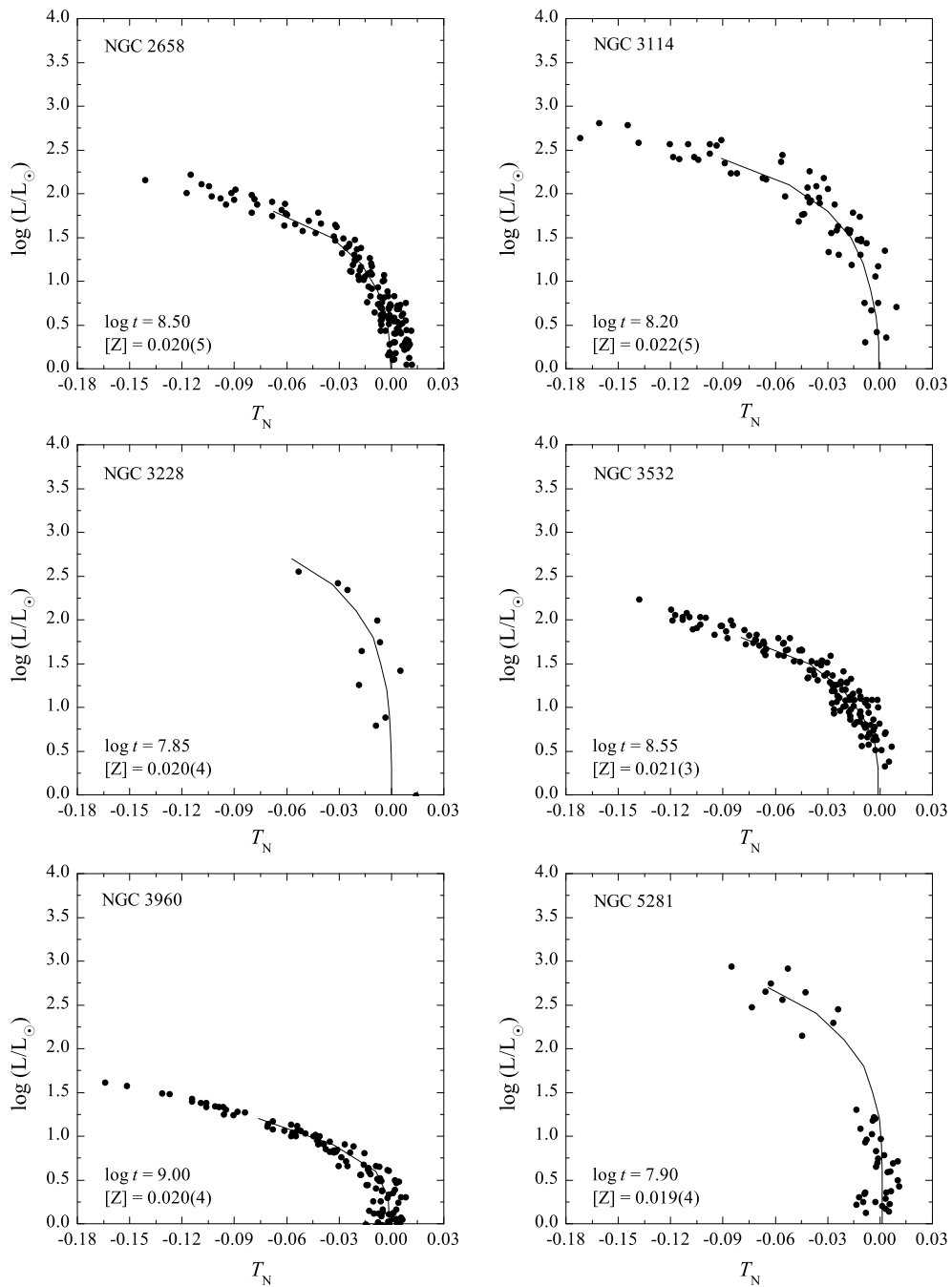


Figure 6.17: Continuation of Figure 6.12.

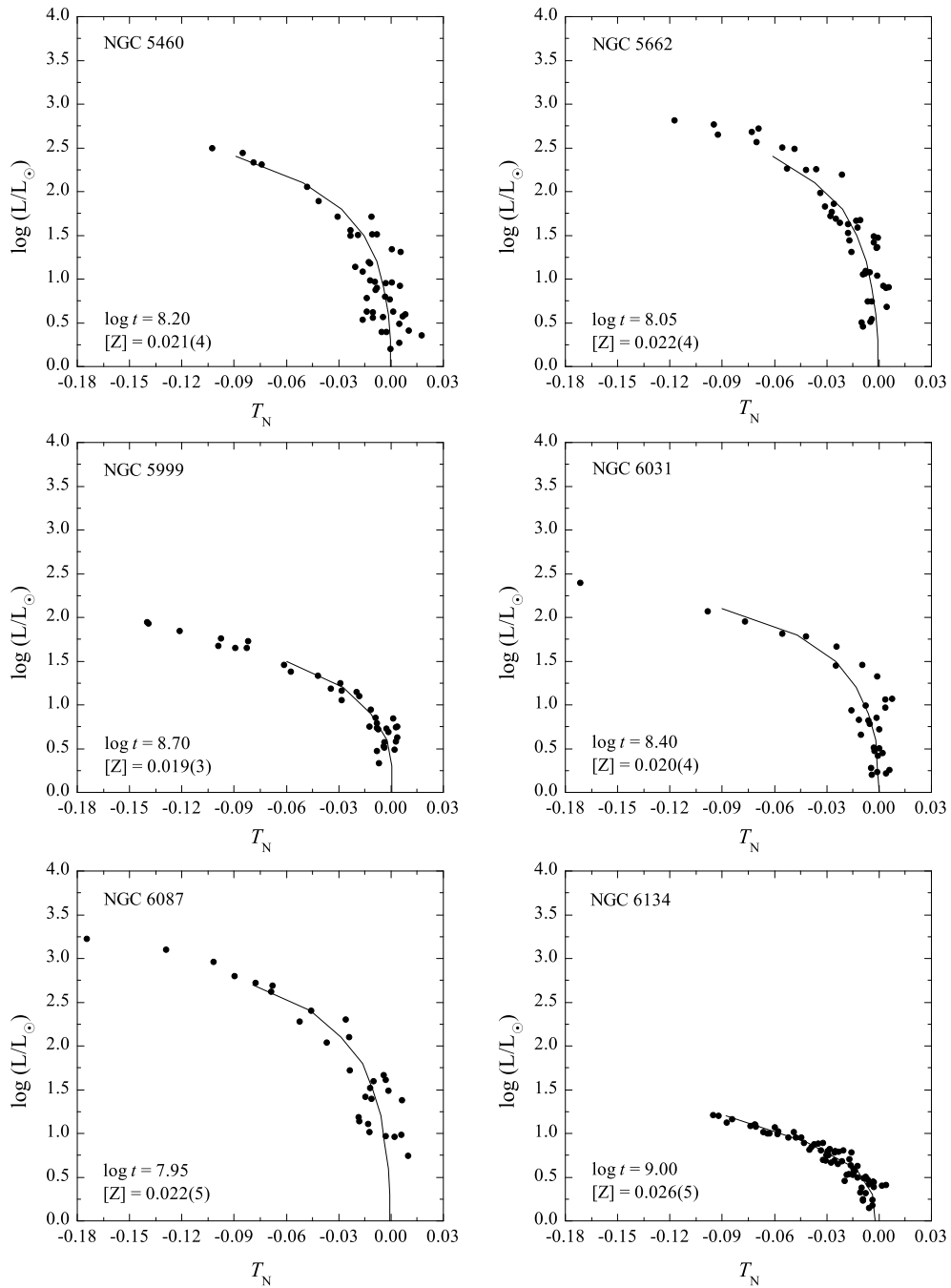


Figure 6.18: Continuation of Figure 6.12.

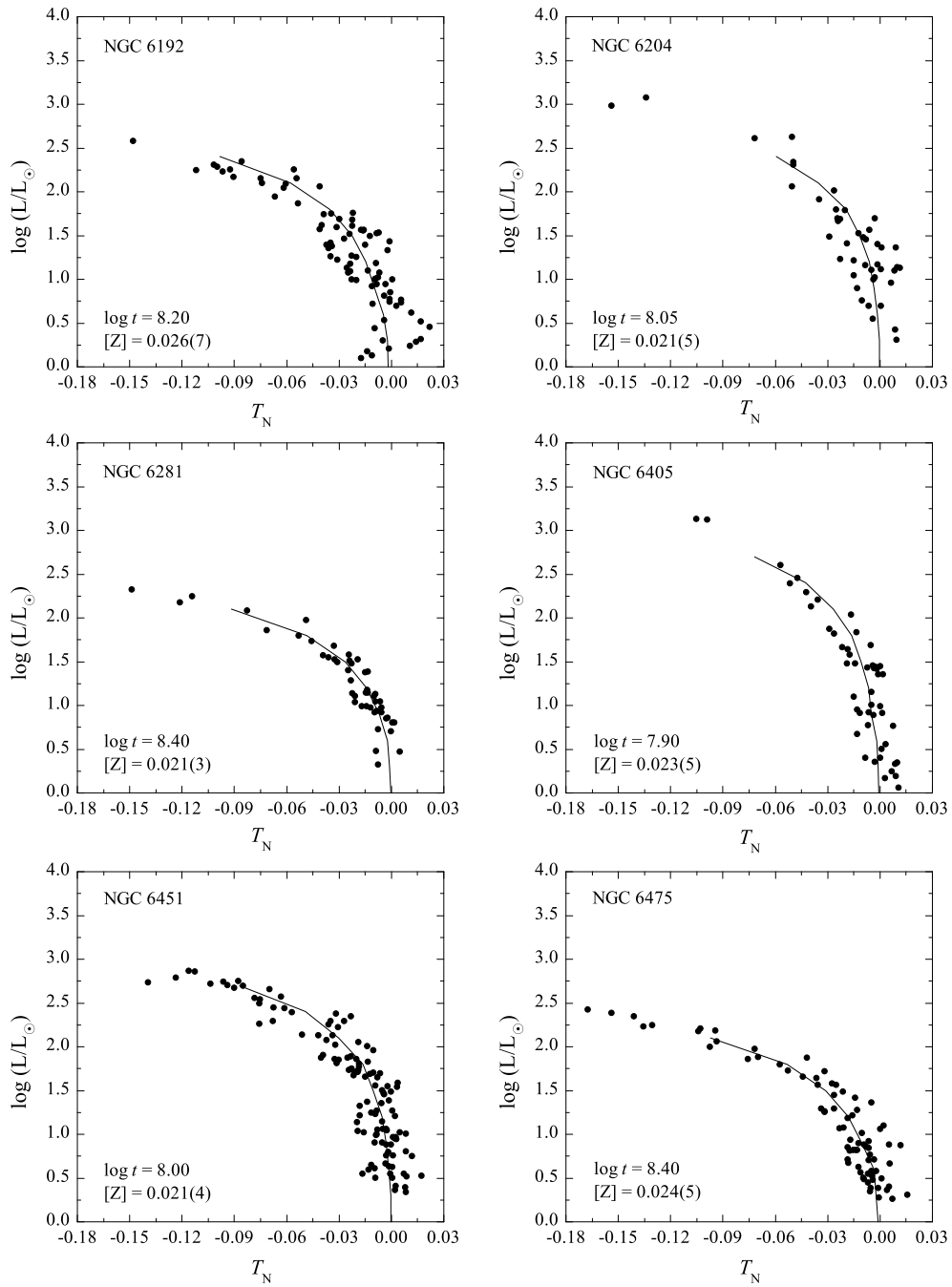


Figure 6.19: Continuation of Figure 6.12.

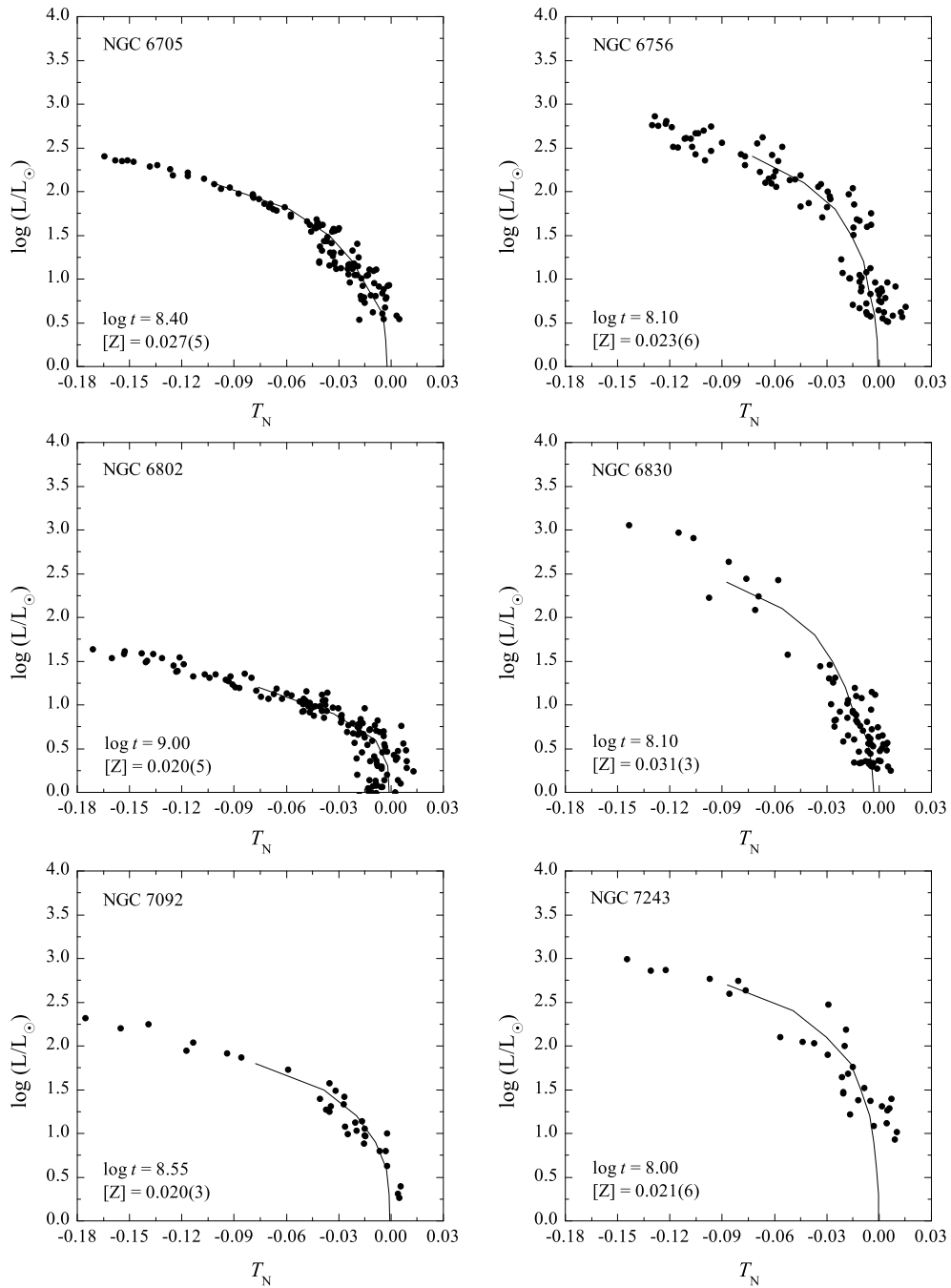


Figure 6.20: Continuation of Figure 6.12.

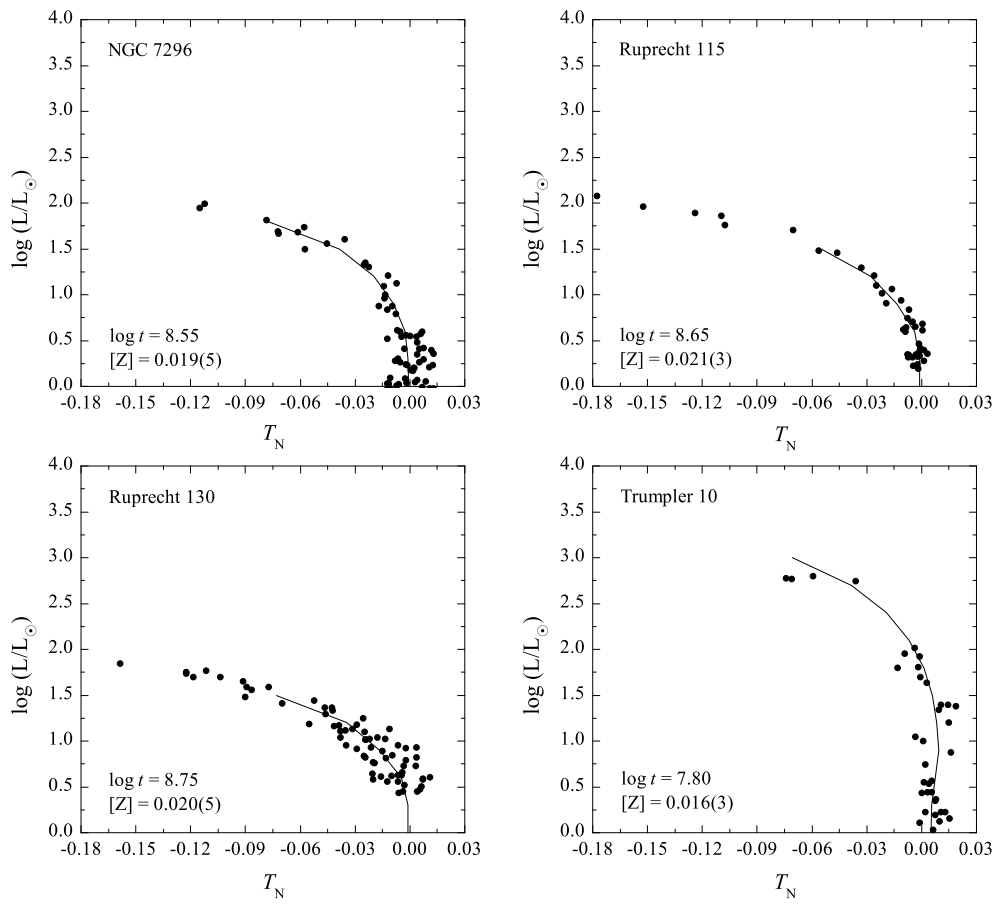


Figure 6.21: Continuation of Figure 6.12.

Table 6.2: The results of the metallicity determination together with spectroscopic literature values.

Cluster	$\log t$	$(m - M)_0$	$E(B - V)$	$[Z]$	$[\text{Fe}/\text{H}]_{grid}$	$[\text{Fe}/\text{H}]_{spec}$	No	Comments
Berkeley 11	7.80	12.20	0.96	0.020 (5)	+0.01 (14)			Rv=2.6
Collinder 140	7.55	8.05	0.04	0.021 (3)	+0.04 (7)			no clear solution
Collinder 272	7.30	11.75	0.43	0.021 (4)	+0.06 (9)			
IC 2391	7.65	5.79	0.01	0.018 (3)	-0.03 (7)	-0.01 (3)	6	
IC 2602	7.85	5.86	0.03	0.019 (3)	+0.00 (8)	-0.02 (2)	10	
IC 4665	7.70	7.70	0.19	0.021 (3)	+0.02 (6)	-0.03 (4)	18	
IC 4725	7.85	9.00	0.45	0.020 (3)	+0.03 (8)			
King 21	7.30	12.40	0.86	0.021 (6)	+0.06 (14)			diff. reddening
Lyngå 1	8.10	11.40	0.45	0.021 (4)	+0.04 (10)			Rv=3.5
Melotte 20 (Alpha Per)	7.75	6.13	0.09	0.021 (5)	+0.05 (13)	+0.15 (11)	2	
Melotte 22 (Pleiades)	8.05	5.48	0.03	0.016 (2)	-0.08 (7)	-0.01 (5)	12	
Melotte 105	8.60	11.84	0.44	0.022 (5)	+0.08 (12)			
Melotte 111 (Coma Ber)	8.85	4.69	0.00	0.018 (2)	-0.04 (5)	-0.01 (8)	13	
NGC 1039	8.25	8.34	0.08	0.021 (4)	+0.05 (10)	+0.02 (6)	7	
NGC 1662	8.60	8.05	0.32	0.021 (3)	+0.05 (8)			low magnitude limit
NGC 1901	8.90	8.20	0.02	0.019 (2)	+0.01 (5)	-0.08	1	few stars
NGC 2099	8.65	10.55	0.30	0.019 (2)	+0.00 (4)	+0.02 (5)	3	
NGC 2232	7.70	7.65	0.03	0.025 (6)	+0.14 (12)	+0.22 (9)	3	
NGC 2287	8.40	9.10	0.02	0.014 (3)	-0.16 (9)	-0.10 (2)	3	
NGC 2343	8.05	9.90	0.20	0.021 (6)	+0.05 (14)			
NGC 2422	8.15	8.52	0.09	0.023 (4)	+0.09 (8)			
NGC 2423	9.00	9.80	0.10	0.024 (5)	+0.11 (10)	+0.08 (5)	6	
NGC 2447	8.75	10.13	0.01	0.020 (3)	+0.03 (7)	-0.03 (5)	12	low magnitude limit
NGC 2451A	7.70	6.35	0.01	0.017 (4)	-0.06 (11)	-0.01 (8)	6	
NGC 2451B	7.70	7.93	0.10	0.020 (3)	+0.02 (9)	-0.01 (8)	3	no clear solution
NGC 2489	8.75	11.30	0.31	0.022 (4)	+0.06 (10)			
NGC 2516	8.25	8.05	0.11	0.020 (5)	+0.03 (12)	+0.05 (11)	2	
NGC 2546	8.15	9.75	0.15	0.020 (4)	+0.01 (9)			
NGC 2567	8.45	11.03	0.13	0.020 (4)	+0.02 (10)	+0.01 (5)	3	
NGC 2632 (Praesepe)	8.80	6.30	0.03	0.027 (5)	+0.17 (9)	+0.19 (10)	11	
NGC 2658	8.50	13.05	0.36	0.020 (5)	+0.02 (12)			
NGC 3114	8.20	9.85	0.07	0.022 (5)	+0.07 (11)	+0.07 (1)	2	
NGC 3228	7.85	8.35	0.04	0.020 (4)	+0.03 (10)			few stars
NGC 3532	8.55	8.34	0.04	0.021 (3)	+0.04 (7)	+0.04 (6)	4	
NGC 3960	9.00	11.65	0.29	0.020 (4)	+0.03 (9)	-0.04 (10)	5	
NGC 5281	7.90	10.70	0.22	0.019 (4)	+0.00 (11)			no clear solution
NGC 5460	8.20	9.20	0.13	0.021 (4)	+0.06 (9)	+0.05 (24)	21	
NGC 5662	8.05	9.31	0.27	0.022 (4)	+0.06 (9)			diff. reddening
NGC 5999	8.70	11.75	0.46	0.019 (3)	+0.00 (8)			
NGC 6031	8.40	11.00	0.44	0.020 (4)	+0.02 (9)			
NGC 6087	7.95	9.60	0.19	0.022 (5)	+0.06 (12)			low magnitude limit

... continues on next page

Table 6.2: ... Continuation

Cluster	$\log t$	$(m - M)_0$	$E(B - V)$	$[Z]$	$[Fe/H]_{grid}$	$[Fe/H]_{spec}$	No	Comments
NGC 6134	9.00	10.00	0.40	0.026 (5)	+0.16 (9)	+0.11 (7)	8	reddening law?
NGC 6192	8.20	11.05	0.63	0.026 (7)	+0.16 (13)	+0.12 (4)	4	diff. reddening
NGC 6204	8.05	10.25	0.47	0.021 (5)	+0.05 (12)			diff. reddening
NGC 6281	8.40	8.65	0.17	0.021 (3)	+0.04 (7)	+0.06 (6)	2	
NGC 6405	7.90	8.45	0.17	0.023 (5)	+0.09 (11)			
NGC 6451	8.00	11.75	0.75	0.021 (4)	+0.04 (10)			
NGC 6475	8.40	7.16	0.07	0.024 (5)	+0.11 (11)	+0.08 (2)	7	
NGC 6705	8.40	11.60	0.39	0.027 (5)	+0.18 (8)	+0.13 (13)	6	
NGC 6756	8.10	12.28	1.03	0.023 (6)	+0.10 (14)			
NGC 6802	9.00	11.65	0.79	0.020 (5)	+0.03 (13)			reddening law?
NGC 6830	8.10	11.90	0.54	0.031 (3)	+0.24 (5)			
NGC 7092	8.55	7.43	0.02	0.020 (3)	+0.02 (9)			
NGC 7243	8.00	9.47	0.24	0.021 (6)	+0.06 (13)			low magnitude limit
NGC 7296	8.50	11.90	0.26	0.021 (6)	+0.04 (14)			
Ruprecht 115	8.65	11.35	0.74	0.021 (3)	+0.04 (7)			
Ruprecht 130	8.75	11.50	1.00	0.020 (5)	+0.03 (14)			
Trumpler 10	7.80	8.05	0.03	0.016 (3)	-0.07 (10)			

Table 6.3: The results of the metallicity determination using $wby\beta$, UBV , and $Geneva$ photometric systems. The number of stars used is also indicated, as well as the spectroscopic and grid determinations as comparison. The presented data are uncorrected in respect to the spectroscopic results.

Cluster	[Fe/H] $wby\beta$	No.	[Fe/H] UBV	No.	[Fe/H] $Geneva$	No.	[Fe/H] grid	[Fe/H] spec
Collinder 140	+0.08 (3)	3	+0.18 (10)	5			+0.04 (7)	
IC 2391	+0.03 (8)	9	-0.07 (9)	7	-0.06 (4)	19	-0.03 (7)	-0.01 (3)
IC 2602	+0.00 (8)	6	-0.08 (7)	4	-0.01 (6)	9	+0.00 (8)	-0.02 (2)
IC 4665	+0.06 (7)	10			+0.00 (9)	12	+0.02 (6)	-0.03 (4)
Melotte 20 (Alpha Per)	+0.06 (5)	43	+0.02 (9)	30	-0.08 (8)	55	+0.05 (13)	+0.15 (11)
Melotte 22 (Pleiades)	+0.05 (5)	31	+0.02 (9)	49	-0.06 (9)	38	-0.08 (7)	-0.01 (5)
Melotte 111 (Coma Ber)	-0.07 (6)	33	-0.07 (7)	18	-0.04 (7)	34	-0.04 (5)	-0.01 (8)
NGC 1039	+0.10 (6)	9	+0.05 (12)	5	-0.01 (8)	9	+0.05 (10)	+0.02 (6)
NGC 1662	+0.16 (4)	17	+0.11 (8)	5	-0.07 (8)	12	+0.05 (8)	
NGC 1901	+0.08 (7)	10	-0.04 (5)	3			+0.01 (5)	-0.08
NGC 2232					+0.01 (8)	4	+0.14 (12)	+0.22 (9)
NGC 2287	-0.07 (6)	12	-0.04 (10)	7	-0.05 (8)	32	-0.16 (9)	-0.10 (2)
NGC 2422	+0.02 (4)	10			+0.04 (5)	17	+0.09 (8)	
NGC 2423	+0.10 (4)	23			-0.02 (8)	4	+0.11 (10)	+0.08 (5)
NGC 2447	+0.06 (4)	14			-0.06 (5)	11	+0.03 (7)	-0.03 (5)
NGC 2451A			-0.04 (6)	6	+0.02 (6)	3	-0.06 (11)	-0.01 (8)
NGC 2516	-0.02 (6)	15	-0.01 (7)	12	-0.05 (8)	21	+0.03 (12)	+0.05 (11)
NGC 2632 (Praesepe)	+0.11 (5)	48	+0.07 (6)	83	+0.18 (8)	44	+0.17 (9)	+0.19 (10)
NGC 3114	+0.09 (3)	7			+0.03 (6)	3	+0.07 (11)	
NGC 3293	+0.08 (4)	5						
NGC 3532	+0.06 (3)	3	-0.07 (2)	3	-0.01 (6)	32	+0.04 (7)	+0.04 (6)
NGC 5460	+0.07 (6)	6	+0.03 (11)	5	+0.00 (9)	3	+0.06 (9)	+0.05 (24)
NGC 5662			+0.05 (11)	5			+0.06 (9)	
NGC 6192			+0.29 (17)	4			+0.16 (13)	+0.12 (4)
NGC 6208			-0.05 (6)	4				
NGC 6281	+0.07 (2)	11	+0.07 (12)	6	-0.01 (7)	20	+0.04 (7)	+0.06 (6)
NGC 6405	+0.10 (4)	13	+0.14 (8)	20	+0.01 (5)	13	+0.09 (11)	
NGC 6475	+0.12 (6)	31	+0.02 (13)	3	-0.02 (7)	43	+0.11 (11)	+0.08 (2)
NGC 7092	+0.05 (6)	4	-0.02 (11)	14	-0.05 (8)	8	+0.02 (9)	
NGC 7243	+0.10 (4)	7			+0.04 (4)	10	+0.06 (13)	
Trumpler 10	+0.13 (1)	3			-0.06 (13)	3	-0.07 (10)	

6.2 The final open cluster parameters

From the current point of view, probably no specific method to determine cluster parameters (which also holds for the new results presented above) can be assumed as superior compared to the others. However, up to now still most determinations are based on “simple” isochrone fitting. Several isochrone sets are available (by the Geneva or Padova group, just to mention two of them) with different input physics used for the calculation. Grocholski & Sarajedini (2003) for example compared five different sets and concluded that no model is able to reproduce observational data in a uniform manner. Furthermore, the fitting procedure is strongly biased on one hand by the respective users and their particular approach as well as by the availability and quality of the used data.

Therefore, in order to try to overcome these problems somehow, we merged our new results with previous determinations, mentioned already at the beginning of Sect 6, to calculate mean values, so that the final results incorporate various methods and approaches. However, for some clusters we adopted directly our new results, since the earlier parameters seem not to be appropriate. Such an example is the open cluster Ruprecht 130. This aggregate was studied for the first time by Piatti et al. (2000) by means of B, V, I photometry and integrated spectra. Based on this combination, they adopted an age of 50 Myr, $E(B - V) = 1.20$, and a distance $d = 2.1$ kpc. Later on, this cluster was studied with Δa photometry by Paunzen et al. (2006b). Using isochrones, they obtained 70 Myr, $d = 1.8$ kpc, and the same reddening.

During inspection of all available photometric data we noticed a difference of ~ -1 mag for the I -magnitude by Piatti et al. (2000), deduced using V and $(V - I)$, compared to the DENIS survey. However, actually the V magnitude is affected, if employing e.g. the Guide Star Catalog or ASAS. Such a difference was already noticed by Paunzen & Maitzen (2002) in NGC 6451, comparing the data by Piatti et al. (1998) with other literature values. Since for that cluster several datasets are available, we determined a shift in V of 0.97 mag, in the sense that Piatti et al. (1998) provide too bright magnitudes, whereas the colour indices are in reasonable agreement. Since the data by Piatti et al. (1998, 2000) for both clusters (NGC 6451 and Ruprecht 130) were obtained within the same observing run (although not during the same night, but the transformation coefficients are in good agreement), we applied this correction also on Ruprecht 130. Using this corrected photometry, the agreement with the I photometry of the DENIS survey is within 0.01 mag. Unfortunately, up to now no further photometry is available (e.g. APASS) to check also $(B - V)$, but a comparison of other clusters observed during the run by Piatti et al. (1998, 2000) showed a reasonable agreement with other studies. Surprisingly, not all of their clusters seem to be affected the same way in the V magnitude. If comparing the listed transformation coefficients given by Piatti et al. (1998) and Piatti et al. (2000), one can already recognize this difference in V of ~ 1 mag. So it seems that randomly one or the other transformation was applied.

We also queried the 2MASS and UKIDSS (DR8 plus) surveys for additional NIR JHK data. Although UKIDSS is supposed to be tightened on 2MASS photometry, we also noticed some offsets and gradients. Using data of these surveys of an extended area around Ruprecht 130, restricted to reliable photometry using the respective flags,

we determined the following dependencies, valid for this area only.

$$\begin{aligned}
 J_{2M} &= J_{UK} + 0.068(39) \\
 (J - H)_{2M} &= 0.133(6) + 1.063(7)(J - H)_{UK} \\
 (J - K)_{2M} &= 0.092(10) + 1.025(8)(J - K)_{UK}
 \end{aligned}$$

Since UKIDSS tends to provide a deep coverage, the brighter stars are saturated, as can be recognized from their quality flags. Hence we combined it with 2MASS data to obtain a final more complete catalogue. Unfortunately, up to now UKIDSS does not cover the complete area - so far the available coverage ends about $2'$ to the east from the cluster center. However, the cluster is not assumed to be much more extended.

The differential grid method was then applied using the compiled catalogue of corrected B, V, I, K photometry and all available colour indices. The final best fit is presented in Figs. 6.21 and Fig. 6.22. In the latter we also show the results, if the parameters of the previous studies are applied to the same stars, but taking into account the shift in V and hence in the distance modulus.

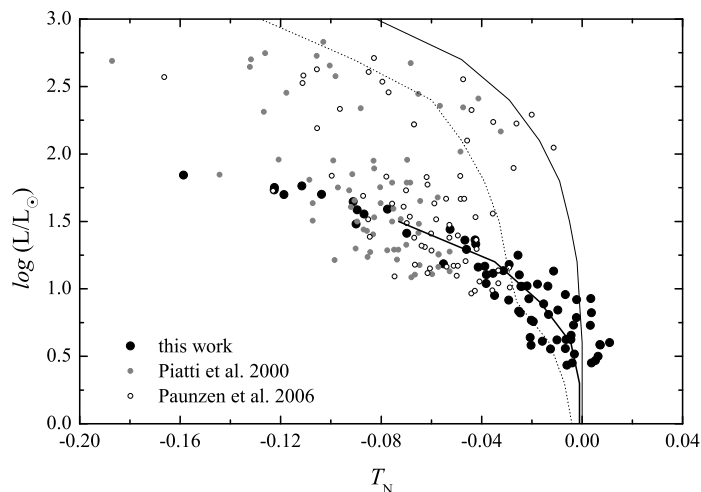


Figure 6.22: The result of the differential grid method for Rup 130 with $\log t = 8.75$ and solar metallicity. Additionally, the parameters listed in Paunzen et al. (2006b) and Piatti et al. (2000) were adopted and applied to the same star sample. The isochrones for $\log t = 7.8$ with solar metallicity (thin line) and $[Z] = 0.04$ (dotted line) are shown as comparison.

As can be seen in Table 6.2, the differential grid method provides parameters which differ significantly compared to the previous studies. Whereas the distance of ~ 2000 pc is in agreement (although 1 mag offset in V), the deduced age is much older (560 Myr) and the reddening 0.2 mag lower. This also clearly shows how strong these parameters are coupled. Applying the parameters by Piatti et al. (2000) and Paunzen et al. (2006b) does not provide a reasonable fit at all (see Fig. 6.22), even if considering an extreme overabundance of $[\text{Fe}/\text{H}] \sim 0.4$.

The obtained parameters were applied on the available colour-magnitude diagrams (Fig. 6.23) using Padova isochrones (for 2MASS/UKIDSS), but also Geneva ones for

the other diagrams, showing an excellent fit. Especially in the NIR diagram, one can see that this older age fits the probable red giant branch rather well - we want to recall again that the parameters are deduced from main-sequence stars only. The obtained extinction values $E(B - V) = 1.0$, $E(V - I) = 1.25$, $E(V - K_s) = 2.70$, $E(J - K_s) = 0.43$, $E(J - H) = 0.28$ are all compatible with a normal reddening law of $R_V = 3.1$.

The extreme disagreement in age with the previous studies can be explained such that in the isochrone fitting procedure more weight to the brightest/bluest objects was given. It seems that also several Blue Stragglers are present, influencing probably the integrated spectra by Piatti et al. (2000), evoking a much younger age. The not negligible influence of Blue Stragglers on the integrated light of open clusters was extensively studied e.g. by Xin et al. (2007).

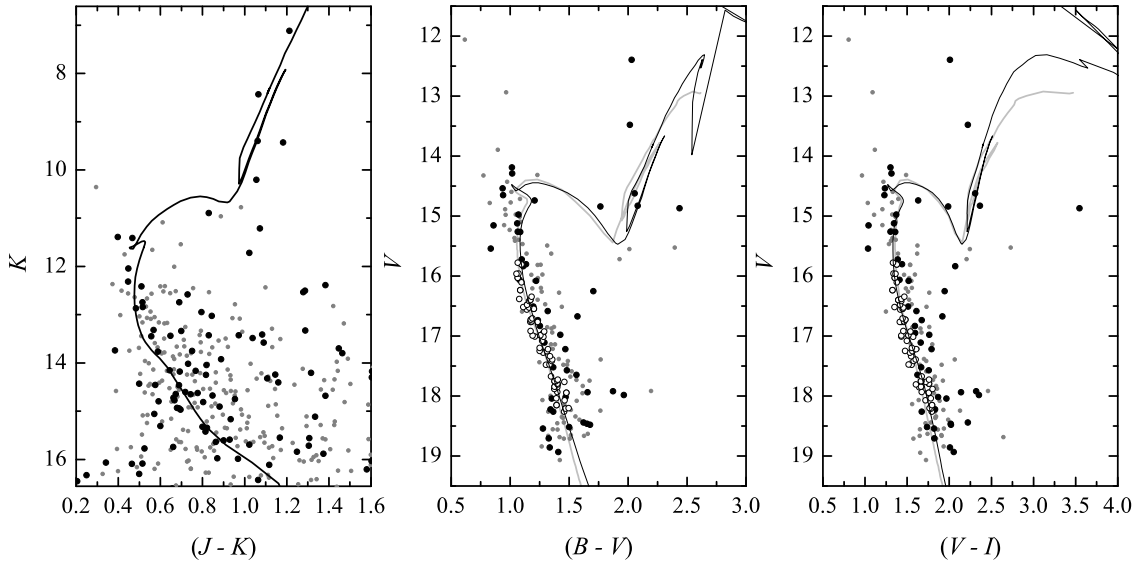


Figure 6.23: The colour-magnitude diagrams (CMD) for the open cluster Rup 130 together with the isochrones for the age $\log t = 8.75$ and solar metallicity. In the left panel the UKIDSS/2MASS CMD is given (restricted to the blue part), whereas larger symbols represent objects within a radius of $1'$ and smaller grey symbols additional objects up to a radius of $2.0'$. This also holds for the other CMDs. Furthermore, in the $(B - V)$ and $(V - I)$ diagrams the stars used for the metallicity-fit within the grid range are indicated as open symbols. The black lines are the Padova isochrones, whereas the grey lines are Geneva ones.

Recently, Bica & Bonatto (2011) performed a structural analysis of this cluster using 2MASS data and a decontamination procedure to eliminate the field population. They classified that object as a borderline case, since only a few stars remained. Using these stars, they fitted an isochrone resulting in a distance of 900 pc, with an extreme extinction of $A_V = 7.3$, and an age of $\log t = 8.0$. However, as can be seen in their figure, the fit was applied on a part of the possible red giant branch (see left panel of our Fig. 6.23), therefore they obtained a much closer distance and an extreme reddening.

Unfortunately, they do not provide a discussion of their result, neither of the high extinction at a rather close distance, nor in comparison to previous studies, although

these are mentioned. We conclude, that the 2MASS data alone do not provide a sufficient deep magnitude limit with reliable photometry.

Apart from Ruprecht 130, we adopted also solely our new results via the grid method for the double cluster NGC 2451A/B, whereby particular attention was paid to discriminate the population of the fore- and background cluster using literature, Hipparcos parallax, and proper motions.

Furthermore, for e.g. NGC 2423 previous studies differ from our determination. All photoelectric studies (no CCD ones are available so far) do not provide a sufficient deep coverage of the main sequence to determine distance accurately. Most distances for that cluster (which are $\sim 20\%$ lower than our adopted one) are probably based on the photographic study by Hassan (1976), whose V magnitudes are about 0.6 mag too bright (see also Sect. 5.1.20).

In contrast, the ages found in the literature are predominantly in agreement with our result, since this cluster shows a rather well defined giant branch. We therefore queried the APASS survey for additional B, V photometry, which offers a magnitude limit of $V \sim 17$. This dataset was merged with photoelectric $UBV, Geneva,$ and $uvby\beta$ measurements after a slight adjustment on their scale. Our study is therefore based on a more complete dataset and supersedes all previous works.

Additionally, for the remaining clusters on which we were not able to apply the differential grid method safely due to either the young age, insufficient data, and/or differential reddening, we performed isochrone fitting using the merged photometric datasets (see Table 6.4) together with Geneva and Padova isochrones. Whenever possible, the stars were individually de-reddened, which is especially important for young aggregates with variable reddening. Again, for two clusters our new results supersede former investigations: NGC 6268 and Ruprecht 120. For the first cluster all previous investigations resulted in much closer distances, and for the other cluster in more distant ones. Also in age rather different results can be found. Since we incorporated not only a single dataset, using also NIR data (2MASS), we decided to adopt our parameters directly.

As mentioned above, in general all additional determinations were merged with available literature results, and finally mean cluster parameters were calculated. The final open cluster parameters, adopted for further analysis, are given in Table 6.5, together with the number of different studies used for the mean values (including our new ones). The distribution of these final parameters is presented in Fig. 6.24.

In this respect it is worth to mention that also parts of literature parameter sets were used for the mean values, since e.g. via ZAMS fitting the distance and reddening can be determined, or the reddening alone via appropriate calibrations. In addition, the age can be estimated e.g. by the bluest colour, turnoff-point etc., even without a proper distance determination, for which a sufficient deep magnitude limit is necessary. However, our results were used as a kind of reference to sort out implausible values. As one can see in Table 6.5, e.g. for NGC 2489 only two studies were used, although numerous ones are available in the literature, but most of them with divergent results (too young and close). Only the most recent one (Piatti et al., 2007), which confirmed membership of several red giants (which were probably not taken into account by the other studies), is in very good agreement with our determination.

Table 6.4: Results of isochrone fitting for some aggregates using all available data.

Cluster	$\log t$	distance [pc]	$E(B - V)$ [mag]
Berkeley 94	6.90	3020	0.68
Collinder 121	7.00	880	0.03
Collinder 132	7.00	470	0.03
Lyngå 14	6.80	2290	1.43
NGC 1502	6.90	830	0.76
NGC 2169	6.95	960	0.19
NGC 2362	6.80	1380	0.10
NGC 2439	7.10	3980	0.41
NGC 3105	7.40	7240	1.08
NGC 3293	6.95	2190	0.27
NGC 6208	9.10	1100	0.22
NGC 6250	7.20	930	0.37
NGC 6268	8.20	1530	0.43
NGC 6396	7.45	1260	0.95
NGC 6611	6.30	1740	0.72
NGC 6834	7.75	2190	0.71
NGC 7235	7.00	2750	0.92
NGC 7510	6.80	2880	1.07
Pismis 20	6.60	2820	1.20
Ruprecht 120	8.35	1650	0.68
Stock 16	6.60	1950	0.50

In open cluster research, rather often the catalogue by Dias et al. (2002) (DAML02) is used as a reference to adopt e.g. cluster parameters, which is a compilation of individual results taken from the literature. We therefore compare our final parameters with those of the latest version (3.2., 26th January 2012) of this catalogue in Fig. 6.25. In general, the reddening coincides rather well within 0.05 mag for 70% of the aggregates. That this parameter is probably the best known one was already shown e.g. by Paunzen & Netopil (2006). The conclusion by this reference that age is the worst known parameter is reflected also in Fig. 6.25 at least for the youngest representatives, where the dispersion is significantly larger than for older open clusters. This is probably the result of a combination of several facts, like that no conspicuous turn-off point can be recognized in young clusters to fit an isochrone properly, as well as the larger influence of star formation time spread.

Generally, in such a comparison one should expect a scatter around zero, noticed at least for the reddening and the age. However, if looking at the middle panel of Fig. 6.25, which shows the differences in distance, one can recognize an overestimate of distance in DAML02 for numerous closer clusters, and the contrary for more distant ones.

We inspected the source of the parameters listed in DAML02 and found that for about 65% of the clusters these were adopted from the WEBDA database, which in turn used those determined by Loktin et al. (2001), who investigated 425 clusters in a homogeneous way. These authors introduced a correction factor of +0.2 mag on the distance modulus (although in their previous study they quoted 0.15 mag), to match their distance scale to the Hyades. Furthermore, they adopted a total-to-selective absorption ratio $R_V = 3.34$ (including some further terms with respect to colour and reddening), which is higher than the typical one in the Milky Way ($R_V = 3.1$) according to Winkler (1997). If taking these differences into account, the distances are in rather good agreement with ours. However, the more distant clusters are still

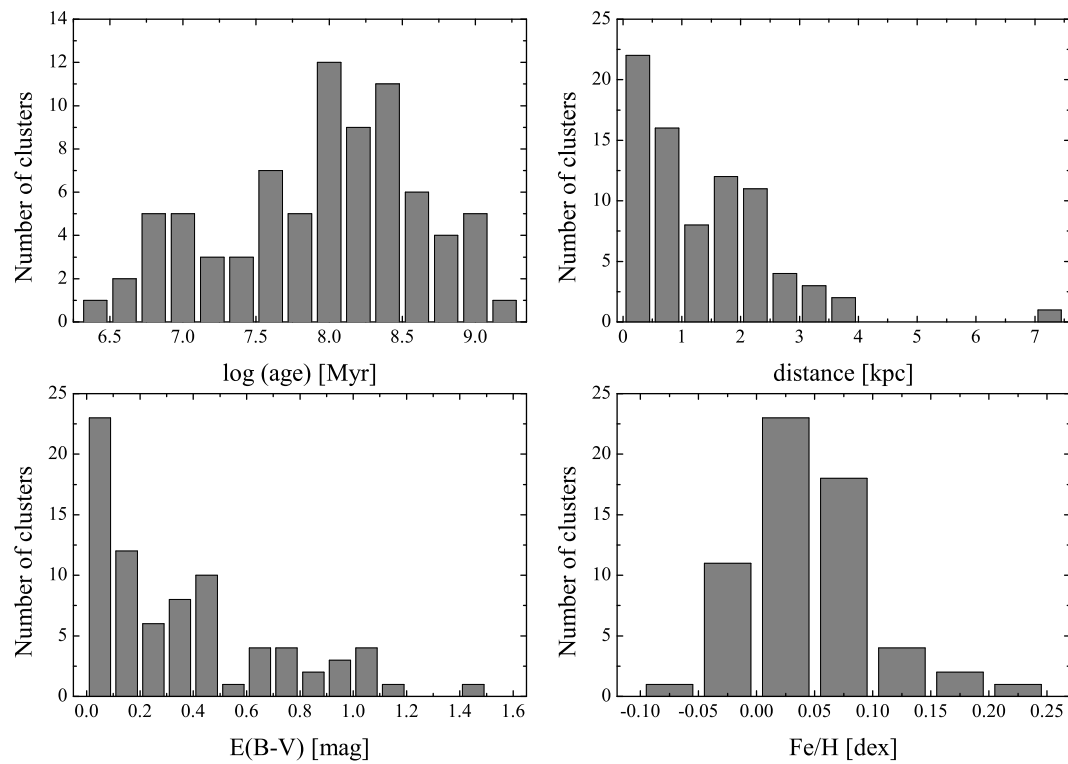


Figure 6.24: The parameter distributions of the open cluster sample.

deviating (overestimated), most probably due to an insufficient magnitude limit, since at that time not many CCD studies were available.

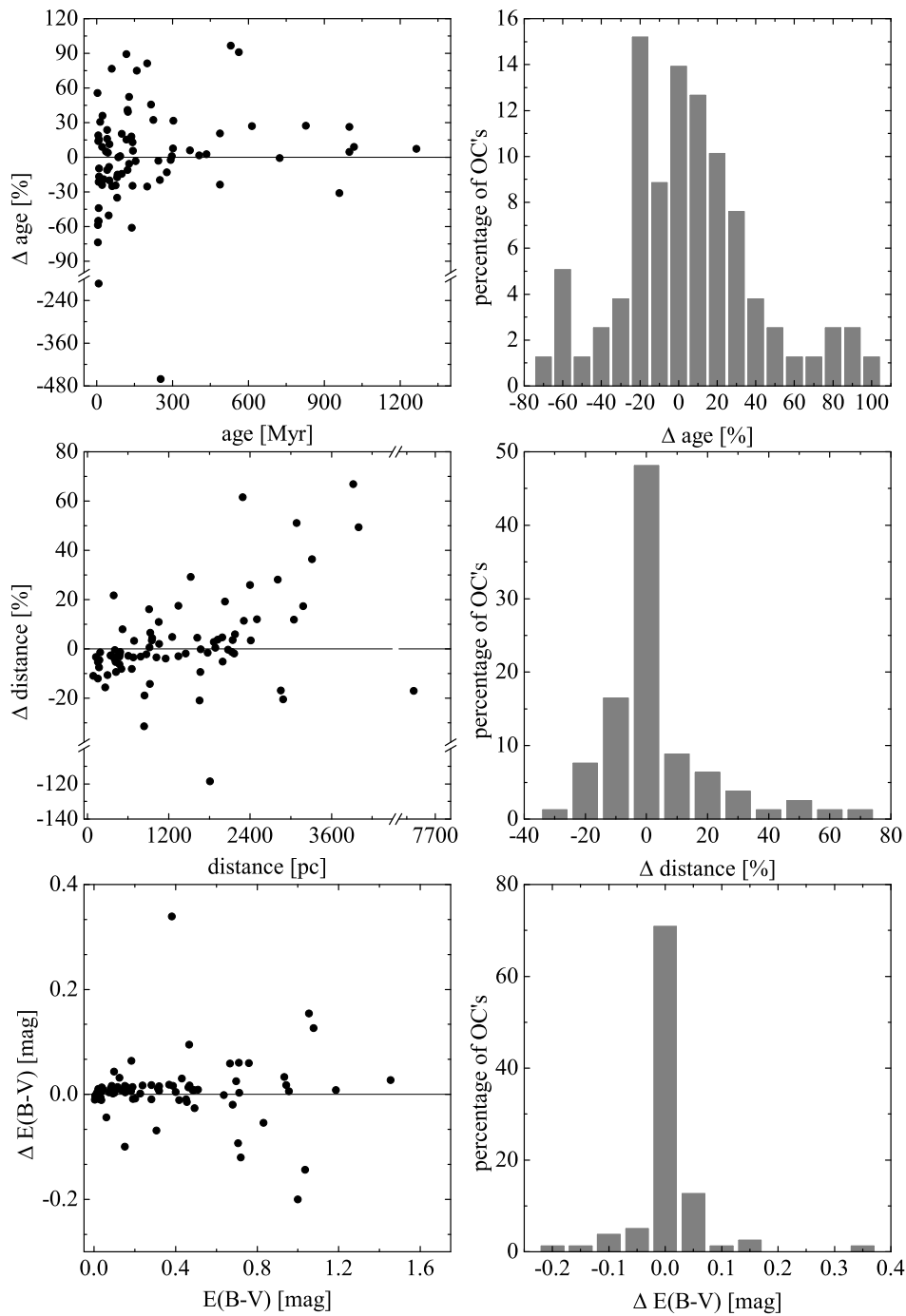


Figure 6.25: Comparison of the final adopted parameters to those listed in the open cluster catalogue by Dias et al. (2002) (DAML02, Version 3.2). Note that in some panels due to outliers the axis is interrupted for a better presentation. In the histograms (right panels) these outliers were omitted. The differences are always calculated in the sense this study minus DAML02.

Table 6.5: The final parameters adopted for the programme open clusters.

Cluster	age [Myr]	σ [Myr]	$E(B - V)$	σ	dist [pc]	σ [pc]	No	[Fe/H]	weight	av. [Fe/H]	σ	No
Berkeley 11	81	28	0.96	0.01	2500	351	6	+0.01	3	+0.01		1
Berkeley 94	9	2	0.67	0.02	3181	362	7					
Collinder 121	8	5	0.03	0.01	836	245	7					
Collinder 132	8	5	0.03	0.01	460	34	7					
Collinder 140	37	10	0.04	0.01	391	31	7	+0.09	2	+0.10	0.09	3
Collinder 272	14	4	0.46	0.02	2310	206	8	+0.06	3	+0.06		1
IC 2391	41	10	0.01	0.00	156	13	9	-0.02	15	-0.02	0.02	5
IC 2602	42	19	0.04	0.01	153	10	11	-0.01	13.5	-0.01	0.03	5
IC 4665	45	13	0.18	0.01	343	12	10	+0.00	13	+0.02	0.03	4
IC 4725	74	12	0.48	0.02	603	38	9	+0.03	3	+0.03		1
King 21	18	3	0.86	0.01	3215	276	2	+0.06	3	+0.06		1
Lyngå 1	118	16	0.47	0.02	1992	146	7	+0.04	3	+0.04		1
Lyngå 14	6	3	1.46	0.03	2291	42	4					
Melotte 20 (Alpha Per)	48	16	0.09	0.01	172	11	10	+0.07	13	+0.05	0.07	5
Melotte 22 (Pleiades)	122	10	0.04	0.01	129	5	12	-0.01	15	-0.01	0.05	5
Melotte 105	303	70	0.49	0.03	2166	130	8	+0.08	3	+0.08		1
Melotte 111 (Coma Ber)	614	87	0.00	0.01	87	6	7	-0.03	15	-0.04	0.03	5
NGC 1039	142	41	0.09	0.02	470	28	9	+0.04	13.5	+0.05	0.03	5
NGC 1502	6	2	0.76	0.01	841	69	11					
NGC 1662	434	49	0.32	0.02	415	31	7	+0.04	9.5	+0.05	0.09	5
NGC 1901	827	24	0.04	0.02	420	12	5	-0.02	9.5	-0.00	0.06	4
NGC 2099	368	56	0.31	0.02	1343	52	9	+0.03	11	+0.04	0.05	3
NGC 2169	10	3	0.19	0.01	1017	66	10					
NGC 2232	49	15	0.02	0.01	350	22	7	+0.18	9.5	+0.13	0.09	3
NGC 2287	244	34	0.02	0.02	657	27	10	-0.07	17	-0.05	0.08	6
NGC 2343	118	34	0.18	0.02	924	92	6	+0.05	3	+0.05		1
NGC 2362	6	3	0.11	0.01	1452	106	11					
NGC 2422	123	21	0.08	0.01	480	16	9	+0.06	7	+0.05	0.05	3
NGC 2423	1000	200	0.10	0.02	912	90	1	+0.09	13.5	+0.08	0.05	5
NGC 2439	14	5	0.39	0.02	3918	293	9					
NGC 2447	487	89	0.03	0.03	1058	31	7	-0.01	13	+0.00	0.04	4
NGC 2451A	50	10	0.01	0.02	186	20	1	-0.03	11.5	-0.02	0.05	4
NGC 2451B	50	10	0.10	0.02	385	40	1	-0.01	7	+0.01	0.02	2
NGC 2489	531	44	0.30	0.01	1810	14	2	+0.08	5	+0.08	0.02	2
NGC 2516	137	27	0.11	0.01	407	24	12	+0.02	15	+0.02	0.04	6
NGC 2546	123	21	0.15	0.01	951	44	7	+0.06	5	+0.07	0.08	2
NGC 2567	297	52	0.14	0.01	1673	58	8	+0.01	11	+0.01	0.00	3
NGC 2632 (Praesepe)	723	76	0.01	0.01	179	7	9	+0.16	17	+0.15	0.05	6
NGC 2658	253	59	0.38	0.02	3998	377	5	+0.02	3	+0.02		1
NGC 3105	22	3	1.08	0.02	7287	1072	7					
NGC 3114	142	31	0.07	0.01	917	20	8	+0.07	11.5	+0.06	0.01	5

... continues on next page

Table 6.5: ... Continuation

Cluster	age [Myr]	σ [Myr]	$E(B - V)$	σ	dist [pc]	σ [pc]	No	[Fe/H]	weight	av. [Fe/H]	σ	No
NGC 3228	86	15	0.03	0.01	503	31	5	+0.03	3	+0.03		1
NGC 3293	8	2	0.28	0.02	2407	170	10	+0.06	0.5	+0.06		1
NGC 3532	293	46	0.04	0.00	486	12	7	+0.03	14	+0.02	0.03	6
NGC 3960	960	144	0.28	0.03	1922	265	5	-0.03	11	-0.04	0.06	3
NGC 5281	60	18	0.23	0.02	1342	170	6	+0.00	1	+0.00		1
NGC 5460	153	39	0.12	0.02	676	76	8	+0.05	12	+0.05	0.01	5
NGC 5662	94	13	0.32	0.02	688	59	9	+0.07	3.5	+0.07	0.01	2
NGC 5999	405	93	0.46	0.02	2178	75	3	-0.00	3	-0.00		1
NGC 6031	215	45	0.47	0.03	1666	130	10	+0.02	3	+0.02		1
NGC 6087	82	16	0.19	0.01	871	35	10	+0.06	3	+0.06		1
NGC 6134	1018	115	0.40	0.03	954	82	10	+0.13	11	+0.15	0.03	3
NGC 6192	143	33	0.64	0.01	1619	81	8	+0.14	9.5	+0.20	0.11	3
NGC 6204	100	24	0.45	0.02	1155	42	10	+0.05	3	+0.05		1
NGC 6208	1265	106	0.20	0.02	1054	124	7	+0.02	2.5	+0.01	0.04	2
NGC 6250	21	5	0.37	0.01	925	58	8					
NGC 6268	158	40	0.43	0.02	1525	150	1					
NGC 6281	278	52	0.15	0.01	520	32	6	+0.05	15	+0.05	0.03	6
NGC 6396	27	4	0.94	0.02	1252	102	5					
NGC 6405	80	14	0.16	0.02	472	18	9	+0.10	9	+0.10	0.05	4
NGC 6451	129	29	0.70	0.03	2074	128	5	+0.04	3	+0.04		1
NGC 6475	250	80	0.06	0.02	260	24	9	+0.08	15.5	+0.07	0.04	6
NGC 6611	3	1	0.71	0.03	1771	110	9					
NGC 6705	200	36	0.42	0.02	1886	171	10	+0.14	11	+0.15	0.02	3
NGC 6756	129	4	1.04	0.01	3085	320	2	+0.10	3	+0.10		1
NGC 6802	977	32	0.82	0.04	2015	205	3	+0.03	3	+0.03		1
NGC 6830	163	52	0.51	0.04	2176	362	2	+0.24	3	+0.24		1
NGC 6834	61	15	0.71	0.01	2145	49	9					
NGC 7092	301	69	0.02	0.02	295	23	8	+0.01	7.5	+0.01	0.02	4
NGC 7235	9	2	0.93	0.02	2850	204	7					
NGC 7243	100	19	0.24	0.01	784	32	7	+0.07	7	+0.07	0.01	3
NGC 7296	316	70	0.26	0.02	2399	240	1	+0.04	3	+0.04		1
NGC 7510	8	2	1.05	0.05	2888	327	6					
Pismis 20	5	2	1.19	0.03	2809	420	9					
Ruprecht 115	487	88	0.71	0.05	2134	275	4	+0.04	3	+0.04		1
Ruprecht 120	224	50	0.68	0.02	1653	170	1					
Ruprecht 130	562	130	1.00	0.02	1995	200	1	+0.03	3	+0.03		1
Stock 16	5	2	0.49	0.02	1863	41	8					
Trumpler 10	41	12	0.04	0.01	407	30	7	-0.04	4	+0.00	0.10	3

Chapter 7

Membership analysis

There are numerous studies available, which are dealing with membership analyses in open clusters. They are either based on proper motions, radial velocities, or photometric criteria. For just a handful of open clusters all data types are available, allowing the most accurate member selection. Radial velocity studies are compared to proper motion not limited in distance, but due to the time consuming observations, studies in this respect are hardly carried out. However, multi object spectrographs, which are to date offered at several observatories, allow a significant reduction of observing time, but still there is a lack of such data. More common are membership studies using proper motion (e.g. Baumgardt et al., 2000; Dias et al., 2001, 2006; Kharchenko et al., 2004). They are either based directly on Hipparcos and Tycho-2 data, or on catalogues like UCAC-2 (Zacharias et al., 2004). The latter is the result of a combination of photographic surveys, analysed in a homogeneous way, but the overall given errors are somewhat larger than for data e.g. by Tycho-2. In the meanwhile, updated versions (UCAC-3 and 4) are available, including additional observations. Roeser et al. (2010), who presented a further proper motion catalogue (PPMXL) using USNO-B1.0 and the 2MASS survey, noticed distortions in the UCAC-3 data north of -20° in declination, which led to the exclusion of Schmidt plate data in the latest UCAC release. As have been already shown e.g. in Sect. 5.1.27 for the cluster NGC 3228, available membership probabilities have to be properly checked before adopting them, since for this cluster they were inversely calculated by Dias et al. (2001), showing a higher membership probability with increasing deviation from the cluster mean. Such a distinctive feature was also found in their results for NGC 6250.

Hipparcos offers parallaxes, which can be used as a further membership criteria, but the limiting magnitude results in a considerable limitation in distance. Our approach of the member selection is shown by means of some open cluster, which should demonstrate the difficulties arising within such a task.

NGC 3532 for example is a rather difficult case, as can be seen in the following. Its peculiar content was studied by Maitzen & Schneider (1987). Using the Δa photometric system, 164 objects were measured in the cluster area, representing the most extensive investigation in the photoelectric survey. They found three significantly deviating objects exhibiting Δa values of more than 60 mmag as well as four mildly ones with Δa in the range of 12–18 mmag. Since this cluster is rather close (~ 500 pc), proper

motions offer an appropriate method for membership analysis. In the literature one can find several studies dealing with this exercise, which are compiled in Table 7.3. All of them are based on proper motions, except the one by Giesekeing (1981), who used radial velocity data. Furthermore, the works by Dias et al. (2001), Dias et al. (2006), and Kharchenko et al. (2004) provide absolute proper motions, a comparison of the mean cluster motion can be found in Table 7.1. The result by Dias et al. (2006) using UCAC-2 data (Zacharias et al., 2004) is deviating compared to the others. Whereas the works by Dias et al. (2001) and Loktin & Beshenov (2003) are based on the Tycho-2 catalogue (Høg et al., 2000), Kharchenko et al. (2004) used a compilation of different sources including Tycho-2. Finally, Baumgardt et al. (2000) used Hipparcos data for their investigation. However, this result is based only on five objects.

The main difference between the two catalogues (UCAC-2/Tycho-2) is the limiting magnitude. Whereas the one by Tycho-2 lies at ~ 12 mag, UCAC-2 provides data for stars down to ~ 16 mag. However, especially for closer (brighter) clusters, a deeper investigation can result in a contrary effect, since with decreasing magnitude the influence of field stars is increasing. Since the provided tables by Dias et al. (2006) list also 2MASS data, we restricted the sample to stars brighter than 10 mag in the K_s magnitude. As mentioned above, new releases are already available (the currently latest is UCAC-4), but we still used the previous version to have a direct comparison of the results based on the same data set. Furthermore, the cluster CMD was examined in order to remove objects which are strongly deviating from the main sequence. Using this limited sample of about 170 stars, we determined a mean cluster motion of $-11.5(2)/3.9(1)$ mas/yr by means of Gaussian fits (see Fig. 7.1) in good agreement with the Tycho-2 results. Inspecting the results by Dias et al. (2006), one can also notice that all stars have probabilities lower than 60%, so according to the latter reference no definite member can be found in this cluster at all. Due to this fact and the deviating cluster motion, the membership probabilities were re-estimated based on the UCAC-2 sample. For this purpose, the parameters of the above mentioned Gaussian fits and the equations below for RA (x) and DE (y), as given by Javakhishvili et al. (2006), were used to calculate the final probabilities, which are listed in Table 7.3.

$$p_x = e^{-2\left(\frac{x-x_0}{\sigma_x}\right)^2}, p_y = e^{-2\left(\frac{y-y_0}{\sigma_y}\right)^2}, p = p_x * p_y$$

Inspecting the final membership probabilities in Table 7.3, one can notice rather divergent results for the individual stars between the different studies, even for those two with more or less the same basis.

Although data for HD 303821 and CP -57 04336 are available in the UCAC-2 catalogue, Dias et al. (2006) have not investigated them because of their restriction of the cluster area (diameter). However, these objects were included in our sample to recalculate membership probabilities.

Additionally, we calculated temperature and luminosity for all CP candidates using the methods described by Netopil et al. (2008), the available photometry, and the determined cluster parameters. The results can be found in Table 7.3 and Fig. 7.2. For all objects sufficient data are available. The availability and quality of the data incorporates also into our membership classification, e.g. if those are available in

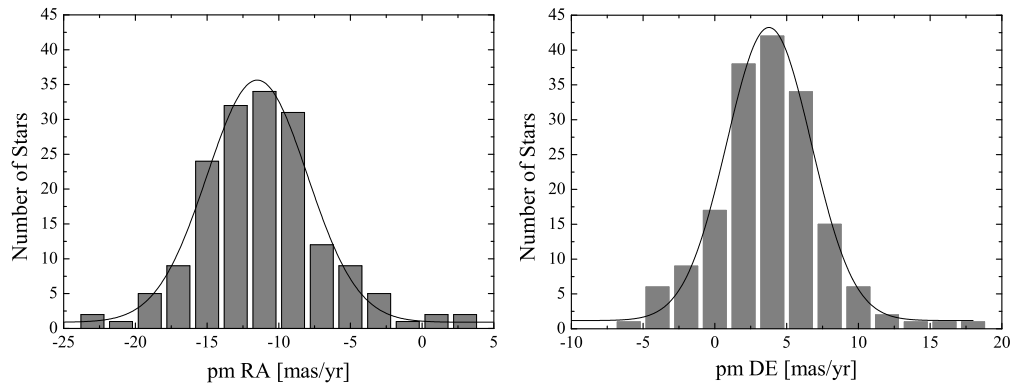


Figure 7.1: The Gaussian fits for the restricted sample of proper motions in RA and DE for stars in NGC 3532 using UCAC-2 data.

Table 7.1: Overview of mean proper motions for the open cluster NGC 3532. The errors of the last digits are given in parenthesis.

Reference	pmRA [mas/yr]	pmDE [mas/yr]
Dias et al. (2001)	-11.00(290)	4.90(290)
Dias et al. (2006)	-7.46(13)	4.57(13)
Kharchenko et al. (2005)	-10.54(23)	4.57(17)
Baumgardt et al. (2000)	-10.70(47)	5.26(43)
Loktin & Beshenov (2003)	-9.25(26)	3.88(19)
this study	-11.5(2)	3.9(1)

Table 7.2: Proper motions of the CP candidates in the open cluster NGC 3532. The indication of errors have been omitted for better readability, all of them are in the order of 2–3 mas/yr. The mean cluster motion was calculated as $-10.0(1.2)/4.7(0.5)$ for RA and DE, respectively.

Star	Tycho-2 [mas/yr]	ASCC [mas/yr]	UCAC-4 [mas/yr]	PPMXL [mas/yr]	kinematic member
HD 96040	-1.1/3.1	-3.2/3.3	-5.0/2.0	-2.6/2.3	pm
HD 96729		-11.49/1.39	-9.7/-0.8	-10.0/2.8	m
HD 303821			-3.8/-9.0	-2.0/-1.6	nm
HD 96619	-9.3/9.8	-9.32/9.76	-7.9/8.0	-10.8/8.3	m
HD 96754	-14.6/10.4	-16.27/8.14	-14.9/7.9	-15.5/9.4	pm
CP -57 04336			-4.7/4.8	-7.0/5.9	m
CP -58 03025			-6.5/-7.0	-12.9/-1.0	pnm

different photometric systems, several measurements in one system are in agreement, but also the detector (photographic plates, photoelectric multiplier, CCD) is taken into account.

Based only on photometric criteria, we conclude that two stars (HD 96619 and CP –57 04336) are members, whereas most others cannot be assigned to the cluster. Since these two objects are rather cool (~ 8900 K), even the treatment as non CPs will not alter the result. No significant difference can be found at such a temperature, if compared to normal star temperature calibrations. One further object (CP –58 03025) is located slightly below the ZAMS but reasonable close to the sequence of all cluster members and was therefore classified as probable member. Several stars are significantly deviating from the ZAMS. If they were calibrated as normal stars, the deviation will be even larger. So, the most outstanding objects in Δa seem to be non-members. The same holds for the most luminous star (HD 96754) near the TAMS in Fig. 7.2. Binarity can influence the brightness by about 0.75 mag, if the components are of equal mass, but even this assumption is not sufficient to correct the deviation. Nevertheless, this star is classified as metallic line Am star in the Michigan spectral survey, which are known to be spectroscopic binaries. The mild Δa value of 13 mmag is in line with those found for some other Am stars (e.g. in Praesepe).

Instead of calculating “hard number” kinematic membership probability values, we classify the stars identical to the photometric criteria above within a less strict scheme (m: member; pm: probable member; pnm: probable non-member; nm: non-member), taking into account the deviation from the cluster mean values (see Table 7.5), the reliability of catalogue entries (e.g. number of epoch data used to calculate proper motion), deviations of the available data if several entries are available for one object, but also the star density in the respective area to account for possible wrong assignment of the individual epoch data. The latter argument is especially important if investigating e.g. rather close-by stars, which were probably not always clearly resolved, depending on the resolution of the individual source data (e.g. POSS plates) used.

Using a combination of the membership classes deduced from proper motion data (see Table 7.2), the photometric criteria, as well as radial velocities and parallax if available, we define a final membership flag. We conclude that out of the 7 CP candidates only HD 96619 and CP –57 04336 can be assigned as cluster member. However, due to the rather low Δa index of 12 mmag, we cannot designate the latter object as a definite member of the CP group. Hence, only one CP star that belongs to NGC 3532 seems to be present.

Landstreet et al. (2007) investigated the CP and cluster membership of the three outstanding Δa objects. For the first two stars in Table 7.3 they have detected in a previous study magnetic fields, what strengthen their CP nature and the Δa results. Furthermore, an abundance analysis of HD 96729 by Saffe et al. (2005) revealed a doubtless Si star nature. For this object also the *Geneva* indices Z and $\Delta(V1 - G)$ show a strong peculiar indication (see Table 7.3). A probable cluster membership was assigned by Landstreet et al. (2007) only for HD 96040, in contrast to our result for this object. Whereas the kinematic membership is in agreement, we define it as probable photometric non-member. Since temperature and luminosity, listed by them, are in perfect agreement with our determinations, their membership classification is probably

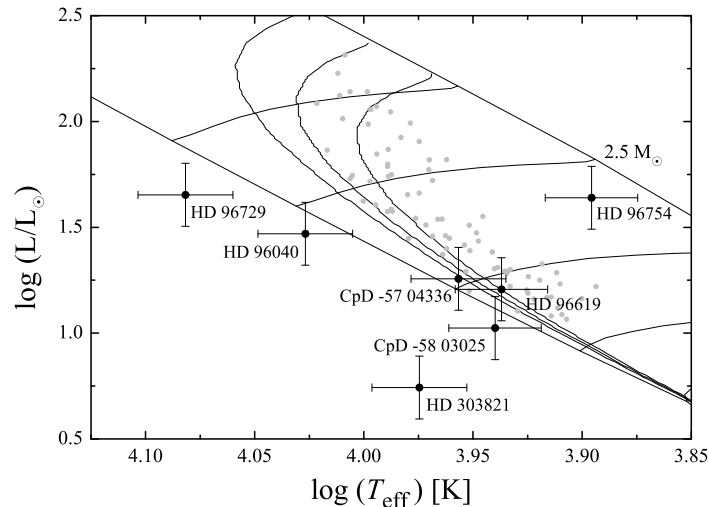


Figure 7.2: The HRD of the open cluster NGC 3532. The black circles represent the probable CP2 members, the smaller grey symbols the normal ones. Furthermore, the Geneva isochrones for solar metallicity at $\log t = 8.3, 8.4, 8.5$ and some mass tracks are plotted.

even less strict than ours. As can be seen in Fig. 7.2, this object is strongly deviating in the HRD, located even below the ZAMS. Since the temperatures calculated by means of UBV , Strömgen data, as well as SED fitting are in perfect agreement, only an unlikely temperature overestimation of about 1300 K will bring the star in line.

A careful membership analysis was performed for all with Δa measured objects, and 82 stars in total remained as members (see Fig. 7.2). Maitzen & Schneider (1987) estimated a number of 70 members, and found membership for HD 96619 and CP -57 04336. However, as shown above only the first star can be designated at least as cluster member, but not as CP star.

Fortunately, there are also somewhat easier cases like NGC 2516. This is a rather CP rich open cluster investigated by Maitzen & Hensberge (1981), located at a distance of about 400 pc and exhibiting an age of $\log t \sim 8.15$. This study included in their sample seven spectroscopically identified peculiar objects, which were confirmed by their positive Δa indices, but the authors were not able to detect any new candidate among the 53 investigated objects. Actually, eight probable peculiar objects are found in this cluster. A visual binary (CP -60 944 A/B) is present, where both components are suspected as peculiar, but Maitzen & Hensberge (1981) were not able to resolve the pair and treated them as a single star due to the separation of about $9.5''$. The spectroscopic study by Dachs (1972) found peculiar nature for both components, whereas Hartoog (1976) was able to confirm a peculiar behaviour only for the component A; the other one was classified as B8III. However, the spectrum for A obtained by Dachs (1972) broke during exposure and was therefore not focused at wavelengths redder than $\sim 3950\text{\AA}$. Maitzen & Hensberge (1981) discussed the possibility of misunderstanding the denominations in these works, an assumption which is supported by Dachs & Kabus (1989) and their comparison with the former results. The latter reference provided new spectroscopic data for A (Hartoogs B) and classified it as B9IVp(Si4200).

Table 7.3: The membership probabilities for the possible CP stars in NGC 3532.

Object	WEBDA #	Δa [mmag]	$Z/\Delta(V1-G)$ [mmag]	K1 ^a [%]	K2 ^b	D1 ^c [%]	D2 ^d [%]	G ^e [%]	K3 ^f [%]	$\log(T_{\text{eff}})$ [K]	$\log(L/L_{\odot})$	HRD/PM ^g	final
HD 96040	413	60		24	b	34/28	4		18/76/100	4.027(22)	1.470(149)	pnm/pm	pnm
HD 96729	449	65	-47/30	91	a	23/90			77/07/100	4.082(22)	1.654(149)	nm/m	pnm
HD 303821	704	61			b	-/1				3.975(22)	0.743(149)	nm/nm	nm
HD 96619	510	12	-6/-14	90	c	23/73	77		38/80/100	3.937(21)	1.207(149)	m/m	m
HD 96754	500	13		0	c	0/8	59	0	18/02/100	3.896(21)	1.640(149)	nm/pm	nm
CP -57 04336	632	18	-34/3	90	c	-/31				3.957(22)	1.257(149)	m/m	m
CP -58 03025	163	15		78	c	1/31				3.940(21)	0.942(149)	pm/pnm	pnm

^aKing (1978a)

^bKoelbloed (1959): a = high probability; c = low probability

^cDias et al. (2006) / this study

^dDias et al. (2001)

^eGiesecking (1981)

^fKharchenko et al. (2004): Probability based on kinematic data / photometry / position

^gmember according to HRD/PM: non-member (nm), probable non-member (pnm), member (m)

Indeed, e.g. also in SIMBAD a wrong identification was found, which was corrected in the meanwhile. In the work by Dachs (1972), the brightest component was called A, the usual convention, but in SIMBAD the coordinates were exchanged. Although the listed basic data (magnitude etc.) were correct, it refers to the weaker eastern component. Examination of the Tycho data revealed that the brighter object CP –60 944A is the western component. This problem was also already noticed by Bagnulo et al. (2006). In the following we adopted the denomination by Dachs (1972). Bagnulo et al. (2006) performed magnetic field measurements for both components, but only for B a probable field was detected. The confusion continued with the follow-up work by Landstreet et al. (2007), where the listed magnetic field measurements were mixed up. It seems that they have exchanged again the already correct given designations, what can be revealed by searching the ESO-Archive, the given observing dates and coordinates. Furthermore, in the radial velocity study by González & Lapasset (2000) another permutation of the stars is most likely. They found a probable binary nature for their listed A component, but Tycho data show hints of duplicity by means of photometry for the weaker one, whereas the other component was classified as a single star. However, if it is indeed a binary cluster member, the mass ratio of the components has to be rather low, what can be explained by the position in the HRD (see Fig. 7.3), where this probable binary is located very close to the corresponding isochrones. If it consists of components with equal masses, a shift to higher luminosities is expected.

In Table 7.4 one can find the rectification for some data of the pair CP –60 944AB. Dachs & Kabus (1989) as well as Pöhlner et al. (2003) suppose a physical connection for them. However, whereas A is a definite member according to several proper motion and radial velocity studies, for B differing results can be found; 0% (Dias et al., 2001), 25% (Kharchenko et al., 2004), and 98% (King, 1978b). Landstreet et al. (2007) defined it as member, since the proper motions differ from cluster mean less than 2σ .

One object (CP–60 981) exhibits a somewhat too mild Δa value of 14 mmag. It was classified as A2 V (p SrCrEu) by Hartoog (1976), but as eclipsing binary without peculiar nature by Debernardi & North (2001). Since also no magnetic field was found by Bagnulo et al. (2006), it was rejected as CP candidate, but remained as cluster member in the sample. Another star (HD 65712) is lying somewhat outside the assumed cluster radius of $15'$, but proper motions as well as its position in the HRD (see Fig. 7.3) are evidence for membership.

We conclude that all stars (except CP–60 981) are indeed CP cluster objects. Unfortunately, all objects are somewhat too faint to be included in the Hipparcos sample. These data (parallax) would be a valuable further membership criteria.

One problem arises due to the above mentioned combined Δa measurements for the pair CP –60 944. So, how many actual CP objects have to be taken into account for further analysis? If Maitzen & Hensberge (1981) were able to separate them, they probably would have obtained a positive result for both objects. However, this can hold for all clusters, which were not completely investigated. One single object more in the target list of each individual cluster can reveal another peculiar candidate. Compared to numerous other clusters, NGC 2516 is a rather well investigated one, showing up such difficulties. We therefore decided to include only one of them, namely component A, whose membership is better confirmed. Since both have similar masses (see Fig.

Table 7.4: Summary of the now hopefully correct rectification for the peculiar visual pair CP –60 944 A/B, whereas A is the brighter western component.

Component	m_V [mag] ^a	RA (2000)	DE (2000)	Spec. Type ^b	B_{rms} [G] ^c
A	8.312	07 56 45.110	-60 48 54.29	B9IVp(Si4200)	120
B	8.761	07 56 46.253	-60 48 58.26	B9.5IVp(Si)	250

^aGeneva photometry

^bDachs & Kabus (1989)

^cLandstreet et al. (2007)

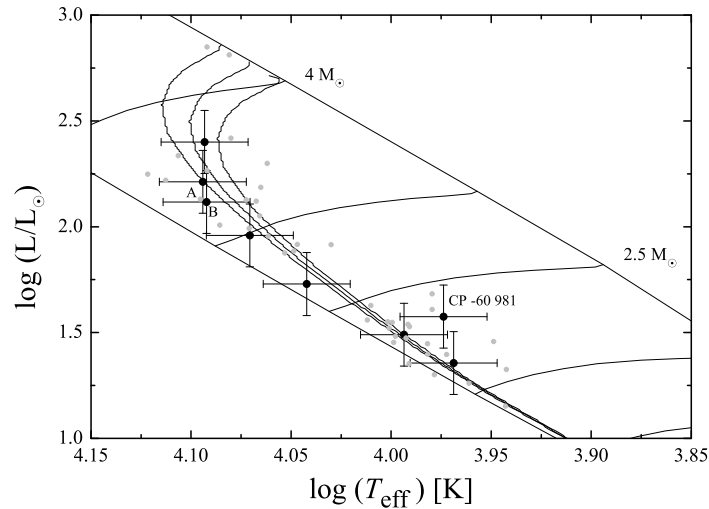


Figure 7.3: The HRD of the open cluster NGC 2516. The black dots represent the possible CP2 members, the smaller grey symbols the normal ones. Furthermore, the Geneva isochrones for solar metallicity at $\log t = 8.10, 8.15, 8.20$ and some mass tracks are plotted. The object CP–60 981 is the only one which is deviating somewhat from the corresponding isochrones, probably due to its binary nature. Both components of CP–60 944 are also indicated.

7.3), the influence whether A or B is chosen is insignificant.

That the currently available proper motion catalogues such as PPMXL and UCAC have to be used with caution can be seen in Fig. 7.4. An area of $5'$ radius around the center of the more distant (1900 pc) and therefore fainter program cluster NGC 3960 was extracted from the above mentioned catalogues. A cross-match was performed using a search radius of $1''$, in order to compile only good matches. Since both catalogues also include 2MASS data, these were used as an additional criteria for the matching. In total, 326 objects with listed proper motions coincide, but of which only 90 (28%) exhibit differences less than 10 mas/yr in both coordinates, if comparing the results of the two catalogues. Using a more strict criteria of 5 mas/yr, only 7% of the sample remains. Beside the rather large scatter, one can notice in Fig. 7.4 also an offset at least in the RA proper motions. Furthermore, there seems to be no magnitude dependency. This result is by far no individual case, what can be seen also e.g. in the study by Paunzen et al. (2012). The investigation of the respective mean cluster motions also revealed a difference of the order of about 5 mas in RA, and a slightly lower one

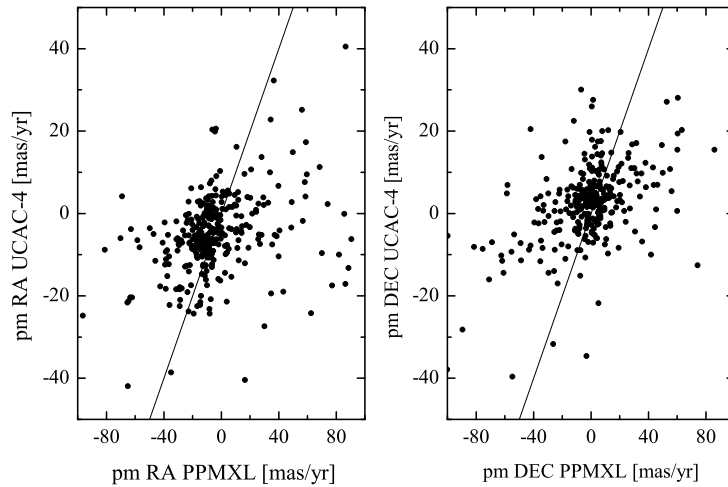


Figure 7.4: The UCAC-4 and PPMXL proper motions for stars in the open cluster NGC 3960. The straight lines represent the 1 to 1 relation. Note that only the inner portion is shown, there are several even larger deviating results.

in DEC.

Nevertheless, proper motions are a valuable source to strengthen membership in combination with other criteria, if the problems mentioned above are taken into account. In Table 7.5 we list the mean cluster motion of the programme clusters, compiled from available catalogues (Dias et al., 2001, 2002; Loktin & Beshenov, 2003; Kharchenko et al., 2005; Dias et al., 2006). These values represent the mean values of the individual results together with their standard deviation. In addition, for several smaller angular size clusters ($\sim 15'$ in diameter), for which only few studies are available, we obtained further mean motions using the PPMXL and UCAC-3/4 catalogues, by restricting the sample as was discussed for NGC 3532.

Table 7.5: The mean proper motions of the programme open clusters, given in mas/yr. An asterisk in the last column indicates that also mean motions were calculated using the PPMXL and/or UCAC catalogues.

Cluster	pmRA	e(pmRA)	pmDE	e(pmRA)	No. of studies
Berkeley 11	-0.59	1.22	-4.16	2.86	5*
Berkeley 94	-1.73	2.62	-0.73	1.54	4*
Collinder 121	-4.44	0.99	4.14	0.41	5
Collinder 132	-4.51	1.74	4.48	1.11	4
Collinder 140	-8.15	0.58	3.97	0.65	7
Collinder 272	-3.88	1.24	-1.87	0.71	4
IC 2391	-24.85	0.36	22.79	0.41	6
IC 2602	-17.36	0.30	10.94	0.42	5
IC 4665	-0.82	0.18	-8.34	1.21	4
IC 4725	-3.06	0.56	-5.37	1.17	6
King 21	0.25	1.87	-1.13	3.01	3*
Lynga 1	-7.46	1.59	-2.31	1.85	6*
Lynga 14	-1.76	1.50	-4.16	0.50	4*
Melotte 20 (Alpha Per)	22.50	0.36	-25.75	0.46	5
Melotte 22 (Pleiades)	19.64	0.28	-44.94	0.10	3
Melotte 105	-4.85	0.92	-2.18	1.95	3*
Melotte 111 (Coma Ber)	-11.40	0.30	-8.93	0.16	4
NGC 1039	-0.03	0.24	-6.82	0.57	6
NGC 1502	-0.39	1.01	-0.17	0.67	6
NGC 1662	-2.27	0.74	-2.16	0.43	6
NGC 1901	1.81	0.86	10.57	1.34	5*
NGC 2099	3.20	0.48	-6.82	0.45	5
NGC 2169	-2.93	0.80	-2.92	0.74	6*
NGC 2232	-4.45	0.83	-2.78	0.58	7
NGC 2287	-4.36	0.22	-0.68	0.40	5
NGC 2343	-0.56	1.32	0.54	1.48	5*
NGC 2362	-2.20	0.08	2.59	0.75	4
NGC 2422	-6.54	1.18	1.48	0.53	8
NGC 2423	0.47	1.20	-2.97	0.90	7*
NGC 2439	-2.28	0.64	1.60	2.21	4
NGC 2447	-3.87	1.24	4.01	1.04	5
NGC 2451A	-21.86	0.33	15.33	0.25	4
NGC 2451B	-10.09	0.03	4.83	0.88	2
NGC 2489	-2.19	1.66	-1.11	1.14	6*
NGC 2516	-3.85	0.33	10.33	1.09	8
NGC 2546	-4.44	1.00	4.21	0.46	5
NGC 2567	-2.70	1.06	3.12	1.28	5
NGC 2632 (Praesepe)	-35.91	0.19	-12.91	0.11	6
NGC 2658	-1.88	0.41	0.76	1.91	3*
NGC 3105	-4.69	1.74	3.25	0.83	3*
NGC 3114	-7.09	0.91	3.69	0.79	7
NGC 3228	-13.33	1.34	0.43	1.05	8*
NGC 3293	-6.90	0.75	2.23	0.94	6*
NGC 3532	-10.04	1.18	4.66	0.50	8
NGC 3960	-8.08	1.98	1.77	1.86	4*
NGC 5281	-5.39	1.11	-2.80	0.83	8*
NGC 5460	-5.97	0.73	-2.55	1.48	6
NGC 5662	-5.16	0.69	-6.07	1.31	5
NGC 5999	-4.22	0.19	-4.66	1.17	2*
NGC 6031	-2.49	1.10	-7.37	1.32	5*
NGC 6087	-1.25	0.61	-3.16	1.36	8*
NGC 6134	-0.54	0.79	-5.55	1.42	6*
NGC 6192	1.17	0.81	-1.21	1.29	5*
NGC 6204	-1.56	1.44	-1.51	1.23	6*
NGC 6208	-0.68	0.30	-3.66	0.88	4*
NGC 6250	1.01	1.33	-3.38	0.52	9*
NGC 6268	0.44	0.68	-0.81	0.30	6*
NGC 6281	-3.21	0.23	-4.28	0.66	6
NGC 6396	-2.29	0.90	-4.47	1.42	4*
NGC 6405	-1.24	0.91	-4.74	1.97	7
NGC 6451	1.20	3.19	-3.27	2.41	3*

... continues on next page

Table 7.5: ... Continuation

Cluster	pmRA	e(pmRA)	pmDE	e(pmRA)	No. of studies
NGC 6475	2.46	0.42	-4.77	0.53	7
NGC 6611	1.44	0.75	-0.52	0.33	3
NGC 6705	-5.56	0.93	-1.60	1.24	7*
NGC 6756	1.00	0.58	-4.30	1.21	3*
NGC 6802	-3.29	2.72	-6.91	1.36	3*
NGC 6830	-0.30	1.21	-4.09	1.18	7*
NGC 6834	-2.25	1.91	-4.45	1.65	7*
NGC 7092	-7.89	0.26	-20.06	0.39	7
NGC 7235	-3.76	0.97	-2.51	0.76	5*
NGC 7243	0.39	1.15	-2.18	0.62	6
NGC 7296	-3.55	0.07	-3.12	0.38	2*
NGC 7510	-2.78	1.11	-1.05	0.55	5*
Pismis 20	-5.48	2.44	-4.88	2.09	4*
Ruprecht 115	-4.28	0.67	-4.25	1.58	3*
Ruprecht 120	-2.73	1.76	-0.57	1.08	3*
Ruprecht 130	-0.87	1.30	-1.72	5.21	3*
Stock 16	-4.73	1.98	-0.12	0.68	6*
Trumpler 10	-11.07	2.88	6.54	0.41	5

Chapter 8

Results

8.1 The final dataset

In the Sections 5.1, 5.2, and 5.3 we have presented the so far available (photoelectric and CCD) Δa studies of 84 open clusters in total, of which three were investigated with both techniques (NGC 2169, NGC 3114, and NGC 6405). Two open clusters (Haffner 15 and Ruprecht 44) were excluded for further analysis due to reasons described in Sections 5.3.3 and 5.3.19, respectively. Hence, 79 open clusters remain for our analysis, whose parameters (the distance, the age, and the reddening) were determined in Sect. 6.2. Furthermore, for the majority of clusters (60) we were able to estimate also metallicity.

A membership analysis for all investigated stars (CP and normal ones) was carried out as described in Sect. 7, resulting in the membership flags m (member), pm (probable member), pnm (probable non-member), and nm (non-member), using mostly photometric and kinematic data, since radial velocities and parallaxes are hardly available. The membership analysis resulted into 102 CP cluster members out of 4137 investigated main-sequence objects, the latter ranging from $\sim 0.9 M_{\odot}$ (e.g. in NGC 6204) up to $\sim 30 M_{\odot}$ in the 3 Myr old cluster NGC 6611. Pre-main sequence stars (PMS, see Sect. 8.5) and objects, which have left the main-sequence already were excluded in order to not falsify a direct comparison with CP stars, which are in principle known to cover the main-sequence. So far, only one slowly rotating single giant star (EK Eri, G8 III-IV) is known to exhibit a large-scale dipole surface magnetic field of 270 G, most likely the remnant of a main-sequence (CP) progenitor, rather than generated by a dynamo (Aurière et al., 2008).

With the exception of a few CP stars, like those in the young (~ 9 Myr) open cluster Berkeley 94, for which no sufficient photometry is available, effective temperature and luminosity were calibrated as described in Section 2.3. For the error analysis, 5% of the determined temperature, and 10% of the cluster distance were adopted. If the standard deviations of the averaged temperatures and distances exceed these values, these were used instead. Furthermore, errors of 0.05 mag for the reddening $E(B - V)$ and total-to-selective extinction ratio R_V (using in general $R_V = 3.1$), respectively, were assumed, as well as 0.1 mag as error for the bolometric correction, which was determined as a function of temperature (see Sect. 2.3). The resulting Hertzsprung-Russell diagram for the CP cluster members can be found in Fig. 8.1. Normal member stars, investigated

within the Δa survey, were treated with the calibrations presented in Sect. 6.1.1 (Table 6.1). If poor available photometric data prevent a proper calibration, we estimated the mass using the absolute magnitudes (deduced from V magnitude and apparent cluster distance modulus) and the isochrones ($Z=0.02$ by Lejeune & Schaerer, 2001) for the adopted cluster age. Otherwise, mass and age were determined within evolutionary grids using the interpolation algorithm by Myakutin & Piskunov (1995). For objects located slightly outside of the grids (in general below the ZAMS, see Fig. 8.1), the mass was estimated using the nearest geometric position on the ZAMS.

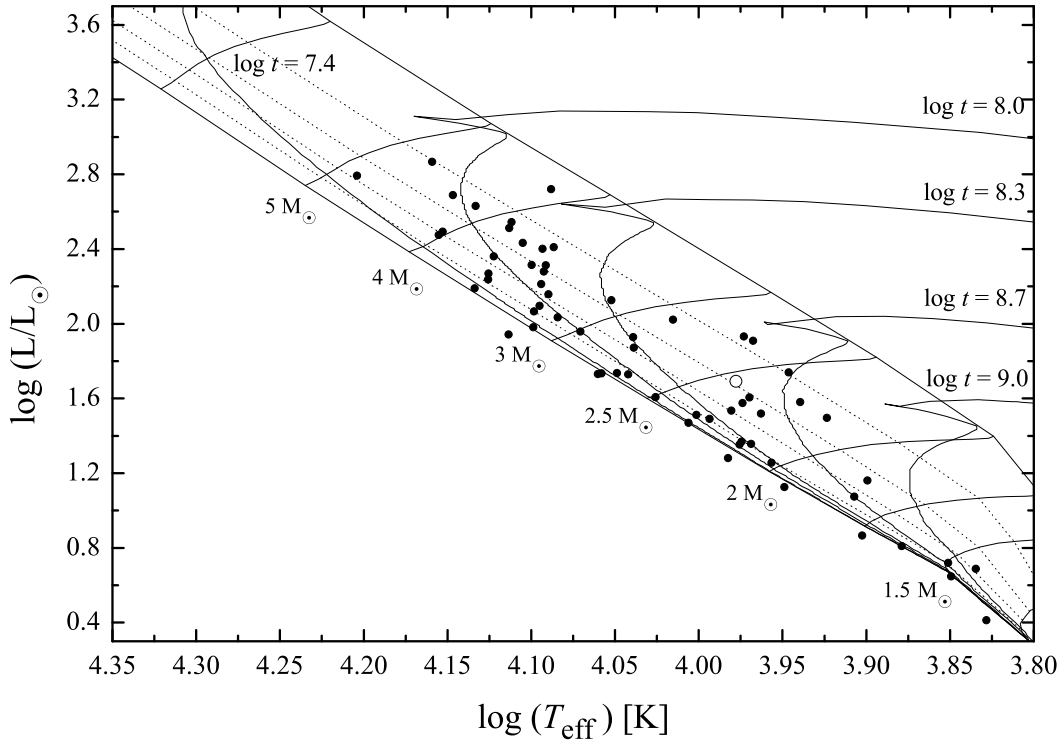


Figure 8.1: The HRD of the compiled cluster member CP stars, detected with Δa photometry, for which sufficient photometry is available to determine effective temperature. Several mass tracks and isochrones are indicated using the evolutionary grids by Schaller et al. (1992) for $Z=0.02$. The dotted lines represent fractional main-sequence ages of 20, 40, 60, and 80%, respectively. Additionally, the position of Stock 16 #12, discussed in Sect. 8.5, is given as open circle. To increase visibility, the individual errors were omitted, but the typical error in temperature and luminosity is shown in the bottom left-hand corner.

As a test of consistency, one can compare the ages interpolated within the grids to the adopted cluster ages (see Fig. 8.2), where we excluded objects located below the ZAMS and the few ones with insufficient photometry. As one can recognise, in general these two determinations nicely agree. The largest deviations are found in the lower mass regime close to the ZAMS (see panel b/c of Fig. 8.2), where already small errors in temperature and luminosity lead to rather large errors in age due to the density of the grids (see the given isochrones in Fig. 8.1). In addition, the fractional ages (elapsed

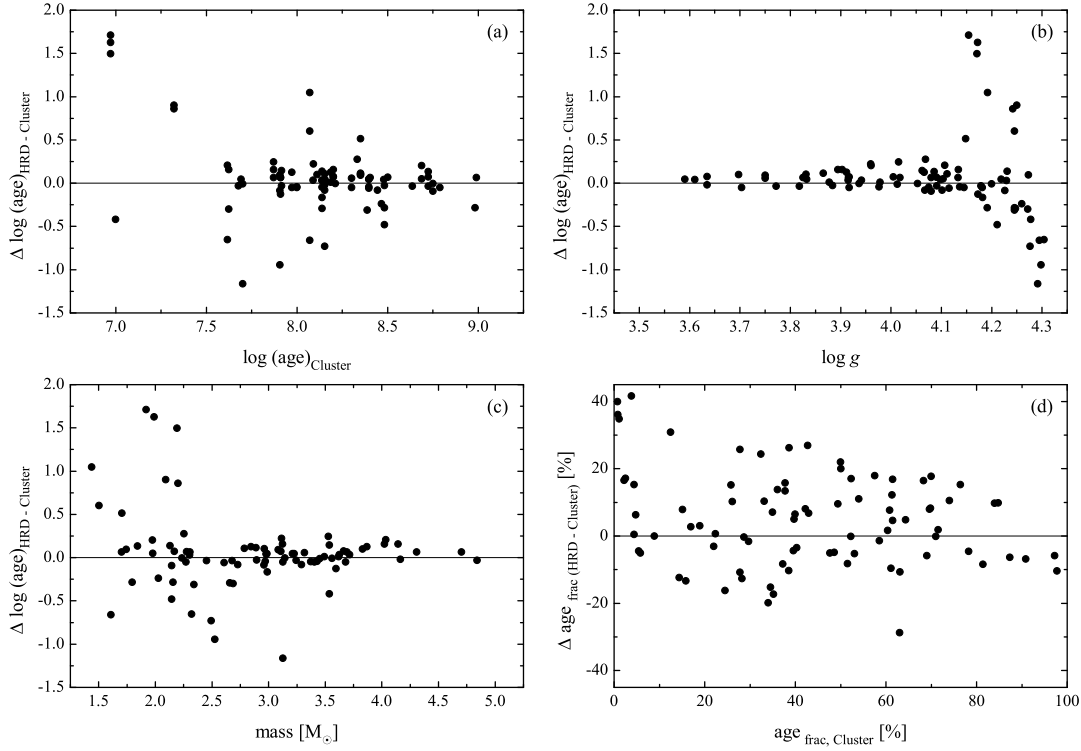


Figure 8.2: The CP stars ages determined by interpolating within the evolutionary grids by Schaller et al. (1992) for $Z=0.02$ compared to the adopted cluster ages in dependence of some properties. Furthermore, the fractional ages (time elapsed on the main-sequence) determined from the position in the HRD are compared to those using the stellar mass, main-sequence lifetimes and cluster age (panel d).

percentage of main-sequence lifetime) derived by interpolating within the evolutionary grids were compared to those using the determined masses, the adopted cluster ages, and the main-sequence lifetimes given in the grids by Schaller et al. (1992) (Fig. 8.2 d). From this figure one can infer an error of about 20 %, if solely using the position in the HRD as a basis.

These results can be in principle also adopted for the analysis of field stars with known parallax presented in Sects. 2.1 and 2.2. However, from the comparisons in Fig. 8.2 one can notice that the ages interpolated within the $Z=0.02$ grids are marginally higher (~ 0.05 in $\log(\text{age})$) than the adopted cluster ages, a slight overestimation is also noticeable for the fractional ages. Possible reasons for this offset can be either that a higher metallicity ($Z \sim 0.025$) is more appropriate, the in general adopted total-to-selective ratio of $R_V = 3.1$ is somewhat too large (this would affect especially higher reddened stars), or systematic effects in temperature and luminosity.

The investigation of magnetic CP stars by Landstreet et al. (2007) showed that the models for $Z=0.02$ (compared to $Z=0.008$ and $Z=0.05$) resulted into the best overall agreement, using grids of the Padova group. They also briefly discussed this finding compared to the “new” (lower) solar metallicity results (e.g. latest estimation $Z=0.0134$

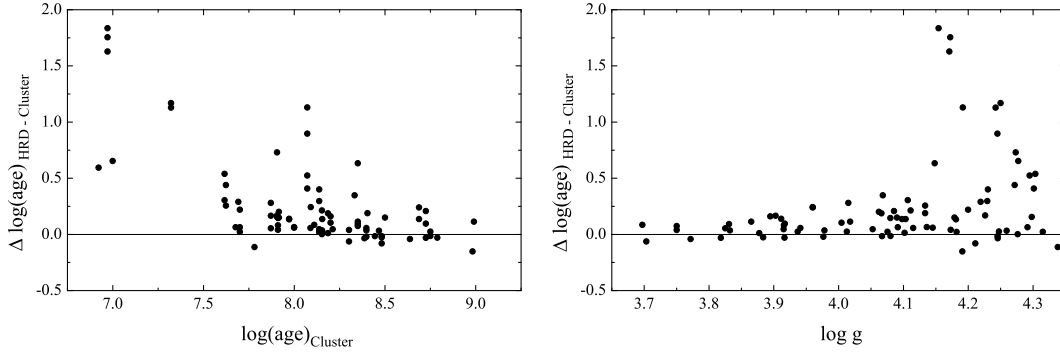


Figure 8.3: The CP stars ages determined by interpolating within the evolutionary grids by Ekström et al. (2012) for $Z=0.014$ (without rotation) compared to the adopted cluster ages. Furthermore, the dependency of the deviation with gravity ($\log g$) is given.

by Asplund et al., 2009). However, they were not able to test such a model, since no proper ones were available that time, which take into account the different ratios of light (CNO) elements to iron peak elements.

Recently, Ekström et al. (2012) presented such updated evolutionary models for $Z=0.014$ with and without rotation. Since CP stars are slow rotators, the latter is a more appropriate choice (see also Sect. 2.1). The comparison of the CP stars ages determined by interpolating in this grid with the adopted cluster ages is shown in Fig. 8.3. One can see systematic differences, with an increase of the deviations towards younger ages and higher gravity. New grids with higher metallicities are available by Mowlavi et al. (2012) for a restricted mass range only ($\leq 3.5 M_{\odot}$), reducing even more the number of objects for a proper comparison. Nevertheless, using their $Z=0.02$ grid results in a much better agreement, but a more detailed investigation is necessary, as soon these models are extended to somewhat higher masses. Please note that according to the revised solar abundances, a metallicity of $Z=0.02$ gives $[\text{Fe}/\text{H}] \sim 0.2$ dex using the corresponding equation by Mowlavi et al. (2012).

One can argue that the found differences are due to the fact that the vast majority of cluster ages were determined with isochrones based on the former solar $Z=0.02$ value (see also Sect. 6.1.1). To our knowledge there is no dedicated work, dealing with the errors in age caused by the use of a wrong metallicity. However, Mowlavi et al. (2012) applied their new grids to two open clusters, one (NGC 3532) also among our targets. They found a reasonable fit to the cluster CMD with a 310 Myr isochrone, by applying a distance of 492 pc, $E(B - V) = 0.04$, and $[\text{Fe}/\text{H}]=0.10$. These parameters are in excellent agreement with our adopted mean values: 355 Myr, 486 pc, $E(B - V) = 0.04$, and $[\text{Fe}/\text{H}]=0.03$ (Table 6.5). We want to remind that we also applied the differential grid method based on the models by Mowlavi et al. (2012) on a cluster with comparable age (NGC 6475, see Sect. 6.1.1 and Fig. 6.9), with a perfect agreement for this parameter (250 Myr). Further data in this respect (especially for younger clusters) are necessary for a profound conclusion, since one can notice in Fig. 8.3 that at older ages the differences are going to be smaller.

8.2 Masses and fractional ages of CP stars.

Since the stellar masses determined in all these various grids do not differ significantly (the differences are well below the adopted errors in mass), we keep the results obtained with the models by Schaller et al. (1992) for $Z=0.02$, to be able to directly compare the results with those presented in Sects. 2.1 and 2.2.

We use the results for 307 field stars investigated in these Sections to compare their mass distribution with the one of the cluster CP stars detected with Δa photometry, shown in Fig. 8.4. The mass distributions of these two samples nicely agree, what is hardly surprising, since probably the majority of stars are born in clusters, but a direct proof was not presented so far. Using the combined sample of field and cluster stars, a Gaussian distribution in the form

$$y = y_0 + \frac{A}{\omega\sqrt{\pi/2}} e^{-2\frac{(x-x_c)^2}{\omega^2}}$$

can be fitted to the data (also shown in Fig 8.4), with $y_0 = 0.40(52)$, $x_c = 2.65(4)$, $\omega = 1.40(8)$, and $A = 47(3)$ for the offset, center, width, and area, respectively. The errors of the last digits are given in parenthesis.

A comparison was performed also for the fractional ages, whose distribution is given in Fig. 8.5. The bin size was set to 20%, to take into account the offset of $\sim 5\%$, noticed in Fig. 8.2. While the field star sample shows a rather homogeneous distribution, the cluster stars seem to exhibit a deficit at the later stages. It is difficult to conclude if that is an intrinsic feature, a selection effect, or just a result due to the lower number of objects. The analysis by Landstreet et al. (2007) showed even a much stronger preference at the very earliest stage, probably the result of the inclusion of numerous very young OB association objects, representing $\sim 35\%$ of their total sample. Combining our two samples (cluster and field CP stars), one obtains $\chi^2 = 4.5$, corresponding to a uniform distribution. Hence, one can conclude that CP stars occupy the whole main-sequence band from the ZAMS to the TAMS (see also Fig. 3 by Pöhl et al., 2005).

As mentioned at the beginning of this Section, we estimated also the masses of the investigated “normal” cluster members, but we have to note that this sample is probably somewhat biased with respect to other chemically peculiar (non-magnetic) groups (e.g. HgMn or Am stars), which are in general not detectable with Δa photometry. However, the number of known HgMn (CP3) stars is rather low (see also Sect. 1), and the Am (CP1) objects are located predominantly in the lower mass regime ($\lesssim 2 M_\odot$; e.g. North, 1993; Paunzen et al., 2013). Accepting this limitation, we are able to derive the incidence of CP stars in dependence on the mass (see Fig. 8.6 and Table 8.1). It shows a Gaussian distribution with a maximum of $\sim 6\%$ in the mass range of 3 to $4 M_\odot$.

The distribution is rather similar to the one presented by Power et al. (2008) using volume limited CP and normal star samples within 100 pc around the Sun, but their CP star sample, consisting of 57 stars, is poorly defined for masses above $\sim 3.5 M_\odot$. They derived a bulk incidence for the CP stars of 1.7%. Using our samples presented above (see Fig. 8.6), we obtain a slightly higher value of $\sim 2.7\%$ (102 CP stars out of

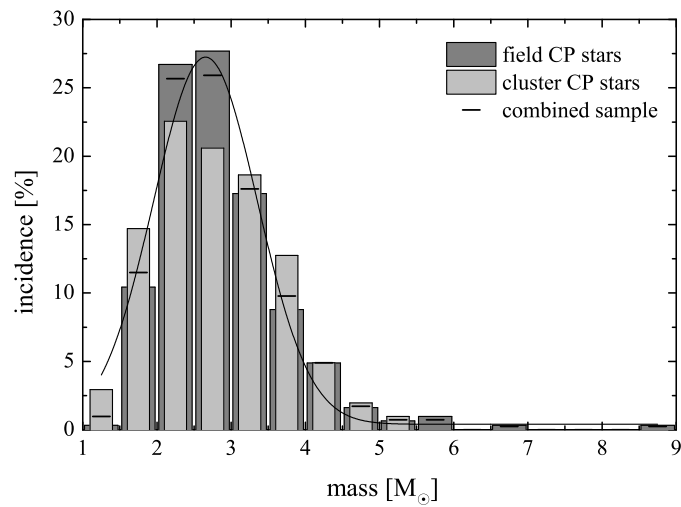


Figure 8.4: The mass distribution of the cluster CP stars compared to CP field objects compiled in the Sects. 2.1 and 2.2. The horizontal lines indicate the percentage if both samples are combined. Furthermore, a Gaussian function was fitted to the total distribution.

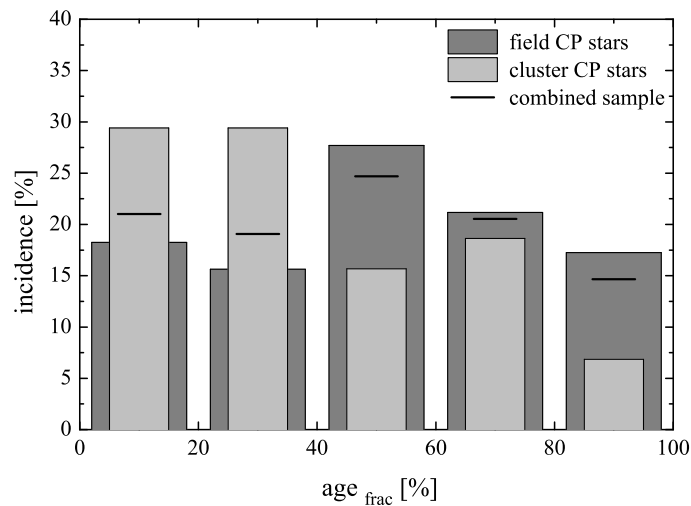


Figure 8.5: The distribution of the fractional ages of the cluster CP stars and the CP field objects compiled in the Sects. 2.1 and 2.2. The horizontal lines indicate the percentage if both samples are combined.

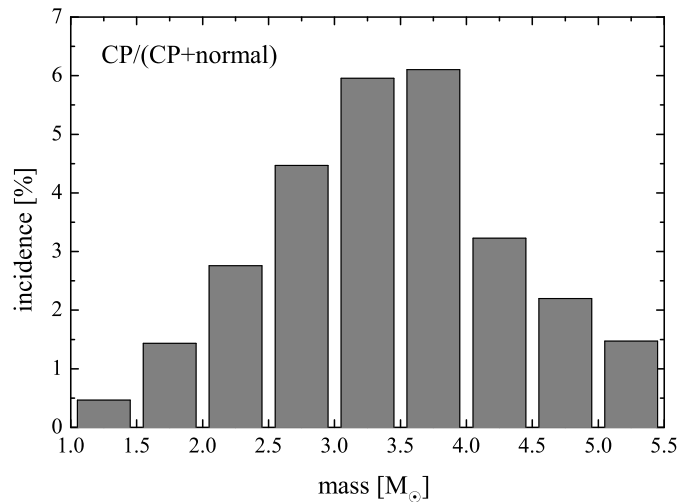


Figure 8.6: The frequency of the (102) cluster CP stars compared to (3742) normal stars for various mass bins, calculated as $\frac{CP}{CP+normal}$.

Table 8.1: Number of cluster CP and normal stars for various mass ranges.

Mass [M _⊙]	# CP stars	# normal stars	frequency [%]
1.0 – 1.5	3	644	0.46
1.5 – 2.0	15	1032	1.43
2.0 – 2.5	23	811	2.76
2.5 – 3.0	21	449	4.47
3.0 – 3.5	19	300	5.96
3.5 – 4.0	13	200	6.10
4.0 – 4.5	5	150	3.23
4.5 – 5.0	2	89	2.20
5.0 – 5.5	1	67	1.47

3844). Also in the work by North (1993) the highest incidence was found in the mass range of 3 to 4 M_⊙, but with a percentage about twice as large than in our analysis.

Investigations with Δa were also carried out in the Large Magellanic Cloud (LMC), and the so far available results are summarized by Paunzen et al. (2006a). They presented the mass distribution of the detected CP candidates (their Fig. 2), which is also in rather good agreement with the one of the galactic representatives shown here. However, the used sample of 35 peculiar LMC stars has to be still increased for a more profound comparison.

Comparing the mass distributions in Figs. 8.4 and 8.6, it is evident that the maximum peak is shifted to somewhat higher masses in the latter diagram (2–3 M_⊙ vs. 3–4 M_⊙). This fact is very probably due to the mass function of stellar populations, where an increase of the number of stars with decreasing mass is observed. Kroupa (2001) estimated the initial mass function (IMF) with a power-law index $\alpha = 2.3 \pm 0.7$, valid for $> 1 M_{\odot}$.

We can use the mass function of our sample to verify somehow its completeness towards the lower mass end. In Fig. 8.7 we present such an analysis for the complete sample (~ 4000 stars) as well as for a young population with an age < 15 Myr (560

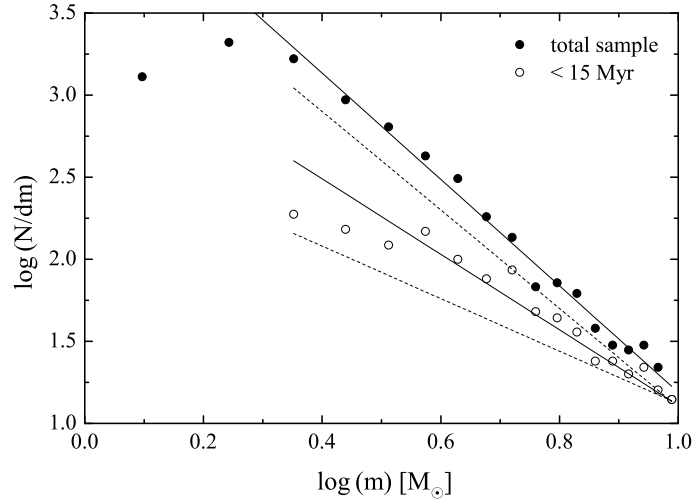


Figure 8.7: The mass functions of the investigated stars, divided into the complete sample and cluster stars younger than 15 Myr. Whereas most mass bins of the latter group are well represented by the universal IMF $\alpha=2.3 \pm 0.7$ (Kroupa, 2001), the complete sample needs $\alpha \sim 3.25$ for a proper fit. The error of the IMF is given as dashed lines. The investigation was restricted to $10 M_{\odot}$ as upper limit, and the bin size was always set to $0.5 M_{\odot}$.

stars), both investigated with identical mass bins of $0.5 M_{\odot}$ and restricted to objects up to $10 M_{\odot}$. Even by the limitation to a rather young age, stellar evolution has already occurred, hence one can not retrace the “real” IMF, and observes the present day mass function instead. Nevertheless, this young subsample is still well represented with $\alpha = 2.3$ (see Fig. 8.7). Since the complete sample incorporates cluster stars up to ~ 1 Gyr, with a continuous decrease of the upper mass limit due to stellar evolution, it is evident that its mass function has to be somewhat steeper. We defined it to $\alpha \sim 3.25$, excluding the two lowest mass bins, where only the lowest mass range ($1 - 1.5 M_{\odot}$) deviates significantly from the relation, but the main mass domain of CP stars ($\sim 1.5 - 7.0 M_{\odot}$; see e.g. Fig. 8.4 or Landstreet et al., 2007) is well covered. Of course, the completeness varies from cluster to cluster, depending on the distance, telescope magnitude limit, but also on the technique used (photoelectric vs. CCD). However, as soon as a sufficient large number of clusters are merged into age groups (or whatever), the bias due to these differences can be reduced.

8.3 Evolution with age

8.3.1 Former investigations

Some former investigations discussed already the possibility of an evolution of the CP phenomenon with age (Abt, 1979; North, 1993).

The first reference used open clusters and associations to study among other peculiar groups also the frequency and evolution with age of magnetic CP objects. This investigation is based on previous works, where he and his collaborators determined

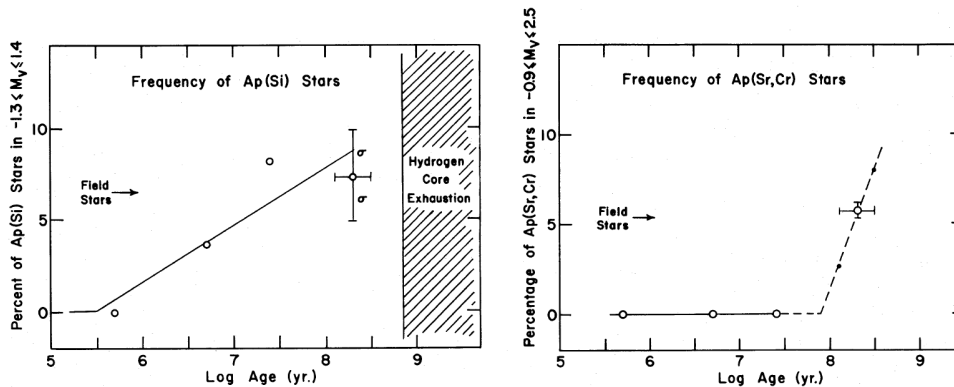


Figure 8.8: The frequency of Si and Sr,Cr stars as shown by Abt (1979).

spectral classifications for 661 stars in 14 open clusters; a rather small number of clusters. In total, 39 magnetic CP stars were found and used for the investigation, divided into four age bins. The results using 20 Si and 19 cooler Sr/Cr objects are shown in Fig. 8.8. Abt (1979) has noted for the Si sample a visual impression that the frequency increases with time, but because of scatter and low confidence level only a slight evidence can be concluded. On the other hand, for the Sr/Cr sample he found a real dependence with a confidence level of 98.8%. However, this result is not surprisingly since cooler objects will not be found at such extent at younger ages; they mostly have still not reached the main sequence.

An analysis based on a considerable larger sample of 73 open clusters (a number comparable to ours) was presented in the proceedings paper by North (1993). The author compiled data from various catalogues, presenting spectral classifications of CP and normal stars in open clusters (e.g. from the predecessor of the WEBDA database). In total, 86 peculiar objects (CP2 and CP4) out of 1345 stars were finally used for the investigation, divided into several mass bins and seven age groups. Whereas for the lower mass CP objects a complete uniformity was found, for the higher mass group at least a slight probability was calculated that an evolution with age exists. These results are therefore more or less the opposite of the study by Abt (1979).

This clearly shows that a large and especially homogeneous sample is necessary for a profound statistical investigation, such as the Δa survey.

Concerning CP stars and their evolution with age it is also worth to mention the work by Landstreet et al. (2007), although they have not investigated the frequency of CP stars. Though, this study examined the evolution of the magnetic field strength using cluster CP objects. They were able to definitely rule out the hypothesis by Hubrig et al. (2000) that magnetic fields of low mass CP stars ($< 3 M_{\odot}$) emerge for the first time at a later stage (after $\sim 30\%$ of their main-sequence lifetime), which was also already disproved by Pöhl et al. (2005). In our sample we have even 12 CP objects with masses below $2 M_{\odot}$ and fractional ages smaller than 15%, which are two-third of the stars in this mass range.

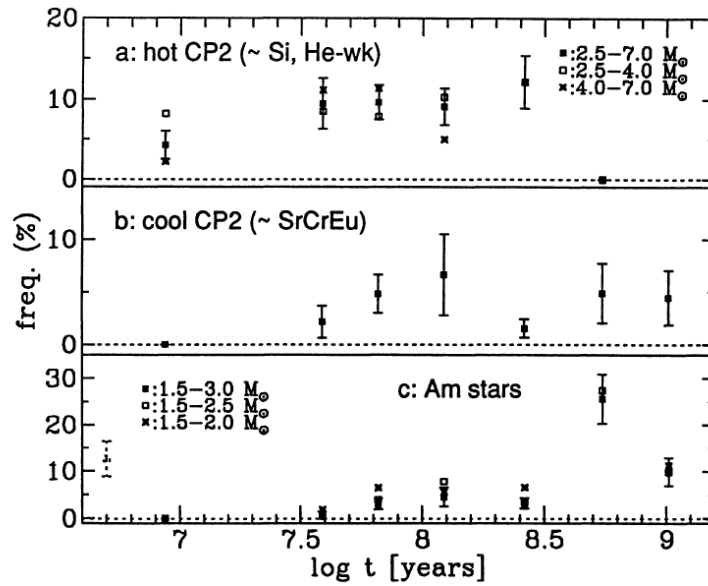


Figure 8.9: The frequency of CP stars as shown by North (1993).

8.3.2 Results based on the Δa survey

With the compilation of via Δa detected CP and normal (non-magnetic) cluster members (Sect. 8.1), their estimated masses, as well as the determined cluster ages (Sect. 6.2), one can examine the frequency of chemically peculiar objects as a function of age as was done for example by Abt (1979) or North (1993).

As already mentioned, our open cluster sample was studied by means of the photoelectric as well as CCD technique, with tree overlapping investigations. For one of these clusters (NGC 2169), the CCD study has not provided measurements for additional stars, hence one can still allocate this open cluster to the photoelectric sample, in contrast to the other two aggregates in common (NGC 3114 and NGC 6405). Therefore, the complete sample can be divided into 36 photoelectric (pe) and 43 CCD open clusters, with 43 (pe) and 59 (CCD) CP star detections. This gives a quite good agreement for the total detection rate of 1.2 and 1.4 CP stars per cluster, for the pe and CCD sample, respectively.

In a first attempt we examine the number of all found CP stars per cluster using age groups, which can be seen in Fig. 8.10. Due to the number of clusters, the two samples were divided into sufficient large bins of 0.5 between $6.5 < \log(\text{age}) < 9.0$, while the few clusters outside this range were merged with the youngest and oldest groups. Beside the second age group, which is unfortunately not covered by photoelectric studies, all groups contain between 4 and 14 open cluster. Except for the oldest age group, incorporating 6 (pe) and 10 (CCD) open clusters, a nice agreement between the two samples can be found. We have to note that these old (pe) clusters are rather poorly studied, three of them with ≤ 11 investigated stars. This investigation already shows the impression that an age dependency exists. Compared to open clusters with ages around 100 Myr ($\log t = 8.0$), in the youngest clusters much less CP stars were detected.

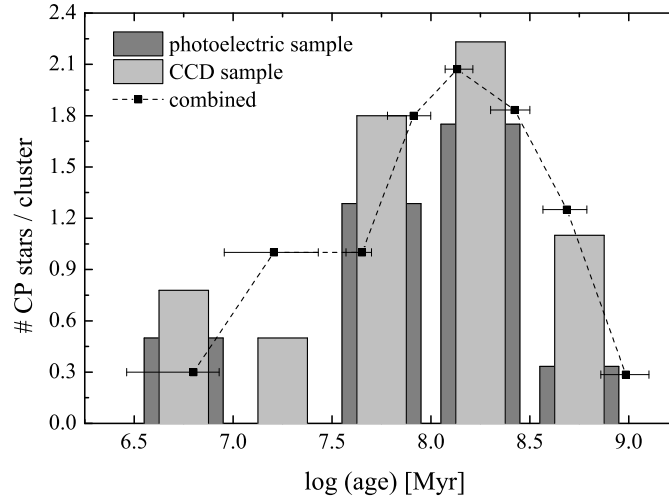


Figure 8.10: The number of CP stars per cluster as a function of age, divided into the photoelectric and CCD sample. Furthermore, the total sample was grouped into somewhat smaller age ranges. The mean ages of the individual groups are given together with covered age range. Please note that the apparent deviations between the sub- and total samples are due to the different binning.

Table 8.2: Number and frequency of all CP member stars per open cluster for the defined age groups.

Group	age(σ) [Myr]	log(age) [Myr]	age range	# clusters	# CP stars	CP / cluster
1	6(2)	6.80	6.46 – 6.93	10	3	0.3
2	16(6)	7.21	6.96 – 7.43	9	9	1.0
3	45(5)	7.65	7.57 – 7.70	9	9	1.0
4	82(14)	7.91	7.78 – 8.00	10	18	1.8
5	136(15)	8.13	8.07 – 8.21	14	29	2.1
6	265(39)	8.42	8.30 – 8.50	12	22	1.8
7	486(82)	8.69	8.57 – 8.79	8	10	1.3
8	967(169)	8.99	8.86 – 9.10	7	2	0.3

Combining the two samples, allows to define more restricted age groups, which are presented in Fig. 8.10 and Table 8.2. These groups were arranged to host a sufficient large number of open clusters, in consideration of gaps in the age distribution (see e.g. Fig. 6.24). The resulting incidence of CP stars indicates a continuous increase up to an age of $\sim \log t = 8.13$ (135 Myr), with a subsequent decrease. As one can see in Table 8.2, all age groups are rather well covered, with a slight deficit at the oldest ages only. In Fig. 8.10 one can notice a discrepancy of the incidence between the second age group of the CCD study and the total sample, respectively, which is due to the selected bin sizes. There are three open clusters (Berkeley 94, NGC 7235, and NGC 2169), all of them $\lesssim 10$ Myr old, exhibiting six CP stars in total. These were included in the second class of the total sample to account for a more or less equal number of clusters in the individual age groups (see Table 8.2).

This kind of analysis assigns an equal weight for each cluster, even for poorly studied ones. Therefore, a probably better approach is to compare the detected CP stars with the non-magnetic member stars. We follow the suggestion by North (1993) or North

et al. (2008) to calculate the individual cluster CP frequencies by using the ratio:

$$\frac{N_{CP}}{N_{normal} + N_{CP}}$$

For a direct comparison, the normal stars have to be restricted to the main mass domain of CP stars ($1.5 - 7.0 M_{\odot}$), already mentioned in Sect. 8.2. As explained there, this range is rather well covered by the investigations, but gets more incomplete towards lower masses. In the HRD (Fig. 8.1) or in Table 8.1 one can notice three CP candidates with masses below this range. These are all members of the open cluster Lyngå 1 (Sect. 5.3.5), whereas one star (Lyngå 1 #85) is probably one of the coolest representatives known. Due to its faintness ($V \sim 16.8$ mag), unfortunately no spectroscopic information is available so far. Since even with generously adopted errors the estimated mass is lower than $1.5 M_{\odot}$, we exclude the latter object from further analysis, but consider it in the error estimations. Nevertheless, this open cluster (with $\log t = 8.07$) still host a considerable number of four CP stars, resulting in the highest incidence found (21 %).

In Fig. 8.11 we present the individual CP frequencies for all open clusters, as in Fig. 8.10 divided to the photoelectric and CCD sample, respectively. In addition, we used a colour code to emphasise open clusters, in which only a few stars were observed. However, a low number of investigated objects does not necessarily imply a quite incomplete investigation. Especially older open clusters do not contain anymore a large number of member stars in the adopted mass range. Since we constrain the analysis on main-sequence stars in the CP mass domain, a considerable number of objects in old clusters are already evolved ones. Stellar evolution and the IMF (see Sect. 8.2) can also explain a low number of main-sequence stars in very young aggregates, where still objects on the pre-main-sequence (PMS) are found.

The latter argument applies e.g. for Stock 16, whose Δa study includes several PMS stars, and also one CP object which has very probably not yet reached the ZAMS (see Sect. 8.5). To be consistent, we have to exclude this star for further analysis. Hence, our final sample consists of 100 CP objects in 79 open clusters.

The individual CP star frequencies in Fig. 8.11 show a quite large scatter, cluster to cluster variations are evident, even if excluding those with few measured stars. This fact shows nicely that it is essential to define age groups, covering several open clusters. Among the “best” studied ones, NGC 2516 (Sect. 7) with an age of $\log t = 8.14$ exhibits the highest incidence (12.8 %; 6 CP stars out of 47). Other open clusters with nearly identical ages are NGC 6204 or NGC 6451, but which do not contain any CP star among 59 and 89 investigated stars, respectively. Looking at the adopted parameters in Table 6.5, one can notice that there is also no difference for the global metallicity (all have solar abundances as most of our programme clusters).

Excluding the young cluster Stock 16 mentioned previously, there are 28 open clusters without a CP star detection. About 30% of them are younger than 15 Myr ($50\% < 50$ Myr), explaining the low incidences found for the youngest groups in Figs. 8.10 and 8.11.

The mean frequencies in Fig. 8.11, derived using the individual results for clusters within an age group, show a similar behaviour as in Fig. 8.10, although the errors are

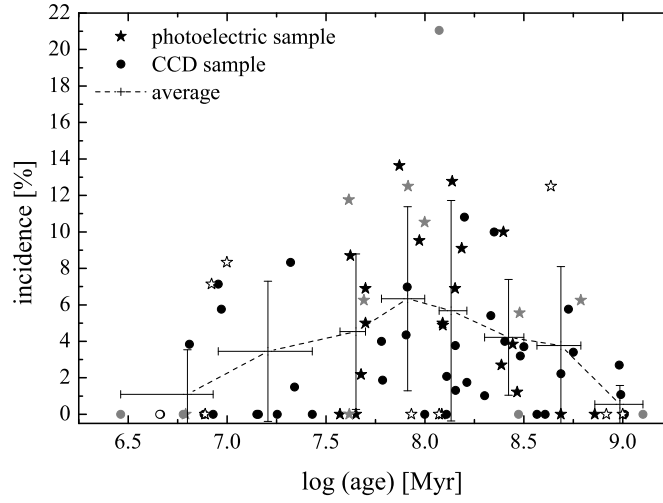


Figure 8.11: The frequency of CP stars in all investigated open clusters, calculated as $CP/(CP+normal)$ using the mass range of 1.5 to $7 M_{\odot}$. Open symbols represent clusters with less than 15 investigated objects, grey symbols < 20 , and black ones with ≥ 20 measured stars. Furthermore, the average frequency and standard deviation was calculated using the age groups listed in Table 8.2. As in Fig. 8.10, the age ranges are also shown.

quite large. However, also here all clusters are equally weighted, without consideration of the number of stars involved. As a next step we therefore follow the approach by Abt (1979) or North (1993) and accumulate all objects (magnetic and non magnetic) within the age groups. The number of observed stars in all open clusters are listed in Table 8.3, and the results can be found in Fig. 8.12 and in Table 8.4.

Table 8.3: The number of observed CP and normal stars within the open clusters. The vertical lines separates the in general used age groups. Open clusters marked with ^a originate from the photoelectric survey. For Stock 16 and Lyngå 1, the number in parenthesis gives the total number of found CP stars, but which were not considered for the analysis, due to PMS nature or too low mass (see text for details).

Cluster	log(age)	# normal total	mass range [M_{\odot}]	CP / normal 1.5 – 7 M_{\odot}	CP / normal 2 – 4 M_{\odot}	CP / normal 1.5 – 3 M_{\odot}	CP / normal 3 – 7 M_{\odot}
NGC 6611	6.46	44	3.1 – 35.4	0 / 19	0 / 5	0 / 0	0 / 19
Stock 16	6.66	10	2.1 – 12.0	0(1) / 7	0(1) / 4	0(1) / 4	0 / 3
Pismis 20	6.66	94	2.2 – 23.1	0 / 82	0 / 55	0 / 25	0 / 57
Lyngå 14	6.78	22	4.3 – 21.4	0 / 16	0 / 0	0 / 0	0 / 16
NGC 2362 ^a	6.79	23	2.3 – 11.9	0 / 18	0 / 11	0 / 6	0 / 12
NGC 1502	6.81	28	1.9 – 8.7	1 / 25	1 / 16	0 / 15	1 / 10
NGC 7510	6.88	69	2.5 – 19.4	0 / 47	0 / 23	0 / 10	0 / 37
Collinder 121 ^a	6.89	8	3.0 – 8.2	0 / 7	0 / 3	0 / 1	0 / 6
Collinder 132 ^a	6.92	15	2.4 – 7.8	1 / 13	1 / 7	1 / 4	0 / 9
NGC 3293	6.93	136	2.0 – 16.0	0 / 112	0 / 78	0 / 50	0 / 62
Berkeley 94	6.96	33	1.7 – 12.1	2 / 26	2 / 10	1 / 10	1 / 16
NGC 7235	6.97	64	1.8 – 15.4	3 / 49	1 / 28	3 / 22	0 / 27
NGC 2169 ^a	7.00	14	2.4 – 13.0	1 / 11	1 / 8	0 / 4	1 / 7
Collinder 272	7.15	59	1.2 – 8.4	0 / 35	0 / 16	0 / 20	0 / 15
NGC 2439	7.16	66	2.0 – 12.8	0 / 56	0 / 36	0 / 25	0 / 31
King 21	7.25	97	1.5 – 8.1	0 / 95	0 / 31	0 / 78	0 / 17
NGC 6250	7.32	29	1.3 – 4.5	2 / 22	2 / 11	2 / 19	0 / 3

... continues on next page

Table 8.3: ... Continuation

Cluster	log(age)	# normal total	mass range [M_{\odot}]	CP / normal 1.5 – 7 M_{\odot}	CP / normal 2 – 4 M_{\odot}	CP / normal 1.5 – 3 M_{\odot}	CP / normal 3 – 7 M_{\odot}
NGC 3105	7.34	83	3.1 – 10.2	1 / 66	0 / 20	0 / 0	1 / 66
NGC 6396	7.43	55	1.4 – 6.9	0 / 51	0 / 27	0 / 36	0 / 15
Collinder 140 ^a	7.57	22	1.7 – 7.2	0 / 20	0 / 11	0 / 15	0 / 5
IC 2391 ^a	7.62	15	1.7 – 6.2	2 / 15	1 / 5	1 / 8	1 / 7
Trumpler 10 ^a	7.62	19	1.7 – 6.9	0 / 19	0 / 11	0 / 12	0 / 7
IC 2602 ^a	7.62	21	1.7 – 5.4	2 / 21	1 / 11	1 / 16	1 / 5
IC 4665 ^a	7.65	24	1.6 – 4.8	0 / 24	0 / 12	0 / 17	0 / 7
Melotte 20 ^a	7.68	45	1.6 – 6.2	1 / 45	0 / 27	0 / 33	1 / 12
NGC 2232 ^a	7.69	16	1.8 – 7.7	1 / 15	1 / 9	0 / 11	1 / 4
NGC 2451A ^a	7.70	19	1.6 – 4.7	1 / 19	1 / 14	0 / 13	1 / 6
NGC 2451B ^a	7.70	28	1.6 – 7.7	2 / 27	2 / 18	1 / 19	1 / 8
NGC 5281	7.78	24	1.6 – 4.3	1 / 24	0 / 11	1 / 15	0 / 9
NGC 6834	7.79	155	1.1 – 5.6	2 / 105	1 / 45	2 / 77	0 / 28
IC 4725 ^a	7.87	19	2.7 – 5.6	3 / 19	1 / 15	0 / 2	3 / 17
NGC 6405	7.90	103	0.9 – 5.4	3 / 66	2 / 42	3 / 44	0 / 22
Berkeley 11	7.91	40	2.2 – 5.4	3 / 40	2 / 32	0 / 22	3 / 18
NGC 6087 ^a	7.91	14	3.1 – 5.2	2 / 14	2 / 8	0 / 0	2 / 14
NGC 3228 ^a	7.93	9	1.9 – 4.1	0 / 9	0 / 7	0 / 5	0 / 4
NGC 5662 ^a	7.97	19	2.1 – 4.9	2 / 19	2 / 13	0 / 10	2 / 9
NGC 7243 ^a	8.00	17	2.2 – 4.8	2 / 17	2 / 9	0 / 6	2 / 11
NGC 6204	8.00	167	0.9 – 4.1	0 / 59	0 / 30	0 / 47	0 / 12
Lyngå 1	8.07	55	1.1 – 3.3	4(5) / 15	0 / 9	4(5) / 12	0 / 3
NGC 2343 ^a	8.07	14	1.9 – 4.2	0 / 14	0 / 11	0 / 10	0 / 4
Melotte 22 ^a	8.09	30	1.6 – 4.8	0 / 30	0 / 15	0 / 22	0 / 8
NGC 2422 ^a	8.09	19	1.9 – 4.3	1 / 19	1 / 16	0 / 15	1 / 4
NGC 2546 ^a	8.09	39	2.3 – 4.3	2 / 39	2 / 33	1 / 16	1 / 23
NGC 6451	8.11	89	1.8 – 4.8	0 / 89	0 / 61	0 / 64	0 / 25
NGC 6756	8.11	47	2.8 – 4.5	1 / 47	1 / 36	0 / 3	1 / 44
NGC 2516 ^a	8.14	41	1.9 – 4.5	6 / 41	6 / 34	4 / 27	2 / 14
NGC 1039 ^a	8.15	27	1.7 – 3.5	2 / 27	2 / 23	2 / 22	0 / 5
NGC 3114	8.15	108	1.4 – 4.3	4 / 102	3 / 79	0 / 78	4 / 24
NGC 6192	8.15	76	1.4 – 3.9	1 / 75	1 / 44	1 / 52	0 / 23
NGC 5460 ^a	8.19	20	2.3 – 4.1	2 / 20	2 / 19	1 / 13	1 / 7
NGC 6268	8.20	39	1.3 – 4.6	4 / 33	4 / 24	1 / 22	3 / 11
NGC 6830	8.21	130	1.1 – 3.6	1 / 56	1 / 26	0 / 44	1 / 12
NGC 6705	8.30	195	1.5 – 3.7	2 / 195	2 / 113	0 / 174	2 / 21
NGC 6031	8.33	113	1.0 – 3.1	2 / 35	1 / 18	2 / 33	0 / 2
Ruprecht 120	8.35	65	1.2 – 3.0	4 / 36	3 / 9	3 / 34	1 / 2
NGC 2287 ^a	8.39	36	1.9 – 3.7	1 / 36	1 / 30	1 / 25	0 / 11
NGC 6475 ^a	8.40	36	1.6 – 3.7	4 / 36	4 / 23	3 / 30	1 / 6
NGC 2658	8.40	48	1.7 – 3.4	2 / 48	2 / 39	2 / 44	0 / 4
NGC 6281 ^a	8.44	25	1.8 – 3.3	1 / 25	1 / 18	1 / 21	0 / 4
NGC 3532 ^a	8.47	81	1.8 – 3.1	1 / 81	1 / 62	1 / 80	0 / 1
NGC 2567	8.47	31	1.2 – 3.0	0 / 17	0 / 9	0 / 17	0 / 0
NGC 7092 ^a	8.48	17	1.8 – 3.3	1 / 17	1 / 13	1 / 15	0 / 2
Melotte 105	8.48	91	1.6 – 3.4	3 / 91	3 / 49	3 / 83	0 / 8
NGC 7296	8.50	26	1.6 – 3.2	1 / 26	1 / 21	1 / 20	0 / 6
NGC 2099	8.57	27	2.0 – 2.7	0 / 27	0 / 27	0 / 27	0 / 0
NGC 5999	8.61	150	1.2 – 2.6	0 / 81	0 / 27	0 / 81	0 / 0
NGC 1662 ^a	8.64	7	2.3 – 2.8	1 / 7	1 / 7	1 / 7	0 / 0
NGC 2447 ^a	8.69	36	1.7 – 2.7	0 / 36	0 / 21	0 / 36	0 / 0
Ruprecht 115	8.69	89	1.5 – 2.7	2 / 88	0 / 38	2 / 88	0 / 0
NGC 2489	8.73	54	1.4 – 2.9	3 / 49	2 / 24	3 / 49	0 / 0
Ruprecht 130	8.75	85	1.5 – 2.2	3 / 85	2 / 20	3 / 85	0 / 0
Melotte 111 ^a	8.79	15	1.5 – 2.5	1 / 15	1 / 4	1 / 15	0 / 0
NGC 2632 ^a	8.86	26	1.6 – 2.7	0 / 26	0 / 12	0 / 26	0 / 0
NGC 1901 ^a	8.92	11	1.7 – 2.3	0 / 11	0 / 4	0 / 11	0 / 0
NGC 3960	8.98	56	1.3 – 2.0	1 / 36	0 / 2	1 / 36	0 / 0
NGC 6802	8.99	154	1.2 – 2.1	1 / 91	0 / 8	1 / 91	0 / 0
NGC 2423 ^a	9.00	11	2.0 – 2.4	0 / 11	0 / 10	0 / 11	0 / 0
NGC 6134	9.01	74	1.2 – 2.2	0 / 36	0 / 4	0 / 36	0 / 0
NGC 6208	9.10	17	1.4 – 1.8	0 / 16	0 / 0	0 / 16	0 / 0

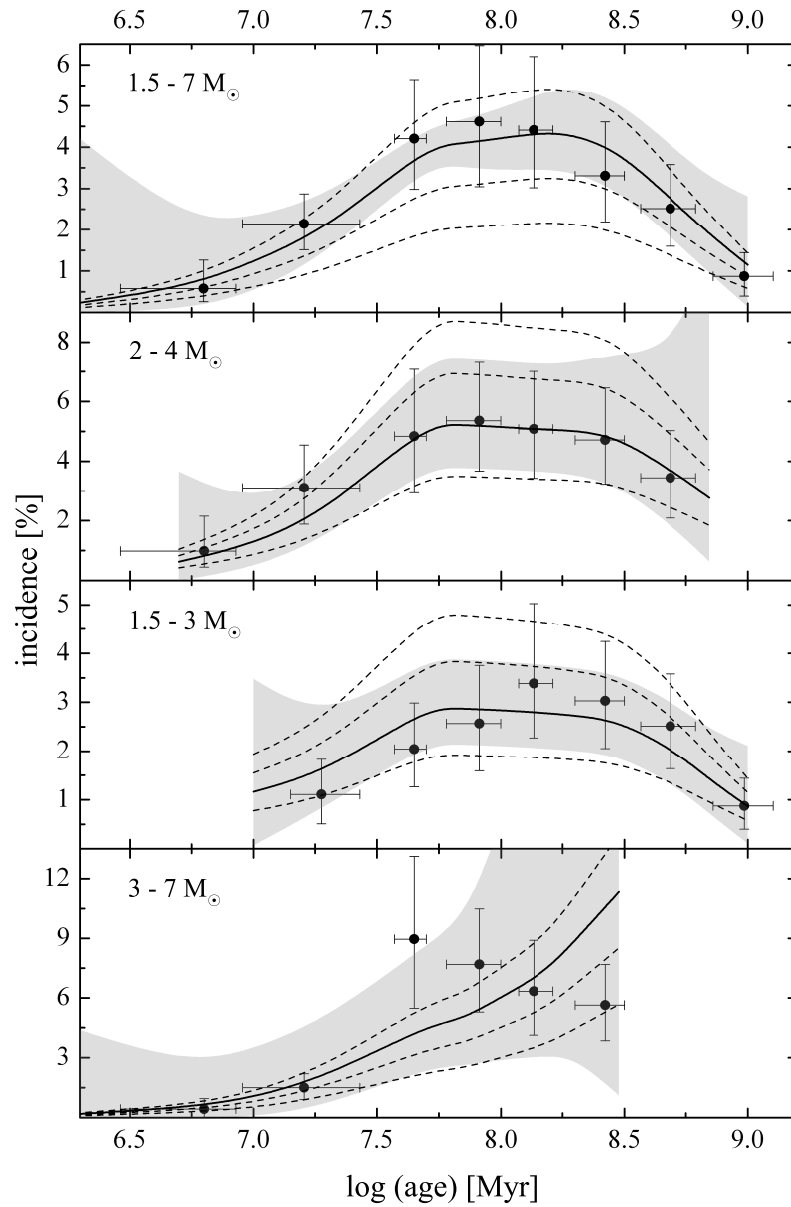


Figure 8.12: The observed frequencies of CP stars for various mass ranges as a function of age by accumulating all stars in each age group. Furthermore, theoretical frequencies taking into account stellar evolution and the IMF are given, assuming a fixed CP content of 2, 3, 4, and 5 stars as well as a maximum of 100 member stars in each simulated cluster. The respective best fitting value is shown as solid line, the adopted errors as grey area (see the text for more details). For the mass subgroups the youngest and/or oldest clusters were not considered due to low or absent population (see Table 8.3).

Table 8.4: The observed CP frequencies for the investigated mass ranges and age groups. In addition, the frequencies are given by removing clusters with few observed stars as described in the text (last column).

	age [Myr]	log(age)	age range	# clusters	# CP	# normal	freq _{comp} (+/-) [%]	freq _{rem} [%]
1.5 – 7 M _⊙	6 (2)	6.80	6.46 – 6.93	10	2	346	0.57 (0.69/0.31)	0.33
	16 (6)	7.21	6.96 – 7.43	9	9	411	2.14 (0.73/0.62)	2.05
	45 (5)	7.65	7.57 – 7.70	9	9	205	4.21 (1.44/1.23)	4.21
	82 (14)	7.91	7.78 – 8.00	10	18	372	4.62 (1.85/1.57)	3.79
	136 (15)	8.13	8.07 – 8.21	14	28	607	4.41 (1.79/1.39)	4.71
	265 (39)	8.42	8.30 – 8.50	12	22	643	3.31 (1.30/1.11)	3.31
	486 (82)	8.69	8.57 – 8.79	8	10	388	2.51 (1.07/0.91)	2.31
	967 (169)	8.99	8.86 – 9.10	7	2	227	0.87 (0.57/0.48)	0.97
2 – 4 M _⊙	6 (2)	6.80	6.46 – 6.93	9	2	202	0.98 (1.17/0.53)	0.54
	16 (6)	7.21	6.96 – 7.43	9	6	187	3.11 (1.44/1.22)	3.05
	45 (5)	7.65	7.57 – 7.70	9	6	118	4.84 (2.24/1.90)	4.24
	82 (14)	7.91	7.78 – 8.00	10	12	212	5.36 (1.96/1.68)	4.71
	136 (15)	8.13	8.07 – 8.21	14	23	430	5.08 (1.93/1.65)	5.41
	265 (39)	8.42	8.30 – 8.50	12	20	404	4.72 (1.74/1.48)	4.82
	486 (82)	8.69	8.57 – 8.79	8	6	168	3.45 (1.58/1.35)	2.48
	19 (5)	7.28	7.15 – 7.43	5	2	178	1.11 (0.72/0.60)	1.11
1.5 – 3 M _⊙	45 (5)	7.65	7.57 – 7.70	9	3	144	2.04 (0.94/0.77)	1.45
	82 (15)	7.91	7.78 – 8.00	9	6	228	2.56 (1.19/0.97)	2.71
	136 (15)	8.13	8.07 – 8.21	14	14	400	3.38 (1.64/1.11)	3.41
	265 (39)	8.42	8.30 – 8.50	12	18	576	3.03 (1.21/0.98)	3.03
	486 (82)	8.69	8.57 – 8.79	8	10	388	2.51 (1.07/0.87)	2.31
	967 (169)	8.99	8.86 – 9.10	7	2	227	0.87 (0.57/0.47)	0.87
	6 (2)	6.80	6.46 – 6.93	10	1	231	0.43 (0.52/0.43)	0.47
3 – 7 M _⊙	16 (6)	7.21	6.96 – 7.43	9	3	197	1.50 (0.70/0.59)	1.06
	45 (5)	7.65	7.57 – 7.70	9	6	61	8.96 (4.16/3.48)	
	82 (14)	7.91	7.78 – 8.00	10	12	144	7.69 (2.80/2.40)	8.33
	136 (15)	8.13	8.07 – 8.21	14	14	207	6.33 (2.58/2.20)	6.31
	262 (39)	8.42	8.30 – 8.50	11	4	67	5.63 (2.06/1.79)	

Beside the complete CP mass range of 1.5 to 7 M_⊙, also sub ranges of 2 – 4 M_⊙ (somehow the main mass domain of CP stars, see Fig. 8.4), 1.5 – 3 M_⊙, as well as the more massive part 3 – 7 M_⊙ were analysed. As can be seen in Fig. 8.12, the apparent evolution of the CP star incidences with age, noticeable already in Figs. 8.10 or 8.11, seems to be confirmed.

If comparing the third age group of Fig. 8.12 (upper panel) with the one in Fig. 8.10 (showing the average number of CP stars per cluster), one can notice that the latter exhibits a considerable lower CP star level. This is due to the low total number of investigated stars in this age group (see also Table 8.4), and all clusters forming this age group originate from the photoelectric survey (see Table 8.3). Otherwise, a mixture of photoelectric and CCD studies are found for the other age groups.

To investigate the influence of open clusters with few observed stars, we recalculated the incidences by excluding clusters with less than 15 investigated stars (normal + CP) in the complete mass range and < 10 objects in the subdivisions of the mass range. The latter was set to a somewhat lower limit, to take into account the lower number of stars if studying restricted mass ranges. In addition, open clusters were also excluded, if their investigation revealed a lower mass limit of the investigated stars, which is considerable higher than found for other clusters in the respective age group. This applies e.g. to Lyngå 14, NGC 3105, IC 4725, NGC 6087, and NGC 6756 in the analysis of the complete mass range, which reduces the number of clusters to 65 in this sample. Strongly hampered is the analysis of the high mass range, where the exclusion

of clusters reduce the available number from 63 to 33. Therefore, the previously defined age groups are poorly covered. For example, in the third age group only Melotte 20 remained, which was assigned to the successive group. Also in the oldest investigated group in this mass range only two clusters (NGC 6705 and NGC 2287) remained, which were merged with the previous group. This way, each group still includes at least seven open cluster clusters, and since the mean ages are not significantly altered (157 Myr compared to 136 Myr using all clusters) one can still directly compare the resulting CP incidences. As one can see in Table 8.4, these values differ only marginally from the former analysis, incorporating all open clusters, regardless of the number of stars involved or covered mass range. Several age groups are even not affected at all.

We have to note that within the mass subsamples not for all originally defined age groups CP frequencies were calculated. For the $2 - 4 M_{\odot}$ range the oldest group was not considered, since it incorporates only 40 main sequence stars in total anymore due to stellar evolution. The same holds for the more massive range of $3 - 7 M_{\odot}$, in which the last two age groups include even no single star, and also the last given age group covers 67 objects only (see Table 8.4). Similarly, we also left out open clusters younger than 10 Myr in the mass range of $1.5 - 3 M_{\odot}$, where most lower mass stars have still not reached the main sequence.

The estimation of errors for the derived CP star incidences is crucial. It should reflect on the one hand the detection rate (incompleteness) of CP stars, the completeness of the whole sample of investigated stars, but also their proper membership determination. The grouping of several clusters to an age class for sure helps to reduce these problems. Paunzen et al. (2005b) investigated the detection probability of the various chemically peculiar groups, depending on the Δa detection limit (see discussion in Sect. 3 and Fig. 3.3). Using their results for the magnetic CP2 and CP4 stars and a detection limit of 15 to 20 mmag, we infer that our sample includes about 80% of the actual CP star content. This value was applied to the CP objects found in the investigated age and mass groups, but at least one overseen object was adopted. Additionally, the low mass CP star in Lyngå 1 and the probable PMS object in Stock 16 were also considered in the corresponding age/mass domains (see discussion earlier in this Section). Furthermore, we assign a 10% uncertainty to the number of studied normal type stars.

It is even more complex to account for the contribution of spuriously included CP stars, due to e.g. a slightly lower reddening than the mean cluster one, or a wrongly assigned membership. These facts especially applies to more distant, faint, and crowded open clusters, in which spectroscopic verifications of the photometrically detected CP stars are still needed. We therefore assign the same error budget as above for the possible overestimation. The resulting errors are indicated in Fig. 8.12 and listed in Table 8.4.

Since all investigations so far showed an evolution of the CP incidences with age, it is worth to inspect if this is an intrinsic feature or just due to “simple” stellar evolution. We want to recall that for a direct comparison of CP to normal stars, our sample was restricted to probable main sequence stars, hence at very young ages most lower mass stars are still on the pre-main sequence phase, whereas towards older ages the more massive objects gradually evolve and leave the main sequence. To reproduce this effect,

we generate a simulated open cluster consisting of 100 member stars in the mass range of $1.5 - 7 M_{\odot}$, distributed according to the initial mass function (IMF, see also Sect. 8.2) with the power law $\alpha=2.3$ (Kroupa, 2001). Furthermore, we used the evolutionary grids by Schaller et al. (1992) to evaluate which mass ranges are present on the main sequence at ages of 1 Myr up to 1 Gyr. Next, we summed up the corresponding number of stars in the simulated open cluster.

Based on the evolutionary models, the defined ages, and the theoretical upper and lower (MS) masses, one can now calculate the respective fractional ages (percentage of main-sequence lifetimes). In this way one obtains for all in Table 8.5 quoted mass ranges a differential percentage (or probability) value P_{frac} , representing the particular covered portion of the main-sequence band. Additionally, the observed mass distribution of the CP stars has to be considered. We therefore used the Gaussian distribution presented in Sect. 8.2 (see Fig. 8.4), to derive the accessible CP percentage (P_{CP}) for all in Table 8.5 given mass ranges. Assuming for simplicity that CP stars are uniformly distributed along the main-sequence, what can be assumed if looking at the complete sample of observed fractional ages in Fig. 8.5 (Sect. 8.2), one can derive for each simulated cluster a kind of total probability $P_{total} = P_{frac} \cdot P_{CP}$ to catch a CP star at a specific age. This was performed also for the investigated mass subgroups (shown e.g. in Table 8.4 and Fig. 8.12), by adopting the respective lower and upper masses. However, since these represent only a part of the total population, the derived percentage values of the fractional ages of the complete mass range have to be used.

If assuming the hypothesis that CP stars have no intrinsic evolution with age beside the general one, the inclusion of a fixed number of CP stars together with applying the derived probabilities and number of stars in the simulated clusters should resemble the observed frequencies. The results can be found in Table 8.5 and are shown in Fig. 8.12. In the latter we present these theoretical incidences using a fixed number of 2, 3, 4, and 5 CP stars, highlighting always the best visual fit to the observed values. In all cases three or four CP stars give the best agreement. An ideal correlation would exist, if all mass ranges can be reproduced well with an equal number of stars. However, the number of observed CP stars in the investigated mass subgroups is probably too small, e.g. the $1.5 - 3 M_{\odot}$ range includes only 55 representatives (out of 100), and the high mass range even only 40 stars in total. The discrepancy to 100 stars, if summing up these two groups, originate from the exclusion of the youngest clusters in the low mass regime. Furthermore, if looking at the mass function presented in Fig. 8.7, there is an apparent incompleteness of the investigated stars towards lower masses.

Also the theoretical values are affected by the probable inadequate use of the IMF and the evolutionary models to generate the number of stars. Nevertheless, within the errors, a good agreement between the observed and theoretical incidences can be found. The errors of the latter were estimated using an uncertainty of 10% for the derived probabilities, as well as ± 10 member stars were considered for the simulated clusters, but assigning at least one or 100 stars at maximum. The error range is shown as grey areas in Fig. 8.12. As can be seen especially in the high mass regime (lower panel), these increase strongly as soon as only a few stars are involved anymore (compare also with Table 8.5).

Concerning the analyses of the low and high mass parts of CP stars, we want to

Table 8.5: The theoretical CP frequencies for the investigated mass ranges as described in the text, whereat P gives the probability in percentage to catch a CP star in the respective mass range, or fractional ages covered in a particular age/mass combination. The given frequencies represent the best fit to the observed ones by adopting a fixed value of CP stars; three for the two middle panels and four in upper and lower one.)

	age [Myr]	log(age)	mass [M_{\odot}]	# members	P_{frac} [%]	P_{CP} [%]	P_{total} [%]	freq [%]
1.5 – 7 M_{\odot}	1	6.00	4.0 – 7.0	17	0.2	5.6	0.0	0.00
	5	6.70	2.7 – 7.0	38	9.7	52.5	5.1	0.54
	10	7.00	2.1 – 7.0	59	21.5	83.7	18.0	1.22
	20	7.30	1.7 – 7.0	87	45.2	97.4	44.0	2.02
	50	7.70	1.5 – 6.8	99	99.7	99.8	99.5	4.02
	70	7.85	1.5 – 6.0	96	98.9	99.1	98.1	4.09
	100	8.00	1.5 – 4.9	91	97.8	98.2	96.0	4.22
	150	8.18	1.5 – 4.2	85	95.9	96.4	92.4	4.35
	200	8.30	1.5 – 3.8	81	94.0	92.5	87.0	4.30
	300	8.48	1.5 – 3.3	74	90.3	79.9	72.2	3.90
	500	8.70	1.5 – 2.7	62	82.7	50.4	41.7	2.69
700	8.85	1.5 – 2.4	53	75.2	33.3	25.1	1.89	
1000	9.00	1.5 – 2.1	41	63.9	18.4	11.8	1.15	
2 – 4 M_{\odot}	5	6.70	2.7 – 4.0	22	9.7	47.4	4.6	0.63
	10	7.00	2.1 – 4.0	42	21.5	78.6	16.9	1.21
	20	7.30	2.0 – 4.0	47	45.2	82.5	37.3	2.38
	50	7.70	2.0 – 4.0	47	99.7	82.5	82.3	5.25
	70	7.85	2.0 – 4.0	47	98.9	82.5	81.6	5.21
	100	8.00	2.0 – 4.0	47	97.8	82.5	80.7	5.15
	150	8.18	2.0 – 4.0	47	95.9	82.5	79.2	5.05
	200	8.30	2.0 – 3.8	45	94.0	80.1	75.4	5.02
	300	8.48	2.0 – 3.3	38	90.3	67.5	61.0	4.81
	500	8.70	2.0 – 2.7	26	82.7	38.0	31.4	3.63
700	8.85	2.0 – 2.4	17	75.2	20.9	15.7	2.78	
1.5 – 3 M_{\odot}	10	7.00	2.1 – 3.0	28	21.5	50.5	10.9	1.16
	20	7.30	1.7 – 3.0	55	45.2	64.2	29.0	1.58
	50	7.70	1.5 – 3.0	69	99.7	66.8	66.6	2.89
	70	7.85	1.5 – 3.0	69	98.9	66.8	66.1	2.87
	100	8.00	1.5 – 3.0	69	97.8	66.8	65.3	2.84
	150	8.18	1.5 – 3.0	69	95.9	66.8	64.1	2.79
	200	8.30	1.5 – 3.0	69	94.0	66.8	62.8	2.73
	300	8.48	1.5 – 3.0	69	90.3	66.8	60.3	2.62
	500	8.70	1.5 – 2.7	62	82.7	50.4	41.7	2.02
	700	8.85	1.5 – 2.4	53	75.2	33.3	25.1	1.42
1000	9.00	1.5 – 2.1	41	63.9	18.4	11.8	0.86	
3 – 7 M_{\odot}	1	6.00	4.0 – 7.0	17	0.2	5.6	0.0	0.00
	5	6.70	3.0 – 7.0	31	9.7	35.8	3.5	0.45
	10	7.00	3.0 – 7.0	31	21.5	35.8	7.7	0.99
	20	7.30	3.0 – 7.0	31	45.2	35.8	16.2	2.08
	50	7.70	3.0 – 6.8	31	99.7	35.6	35.5	4.57
	70	7.85	3.0 – 6.0	28	98.9	34.9	34.5	4.93
	100	8.00	3.0 – 4.9	22	97.8	33.9	33.2	6.03
	150	8.18	3.0 – 4.2	17	95.9	32.1	30.8	7.26
	200	8.30	3.0 – 3.8	12	94.0	28.3	26.6	8.88
	300	8.48	3.0 – 3.3	5	90.3	15.7	14.2	11.35

remind that in addition to the smaller sample, they are also probably influenced by a lower detection rate with Δa (see the temperature dependency in Fig. 3.4, Sect. 3). Therefore, we assume that the $2 - 4 M_{\odot}$ mass range represents the incidence of CP stars much better. With a frequency of about five percent at maximum it also reflects the CP occurrences of 5-10% quoted in the literature (e.g. Wolff, 1968; Abt, 1979), though at the lower end.

Based on the overall agreement of the observed and theoretical CP incidences, one can conclude that very probably no intrinsic evolution with age exists. The number of magnetic chemically peculiar stars remain constant up to about 1 Gyr, when most of them are already evolved and convection destroyed the peculiarities. Furthermore, the CP stars seem to be developed as soon as the stars have arrived on the main-sequence (or even before). This is a further strong hint that the magnetic field is of fossil origin (see e.g. Sect. 2.2). If a dynamo plays an additional key role to generate the magnetic fields of CP stars, one would expect an additional increase of their number with age.

8.4 Dependencies beside age

In the previous section we have already shortly discussed the large scatter of the individual cluster CP incidences, presented in Fig. 8.11. There seems to be no apparent correlation with metallicity. Remind the comparison of the CP rich cluster NGC 2516 with the zero results in NGC 6204 or NGC 6451, all having similar (solar) metallicities. In this age range there are also two clusters (NGC 6192 and NGC 6830), exhibiting the highest metallicity ($[Fe/H] \sim 0.2$ dex) in our sample, but show a CP incidence of about 1.5%, or one third only of the average incidence in this age range (see Fig. 8.12).

Extreme underabundant aggregates are not present in our sample, but one can consider the Δa results for the LMC (Paunzen et al., 2006a) instead, which has a much lower overall metallicity ($[Fe/H] \sim -0.4$ dex) than the Milky Way. Since the CP incidences derived for the LMC clusters NGC 1711, NGC 1866, and NGC 2136/7, which span an age range of 7.2 to 8.1 in $\log(t)$, do not strongly deviate, we calculated a mean CP frequency of $\sim 1.9\%$, i.e. about half the mean Milky Way value but comparable to the aforementioned overabundant galactic clusters. However, the number of investigated LMC clusters is rather small and probably also here as soon as the sample is significantly increased, strong divergent results are possible to enhance the mean CP incidence. Furthermore, due to the different evolution of the LMC, a direct comparison is probably misleading, also their clusters are of different morphology; they are much more compact than open clusters in the Milky Way and are rather similar to globular clusters, but with a much younger age.

The apparent age dependency of the CP incidence complicates an investigation of a possible connection with other parameters, which maybe favour the formation of CP stars. For a proper analysis, one has to restrict the sample to specific age groups. If using the age groups three to five, which exhibit a similar CP incidence (see Fig. 8.12), 33 open clusters remain. Since the overwhelming majority have metallicities in the range $[Fe/H] \pm 0.1$ dex, it is out of scope to find a probable correlation, especially if keeping in mind their uncertainties.

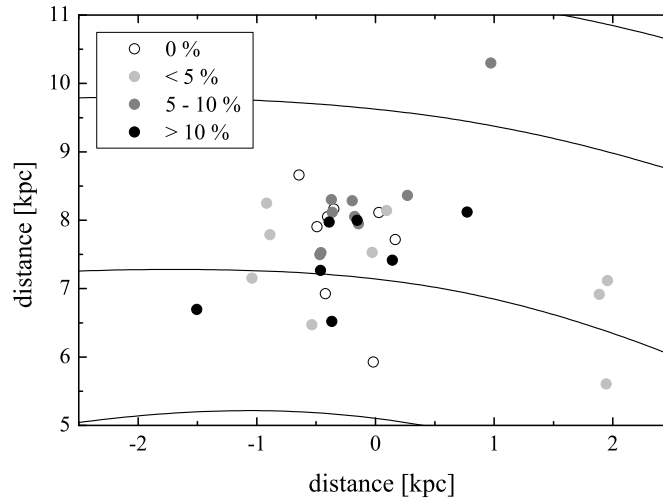


Figure 8.13: The galactic location of the open clusters from the age groups three to five. These were subdivided into a few groups with respect to their CP incidence. Furthermore, the spiralarm models by Hou et al. (2009) are shown. The position of the Sun is at 0/8.0 kpc.

To study a possible dependency with galactocentric distances (R_{GC} , using 8 kpc as solar distance), the above mentioned subsample was divided into three distance ranges, covering nine to twelve open clusters each. We derived 3.4, 5.8, and 4.2%, for the distance groups $R_{GC} < 7.5$, $7.5 - 8.1$, and $8.1 - 8.7$ kpc, respectively. The open cluster Berkeley 11 was excluded, since with $R_{GC} = 10.3$ kpc it is located far beyond the third defined group. Its inclusion would slightly enhance the incidence of this group to about 4.6%. Within the typical errors of $\sim 1.5\%$, deduced for such kind of analysis (see Sect. 8.3.2), one can not infer a dependency. We want to note that the second group, reflecting somehow the solar position and showing the highest percentage, contains the CP rich open cluster NGC 2516. Its exclusion would reduce the derived incidence by about one percent.

Also, if inspecting the galactic location of these open clusters (Fig. 8.13), one can not notice a preference of CP rich open clusters compared to CP free ones, all are populating the same regions. Certainly, to find a correlation with their place of origin, their position has to be dated back using age and their motion as was performed e.g. by Dias & Lépine (2005). However, such information with needed precision is available for a few open clusters only (especially radial velocity data). The youngest aggregates would help out of this dilemma somehow, since they have not moved that much from their birthplace, but there are only 13 clusters younger than 10 Myr in our sample, too few for a proper statistical study. Furthermore, since at such ages not the complete CP mass range has arrived yet on the main-sequence, such an analysis is additionally affected.

Maitzen et al. (2008) suggested that the formation of CP stars is more efficient in compact less populated clusters than in more extended richer ones, but they have neither performed a dedicated membership analysis of the Δa sample, nor they have taken into account the age dependency presented in Sect. 8.3.2. Therefore, a revision

of their assumption is necessary using the cluster subsample with nearly identical CP incidences (the age groups 3 to 5). The calculation of cluster volumes is strongly influenced by the uncertainties of the cluster distances and angular diameters, as well as by assuming a spherical shape. In Sect. 6.2 we already derived the cluster distances, and one can adopt a 10 % uncertainty for this parameter as used in Sect 8.1. Concerning cluster radii, the errors are even more difficult to define. In principle, the radii can be estimated by the stellar overdensity, a radial density profile of the respective area, and the fitting of a profile (e.g. King profile; King, 1962). However, in the literature often rather different approaches for this profile are used, making a direct comparison difficult.

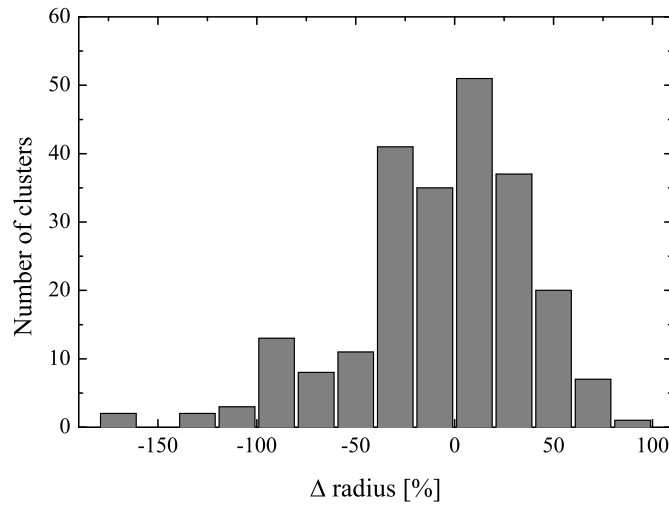


Figure 8.14: Comparison of limiting radius determinations by Bukowiecki et al. (2011) and Kharchenko et al. (2012), using the latter as reference.

Kharchenko et al. (2005) have performed such an analysis for several hundreds of clusters using their (optical) ASCC catalogue, which is on the basis of the TYCHO-2 and Hipparcos catalogues. Recently, Bukowiecki et al. (2011) and Kharchenko et al. (2012) published numerous open cluster parameters (including radii), determined from near-infrared (NIR) 2MASS data. One difference between both comprehensive studies is that Kharchenko et al. (2012) also included membership probabilities deduced from proper motion data. In total, 231 open clusters are in common, offering a sufficient large sample to evaluate the accuracy of cluster radii. However, both are using different definitions of the core and limiting/tidal radius, complicating a comparison. Kharchenko et al. (2012) list parameters determined on the one hand by eye, as well as using a dedicated King profile. Their eye fitted limiting radius (when the stellar density vanishes into the one of the field) corresponds probably best with the limiting radius defined by Bukowiecki et al. (2011). The comparison is presented in Fig. 8.14. One can notice that several cluster radii are significantly underestimated (using the results by Kharchenko et al. (2012) as reference), which are all among the smaller sized clusters. We calculated a median deviation of about 25 %, which is in line with the

Table 8.6: The CP incidences in dependence of the cluster volumes, derived by summing up all members (CP + normal) in the respective volume ranges (using clusters from the age groups three to five). The upper panel gives the results for the core radius, the lower panel if adopting the corona radius instead.

volume range [pc ³]	# clusters	# CP / normal	incidence [%]
1.4 – 9.9	10	13 / 264	4.7
10.2 – 24.2	10	20 / 424	4.5
25.2 – 63.3	11	19 / 412	4.4
16.5 – 181.7	9	10 / 271	3.7
206.0 – 464.4	10	21 / 388	5.1
514.2 – 1630.2	11	21 / 421	4.8

relative error of about 20 % quoted by Piskunov et al. (2007) for their tidal radii of close open clusters.

Unfortunately, there are only a few of our programme clusters included in the lists of Bukowiecki et al. (2011) and Kharchenko et al. (2012), in contrast to the study by Kharchenko et al. (2005), covering most of our subsample (except Berkeley 11, NGC 6451, NGC 6756, and NGC 6834). Their given core radius was defined as the distance where the decrease of the stellar density stops abruptly, reflecting somehow the main (central) area of the cluster with the vast majority of probable members. This parameter resembles also quite good the diameters estimated by Lyngå (1987). Using the results by Kharchenko et al. (2005), we found that the more extended corona radius (i.e. the actual radius of a cluster) is on average about 2.5 times larger than the respective core values. We therefore used for the above listed missing four clusters half the diameter by Lyngå (1987) as core radius and applied the factor 2.5 to obtain their corona radii. A comparison of the results by Kharchenko et al. (2005) and Kharchenko et al. (2012) gives a similar distribution of the deviations as presented in Fig. 8.14, but significantly less open clusters are in common (92 objects). Both references used the same approach, but datasets differing in limiting magnitude as well as in wavelength (optical vs. NIR).

With the derived cluster distances and the compiled radii (using core as well as corona radius) we calculated the respective cluster volumes. Please note that if one fully utilise the adopted error margins (10 % error in distance and 25 % for the cluster radius as estimated above), the resulting error for the volumes can reach up to about 250 %!

In Table 8.6 we summarized the obtained CP incidences by dividing the cluster sample into volume ranges. As can be seen especially for the results based on the core radius, which is very probably better covered by the photometric Δa investigations, by no means a dependency with the compactness of a cluster can be found, they all agree within a few tenths of percent. If using the corona radius (lower panel of Table 8.6), the data would suggest a slight lack of CP stars in smaller clusters, but the results are also still in agreement within the typical errors for the incidences of 1.5 % (ignoring the additional large errors introduced by the volume determinations).

Some extreme spacious open clusters were excluded, since they would form a further too less populated group. These are Melotte 20 (250/28000 pc³), NGC 2546 (300/4300 pc³), and the Pleiades (63/12600 pc³), listing the respective volumes for the core and corona radius in parentheses. Due to the apparent radii of the latter aggregate

(1.1/6.4°) it was included in the investigation of the core radius, but not in the one of the extended area.

Hence, based on the presented sample we are not able to find any further dependency, which favours the formation of CP stars. These are probably connected with initial conditions within the star forming regions. One possibility is the original magnetic field in the respective molecular cloud. For example, Curran & Chrysostomou (2007) investigated the magnetic fields of 16 star forming regions and found a variety of morphologies for the magnetic field, with some very ordered fields. This also clearly shows that the efforts have to be significantly increased among the youngest open clusters, to provide better clues about the formation of CP stars.

8.5 The early stage of chemically peculiar stars

In the previous chapters we have shown that the incidence of chemically peculiar stars on the main sequence remains in principle constant with age and that the found behaviour (increase / decrease) is just a result of stellar evolution in the sense that stars have not yet reached or left the main sequence already. Concerning stellar evolution it is important to constrain the time necessary to develop the chemical peculiarities, hence when diffusion starts to act efficiently. The magnetic field seems to be an important ingredient to develop the chemical peculiarities, in the sense that it slows down stellar rotation. Up to now in some pre-main sequence (PMS) stars (Herbig Ae/Be; see Herbig, 1960) strong magnetic fields were detected, strengthening the conclusion that the magnetic field is probably of fossil origin (e.g. Braithwaite et al., 2010). Recently, Alecian et al. (2013) presented a polarimetric survey of 70 Herbig Ae/Be objects, with six detections of a magnetic field. This results in a frequency of 8.6 %, which is only somewhat higher than the main-sequence CP incidence derived here (Sect. 8.3.2).

However, still no definite prototype is known showing both - a magnetic field and the typical chemical abundances of CP stars. The first of such an announcement was made by Wade et al. (2005) for the star HD 72106A, but later Folsom et al. (2008) deny the PMS phase of it. However, it is still an extremely young representative, which has spent only $\sim 1.5\%$ of its main-sequence lifetime. Similarly, Alecian et al. (2008) proposed the $10.2 M_{\odot}$ He-strong star W601 in the very young open cluster NGC 6611 to be such a candidate, but Martayan et al. (2008) also call the PMS phase into question, since e.g. no infrared excess is noticeable. Later, Hubrig et al. (2010) claimed that they detected chemical spots and resolved magnetically split lines in the star HD 101412, but Cowley et al. (2010) assigned it rather to the class of metal weak λ Bootis stars according to the found abundance pattern. Folsom et al. (2012) confirm this classification, though among their sample of 20 studied Herbig Ae/Be objects about half are showing such a characteristic. They also noted that magnetic Herbig stars do not exhibit chemical compositions remarkably different from the normal stars. However, for one object (V380 Ori A) the reference quote a weak but unsure Ap/Bp peculiarity (see discussion by Folsom et al., 2012).

This demonstrates that it is essential to search for such objects within the lower mass regime, since the duration of the PMS phase is somewhat longer (~ 5 Myr for

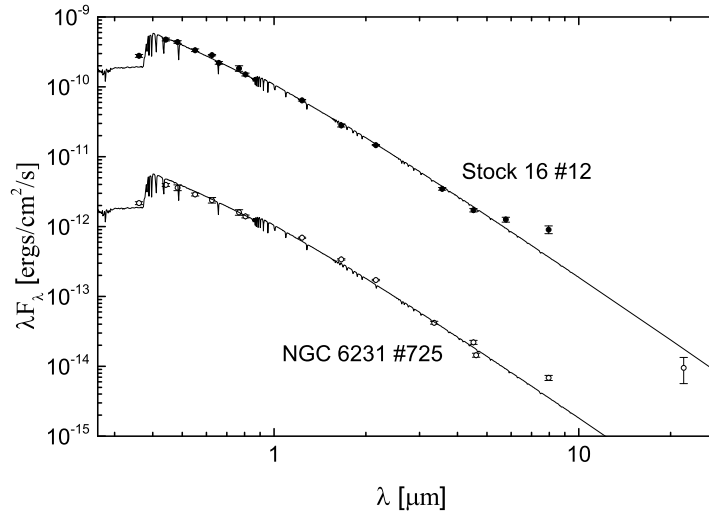


Figure 8.15: Spectral energy distribution (SED) for Stock 16 #12 and NGC 6231 #725, the latter shifted to lower fluxes by two orders. Additionally, synthetic spectra (Kurucz ATLAS 9) with a temperature of 9500 K is given for both objects.

a $3 M_{\odot}$ star; Bernasconi & Maeder, 1996), preferably within open clusters to take advantage of the constraint in age. However, that implies fainter magnitudes, which makes a pre-selection of proper PMS CP candidates solely via spectroscopy rather time consuming.

In our Δa survey also several young open clusters were studied, but most turned out to be free of CP stars. Nevertheless, one detected CP star (Stock 16 #12) with a Δa of +24 mmag seems to be still in its PMS phase due to the young cluster age of ~ 5 Myr (see Table 6.5) and the estimated mass of $\sim 2.5 M_{\odot}$. Furthermore, the spectral energy distribution, constructed using all available photometry (WEBDA, 2MASS, DENIS, APASS, and Spitzer GLIMPSE), shows an infrared (IR) excess starting at $5.8 \mu\text{m}$ (Fig. 8.15), indicating that probably still some circumstellar dust is present. An IR excess and emission (at least in $H\alpha$) are strong indications for a PMS star (see e.g. Martayan et al., 2008). A further criterion to infer a PMS nature is the position in the HRD (see Fig. 8.16 and Table 8.7). We used the new PMS tracks by Lagarde et al. (2012) to determine the mass and age of the object, resulting in $2.43 \pm 0.15 M_{\odot}$ and 3.7 ± 0.6 Myr, respectively.

The spectral classification by Paunzen et al. (2011c) shows a Si nature for Stock 16 #12 (A2 Si), together with strong metal lines. Although a young cluster age was given and the position in the HRD deviates somewhat from the ZAMS, they do not discuss the possibility of a PMS nature. Since the data do not cover $H\alpha$, additional spectra were taken at the CASLEO observatory (see Sect. 3.1 for details). Beside a further exposure of the blue part (as presented by Paunzen et al., 2011c), also spectra covering the region around $H\alpha$ were obtained, shown in Figs. 8.17 and 8.18, respectively. A slightly earlier spectral type of A1 Si was determined, comparable within the typical errors (~ 2 subclasses) to the former result. No clear emission can be noticed in the spectra, what is hardly surprising, since emission would influence the detection as CP

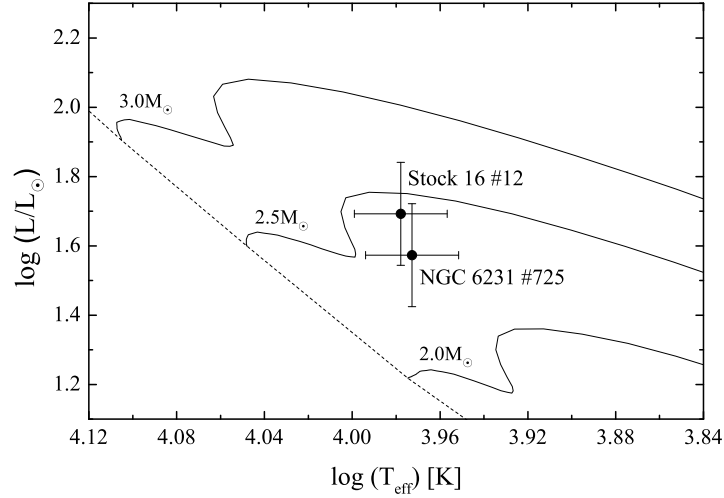


Figure 8.16: The position of Stock 16 #12 and NGC 6231 #725 in the HRD. The new PMS evolutionary tracks by Lagarde et al. (2012) using their standard model for some masses are given; the ZAMS for the $Z=0.014$ model is indicated as dashed line.

Table 8.7: The parameters determined for the PMS candidates.

Star	distance ^a [pc]	$\log(T_{\text{eff}})$ [K]	$\log(L/L_{\odot})$	mass ^b [M_{\odot}]	age [Myr]	Spec
Stock 16 #12	1863(41)	3.978(21)	1.693(149)	2.43(15)	3.7(6)	A1 Si
NGC 6231 #725	1745(146)	3.973(21)	1.573(149)	2.28(13)	4.3(6)	A2

^amean cluster distance and standard deviation using literature values

^bmass and age estimated using PMS grids

star with a positive Δa index. In the study by Paunzen et al. (2005c) on Stock 16 several PMS objects were also covered, showing negative Δa values due to emission. Hence, using photometric peculiarity indices, one can probably identify CP stars only, which have already accreted most of their surrounding material and are transition objects between PMS phase and main-sequence.

We queried the literature to find additional PMS CP candidates beside Stock 16 #12, and recognized NGC 6231 #725 (according to WEBDA), identified by Raboud et al. (1997) using *Geneva* CCD photometry (identifier S168 in their paper). Unfortunately, not all photometric data are available, but at least some *Geneva* colours and indices (like X/Y/Z) are given in the online material. The peculiarity index Z exhibits significant -0.04 mag, and Raboud et al. (1997) classified the star as A0V (Ap?) according to the photometry. It shows a similar IR-excess like the object in Stock 16 (Fig. 8.15), but since also WISE infrared data are available (Wright et al., 2010), the SED is extended up to $22 \mu\text{m}$, showing a more prominent excess.

The spectral classification (Figs. 8.17 and 8.18) resulted in a A2 type star, without a noticeable chemical peculiarity. To estimate the position in the HRD, the effective temperature was derived using calibrations for normal type stars based on *Geneva* and

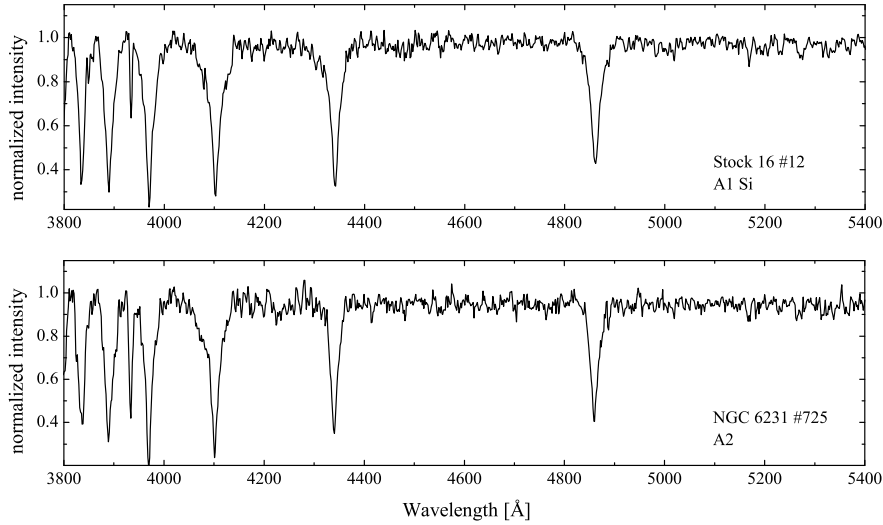


Figure 8.17: Classification resolution spectra for Stock 16 #12 and NGC 6231 #725 taken at CASLEO observatory.

UBV photometry, and the luminosity using a mean cluster distance compiled from the literature (1745 ± 146 pc). Like for the star in Stock 16, we adopted a 10% error for the distance instead, as well as 5% for the effective temperature. These errors also account for, if temperature calibrations and bolometric corrections for CP stars are justified for this object. Using the evolutionary models by Lagarde et al. (2012) we estimated a mass of $2.28 \pm 0.13 M_{\odot}$ and an age of 4.3 ± 0.6 Myr for NGC 6231 #725.

Sana et al. (2007) investigated this cluster using optical and X-ray (XMM) data and found PMS stars up to a mass of $3.0 M_{\odot}$. Concerning cluster age they concluded that star formation started more than 10 Myr ago, with a starburst-like event $\sim 1\text{--}4$ Myr ago, when most of the cluster stars were formed. Although the IR-excess and the detection as X-ray source further strengthen the PMS nature of NGC 6231 #725, also for this star no balmer line emission can be noticed (see Fig. 8.18). Since no chemical peculiarity was found in the classification resolution spectra, this object exhibits probably only a magnetic field yet (as found for some Herbig Ae/Be's), producing the *Geneva Z* index of -0.04 mag (see discussion in Sect. 3). High resolution spectroscopy for an abundance analysis and polarimetric measurements to deduce the magnetic field strength for these two objects are desirable for a more profound conclusion.

Recently, Vick et al. (2011) computed stellar evolution models with mass loss in the mass range of 1.5 to $2.8 M_{\odot}$ to determine at what age the effect of atomic diffusion results in the typical abundances found in CP stars. For their $2.5 M_{\odot}$ model they found that until 3 Myr the abundances would be roughly normal. Since NGC 6231 #725 is slightly less massive, the duration to develop peculiarities is somewhat longer (~ 4 Myr). Hence, the object is probably still too young to show chemical peculiarities, in contrast to Stock 16 #12. However, as mentioned above, more detailed investigations

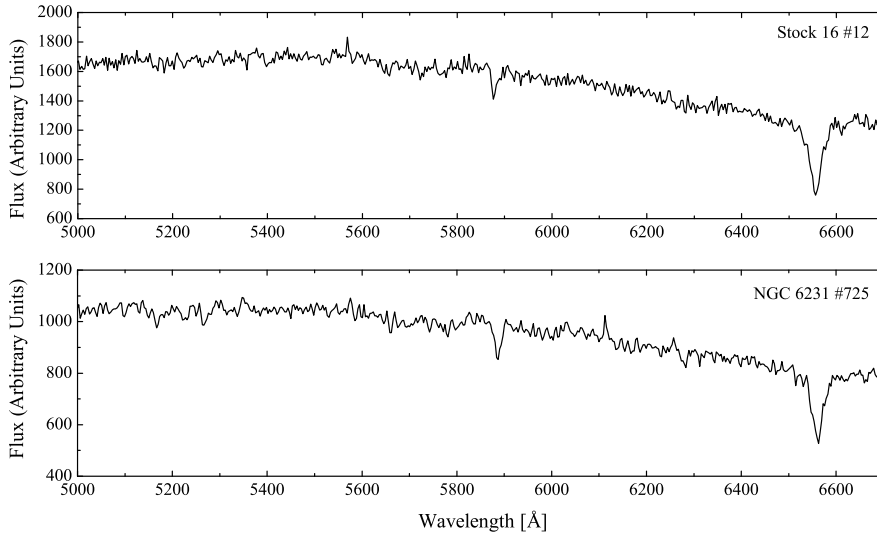


Figure 8.18: Classification resolution spectra covering $H\alpha$ for Stock 16 #12 and NGC 6231 #725 taken at CASLEO observatory. These are not normalized for a better recognition of the probable flux depressions at $\sim 5200 \text{ \AA}$.

based on high-resolution and high S/N data are still necessary, whose acquisitions are rather time consuming due to the V magnitudes of ~ 13.5 mag.

In order to increase the sample of such stars and to further constrain the necessary time to develop CP characteristics, a considerable number of very young open clusters have to be evaluated either using Δa photometry or directly with spectroscopic data (e.g. with those of the LAMOST survey; see Sect. 3.1). To allow efficient follow-up observations due to the brightness of the candidates, these clusters should be preferable also rather close, which limits the number of targets drastically. For example, in WEBDA there are only 14 open clusters listed with an age younger than 10 Myr within 1 kpc around the Sun.

Chapter 9

Outlook

Although the analysis presented in this thesis is already based on the CP content of 79 open clusters, the sample has to be still increased to obtain a much better coverage of the age groups, to decrease the influence of single CP rich/poor populated clusters, or even to narrow down the respective age ranges. Special attention should be paid to enhance the sample of the youngest age group(s). This would help on the one hand to investigate a possible dependency with galactic location in more detail, but also allows to enlarge the number of detected very young (PMS) CP stars, to further constrain the necessary time for the development of chemical peculiarities. The same holds for the CP content of the Large Magellanic Cloud, which is rather poorly defined. For both environments (Milky Way and Magellanic Clouds) we have still some Δa observations in stock, which are going to be analysed.

As discussed in Sect. 7, the determination of cluster membership can be a rather difficult task. With the current available data, especially the more distant and crowded open clusters are very probably strongly affected in this respect. The upcoming Gaia mission will provide an incredible picture of the open clusters with the measured proper motions, parallaxes, and radial velocities. As soon as the data catalogues are available, membership of the cluster stars has to be re-evaluated. Furthermore, with the sample of true members also the cluster parameters can be much better derived.

With the onset of photometric surveys like APASS, IPHAS, Pan-STARRS, Skymapper, and UKIDSS, just to mention a view of them, which will or already provide homogeneous photometry in different passbands, cluster research benefits significantly. Furthermore, also the accuracy of effective temperature determinations for individual objects (like CP stars) will be increased. Hence, for example the differential grid method (see Sect. 6.1.1) can be applied more homogeneously.

Finally, the sample of CP stars, for which all main properties (effective temperature, rotation period, magnetic field strength, and abundances) are well defined, has to be significantly improved (see Sect. 2). With such a data set at hand, the dependencies between all these parameters can be studied in more detail.

Appendix A

The data

In Table A.1 one can find the membership analysis of all compiled CP candidates. The stars were classified as m (member), pm (probable member), pnm (probable non-member), or nm (non-member) according to available proper motion data, radial velocity measurements, Hipparcos parallaxes, as well as based on their position in the colour-magnitude diagrams and HRD. A question mark is given, if the available data are inconclusive (e.g. strong differing proper motion entries in the PPMXL and UCAC-4 catalogues). The final membership flags incorporate the individual determinations, but also spectral types (e.g. disagreement with absolute magnitude or temperature) and memberships listed in the literature. Furthermore, a flag concerning the probable CP nature is given (1 CP / 0 non-CP), which takes into account spectral types (see Sect. 3.1), magnetic field measurements, temperature, or unusual large Δa indices (which are mostly due to non-membership). For some objects the ID of the respective Δa work was adopted (marked by ^a) instead of a WEBDA number.

In Table A.2, beside the mean cluster age, the main parameters (temperature, luminosity, mass, and fractional ages) for the remaining 102 CP cluster members are given. The errors of temperature and luminosity were omitted, since the used error budget is explained in Sect 8.1, but we list the number of different temperature calibrations involved to derive the mean effective temperature (see Sect. 2.3). For a few stars direct temperatures (dt) were adopted from the work by Netopil et al. (2008). We also list the used reddening in magnitudes, which were determined individually as far as possible. If the mean cluster result was used instead, the reddening value is given in italic style. Some stellar masses are also marked this way, if the available photometric data are too poor to derive reliable temperatures. In such cases, the masses were estimated using absolute magnitudes and isochrones for the cluster age.

Table A.1: Membership analysis of the detected CP candidates.

Cluster	Webda #	HD/DM	RA (2000) deg	DE (2000) deg	V mag	Δa mmag	PM	RV	π membership flag	CMD/HRD	final	CP flag
Berkeley 11	128		65.14775	44.95878	13.32	42	pm			m	pm	1
Berkeley 11	188		65.13438	44.94478	14.61	45	?			pm	pm	1
Berkeley 11	255		65.15095	44.92958	15.64	111	pnm			nm	nm	0
Berkeley 11	313		65.17708	44.91944	13.96	33	pm			m	pm	1
Berkeley 11	322		65.11345	44.91823	16.34	91				nm	nm	1
Berkeley 94	4		335.73025	55.89722	15.30	42	?			pm	pm	1
Berkeley 94	176		335.66954	55.86918	16.32	88	m			pm	pm	1
Collinder 121	9	51088	103.72521	-24.71811	8.26	34	m			nm	nm	1
Collinder 132	27	56343	108.82776	-31.90968	9.25	35	pm		pm	m	pm	1
Collinder 140	60	CpD -31 1517	110.83949	-31.83523	10.72	39	pnm			nm	nm	1
IC 2391	17	74168	130.03479	-51.94156	7.49	21	nm		nm	nm	nm	1
IC 2391	18	74169	129.99737	-53.26096	7.25	43	m	m		m	m	1
IC 2391	31	74535	130.57835	-53.09995	5.51	26	m	m	m	m	m	1
IC 2602	17	92385	159.57314	-65.04193	6.74	19	m	?	m	m	m	1
IC 2602	27	92664	160.04766	-65.10021	5.51	26	m	?	m	m	m	1
IC 4725	98	BD -19 5044L	277.93566	-19.12044	10.19	16	pm			m	pm	1
IC 4725	153	170860	278.11256	-19.09878	9.41	22	m	?		m	pm	1
IC 4725	167	170836	278.05123	-19.27573	8.96	46	m	m		m	m	1
King 21	137 ^a		357.46527	62.71098	14.85	41	pnm			nm	nm	1
King 21	151 ^a		357.45343	62.66392	17.68	84	pm			nm	nm	0
King 21	152 ^a		357.45525	62.71651	14.42	36	pnm			nm	nm	0
King 21	55 ^a		357.52227	62.69245	16.17	59	pnm			nm	nm	1
King 21	85 ^a		357.50077	62.71519	16.35	85	pnm			nm	nm	0
Lyngå 1	40		210.01450	-62.16519	14.15	51	pnm			nm	nm	1
Lyngå 1	52		209.99865	-62.18236	15.81	37	pm			m	pm	1
Lyngå 1	53		210.07233	-62.15314	16.22	26	m			m	m	1
Lyngå 1	57		210.00665	-62.16927	16.04	22				m	pm	1
Lyngå 1	58		210.08982	-62.13196	16.13	48	pm			m	pm	1
Lyngå 1	85		209.99084	-62.15902	16.82	22	pm			m	pm	1
Melotte 20	985	21699	53.03584	48.02348	5.47	18	m	m	m	m	m	1
Melotte 105	74		169.93815	-63.48745	14.74	15				m	pm	1
Melotte 105	107		169.93011	-63.48161	13.15	15				m	pm	1
Melotte 105	118		169.92522	-63.47604	14.77	19				m	pm	1
Melotte 105	133		169.92129	-63.47534	13.15	17				m	pm	0
Melotte 111	146	108662	187.22794	25.91285	5.28	43	nm	m	pm	pnm	pnm	1
Melotte 111	160	108945	187.75233	24.56717	5.47	21	m	m	m	m	m	1
NGC 1039	154	16605	40.24558	42.87127	9.67	56	m	pnm		m	pm	1
NGC 1039	307	16728	40.55486	42.69928	7.96	15	m	m	pnm	m	m	1
NGC 1502	27		61.91987	62.26124	12.46	88	m			pm	pm	1
NGC 1662	4	30598	72.36108	10.98840	9.12	17	m		pnm	m	pm	1

... continues on next page

Table A.1: ... Continuation

Cluster	Webda #	HD/DM	RA (2000) deg	DE (2000) deg	V mag	Δa mmag	PM	RV	π	CMD/HRD membership flag	final	CP flag
NGC 2169	12		92.10051	13.94663	10.80	42	m	m		m	m	1
NGC 2232	9	45583	97.04486	-4.89903	7.99	67	m	?	m	m	m	1
NGC 2287	56	49299	101.73587	-20.65196	10.21	74	m	m		pm	m	1
NGC 2422	89	61045	114.19652	-14.56160	8.02	34	m	m	m	pm	m	1
NGC 2423	213	61044	114.19590	-13.99931	8.64	12	pnm			nm	nm	0
NGC 2423	236	61098	114.28267	-13.86975	9.01	18	pm	pnm		nm	pnm	0
NGC 2451A/B	250	62992	116.25672	-38.15841	7.89	19	nm			pnm	nm	1
NGC 2451A	277	63401	116.77399	-39.33100	6.34	38	m	m	m	m	m	1
NGC 2451B	162	61622	114.61372	-39.69288	8.58	33	m			m	m	1
NGC 2451B	207	62251	115.36524	-38.17421	8.96	38	m			m	m	1
NGC 2489	40		119.04975	-30.04211	13.21	32	?			m	pm	1
NGC 2489	43		119.09800	-30.03650	14.05	31	m			m	m	1
NGC 2489	58		119.02200	-30.05772	12.63	52	m			m	m	1
NGC 2516	15	65987	119.51213	-60.61479	7.63	35	m	m	pm	pm	m	1
NGC 2516	24	66318	119.86445	-60.79643	9.65	74	m	m		pm	m	1
NGC 2516	26	66295	119.83874	-60.81567	9.11	45	m	m		pm	m	1
NGC 2516	38	CpD -60 981	119.54365	-60.86596	9.53	14	m			pm	pm	0
NGC 2516	127	CpD -60 978	119.51042	-60.81301	8.94	25	m	m		m	m	1
NGC 2516	208	CpD -60 944A	119.18794	-60.81508	8.35	21	m	m		m	m	1
NGC 2516	230	65712	119.09451	-61.28393	9.41	70	m			pm	pm	1
NGC 2546	197		122.94322	-37.81874	11.14	31	m			m	m	1
NGC 2546	258		122.85019	-37.45934	10.54	30	pm			nm	nm	0
NGC 2546	567	CpD -37 2043	123.24906	-37.91575	10.36	46	pm			m	pm	1
NGC 2632	224	73618	129.98540	19.55299	7.34	22	m	m		pm	m	0
NGC 2632	276	73711	130.07541	19.53199	7.55	20	m	m		pm	m	0
NGC 2632	279	73709	130.08645	19.68673	7.70	18	m	m		m	m	0
NGC 2658	110		130.86322	-32.66868	15.31	26	m			m	m	1
NGC 2658	158		130.85115	-32.64398	15.98	34	?			m	pm	1
NGC 3105	423		150.18956	-54.78192	16.79	31				m	pm	1
NGC 3114	22	CpD -59 1669	150.38602	-59.93660	11.61	29	m			nm	pnm	1
NGC 3114	25	87240	150.43370	-59.85005	9.64	30	pm	m		m	m	1
NGC 3114	80	304841	150.59188	-59.99938	9.96	36	pm	m		m	m	1
NGC 3114	108	87405	150.70082	-59.95838	8.50	17	m	nm	pm	m	pm	1
NGC 3114	184	CpD -59 1807	150.97187	-60.13783	11.39	59	pm			nm	pnm	1
NGC 3114	234	304842	150.66592	-59.96519	9.73	19	pm	m		m	m	1
NGC 3228	3	89856	155.23048	-51.86158	9.05	32	m		m	nm	pnm	1
NGC 3228	16	298053	155.45113	-51.83614	10.69	15	m			m	m	0
NGC 3532	163	CpD -58 3025	166.17648	-58.78327	10.96	15	pnm			pm	pnm	1
NGC 3532	413	96040	165.95337	-58.57687	9.98	60	pm			pnm	pnm	1
NGC 3532	449	96729	166.89582	-58.67979	9.98	65	m			nm	pnm	1
NGC 3532	500	96754	166.92235	-58.50632	9.08	13	pm	nm		nm	nm	0

... continues on next page

Table A.1: ... Continuation

Cluster	Webda #	HD/DM	RA (2000) deg	DE (2000) deg	V mag	Δa mmag	PM	RV	π	CMD/HRD membership flag	final	CP flag
NGC 3532	510	96619	166.73791	-58.46863	10.14	12	m			m	m	0
NGC 3532	632	CpD -57 4336	167.13679	-58.52869	10.39	18	m			m	m	1
NGC 3532	704	303821	167.20072	-59.05890	11.51	61	nm			nm	nm	1
NGC 3960	1		177.60638	-55.65052	14.31	85	pm			m	pm	1
NGC 5281	45		206.64955	-62.90516	13.28	49	pm			pm	pm	1
NGC 5460	55	123225	211.89709	-48.33011	8.84	14	m			m	m	1
NGC 5460	142	122983	211.55709	-48.38685	9.84	20	m			m	m	1
NGC 5662	85	CpD -56 6330	218.86584	-56.61138	10.60	33	pm			m	pm	1
NGC 5662	187	127924	219.00639	-56.46014	9.21	29	m		pm	m	m	1
NGC 5999	119		238.01406	-56.49520	14.71	92	pnm			pm	nm	0
NGC 5999	148		238.00227	-56.46837	14.92	72	nm			nm	nm	0
NGC 5999	1693 ^a		237.99268	-56.44838	15.42	78	?			nm	nm	0
NGC 6031	73		241.93408	-54.03214	13.53	20	pm			m	pm	1
NGC 6031	85		241.93942	-53.97742	15.10	28	?			m	pm	1
NGC 6087	5	146555	244.99728	-57.90785	10.28	38	m			pm	m	1
NGC 6087	25	CpD -57 7817	244.70697	-57.90843	10.03	27	m			m	m	1
NGC 6192	68		250.06550	-43.35408	13.34	30	?			m	pm	1
NGC 6250	15		254.52205	-45.89383	11.99	65	m			m	m	1
NGC 6250	28		254.51458	-45.99297	12.43	26	m			m	m	1
NGC 6268	21	322549	255.58371	-39.70566	11.13	19	m			m	m	1
NGC 6268	23		255.55367	-39.69672	13.64	12	?			pnm	pnm	0
NGC 6268	39		255.56750	-39.72375	12.17	23	pm			m	pm	1
NGC 6268	80		255.54788	-39.74975	11.97	56	pm			m	pm	1
NGC 6268	121		255.57583	-39.70325	12.94	18	?			m	pm	1
NGC 6281	15	153948	256.06514	-38.05175	9.36	40	m	pm		m	m	1
NGC 6405	7	CpD -32 4732	265.10471	-32.10309	10.90	32	m			m	m	1
NGC 6405	19	318100	265.05268	-32.15912	9.81	55	m	m		m	m	1
NGC 6405	77	318107	264.92185	-32.29932	9.36	85	m			m	m	1
NGC 6451	714		267.61696	-30.19663	16.02	78	nm			nm	nm	0
NGC 6475	14	162305	267.97033	-34.78244	7.82	16	m	m		m	m	1
NGC 6475	23	320764	268.04125	-34.89453	8.92	20	m	m		m	m	0
NGC 6475	55	162576	268.31658	-34.62085	6.98	19	m	m	m	m	m	1
NGC 6475	59	162588	268.34760	-35.01695	7.27	19	m	m		m	m	1
NGC 6475	88	162725	268.49223	-34.83105	6.42	35	m	m	m	m	m	1
NGC 6705	863		282.78900	-6.26015	12.13	37	m			m	m	1
NGC 6705	987		282.77450	-6.28557	11.81	45	nm			m	pm	1
NGC 6756	24		287.18226	4.71505	14.49	49				m	pm	1
NGC 6756	33		287.19032	4.69903	14.93	52	pnm			pnm	nm	1
NGC 6802	42		292.65405	20.25927	13.15	46	pm			pm	pm	0
NGC 6802	100		292.64814	20.23071	14.50	155				pm	pm	0
NGC 6802	138		292.64245	20.25624	14.79	119	?			pm	pm	0

... continues on next page

Table A.1: ... Continuation

Cluster	Webda #	HD/DM	RA (2000) deg	DE (2000) deg	V mag	Δa mmag	PM	RV	π	CMD/HRD membership flag	final	CP flag
NGC 6802	6617		292.63857	20.25473	16.16	27	pm			pm	pm	1
NGC 6802	208 ^a		292.66799	20.24579	17.01	41	pnm			nm	nm	1
NGC 6830	38		297.77905	23.06877	13.04	38	?			nm	nm	1
NGC 6830	159		297.71341	23.13426	14.14	36	nm			nm	nm	1
NGC 6830	166		297.73448	23.12524	13.25	35	m			m	m	1
NGC 6830	180		297.76257	23.10825	14.36	42	pnm			nm	nm	1
NGC 6834	412		298.05514	29.41128	16.40	36				pm	pm	1
NGC 6834	2071		298.05498	29.40675	15.31	41				pm	pm	1
NGC 7092	118	205331	323.29213	48.30340	6.84	16	m	m	m	m	m	1
NGC 7235	410		333.05268	57.26377	16.39	31	?			pm	pm	1
NGC 7235	416		333.07044	57.25493	16.86	48	?			pm	pm	1
NGC 7235	458		333.19376	57.23196	16.74	56	pm			pm	pm	1
NGC 7243	370		333.91202	49.95451	9.97	46	m	m	pm	m	m	1
NGC 7243	490	BD +49 3789	333.79751	49.75846	10.14	27	m	pm		m	m	1
NGC 7296	14		337.04441	52.30388	13.68	23	m			m	m	1
Ruprecht 115	3		243.24379	-52.41051	15.90	197	pm			nm	pnm	0
Ruprecht 115	7		243.23109	-52.39202	13.52	58	?			nm	nm	1
Ruprecht 115	11		243.22903	-52.40028	15.36	57	pm			m	pm	1
Ruprecht 115	30		243.25952	-52.39045	15.28	302	?			nm	nm	0
Ruprecht 115	38		243.23934	-52.41610	15.26	43	?			m	pm	1
Ruprecht 115	57		243.19578	-52.38725	15.83	51	?			nm	nm	1
Ruprecht 115	63		243.25253	-52.40733	15.42	38	?			pnm	pnm	1
Ruprecht 115	93		243.25846	-52.40676	16.22	60	?			nm	nm	1
Ruprecht 115	178		243.20099	-52.38132	16.41	69	?			pnm	pnm	1
Ruprecht 115	90 ^a		243.23086	-52.35828	14.77	53	?			nm	pnm	1
Ruprecht 120	34		248.81721	-48.28621	13.09	53	?			m	pm	1
Ruprecht 120	35		248.81630	-48.28564	12.96	52	?			m	pm	1
Ruprecht 120	38		248.78105	-48.28184	12.73	66	?			m	pm	1
Ruprecht 120	116		248.75632	-48.28269	15.48	19	?			pnm	pnm	0
Ruprecht 120	490 ^a		248.81554	-48.28235	15.41	17	?			m	pm	1
Ruprecht 120	604 ^a		248.77925	-48.34283	17.23	22	?			nm	nm	1
Ruprecht 120	616 ^a		248.77389	-48.24712	17.12	18	?			pnm	pnm	0
Ruprecht 120	623 ^a		248.77079	-48.33944	16.71	22	?			nm	nm	1
Ruprecht 130	1		266.92371	-30.08662	15.77	33	m			m	m	1
Ruprecht 130	7		266.92036	-30.09092	15.47	48	pnm			pm	pm	1
Ruprecht 130	108		266.86523	-30.11858	12.93	60	pm			nm	pnm	0
Ruprecht 130	570		266.92978	-30.08639	15.69	35	?			pnm	nm	1
Ruprecht 130	638		266.87637	-30.06126	17.13	48	pm			m	pm	1
Stock 16	12		199.71338	-62.48914	13.38	24	m			pm	pm	1

Table A.2: Final parameters for the cluster CP members.

Cluster	Webda #	$\log(\text{age})_{cl}$	E(B-V)	$\log(T_{\text{eff}})$	# Teff	$\log(L/L_{\odot})$	M/M $_{\odot}$	t_{frac}
Berkeley 11	128	7.91	0.90	4.147	1	2.69	4.31 ± 0.31	0.61 ± 0.33
Berkeley 11	188	7.91	1.04	4.126	1	2.27	3.59 ± 0.22	0.37 ± 0.19
Berkeley 11	313	7.91	0.89	4.122	1	2.36	3.69 ± 0.23	0.40 ± 0.21
Berkeley 94	4	6.96	0.67				3.00 ± 0.35	0.03 ± 0.01
Berkeley 94	176	6.96	0.67				2.07 ± 0.20	0.01 ± 0.01
Collinder 132	27	6.92	0.02	4.060	5	1.73	2.73 ± 0.14	0.02 ± 0.01
IC 2391	18	7.62	0.01	4.006	5	1.47	2.32 ± 0.12	0.06 ± 0.02
IC 2391	31	7.62	0.01	4.153	3	2.49	4.03 ± 0.22	0.26 ± 0.10
IC 2602	17	7.62	0.01	4.049	5	1.74	2.68 ± 0.14	0.09 ± 0.05
IC 2602	27	7.62	0.00	4.155	dt	2.48	4.02 ± 0.22	0.26 ± 0.16
IC 4725	98	7.87	0.53	4.100	3	2.31	3.53 ± 0.20	0.32 ± 0.10
IC 4725	153	7.87	0.47	4.133	3	2.63	4.14 ± 0.25	0.50 ± 0.17
IC 4725	167	7.87	0.46	4.159	4	2.87	4.70 ± 0.30	0.70 ± 0.22
Lyngå 1	52	8.07	0.47	3.879	2	0.81	1.61 ± 0.07	0.05 ± 0.02
Lyngå 1	53	8.07	0.47	3.849	2	0.65	1.47 ± 0.07	0.04 ± 0.01
Lyngå 1	57	8.07	0.47	3.851	1	0.72	1.50 ± 0.06	0.04 ± 0.01
Lyngå 1	58	8.07	0.47	3.835	2	0.69	1.44 ± 0.10	0.04 ± 0.01
Lyngå 1	85	8.07	0.47	3.828	2	0.41	1.36 ± 0.06	0.03 ± 0.01
Melotte 20	985	7.68	0.06	4.204	dt	2.79	4.84 ± 0.27	0.48 ± 0.21
Melotte 105	74	8.48	0.52	3.976	3	1.35	2.14 ± 0.12	0.34 ± 0.13
Melotte 105	107	8.48	0.50	4.015	2	2.02	2.89 ± 0.19	0.78 ± 0.32
Melotte 105	118	8.48	0.55	3.975	3	1.37	2.15 ± 0.12	0.34 ± 0.13
Melotte 111	160	8.79	0.00	3.940	dt	1.58	2.27 ± 0.15	0.81 ± 0.27
NGC 1039	154	8.15	0.10	4.026	5	1.61	2.49 ± 0.13	0.24 ± 0.11
NGC 1039	307	8.15	0.07	4.039	5	1.87	2.78 ± 0.20	0.33 ± 0.16
NGC 1502	27	6.81	0.70	4.114	2	1.94	3.17 ± 0.17	0.02 ± 0.01
NGC 1662	4	8.64	0.33	3.968	6	1.91	2.68 ± 0.19	0.91 ± 0.27
NGC 2169	12	7.00	0.19	4.134	3	2.19	3.54 ± 0.20	0.04 ± 0.02
NGC 2232	9	7.69	0.01	4.098	5	2.07	3.22 ± 0.18	0.17 ± 0.08
NGC 2287	56	8.39	0.00	4.001	6	1.51	2.34 ± 0.12	0.35 ± 0.10
NGC 2422	89	8.09	0.08	4.105	4	2.43	3.71 ± 0.22	0.61 ± 0.21
NGC 2451A	277	7.70	0.00	4.126	5	2.24	3.56 ± 0.19	0.22 ± 0.08
NGC 2451B	162	7.70	0.06	4.099	4	1.98	3.13 ± 0.17	0.16 ± 0.05
NGC 2451B	207	7.70	0.06	4.058	3	1.74	2.72 ± 0.14	0.11 ± 0.04
NGC 2489	40	8.73	0.30	3.924	1	1.50	2.17 ± 0.15	0.61 ± 0.17
NGC 2489	43	8.73	0.30	3.899	1	1.16	1.84 ± 0.11	0.38 ± 0.10
NGC 2489	58	8.73	0.30	3.946	1	1.74	2.45 ± 0.17	0.87 ± 0.24
NGC 2516	15	8.14	0.06	4.093	6	2.40	3.62 ± 0.22	0.64 ± 0.23
NGC 2516	24	8.14	0.06	3.969	6	1.36	2.13 ± 0.11	0.15 ± 0.05
NGC 2516	26	8.14	0.09	4.042	4	1.73	2.66 ± 0.14	0.28 ± 0.10
NGC 2516	127	8.14	0.17	4.071	4	1.96	2.99 ± 0.16	0.39 ± 0.13
NGC 2516	208	8.14	0.14	4.094	5	2.21	3.37 ± 0.19	0.53 ± 0.18
NGC 2516	230	8.14	0.07	3.994	5	1.49	2.30 ± 0.12	0.19 ± 0.07
NGC 2546	197	8.09	0.15	3.970	2	1.61	2.71 ± 0.20	0.27 ± 0.10
NGC 2546	567	8.09	0.21	4.052	2	2.13	3.11 ± 0.19	0.39 ± 0.13
NGC 2658	110	8.40	0.42	3.981	3	1.54	2.30 ± 0.13	0.35 ± 0.14
NGC 2658	158	8.40	0.43	3.983	2	1.28	2.12 ± 0.11	0.28 ± 0.11
NGC 3105	423	7.34	1.08	4.112	1	2.54	5.40 ± 0.60	0.26 ± 0.04
NGC 3114	25	8.15	0.08	4.091	6	2.31	3.49 ± 0.20	0.60 ± 0.23
NGC 3114	80	8.15	0.06	4.090	5	2.16	3.29 ± 0.18	0.52 ± 0.19
NGC 3114	108	8.15	0.04	4.088	6	2.72	4.16 ± 0.28	0.97 ± 0.39
NGC 3114	234	8.15	0.08	4.093	3	2.28	3.45 ± 0.20	0.59 ± 0.22
NGC 3532	632	8.47	0.11	3.957	3	1.26	2.03 ± 0.11	0.28 ± 0.09
NGC 3960	1	8.98	0.28	3.907	2	1.08	1.80 ± 0.11	0.63 ± 0.22
NGC 5281	45	7.78	0.23	3.949	1	1.13	1.93 ± 0.10	0.05 ± 0.02
NGC 5460	55	8.19	0.12	4.087	5	2.41	3.62 ± 0.24	0.71 ± 0.31
NGC 5460	142	8.19	0.14	4.039	3	1.93	2.84 ± 0.17	0.38 ± 0.16
NGC 5662	85	7.97	0.38	4.084	3	2.03	3.13 ± 0.17	0.30 ± 0.08
NGC 5662	187	7.97	0.26	4.113	6	2.51	3.87 ± 0.23	0.52 ± 0.16
NGC 6031	73	8.33	0.47	3.963	2	1.52	2.25 ± 0.13	0.28 ± 0.11
NGC 6031	85	8.33	0.47	3.902	2	0.87	1.68 ± 0.08	0.11 ± 0.04
NGC 6087	5	7.91	0.14	4.095	4	2.10	3.24 ± 0.18	0.29 ± 0.10
NGC 6087	25	7.91	0.20	4.107	3	2.30	3.54 ± 0.20	0.36 ± 0.12
NGC 6192	68	8.15	0.67	4.059	1	1.99	2.98 ± 0.16	0.40 ± 0.15

... continues on next page

Table A.2: ... Continuation

Cluster	Webda #	$\log(\text{age})_{cl}$	E(B-V)	$\log(T_{\text{eff}})$	# Teff	$\log(L/L_{\odot})$	M/M $_{\odot}$	t_{frac}
NGC 6250	15	7.32	0.27	3.981	3	1.41	2.20 ± 0.12	0.03 ± 0.01
NGC 6250	28	7.32	0.35	3.966	3	1.32	2.09 ± 0.11	0.02 ± 0.01
NGC 6268	21	8.20	0.43	4.046	1	2.50	3.66 ± 0.25	0.76 ± 0.29
NGC 6268	39	8.20	0.43	4.059	1	2.11	3.11 ± 0.18	0.49 ± 0.18
NGC 6268	80	8.20	0.43	4.042	2	2.15	3.12 ± 0.20	0.50 ± 0.19
NGC 6268	121	8.20	0.43	3.975	2	1.65	2.73 ± 0.20	0.35 ± 0.14
NGC 6281	15	8.44	0.13	4.026	4	1.85	2.73 ± 0.16	0.61 ± 0.21
NGC 6405	7	7.90	0.08	3.907	3	0.98	1.74 ± 0.08	0.05 ± 0.02
NGC 6405	19	7.90	0.14	4.033	6	1.62	2.53 ± 0.13	0.14 ± 0.05
NGC 6405	77	7.90	0.17	4.073	6	1.92	2.96 ± 0.16	0.22 ± 0.07
NGC 6475	14	8.40	0.05	4.018	3	1.76	2.61 ± 0.15	0.49 ± 0.23
NGC 6475	55	8.40	0.05	4.016	4	2.09	2.98 ± 0.20	0.70 ± 0.35
NGC 6475	59	8.40	0.07	4.040	3	2.04	2.97 ± 0.18	0.69 ± 0.33
NGC 6475	88	8.40	0.05	3.993	6	2.27	3.21 ± 0.20	0.85 ± 0.41
NGC 6705	863	8.30	0.46	4.036	1	2.30	3.32 ± 0.23	0.74 ± 0.27
NGC 6705	987	8.30	0.47	4.061	1	2.49	3.68 ± 0.25	0.98 ± 0.36
NGC 6756	24	8.11	1.03	4.073	2	2.56	3.83 ± 0.27	0.70 ± 0.15
NGC 6802	6617	8.99	0.81	3.860	2	1.04	1.70 ± 0.11	0.54 ± 0.13
NGC 6830	166	8.21	0.51	4.069	1	2.10	3.14 ± 0.24	0.52 ± 0.27
NGC 6834	412	7.79	0.71	3.927	1	0.87	1.66 ± 0.10	0.03 ± 0.01
NGC 6834	2071	7.79	0.71	4.018	1	1.41	2.33 ± 0.12	0.09 ± 0.03
NGC 7092	118	8.48	0.01	3.971	7	2.13	2.98 ± 0.18	0.84 ± 0.33
NGC 7235	410	6.97	0.93	3.970	1	1.43	2.19 ± 0.12	0.01 ± 0.01
NGC 7235	416	6.97	0.93	3.924	2	1.21	1.92 ± 0.11	0.01 ± 0.01
NGC 7235	458	6.97	0.93	3.938	2	1.26	1.99 ± 0.11	0.01 ± 0.01
NGC 7243	370	8.00	0.17	4.106	4	2.19	3.40 ± 0.18	0.40 ± 0.13
NGC 7243	490	8.00	0.24	4.107	4	2.21	3.43 ± 0.19	0.40 ± 0.13
NGC 7296	14	8.50	0.26	3.970	2	1.53	2.28 ± 0.13	0.42 ± 0.16
Ruprecht 115	11	8.69	0.71	3.926	2	1.28	1.98 ± 0.13	0.43 ± 0.17
Ruprecht 115	38	8.69	0.71	3.900	1	1.32	1.97 ± 0.15	0.43 ± 0.18
Ruprecht 120	34	8.35	0.68	4.012	1	2.03	2.89 ± 0.19	0.58 ± 0.22
Ruprecht 120	35	8.35	0.68	4.014	1	2.08	2.96 ± 0.20	0.61 ± 0.23
Ruprecht 120	38	8.35	0.68	4.012	1	2.17	3.08 ± 0.21	0.68 ± 0.26
Ruprecht 120	490 ^a	8.35	0.68	3.883	2	1.00	1.70 ± 0.10	0.12 ± 0.05
Ruprecht 130	1	8.75	1.00	3.949	1	1.43	2.14 ± 0.13	0.63 ± 0.24
Ruprecht 130	7	8.75	1.00	3.938	1	1.55	2.23 ± 0.15	0.71 ± 0.28
Ruprecht 130	638	8.75	1.00	3.904	1	0.87	1.68 ± 0.11	0.30 ± 0.12
Stock 16	12	6.66	0.46	3.978	2	1.69	2.43 ± 0.15	PMS

References

- Abt H. A., 1975, *PASP*, 87, 417
- Abt H. A., 1979, *AJ*, 84, 1591
- Abt H. A., 2001, *AJ*, 122, 2008
- Abt H. A., 2009, *AJ*, 138, 28
- Abt H. A. & Levato H., 1977, *PASP*, 89, 648
- Abt H. A. & Levato H., 1978, *PASP*, 90, 201
- Abt H. A., Levato H., & Grosso M., 2002, *ApJ*, 573, 359
- Abt H. A. & Morrell N. I., 1995, *ApJS*, 99, 135
- Adelman S. J., 1980, *A&A*, 86, 149
- Adelman S. J., 2008, *PASP*, 120, 595
- Alecian E., Wade G. A., Catala C., et al., 2008, *A&A*, 481, L99
- Alecian E., Wade G. A., Catala C., et al., 2013, *MNRAS*, 429, 1001
- Alonso A., Arribas S., & Martínez-Roger C., 1996, *A&A*, 313, 873
- Anders E. & Grevesse N., 1989, *Geochim. Cosmochim. Acta*, 53, 197
- Asplund M., Grevesse N., Sauval A. J., & Jacques S.P., 2009, *ARA&A*, 47, 481
- Aurière M., Wade G. A., Silvester J., et al., 2007, *A&A*, 475, 1053
- Aurière M., Konstantinova-Antova R., Petit P., et al., 2008, *A&A*, 491, 499
- Babcock H. W., 1947, *ApJ*, 105, 105
- Babcock H. W., 1958, *ApJS*, 3, 141
- Babcock H. W., 1960, *ApJ*, 132, 521
- Bagnulo S., Landstreet J. D., Mason E., et al., 2006, *A&A*, 450, 777
- Balega Y. Y., Dyachenko V. V., Maksimov A. F., et al., 2012, *Astrophysical Bulletin*, 67, 44
- Balona L. A., 1984, *MNRAS*, 211, 973
- Balona L. A., 1994, *MNRAS*, 268, 119
- Baumgardt H., 1998, *A&A*, 340, 402
- Baumgardt H., Dettbarn C., & Wielen R., 2000, *A&AS*, 146, 251
- Bayer C., Maitzen H. M., Paunzen E., Rode-Paunzen M., & Sperl M., 2000, *A&AS*, 147, 99

- Bernasconi P. A. & Maeder A., 1996, *A&A*, 307, 829
- Berthet S., 1990, *A&A*, 236, 440
- Bessell M. S., 1983, *PASP*, 95, 480
- Bessell M. S., 2005, *ARA&A*, 43, 293
- Bessell M. S., Castelli F., & Plez B., 1998, *A&A*, 333, 231
- Bica E. & Bonatto C., 2011, *A&A*, 530, 32
- Bidelman, W. P., 1983, *AJ*, 88, 1182
- Boesgaard, A. M. & Friel E. D., 1990, *ApJ*, 351, 467
- Bohlender D. A., Rice J. B., & Hechler P., 2010, *A&A*, 520, 44
- Braithwaite J. & Spruit H. C., 2004, *Nature*, 431, 819
- Braithwaite J., Akgün T., Alecian E., et al., 2010, *Highlights of Astronomy*, 15, 161
- Bruntt H., North J. R., Cunha M., et al., 2008, *MNRAS*, 386, 2039
- Bukowiecki Ł., Maciejewski G., Konorski P., & Strobel A., 2011, *Acta Astronomica*, 61, 231
- Bychkov V. D., Bychkova L. V., & Madej J., 2005, *A&A*, 430, 1143
- Carpenter J. M., 2001, *AJ*, 121, 2851
- Carraro G., de La Fuente Marcos R., Villanova S., et al., 2007, *A&A*, 466, 931
- Carrera R. & Pancino E., 2011, *A&A*, 535, 30
- Carretta E., Bragaglia A., Gratton R. G., & Tosi M., 2005, *A&A*, 441, 131
- Carrier F., Burki G., & Richard C., et al., 1999, *A&A*, 341, 469
- Carrier F., North P., Udry S., & Babel J., 2002, *A&A*, 394, 151
- Chen L., Hou J. L., & Wang J. J., 2003, *AJ*, 125, 1397
- Claret A., Paunzen E., & Maitzen H. M., 1993, *A&A*, 412, 91
- Clariá J. J., 1977, *PASP*, 89, 803
- Clariá J. J., Mermilliod J.-C., Piatti A. E., & Parisi M.C., 2006, *A&A*, 453, 91
- Clariá J. J., Piatti A. E., Mermilliod J.-C., & Palma T., 2008, *Astron. Nachrichten*, 329, 609
- Code A. D., Davis J., Bless R. C., & Hanbury Brown R., 1976, *ApJ*, 203, 417
- Cowley C. R., Hubrig S., González J. F., & Savanov I., 2010, *A&A*, 523, 65
- Cramer N. & Maeder A., 1979, *A&A*, 78, 305
- Crawford C. L. & Mandwewala N., 1976, *PASP*, 88, 917
- Curran R. L. & Chrysostomou A., 2007, *MNRAS*, 382, 699
- Cutri, R. M., Skrutskie, M. F., van Dyk, S., et al., 2003, 2MASS All Sky Catalog of point sources. The IRSA 2MASS All-Sky Point Source Catalog, NASA/IPAC Infrared Science Archive.
- Dachs J., 1972, *A&A*, 21, 373

- Dachs J. & Kabus H., 1989, *A&AS*, 78, 25
- Daflon S., Cunha K., & Becker S. R., 1999, *ApJ*, 522, 950
- Daflon S., Cunha K., & Butler K., 2004, *ApJ*, 604, 362
- Debernardi Y. & North P., 2001, *A&A*, 374, 204
- Delgado A. J., Alfaro E. J., & Cabrera-Caño J., 1997, *AJ*, 113, 713
- De Silva G. M., Freeman K. C., Asplund M., et al., 2007, *AJ*, 133, 1161
- Dias W. S., Lépine J. R. D., & Alessi B. S., 2001, *A&A*, 376, 441
- Dias W. S., Alessi B. S., Moitinho A., & Lépine J. R. D., 2002, *A&A*, 389, 871
- Dias W. S., Assafin M., Flório V., Alessi B. S., & Líbero V., 2006, *A&A*, 446, 949
- Dias W. S. & Lépine J. R. D., 2005, *ApJ*, 629, 825
- Di Benedetto G. P., 1998, *A&A*, 339, 858
- Eggen O. J., 1981, *ApJ*, 247, 507
- Eggen O. J., 1983a, *AJ*, 88, 197
- Eggen O. J., 1983b, *AJ*, 88, 386
- Ekström S., Meynet G., Maeder A., & Barblan F., 2008, *A&A*, 478, 467
- Ekström S., Georgy C., Eggenberger P., et al., 2012, *A&A*, 537, 146
- Elkin V. G., Mathys G., Kurtz D. W., Hubrig S., & Freyhammer L. M., 2010, *MNRAS*, 402, 1883
- Elkin V. G., Kurtz D. W., & Nitschelm C., 2012, *MNRAS*, 420, 2727
- Fenkart R. P., Binggeli B., Good D., et al., 1977, *A&AS*, 30, 307
- Flower P. J., 1996, *ApJ*, 469, 355
- Folsom C. P., Wade G. A., Bagnulo S., & Landstreet J.D., 2007, *MNRAS*, 376, 361
- Folsom C. P., Wade G. A., Kochukhov O., et al., 2008, *MNRAS*, 391, 901
- Folsom C. P., Bagnulo S., Wade G. A., et al., 2012, *MNRAS*, 422, 2072
- Fossati L., Bagnulo S., Monier R., et al., 2007, *A&A*, 476, 911
- Friel E. D. & Janes K. A., 1993, *A&A*, 267, 75
- Friel E. D., Jacobson H. R., Barrett E., et al., 2003, *AJ*, 126, 2372
- Froebrich D., Scholz A., & Raftery C. L., 2007, *MNRAS*, 374, 399
- Giesecking F., 1981, *A&A*, 99, 155
- Gilmore G., Randich S., Asplund M., et al., 2012, *The Messenger*, 147, 25
- Glagolevskii Yu. V., Ryabchikova T. A., & Chountonov G. A., 2005, *Astronomy Letters*, 31, 327
- Glebocki R. & Gnacinski P., 2005, *ESA*, SP-560, 571
- Gonzalez G. & Lambert D.L., 1996, *AJ*, 111, 424
- Gonzalez G. & Wallerstein G., 2000, *PASP*, 112, 1081
- González J. F. & Lapasset E., 2000, *AJ*, 119, 2296

- Gratton R., 2000, in *Stellar Clusters and Associations: Convection, Rotation, and Dynamos*, ed. R. Pallavicini, G. Micela, and S. Sciortino, ASP Conference, 198, 225
- Gray R. O. & Corbally C. J., 2002, *AJ*, 124, 989
- Gray R. O. & Garrison R. F., 1987, *ApJS*, 65, 581
- Gray R. O. & Garrison R. F., 1989a, *ApJS*, 69, 301
- Gray R. O. & Garrison R. F., 1989b, *ApJS*, 70, 623
- Grenier S., Baylac M. O., Rolland L., et al., 1999, *A&AS*, 137, 451
- Grocholski A. J. & Sarajedini A., 2003, *MNRAS*, 345, 1015
- Harmanec P. & Božić H., 2001, *A&A*, 369, 1140
- Harmanec P. & Prša A., 2011, *PASP*, 123, 976
- Harris G. L. H., Fitzgerald M. P. V., Mehta S., & Reed B. C., 1993, *AJ*, 106, 1533
- Hartoog M. R., 1976, *ApJ*, 205, 807
- Hartoog M. R. & Cowley A.P., 1979, *ApJ*, 228, 229
- Hassan S .M., 1976, *A&AS*, 26, 13
- Hauck B., 1974, *A&A*, 32, 447
- Hauck B., 1985, in *Calibration of fundamental stellar quantities*, ed. Hayes, D. S., Pasinetti, L. E., & Philip, A. G. D., *IAU Symp.*, 111, 271
- Hauck B. & Künzli M., 1996, *Baltic Astronomy*, 5, 303
- Hauck B. & North, P., 1982, *A&A*, 114, 23
- Hauck B. & North, P., 1993, *A&A*, 269, 403
- Herbig G.H., 1960, *ApJS*, 4, 337
- Heiter U., Soubiran C., Netopil M., & Paunzen E., 2013, *A&A*, in preparation
- Hillenbrand L. A., Massey P., Strom S. E., & Merrill K. M., 1993, *AJ*, 106, 1906
- Høg E., Fabricius C., Makarov V. V., et al., 2000, *A&A*, 355, L27
- Hou L. G., Han J. L., & Shi W. B., 2009, *A&A*, 499, 473
- Huang W., Gies D. R., & McSwain M. V., 2010, *ApJ*, 722, 605
- Hubrig S., North P., & Mathys G., 2000, *ApJ*, 539, 352
- Hubrig S., Schöller M., Savanov I., et al., 2010, *Astron. Nachrichten*, 331, 361
- Ianna P. A., 1970, *PASP*, 82, 825
- Ianna P. A., Adler D. S., & Faudree E. F., 1987, *AJ*, 93, 347
- Jamar C., 1977, *A&A*, 56, 413
- Jamar C., 1978, *A&A*, 70, 379
- Janes K. & Adler D., 1982, *ApJS*, 49, 425
- Janes K. A. & Hoq S., 2011, *AJ*, 141, 92
- Javakhishvili G., Kukhianidze V., Todua M., & Inasaridze R., 2006, *A&A*, 447, 915
- Jenkner H. & Maitzen H. M., 1987, *A&AS*, 71, 255

- Jilinski E. G., Frolov V. N., Ananjevskaja J. K., Straume J., & Drake N.A., 2003, *A&A*, 401, 531
- Johnson H. L., 1958, *Lowell Observatory*, 4, 37
- Kaltcheva N. T., 2000, *MNRAS*, 318, 1023
- Kaltcheva N., Gredel R., & Fabricius C., 2001, *A&A*, 372, 95
- Kaltcheva N. & Makarov V., 2007, *ApJ*, 667, L155
- Karataş Y. & Schuster W. J., 2006, *MNRAS*, 371, 1793
- Khan S. A. & Shulyak D. V., 2006, *A&A*, 448, 1153
- Khan S. A. & Shulyak D. V., 2007, *A&A*, 469, 1083
- Kharchenko N. V., Piskunov A. E., Roeser S., Schilbach E., & Scholz R.-D., 2004, *Astron. Nachrichten*, 325, 740
- Kharchenko N. V., Piskunov A. E., Roeser S., Schilbach E., & Scholz R.-D., 2005, *A&A*, 438, 1163
- Kharchenko N. V., Piskunov A. E., Schilbach E., Röser S., & Scholz R.-D., 2012, *A&A*, 543, 156
- King D. S., 1978, *Sydney Obs. Pap. No. 79*
- King D. S., 1978, *Sydney Obs. Pap. No. 81*
- King D. S., 1982, *Sydney Obs. Pap. No. 93*
- King I., 1962, *AJ*, 67, 471
- Kochukhov O., 2011, *The Physics of Sun and Star Spots, Proceedings of the International Astronomical Union, IAU Symposium*, 273, 249
- Kochukhov O., Khan S., & Shulyak D., 2005, *A&A*, 433, 671
- Kodaira K., 1969, *ApJ*, 157, 59
- Koelbloed D., 1959, *Bull. Astron. Inst. Netherlands* 14, 265
- Koen C. & Eyer L., 2002, *MNRAS*, 331, 45
- Kroupa P., 2001, *MNRAS*, 322, 231
- Kudryavtsev D. O., Romanyuk I. I., Elkin V. G., & Paunzen E., 2006, *MNRAS*, 372, 1804
- Künzli M., North P., Kurucz R. L., & Nicolet B., 1997, *A&AS*, 122, 51
- Kupka F., Paunzen E., & Maitzen H. M., 2003, *MNRAS*, 341, 849
- Kupka F., Paunzen E., Iliev I.Kh., & Maitzen H. M., 2004, *MNRAS*, 352, 863
- Kurucz R. L., 1979, *ApJS*, 40, 1
- Kurucz R. L., 1993, *CD-ROM 13*, Cambridge, Mass.: Smithsonian Astrophysical Observatory
- Lagarde N., Decressin T., Charbonnel C., et al., 2012, *A&A*, 543, 108
- Landstreet J. D., 1970, *ApJ*, 159, 1001

- Landstreet J. D., 2011, Science from Small to Large Telescopes. Proceedings of a Workshop held at Fairmont Le Manoir Richelieu, La Malbaie, Quebec, Canada 6-11 July 2008. Edited by Pierre Bastien, Nadine Manset, Dan P. Clemens, and Nicole St-Louis, ASP Conference Series, 449, 249
- Landstreet J. D. & Mathys G., 2000, *A&A*, 359, 213
- Landstreet J. D., Bagnulo S., Andretta V., et al., 2007, *A&A*, 470, 685
- Landstreet J. D., Silaj J., Andretta V., et al., 2008, *A&A*, 481, 465
- Lanz T., 1984, *A&A*, 139, 161
- Lefever K., Puls J., Morel T., et al., 2010, *A&A*, 515, A74
- Lejeune T. & Schaerer D., 2001, *A&A*, 366, 538
- Leone F. & Catanzaro G., 1999, *A&A*, 343, 273
- Levato H. & Malaroda S., 1975, *PASP*, 87, 173
- Lindoff U., 1968, *Ark. Astron.*, 5, 63
- Lindoff U., 1972, *A&AS*, 7, 231
- Lipski L. & Stępień K., 2008, *MNRAS*, 385, 481
- Loktin A. V. & Beshenov G. V., 2003, *Astronomy Reports*, 47, 6
- Loktin A. V., Gerasimenko T. P., & Malysheva L. K., 2001, *Astronomical and Astrophysical Transactions*, 20, 607
- Luck R. E., Andrievsky S. M., Kovtyukh V. V., Korotin S. A., & Beletsky Yu. V., 2000, *A&A*, 361, 189
- LyngåG., 1987, *Catalogue of Open Cluster Data (5th Ed.)*, CDS Strasbourg
- Lyubimkov L. S., Rachkovskaya T. M., Rostopchin S. I., & Lambert D., 2002, *MNRAS*, 333, 9
- Maitzen H. M., 1976, *A&A*, 51, 223
- Maitzen H. M., 1981, *A&A*, 95, 213
- Maitzen H. M., 1982, *A&A*, 115, 275
- Maitzen H. M., 1985, *A&AS*, 62, 129
- Maitzen H. M., 1993, *A&AS*, 102, 1
- Maitzen H. M. & Catalano F. A., 1986, *A&AS*, 66, 37
- Maitzen H. M. & Floquet M., 1981, *A&A*, 100, 3
- Maitzen H. M. & Hensberge H., 1981, *A&A*, 96, 151
- Maitzen H. M. & Pavlovski K., 1987a, *A&AS*, 71, 441
- Maitzen H. M. & Pavlovski K., 1987b, *A&A*, 178, 313
- Maitzen H. M. & Schneider H., 1984, *A&A*, 138, 189
- Maitzen H. M. & Schneider H., 1987, *A&AS*, 71, 431
- Maitzen H. M. & Seggewiss W., 1980, *A&A*, 83, 328
- Maitzen H. M. & Vogt N., 1983, *A&A*, 123, 48

- Maitzen H. M. & Wood H. J., 1983, *A&A*, 126, 80
- Maitzen H. M., Pavlovski K., Catalano F. A., et al., 1986, *A&AS*, 65, 497
- Maitzen H. M., Schneider H., & Weiss W.W., 1988, *A&AS*, 75, 391
- Maitzen H. M., Paunzen E., & Rode M., 1997, *A&A*, 327, 636
- Maitzen H. M., Paunzen E., & Netopil M., 2008, *Contrib. of the Astron. Obs. Skalnaté Pleso*, 38, 385
- Marakov V. V. & Kaplan G. H., 2005, *AJ*, 129, 2420
- Martayan C., Floquet M., Hubert A. M., et al., 2008, *A&A*, 489, 459
- Masana E., Jordi C., Maitzen H. M., & Torra J., 1998, *A&AS*, 128, 265
- Mathys G., 2009, *Solar Polarization 5: In Honor of Jan Stenflo*, Proceedings of the conference held 17-21 September, 2007 at Centro Stefano Franscini–Monte Verità, Ascona, Switzerland. Edited by Svetlana V. Berdyugina, K. N. Nagendra, and Renzo Ramelli, *ASP Conference Series*, 405, 473
- Mathys G., Hubrig S., Landstreet J. D., Lanz T., & Manfroid J., 1997, *A&AS*, 123, 353
- Maury A. C. & Pickering E. C., 1897, *Annals of Harvard College Observatory*, 28, 1
- McNamara B. J., Pratt N. M., & Sanders W. L., 1977, *A&AS*, 27, 117
- McSwain M. V. & Gies D. R., 2005, *ApJS*, 161, 118
- Mégessier C., 1988, *A&AS*, 72, 551
- Mermilliod J.-C., 1995, in *Information & On-Line Data in Astronomy*, eds. D. Egret and M. A. Albrecht, *Astrophysics and Space Science Library*, Vol. 203, 127
- Mermilliod J.-C., Hauck B., & Mermilliod M., 1997, *A&AS*, 124, 349
- Mermilliod J.-C., Mayor M., & Udry S., 2008, *A&A*, 485, 303
- Michaud G., 1970, *ApJ*, 160, 641
- Mikulášek Z., Krtička J., Henry G. W., et al., 2008, *A&A*, 485, 585
- Mohan V. & Pandey A. K., 1984, *Bulletin of the Astronomical Society of India*, 12, 217
- Moon T. T. & Dworetzky M. M., 1985, *MNRAS*, 217, 305
- Morel T., Hubrig S., & Briquet M., 2008, *A&A*, 481, 453
- Moss D., 1989, *MNRAS*, 236, 629
- Mowlavi N., Eggenberger P., Meynet G., et al., 2012, *A&A*, 541, 41
- Myakutin V. I., & Piskunov A. E., 1995, *Astronomy Reports*, 39, 316
- Napiwotzki R., Schoenberner D., & Wenske V., 1993, *A&A*, 268, 653
- Netopil M., Paunzen E., Maitzen H. M., et al., 2005, *Astron. Nachrichten*, 326, 734
- Netopil M., Paunzen E., Maitzen H. M., et al., 2007, *A&A*, 462, 591
- Netopil M., Paunzen E., Maitzen H. M., North P., & Hubrig S., 2008, *A&A*, 491, 545
- Nieva M.-F. & Simón-Díaz S., 2011, *A&A*, 532, A2

- North P., 1993, in Peculiar versus Normal Phenomena in A-type and Related Stars, ed. M. M. Dworetzky, F. Castelli, & R. Faraggiana, IAU Coll. 138, 577
- North P., 1998, *A&A*, 334, 181
- North P. & Cramer N., 1981, in Chemically peculiar stars of the upper main sequence, International Conference on Astrophysics, 23rd, Liège, Belgium, June 23-26, 1981, Reports, Liège, Université de Liège, 55
- North P., Carquillat J. M., Ginestet N., Carrier F., & Udry S., 1998, *A&AS*, 130, 223
- North P., Babel J., & Erspamer D., 2008, *Contrib. of the Astron. Obs. Skalnaté Pleso*, 38, 375
- Orellana R. B., de Biasi M. S., Bustos Fierro I. H., & Calderón J. H., 2010, *A&A*, 521, 39
- Pandey A. K., Upadhyay K., Nakada Y., & Ogura K., 2003, *A&A*, 397, 191
- Paunzen E. & Maitzen H. M., 2001, *A&A*, 373, 153
- Paunzen E. & Maitzen H. M., 2002, *A&A*, 385, 867
- Paunzen E. & Netopil M., 2006, *MNRAS*, 371, 1641
- Paunzen E., Pintado O.I., & Maitzen H. M., 2002, *A&A*, 395, 823
- Paunzen E., Maitzen H. M., Rakos K. D., & Schombert J., 2003a, *A&A*, 403, 937
- Paunzen E., Pintado O.I., & Maitzen H. M., 2003b, *A&A*, 412, 721
- Paunzen E., Schnell A., & Maitzen H. M., 2005a, *A&A*, 444, 941
- Paunzen E., Stütz Ch., & Maitzen H. M., 2005b, *A&A*, 441, 631
- Paunzen E., Netopil M., Iliev I. Kh., et al., 2005c, *A&A*, 443, 157
- Paunzen E., Maitzen H. M., Pintado O. I., et al., 2006a, *A&A*, 459, 871
- Paunzen E., Netopil M., Iliev I. Kh., et al., 2006b, *A&A*, 454, 171
- Paunzen E., Schnell A., & Maitzen H. M., 2006c, *A&A*, 458, 293
- Paunzen E., Heiter U., Netopil M., & Soubiran C., 2010, *A&A*, 517, 32
- Paunzen E., Netopil M., & Bord D. J., 2011a, *MNRAS*, 411, 260
- Paunzen E., Hensberge H., Maitzen H. M., et al., 2011b, *A&A*, 525, 16
- Paunzen E., Netopil M., Pintado O. I., et al., 2011c, *Astron. Nachrichten*, 332, 77
- Paunzen E., Hermansson L., & Holmström P., 2012, *A&A*, 542, 68
- Paunzen E., Wraight K. T., Fossati L., et al., 2013, *MNRAS*, 429, 119
- Perryman M. A. C., Lindegren L., Kovalevsky J., et al., 1997, *A&A*, 323, L49
- Peterson D. M., Hummel C. A., Pauls T. A., et al., 2006, *Nature*, 440, 896
- Piatti A. E., Claría J. J., & Bica E., 1998, *ApJS*, 116, 263
- Piatti A. E., Claría J. J., & Bica E., 1999, *MNRAS*, 303, 65
- Piatti A. E., Claría J. J., & Bica E., 2000, *A&A*, 360, 529
- Piatti A. E., Claría J. J., Mermilliod J.-C., Parisi M. C., & Ahumada A.V., 2007, *MNRAS*, 377, 1737

- Piskunov A. E., Schilbach E., Kharchenko N. V., Röser S., & Scholz R.-D., 2007, *A&A*, 468, 151
- Platais I., Melo C., Mermilliod J.-C., et al., 2007, *A&A*, 461, 509
- Power J., Wade G. A., Aurière M., Silvester J., & Hanes D., 2008, *Contrib. of the Astron. Obs. Skalnaté Pleso*, 38, 443
- Pöhl H. & Paunzen E., 2010, *A&A*, 514, 81
- Pöhl H., Maitzen H. M., & Paunzen E., 2003, *A&A*, 402, 247
- Pöhl H., Paunzen E., & Maitzen H. M., 2005, *A&A*, 441, 1111
- Preston G. W., 1967, *ApJ*, 150, 547
- Preston G. W., 1974, *ARA&A*, 12, 257
- Przybilla N., Nieva M.-F., & Butler K., 2008, *ApJ*, 688, L103
- Raboud D., Cramer N., & Bernasconi P. A., 1997, *A&A*, 325, 167
- Ramsay G. & Pollaco D. L., 1992, *A&AS*, 94, 73
- Renson P., & Catalano F. A., 2001, *A&A*, 378, 113
- Renson P., & Manfroid J., 2009, *A&A*, 498, 961
- Rice J. B. & Wehlau W. H., 1994, *A&A*, 291, 825
- Robichon N., Arenou F., Mermilliod J.-C., & Turon C., 1999, *A&A*, 345, 471
- Robitaille T. P., Whitney B. A., Indebetouw R., & Wood K., 2007, *APJS*, 169, 328
- Roeser S., Demleitner M., & Schilbach E., 2010, *AJ*, 139, 2440
- Romanyuk I. I. & Kudryavtsev D. O., 2008, *Astrophysical Bulletin*, 63, 139
- Romanyuk I. I., 2010, *Astrophysical Bulletin*, 65, 347
- Ryabchikova T. A., 2005, *Astronomy Letters*, 31, 388
- Saffe C., Levato H., & López-García Z., 2005, *Revista Mexicana de Astronomía y Astrofísica*, 41, 415
- Sana H., Rauw G., Sung H., Gosset E., & Vreux J. M., 2007, *MNRAS*, 377, 94
- Sanner J., Brunzendorf J., Will J.-M., & Geffert M., 2001, *A&A*, 369, 511
- Schaller G., Schaerer D., Meynet G., & Maeder A., 1992, *A&AS*, 96, 269
- Schneider H. & Weiss W. W., 1988, *A&AS*, 75, 353
- Schnell A., 2008, *CAOSP*, 38, 87
- Sekiguchi M. & Fukugita M., 2000, *AJ*, 120, 1072
- Semenko E. A., Kudryavtsev D. O., Ryabchikova T. A., & Romanyuk I. I., 2008, *Astrophysical Bulletin*, 63, 128
- Sestito P., Randich S., Mermilliod J.-C., & Pallavicini R., 2003, *A&A*, 407, 289
- Sestito P., Bragaglia A., Randich S., et al., 2008, *A&A*, 488, 943
- Shulyak D., Kochukhov O., & Khan S., 2008, *A&A*, 487, 689
- Shulyak D. V., Ryabchikova T., Kildiyarova R., & Kochukhov O., 2010, *A&A*, 520, 88

- Simón-Díaz S., 2010, *A&A*, 510, A22
- Skiff B. A., 2012, *General Catalogue of Stellar Spectral Classifications; CDS/ADC Collection of Electronic Catalogues*, 1, 2023 (2009)
- Stępień K., 1994, in *Chemically peculiar and magnetic stars*, ed. J. Zverko, & J. Žižňovský (Tatranska Lomnica, Slovak Republic), 8
- Stępień K., 2000, *A&A*, 353, 227
- Stępień K. & Landstreet J. D., 2002, *A&A*, 384, 554
- Stetson P. B., 2000, *PASP*, 112, 925
- Stibbs D. W. N., 1950, *MNRAS*, 110, 395
- Stütz Ch. & Paunzen E., 2006, *A&A*, 458L, 17
- Tadross A. L., 2001, *New Astronomy*, 6, 293
- Tadross A. L., 2003, *New Astronomy*, 8, 737
- Tadross A. L., 2006, *Astronomische Nachrichten*, 327, 714
- Thogersen E. N., Friel E. D., & Fallon B. V., 1993, *PASP*, 105, 1253
- Turner D. G., 1985, *ApJ*, 292, 148
- Twarog B. A., Ashman K. M., & Anthony-Twarog B. J., 1997, *AJ*, 114, 2556
- van den Berg S., 2006, *AJ*, 131, 1559
- van Leeuwen F., 2007, *A&A*, 474, 653
- van Leeuwen F., 2009, *A&A*, 497, 209
- Vázquez R. A., Baume G. L., Feinstein C., Nuñez J. A., & Vergne M. M., 2005, *A&A*, 430, 471
- Vázquez R. A., Giorgi E. E., Brusasco M. A., Baume G., & Solivella G. R., 2003, *Revista Mexicana de Astronomía y Astrofísica*, 39, 89
- Vázquez R. A., May J., Carraro G., et al., 2008, *ApJ*, 672, 930
- Vick M., Michaud G., Richer J., & Richard O., 2011, *A&A*, 526, 37
- Villanova S., Carraro G., & Saviane I., 2009, *A&A*, 504, 845
- Vogt N. & Moffat A. F. J., 1972, *A&AS*, 7, 133
- Wade G. A., Debernardi Y, Mathys G., et al., 2000, *A&A*, 361, 991
- Wade G. A., Drouin D., Bagnulo S., et al., 2005, *A&A*, 442, L31
- Wade G. A., Bagnulo S., Drouin D., et al., 2007, *MNRAS*, 376, 1145
- Winkler H., 1997, *MNRAS*, 287, 481
- Wolff S. C., 1968, *PASP*, 80, 281
- Wraight K. T., Fossati L., Netopil M., et al., 2011, *MNRAS*, 420, 757
- Wright E. L., Eisenhardt P. R. M., Mainzer A. K., et al., 2010, *AJ*, 140, 1868
- Xin Y., Deng L., & Han Z. W., 2007, *ApJ*, 660, 319
- Yadav R. K. S. & Sagar R., 2002, *MNRAS*, 337, 133
- Young A. & Martin A. E., 1973, *ApJ*, 181, 805
- Zacharias N., Urban S. E., Zacharias M. I., et al., 2004, *AJ*, 127, 3043

List of Abbreviations

2MASS	The Two Micron All Sky Survey
AAVSO	American Association of variable star observers
APASS	The AAVSO Photometric All-Sky Survey
ASAS	All Sky Automated Survey
ASCC	All-sky Compiled Catalogue of 2.5 million stars
Be/Ae	Emission line objects with spectral types B and A
CMD	Colour magnitude diagram
CP	Chemically peculiar stars; the magnetic groups
DAML02	Catalog of Optically Visible Open Clusters and Candidates by Dias et al. (2002)
GCPD	General Catalogue of Photometric Data
HRD	Hertzsprung–Russell diagram
IMF	Initial mass function
LAMOST	Large Sky Area Multi-Object Fiber Spectroscopic Telescope
NIR	Near-infrared
PMS	Pre-main sequence
PPMXL	Positions and Proper Motions Extended (astrometric and photometric catalogue)
SDSS	Sloan Digital Sky Survey
SED	Spectral energy distribution
STEREO	Solar Terrestrial Relations Observatory
Superwasp	Super Wide Angle Search for Planets
TASS	The Amateur Sky Survey
UCAC	The US Naval Observatory CCD Astrograph Catalog
UKIDSS	The UKIRT (United Kingdom Infrared Telescope) Infrared Deep Sky Survey
WEBDA	The database for galactic open clusters (http://www.univie.ac.at/webda)
ZAMS/TAMS	Zero/Terminal age main-sequence

List of Figures

1.1	The observed abundances pattern in some groups of chemically peculiar stars, taken from Preston (1974).	2
2.1	The HRD of the stars used for the analysis. Large filled circles represent single stars within the main-sequence band and with available periods, whereas the smaller symbols represent the remaining sample. Open circles are CP members of OB associations.	7
2.2	The distribution of observed $v \sin i$ for CP stars compared to normal main-sequence stars. Additionally, the smaller insert shows the percentage of CP stars to normal ones. Whereas the black columns represent the complete sample, the grey columns gives the sample restricted to stars within 100 pc.	8
2.3	The distribution of the inclination for CP stars. The open bar represents objects including also stars with $(v \sin i - V_{eq}) \leq 10 \text{ km s}^{-1}$ (see text).	9
2.4	The HRD of the cleaned field star CP sample and the slow rotating normal objects with $v \sin i < 50 \text{ km s}^{-1}$, the latter represented by star symbols.	10
2.5	The gravity/period relation for chemically peculiar stars. The thick lines represent the $3 M_{\odot}$ models by Ekström et al. (2008) for initial (ZAMS) values of $\Omega/\Omega_{crit} = 0.1, 0.3, \text{ and } 0.5$ (from top to bottom). The dotted lines show the evolution assuming a simple model with conservation of angular momentum ($P_{rot} \propto R^2$). The subsample of $2.4 \text{ to } 3.5 M_{\odot}$ stars are given by larger grey symbols and their mean values (plus standard deviation) by the crosses. Furthermore, the models were interpolated to $\Omega/\Omega_{crit} = 0.22$ ($v/v_{crit} \sim 0.15$) shown as grey line.	12
2.6	The mass/equatorial velocity relation on the ZAMS. Small dots represent the sample defined in Sect. 2.1, open circles are CP stars in OB associations listed by Landstreet et al. (2007), and the crosses equatorial velocities deduced using the mean v/v_{crit} velocities of the field star sample. Additionally, the linear fit of these averages is given as straight line.	14
2.7	The HRD of the stars used for the investigation of the magnetic field. Large filled circles represent the adjusted sample (see text), whereas the smaller symbols represent the remaining stars.	17

2.8	The magnetic field as a function of gravity for various mass ranges. The full lines assume initial magnetic field strengths of 1.5, 7.5, and 30 kG, respectively, decreasing with $(R/R_Z)^2$. The $3 M_\odot$ evolutionary model by Schaller et al. (1992) was used for that purpose.	18
2.9	The distribution of the magnetic field strengths at the ZAMS.	19
2.10	The magnetic field strength at the ZAMS vs. equatorial velocities.	20
2.11	The <i>Geneva</i> peculiarity indices $\Delta(V1-G)$ and Z compared to equatorial velocities, surface magnetic field strength ($\log B_s$), and iron abundances. In the upper panel also the young magnetic association members are given with grey symbols. The symbol size corresponds with the effective temperature.	21
2.12	Histogram of the number of individual temperature determinations for CP2 stars.	22
2.13	The temperature deviations for CP2 objects determined by Netopil et al. (2008).	23
2.14	The temperature deviations for CP4 objects determined by Netopil et al. (2008). The dark grey portion serves to discriminate He-weak objects from He-rich stars.	23
2.15	The corrections for CP3 and CP4 objects based on Geneva photometry by Netopil et al. (2008). The upper line shows the one-to-one relation, the middle line the determined fit, and the lower one the CP2 relation as comparison. Furthermore, the position of the strong magnetic star HD 137509 is given.	24
2.16	The temperatures for CP2 stars deduced using SED fitting compared to spectroscopic temperatures.	25
2.17	The “blueing effect” of CP2 (filled circles) and CP4 (open circles) objects as a function of temperature. Additionally, the group of roAp stars is given separately as open squares. Smaller symbols indicates that only one fundamental temperature is available. The lower vertical line represents the typical maximal blueing of 0.05 mag. The error bars correspond to the standard deviation of the averaged temperatures and the resulting errors for the colour indices.	27
2.18	The bolometric corrections for CP2/4 objects by Netopil et al. (2008). There is only data for a few CP3 stars available, insufficient to conclude about their behaviour.	28
3.1	The filter curves of the most recent Δa system, produced by Custom Scientific in 2005.	30
3.2	The CMD (left panel) and diagnostic Δa diagram (right panel) for the open cluster Ruprecht 115 taken from Netopil et al. (2007). The isochrone for an age of $\log t = 8.6$ is over plotted. In the right panel, the vertical line represents the transformed position of spectral type A0. The detected chemically peculiar objects are shown with star symbols, non-members with small open circles.	31

3.3	The detection probability of the Δa system for various peculiar groups as a function of the detection limit investigated by Paunzen et al. (2005b). Additionally, the group of supergiants (luminosity class I/II) is also given (see the latter reference for details), which can be easily distinguished from classical CP stars by their photometric properties.	32
3.4	Temperature dependency of $\Delta a / \Delta(V1 - G)$ and abundances of some selected elements. In the upper panel the black circles represent direct Δa measurements, whereas open circles are <i>Geneva</i> $\Delta(V1 - G)$ values shifted by +15 mmag in order to bring them on the scale of Δa . The solid lines indicate the zero point of Δa at ~ 7400 K and the dotted line a Δa limit of +15 mmag. The position of the strong magnetic star HD 137509 is given with star symbols (see discussion in the text).	34
3.5	The photometric peculiarity indices Δa and $\Delta(V1 - G)$ compared to iron abundances. Again, <i>Geneva</i> $\Delta(V1 - G)$ values were shifted by +15 mmag in order to bring them approximately on the scale of Δa	35
3.6	Spectroscopic confirmation of an extragalactic CP star by Paunzen et al. (2011a). The measured equivalent widths of the Si doublet ($\sim 0.3 \text{ \AA}$) are about two times larger compared to normal late B type stars.	37
3.7	Classification resolution spectroscopy of some further open cluster CP candidates taken at CASLEO observatory.	39
3.8	Classification resolution spectroscopy of some further open cluster CP candidates taken at ROZHEN observatory.	40
4.1	Distribution of age, distance, reddening, and metallicity of the clusters in the updated catalogue by Dias et al. (2002).	42
4.2	The positions of open clusters within the Milky Way by using the updated catalogue by Dias et al. (2002). Furthermore, the spiralarm models by Hou et al. (2009) are given. The galactic center is at 0/0, the position of the Sun at 0/8.0 kpc. The youngest open clusters are highlighted to demonstrate their capability as spiral arm tracers.	43
4.3	Comparison of two different studies presenting $(B - V)$ data for NGC 1513 taken from the WEBDA database. In an ideal case, there has to be a small scatter around zero at the ordinate.	44
5.1	The Tycho2 proper motions of the stars in the area of NGC 3228. The membership probabilities by Dias et al. (2001) are given with increasing size of the symbols (larger symbols represent higher probability). The cross indicates the listed mean cluster motion, the grey symbol the proper motion of the CP candidate HD 89856.	55
6.1	The distribution of the mean absolute errors of the distance and age as well as the standard deviation of the reddening for the complete sample of 395 open clusters with more than three independent measurements from the literature; taken from Paunzen & Netopil (2006).	74
6.2	Geneva isochrones for $\log t=8.0$ in the $(B - V)_0/M_V$ plane for some metallicities.	75

6.3	Comparison of available high resolution and high S/N metallicity determinations for the open cluster Collinder 261, taken from Heiter et al. (2013).	76
6.4	The differential evolutionary tracks by Pöhl & Paunzen (2010), which were used to deduce metallicity, as well as the other open cluster parameters. T_N stands for to the ZAMS normalised effective temperatures.	77
6.5	Empirical temperature calibration for the colour index ($V - R$) on the Cousins systems.	79
6.6	Empirical temperature calibration for normal B-type stars (the restricted sample) using the $UBVQ$ -Index. Open circles represent supergiants (luminosity class I a/b).	80
6.7	Empirical temperature calibration for normal B-type stars (the restricted sample) using the reddening free $[u - b]$ Strömgren index. Open circles represent supergiants (luminosity class I a/b).	81
6.8	Comparison of the temperature scale in the present work to various literature results using the restricted sample defined above.	83
6.9	Comparison of the old and new differential grids applied to NGC 6475. For better visibility, the results based on the new grids were shifted by $T_N = 0.07$ to the left. Additionally, some isochrones for the same age but for different metallicities are shown as comparison with dashed lines: $Z=0.010/0.040$ (old grid) and $Z=0.010/0.030$ (new grid)	85
6.10	Comparison of the metallicity estimates using the method by Pöhl & Paunzen (2010) to spectroscopic values. The one-to-one relation is given as straight line.	86
6.11	Comparison of photometric and low-resolution metallicity mean values listed by Twarog et al. (1997) compared to high resolution spectroscopic results by Heiter et al. (2013) and additional sources listed by Carrera & Pancino (2011). The one-to-one relation is given as straight line.	88
6.12	The best fits of the differential grids by Pöhl & Paunzen (2010) to the program open clusters, in order to determine the fundamental parameters including metallicity. For clarity, T_N is the to the ZAMS normalised effective temperature. An equal scale is used for a better recognition of different ages and metallicities. Due to interpolation in the available grids, the hotter stars are sometimes not covered by the isochrone.	89
6.13	Continuation of Figure 6.12.	90
6.14	Continuation of Figure 6.12.	91
6.15	Continuation of Figure 6.12.	92
6.16	Continuation of Figure 6.12.	93
6.17	Continuation of Figure 6.12.	94
6.18	Continuation of Figure 6.12.	95
6.19	Continuation of Figure 6.12.	96
6.20	Continuation of Figure 6.12.	97
6.21	Continuation of Figure 6.12.	98

-
- 6.22 The result of the differential grid method for Rup 130 with $\log t = 8.75$ and solar metallicity. Additionally, the parameters listed in Paunzen et al. (2006b) and Piatti et al. (2000) were adopted and applied to the same star sample. The isochrones for $\log t = 7.8$ with solar metallicity (thin line) and $[Z] = 0.04$ (dotted line) are shown as comparison. 103
- 6.23 The colour-magnitude diagrams (CMD) for the open cluster Rup 130 together with the isochrones for the age $\log t = 8.75$ and solar metallicity. In the left panel the UKIDSS/2MASS CMD is given (restricted to the blue part), whereas larger symbols represent objects within a radius of $1'$ and smaller grey symbols additional objects up to a radius of $2.0'$. This also holds for the other CMDs. Furthermore, in the $(B - V)$ and $(V - I)$ diagrams the stars used for the metallicity-fit within the grid range are indicated as open symbols. The black lines are the Padova isochrones, whereas the grey lines are Geneva ones. 104
- 6.24 The parameter distributions of the open cluster sample. 107
- 6.25 Comparison of the final adopted parameters to those listed in the open cluster catalogue by Dias et al. (2002) (DAML02, Version 3.2). Note that in some panels due to outliers the axis is interrupted for a better presentation. In the histograms (right panels) these outliers were omitted. The differences are always calculated in the sense this study minus DAML02. 108
- 7.1 The Gaussian fits for the restricted sample of proper motions in RA and DE for stars in NGC 3532 using UCAC-2 data. 113
- 7.2 The HRD of the open cluster NGC 3532. The black circles represent the probable CP2 members, the smaller grey symbols the normal ones. Furthermore, the Geneva isochrones for solar metallicity at $\log t = 8.3, 8.4, 8.5$ and some mass tracks are plotted. 115
- 7.3 The HRD of the open cluster NGC 2516. The black dots represent the possible CP2 members, the smaller grey symbols the normal ones. Furthermore, the Geneva isochrones for solar metallicity at $\log t = 8.10, 8.15, 8.20$ and some mass tracks are plotted. The object CP-60 981 is the only one which is deviating somewhat from the corresponding isochrones, probably due to its binary nature. Both components of CP-60 944 are also indicated. 118
- 7.4 The UCAC-4 and PPMXL proper motions for stars in the open cluster NGC 3960. The straight lines represent the 1 to 1 relation. Note that only the inner portion is shown, there are several even larger deviating results. 119

8.1	The HRD of the compiled cluster member CP stars, detected with Δa photometry, for which sufficient photometry is available to determine effective temperature. Several mass tracks and isochrones are indicated using the evolutionary grids by Schaller et al. (1992) for $Z=0.02$. The dotted lines represent fractional main-sequence ages of 20, 40, 60, and 80%, respectively. Additionally, the position of Stock 16 #12, discussed in Sect. 8.5, is given as open circle. To increase visibility, the individual errors were omitted, but the typical error in temperature and luminosity is shown in the bottom left-hand corner.	124
8.2	The CP stars ages determined by interpolating within the evolutionary grids by Schaller et al. (1992) for $Z=0.02$ compared to the adopted cluster ages in dependence of some properties. Furthermore, the fractional ages (time elapsed on the main-sequence) determined from the position in the HRD are compared to those using the stellar mass, main-sequence lifetimes and cluster age (panel d).	125
8.3	The CP stars ages determined by interpolating within the evolutionary grids by Ekström et al. (2012) for $Z=0.014$ (without rotation) compared to the adopted cluster ages. Furthermore, the dependency of the deviation with gravity ($\log g$) is given.	126
8.4	The mass distribution of the cluster CP stars compared to CP field objects compiled in the Sects. 2.1 and 2.2. The horizontal lines indicate the percentage if both samples are combined. Furthermore, a Gaussian function was fitted to the total distribution.	128
8.5	The distribution of the fractional ages of the cluster CP stars and the CP field objects compiled in the Sects. 2.1 and 2.2. The horizontal lines indicate the percentage if both samples are combined.	128
8.6	The frequency of the (102) cluster CP stars compared to (3742) normal stars for various mass bins, calculated as $\frac{CP}{CP+normal}$	129
8.7	The mass functions of the investigated stars, divided into the complete sample and cluster stars younger than 15 Myr. Whereas most mass bins of the latter group are well represented by the universal IMF $\alpha=2.3 \pm 0.7$ (Kroupa, 2001), the complete sample needs $\alpha \sim 3.25$ for a proper fit. The error of the IMF is given as dashed lines. The investigation was restricted to $10 M_{\odot}$ as upper limit, and the bin size was always set to $0.5 M_{\odot}$	130
8.8	The frequency of Si and Sr,Cr stars as shown by Abt (1979).	131
8.9	The frequency of CP stars as shown by North (1993).	132
8.10	The number of CP stars per cluster as a function of age, divided into the photoelectric and CCD sample. Furthermore, the total sample was grouped into somewhat smaller age ranges. The mean ages of the individual groups are given together with covered age range. Please note that the apparent deviations between the sub- and total samples are due to the different binning.	133

8.11	The frequency of CP stars in all investigated open clusters, calculated as CP/(CP+normal) using the mass range of 1.5 to 7 M_{\odot} . Open symbols represent clusters with less than 15 investigated objects, grey symbols < 20, and black ones with ≥ 20 measured stars. Furthermore, the average frequency and standard deviation was calculated using the age groups listed in Table 8.2. As in Fig. 8.10, the age ranges are also shown. . . .	135
8.12	The observed frequencies of CP stars for various mass ranges as a function of age by accumulating all stars in each age group. Furthermore, theoretical frequencies taking into account stellar evolution and the IMF are given, assuming a fixed CP content of 2, 3, 4, and 5 stars as well as a maximum of 100 member stars in each simulated cluster. The respective best fitting value is shown as solid line, the adopted errors as grey area (see the text for more details). For the mass subgroups the youngest and/or oldest clusters were not considered due to low or absent population (see Table 8.3).	137
8.13	The galactic location of the open clusters from the age groups three to five. These were subdivided into a few groups with respect to their CP incidence. Furthermore, the spiralarm models by Hou et al. (2009) are shown. The position of the Sun is at 0/8.0 kpc.	143
8.14	Comparison of limiting radius determinations by Bukowiecki et al. (2011) and Kharchenko et al. (2012), using the latter as reference.	144
8.15	Spectral energy distribution (SED) for Stock 16 #12 and NGC 6231 #725, the latter shifted to lower fluxes by two orders. Additionally, synthetic spectra (Kurucz ATLAS 9) with a temperature of 9500 K is given for both objects.	147
8.16	The position of Stock 16 #12 and NGC 6231 #725 in the HRD. The new PMS evolutionary tracks by Lagarde et al. (2012) using their standard model for some masses are given; the ZAMS for the Z=0.014 model is indicated as dashed line.	148
8.17	Classification resolution spectra for Stock 16 #12 and NGC 6231 #725 taken at CASLEO observatory.	149
8.18	Classification resolution spectra covering $H\alpha$ for Stock 16 #12 and NGC 6231 #725 taken at CASLEO observatory. These are not normalized for a better recognition of the probable flux depressions at $\sim 5200 \text{ \AA}$	150

List of Tables

1.1	The classification scheme by Preston (1974).	2
2.1	The temperature calibrations for the individual CP groups and photometric systems determined by Netopil et al. (2008).	28
3.1	The characteristics of the recent Δa filter set.	29
3.2	Spectral classifications for some additional CP candidates based on data obtained at CASLEO (upper panel) and ROZHEN observatory (lower panel).	38
6.1	Adopted temperature calibrations.	83
6.2	The results of the metallicity determination together with spectroscopic literature values.	99
6.2	... Continuation	100
6.3	The results of the metallicity determination using $uvby\beta$, UBV , and <i>Geneva</i> photometric systems. The number of stars used is also indicated, as well as the spectroscopic and grid determinations as comparison. The presented data are uncorrected in respect to the spectroscopic results.	101
6.4	Results of isochrone fitting for some aggregates using all available data.	106
6.5	The final parameters adopted for the programme open clusters.	109
6.5	... Continuation	110
7.1	Overview of mean proper motions for the open cluster NGC 3532. The errors of the last digits are given in parenthesis.	113
7.2	Proper motions of the CP candidates in the open cluster NGC 3532. The indication of errors have been omitted for better readability, all of them are in the order of 2 – 3 mas/yr. The mean cluster motion was calculated as $-10.0(1.2)/4.7(0.5)$ for RA and DE, respectively.	113
7.3	The membership probabilities for the possible CP stars in NGC 3532.	116
7.4	Summary of the now hopefully correct rectification for the peculiar visual pair CP –60 944 A/B, whereas A is the brighter western component.	118
7.5	The mean proper motions of the programme open clusters, given in mas/yr. An asterisk in the last column indicates that also mean motions were calculated using the PPMXL and/or UCAC catalogues.	120
7.5	... Continuation	121

8.1	Number of cluster CP and normal stars for various mass ranges.	129
8.2	Number and frequency of all CP member stars per open cluster for the defined age groups.	133
8.3	The number of observed CP and normal stars within the open clusters. The vertical lines separates the in general used age groups. Open clusters marked with ^a originate from the photoelectric survey. For Stock 16 and Lyngå 1, the number in parenthesis gives the total number of found CP stars, but which were not considered for the analysis, due to PMS nature or too low mass (see text for details).	135
8.3	... Continuation	136
8.4	The observed CP frequencies for the investigated mass ranges and age groups. In addition, the frequencies are given by removing clusters with few observed stars as described in the text (last column).	138
8.5	The theoretical CP frequencies for the investigated mass ranges as described in the text, whereat P gives the probability in percentage to catch a CP star in the respective mass range, or fractional ages covered in a particular age/mass combination. The given frequencies represent the best fit to the observed ones by adopting a fixed value of CP stars; three for the two middle panels and four in upper and lower one.) . . .	141
8.6	The CP incidences in dependence of the cluster volumes, derived by summing up all members (CP + normal) in the respective volume ranges (using clusters from the age groups three to five). The upper panel gives the results for the core radius, the lower panel if adopting the corona radius instead.	145
8.7	The parameters determined for the PMS candidates.	148
A.1	Membership analysis of the detected CP candidates.	154
A.1	... Continuation	155
A.1	... Continuation	156
A.1	... Continuation	157
A.2	Final parameters for the cluster CP members.	158
A.2	... Continuation	159

Acknowledgements

First of all, I would like to thank my parents for their support of my arising interest in astronomy during adolescence, and later on for the possibility to start my studies on this topic. In this respect (and for taking care during childhood), I also have to thank my brother Heinz, who introduced me into the “StarTrek” universe, probably evoking my interest in science.

Beside trying to make my hobby into a profession, the start of my studies in astronomy was the best decision, since I was able to meet my beloved better half Barbara. Even after twelve years of relationship I still admire her always positive mood and I’m thankful for each elapsed and future minute spent by her side.

Across the oceans across the seas, over forests of blackened trees.
Through valleys so still we dare not breathe,
to be by your side.

...

Into the night as the stars collide,
across the borders that divide forests of stone standing petrified,
to be by your side.

©Nick Cave

Furthermore, I wish to express my gratitude in particular to Hans Michael Maitzen and Ernst Paunzen, but also to all other former and present research group members (especially Monika and Harald), for their support, informative discussions (or chats), and friendship. I have to apologise that it sometimes took rather long to provide results, especially the completion of this thesis.

I would like to finish with the well known phrase “*Per aspera ad astra*”, written as personal note by my German teacher in the annual book at the end of school. She was right ...

Curriculum vitae

Martin Netopil

Born: January 15th 1976 in Vienna, Austria

Citizenship: Austria

Marital status: single

Address: Pannaschgasse 6/3/7, 1050 Vienna, Austria

e-mail: Martin.Netopil@univie.ac.at

Education

1982 - 1986	primary school - Schäffergasse, 1040 Vienna
1986 - 1990	grammar school - BRG4 Waltergasse, 1050 Vienna
1990 - 1995	Vienna Business School (HAK I), 1010 Vienna
June 1 st 1995	School leaving examination at Vienna Business School
Oct. 1995	enrolment at University of Vienna
March 4 th 2004	M.Sc. in Astronomy; Thesis: "PU Vulpeculae, an eclipsing symbiotic novae"
March 17 th 2004	start of PhD study in Astronomy; Thesis: "The incidence of chemically peculiar stars in open clusters"

Employment history

1995 – 2001	Contracts of work and service at Otis Elevator Company (Purchase and Marketing departments)
1998 – 2008	Tutor at the Institute of Astronomy for different lab courses
2001 – 2002	Contracts of work and service at the library of the Austrian Academy of Sciences
10.2002 – 05.2003	Military Service
2005	Research grant by University of Vienna - "Determination of astrophysical parameters of northern galactic open clusters"
2006 – 2008	Full time employment within FWF-Project P17920 "Δa photometry of open clusters"
01.2009 – 10.2009	Research grant by University of Vienna - "An international campaign to monitor variable stars in open clusters"

- 10.2009 – 03.2010 MOEL Plus grant (# 388) by the ÖFG at the Hvar Observatory, University of Zagreb - “The Austro-Croatian galactic open cluster survey”
- 09.2010 – 02.2011 MOEL Plus grant (# 446) by the ÖFG at the Masaryk University, Brno - “Variability of chemically peculiar stars”

Lectures

- WS 2006/07 280386 Basic techniques for scientific research I
- SS 2008 280117 Observatory exercises, O4-1
280127 Star Clusters as galactic modules

Research stays and observing experience

Masaryk University (Czech Republic), University of Zagreb (Croatia), ESO La Silla (Chile), ESO Paranal (Chile), Asiago Observatory (Italy), CASLEO Observatory (Argentina), Hvar Observatory (Croatia), L. Figl Observatory (Austria)

International Conferences

- 44th Conf. on Variable stars of the Czech Astron. Soc., Nov. 2012, Brno (talk)
- JENAM 2010, Sept. 2010, Lisbon (invited talk)
- Binaries - key to comprehension of the Universe, June 2009, Brno (Poster)
- JENAM 2008, Sept. 2008, Vienna (Poster)
- CP#AP Workshop 2007, Sept. 2007, Vienna (Co-Chair, Poster)
- IAU Symp. 224 - The A-Star Puzzle, July 2004, Poprad (Poster)

Participation in bilateral projects

- ÖAD WTZ-projects with Croatia: 10/2004, 15/2006, 18/2008, and 14/2010
- ÖAD WTZ-projects with Czech Republic: 11/2008, 10/2010, and 10/2012

Additional skills

- Languages: German (native), English (fluently), French and Spanish (basics)
- Programming languages: Fortran 77/90, C/C++, Perl, php/cgi
- System administration: Linux, Windows

Research funds

- Vienna University research grants (Forschungsstipendium) in 2005 and 2009
- MOEL-Plus abroad grants by ÖFG: #388 (University of Zagreb - Croatia), #446 (Masaryk University - Brno, Czech Republic)
- Several other University grants for short research stays.

Member of the Österreichische Gesellschaft für Astronomie und Astrophysik (ÖGAA) since 2002

LIST OF REFEREED PUBLICATIONS

- A photometric study of chemically peculiar stars with the STEREO satellites - II. Non-magnetic chemically peculiar stars
Paunzen, E., Wraight, K. T., Fossati, L., Netopil, M., White, G. J., Bewsher, D., 2013, MNRAS, 429, 119
- The Hvar survey for roAp stars. I. The survey observations
Paunzen, E., Netopil, M., Rode-Paunzen, M., Handler, G., Božić, H., Ruždjak, D., Sudar, D., 2012, A&A, 542, 89
- A photometric study of chemically peculiar stars with the STEREO satellites - I. Magnetic chemically peculiar stars
Wraight, K. T., Fossati, L., Netopil, M., Paunzen, E., Rode-Paunzen, M., Bewsher, D., Norton, A. J., White, Glenn J., 2012, MNRAS, 420, 757
- The first spectroscopic verification of an extragalactic classical chemically peculiar star
Paunzen, E., Netopil, M., Bord, D.J., 2011, MNRAS, 411, 260
- New spectroscopic classifications of 35 chemically peculiar candidate stars
Paunzen, E., Netopil, M., Pintado, O. I., Rode-Paunzen, M., 2011, Astron. Nachr., 332, 77
- A photometric long-term study of chemically peculiar stars in open clusters
Paunzen, E., Hensberge, H., Maitzen, H.M., Netopil, M., Trigilio, C., Fossati, L., Heiter, U., Pranka, M. 2011, A&A, 525, 16
- On the metallicity of open clusters I. Photometry
Paunzen, E., Heiter, U., Netopil, M., Soubiran, C., 2010, A&A, 517, 32
- A high-resolution study of isotopic composition and chemical abundances of blue horizontal branch stars in the globular clusters NGC 6397 and NGC 6752
Hubrig, S., Castelli, F., de Silva, G., González, J. F., Momany, Y., Netopil, M., Moehler, S., 2009, A&A, 499, 865
- Chemically peculiar stars and their temperature calibration
Netopil, M., Paunzen, E., Maitzen, H.M., North, P., Hubrig, S., 2008, A&A, 491, 545
- CCD photometric search for peculiar stars in open clusters. VIII. King 21, NGC 3293, NGC 5999, NGC 6802, NGC 6830, Ruprecht 44, Ruprecht 115, and Ruprecht 120
Netopil, M., Paunzen, E., Maitzen, H.M., Pintado, O.I., Claret, A., Miranda L.F., Iliev, I.Kh., Casanova, V., 2007, A&A, 462, 591
- Investigating star formation in the young open cluster NGC 6383
Paunzen, E., Netopil, M., & Zwintz, K., 2007, A&A, 462, 157

- Chemically peculiar stars in the Large Magellanic Cloud
Paunzen, E., Maitzen, H. M., Pintado, O. I., Claret, A., Iliev, I. Kh., Netopil, M., 2006, *A&A*, 459, 871
- On the current status of open-cluster parameters
Paunzen, E., & Netopil, M., 2006, *MNRAS*, 371, 1641
- Photometric survey of marginally investigated open clusters. I. Basel 11b, King 14, Czernik 43
Netopil, M., Maitzen, H. M., Paunzen, E., Claret, A., 2006, *A&A*, 454, 179
- CCD photometric search for peculiar stars in open clusters. VII. Berkeley 11, Berkeley 94, Haffner 15, Lyngå 1, NGC 6031, NGC 6405, NGC 6834 and Ruprecht 130
Paunzen, E., Netopil, M., Iliev, I. Kh., Maitzen, H. M., Claret, A., Pintado, O. I., 2006, *A&A*, 454, 171
- CCD photometric search for peculiar stars in open clusters. VI. NGC 1502, NGC 3105, Stock 16, NGC 6268, NGC 7235 and NGC 7510
Paunzen, E., Netopil, M., Iliev, I. Kh., Maitzen, H. M., Claret, A., Pintado, O. I., 2005, *A&A*, 443, 157
- CCD- Δa and BVR photometry of NGC 7296
Netopil, M., Paunzen, E., Maitzen, H. M., Claret, A., Pavlovski, K., Tamajo, E., *Astron. Nachr.*, 326, 734

LIST OF PROCEEDINGS PUBLICATIONS

- Developments of the Open Cluster Database WEBDA
Netopil, M., Paunzen, E., Stütz, Ch., 2012, in *Star Clusters in the Era of Large Surveys, Astrophysics and Space Science Proceedings*, 53
- Búsqueda de estrellas químicamente peculiares en cúmulos abiertos
Jaque, M., Fraga, L., Paunzen, E., Netopil, M., 2011, *Boletín de la Asociación Argentina de Astronomía*, 54, 167
- Variable Star Survey in Galactic Open Clusters
Netopil, M., Paunzen, E., 2010, in *Binaries - Key to Comprehension of the Universe*, *Astronomical Society of the Pacific*, 145
- A high-spectral-resolution study of abundances and isotopic composition of BHB stars in NGC 6397 and NGC 6752
Hubrig, S., Castelli, F., De Silva, G., González, J. F., Momany, Y., Netopil, M., Moehler, S., 2010, in *Star clusters: basic galactic building blocks throughout time and space*, *IAU Symposium, Volume 266*, 421
- What can we expect from a census of Ap stars in open star clusters in the Galaxy and beyond?
Maitzen, H.M., Paunzen, E., Netopil, M., 2008, *Contrib. of the Astron. Obs. Skalnaté Pleso*, 38, 385

-
- (Extra) galactic stellar aggregates
Netopil, M., Paunzen, E., Maitzen, H.M., 2008, *Contrib. of the Astron. Obs. Skalnaté Pleso*, 38, 431
 - New developments on the field of chemically peculiar stars in the milky way and the LMC.
Maitzen, H. M., Paunzen, E., Pöhl, H., Rode-Paunzen, M., Netopil, M., Stütz, C., Baum, H., Alvear-Gomez, M. L., 2005, *Astron. Nachr.*, 326, 661
 - The Δa research group
Maitzen, H. M., Paunzen, E., Pöhl, H., Rode-Paunzen, M., Netopil, M., Stütz, Ch., Baum, H., 2004, in *The A-Star Puzzle*, IAU Symposium, Volume 224, 743
 - A Quarter Century PU Vulpeculae
Netopil, M., 2002, *Hvar Observatory Bulletin*, 26, 37

BOOKS

- Proceedings of the CP#AP Workshop 2007
edited by: J. Žižňovský, J. Zverko, E. Paunzen, M. Netopil, 2008, *Contrib. of the Astron. Obs. Skalnaté Pleso*, 38/2

OTHER PUBLICATIONS

- Das Observatorium auf Hvar und das Austro-Kroatische 1m-Teleskop
H. M. Maitzen, E. Paunzen, M. Netopil, 2013, *Der Sternenbote*, 1, 2
- Erste spektroskopische Bestätigung von extragalaktischen chemisch pekuliären Sternen
E. Paunzen, M. Netopil, 2011, *Der Sternenbote*, 6, 106